

## **Distribution Agreement**

In presenting this thesis or dissertation as a partial fulfillment of the requirements for an advanced degree from Emory University, I hereby grant to Emory University and its agents the non-exclusive license to archive, make accessible, and display my thesis or dissertation in whole or in part in all forms of media, now or hereafter known, including display on the world wide web. I understand that I may select some access restrictions as part of the online submission of this thesis or dissertation. I retain all ownership rights to the copyright of the thesis or dissertation. I also retain the right to use in future works (such as articles or books) all or part of this thesis or dissertation.

Signature:

\_\_\_\_\_  
Erica Denise Bizzell

\_\_\_\_\_  
Date

Mycobacterial serine proteases and modulation of host immunity

By

Erica Denise Bizzell  
Doctor of Philosophy

Graduate Division of Biological and Biomedical Sciences  
Microbiology and Molecular Genetics

---

Jyothi Rengarajan, Ph.D.  
Advisor

---

Daniel Kalman, Ph.D.  
Committee Member

---

Charles Moran, Ph.D.  
Committee Member

---

William Shafer, Ph.D.  
Committee Member

---

David Weiss, Ph.D.  
Committee Member

Accepted:

---

Lisa A. Tedesco, Ph.D.  
Dean of the James T. Laney School of Graduate Studies

---

Date

Mycobacterial serine proteases and modulation of host immunity

By

Erica Denise Bizzell  
B.S., Towson University, 2008

Advisor: Jyothi Rengarajan, Ph.D.

An abstract of  
A dissertation submitted to the Faculty of the  
James T. Laney School of Graduate Studies of Emory University  
in partial fulfillment of the requirements for the degree of  
Doctor of Philosophy

Graduate Division of Biological and Biomedical Sciences  
Microbiology and Molecular Genetics

2017

## ABSTRACT

Mycobacterial serine proteases and modulation of host immunity

By

Erica Denise Bizzell

Tuberculosis (TB), which is caused by the bacterial pathogen, *Mycobacterium tuberculosis* (Mtb), is the deadliest infectious disease worldwide. Mtb employs a variety of mechanisms to evade host immune responses, allowing the pathogen to establish and maintain infection of its host. The current available TB vaccine, BCG, is poorly protective and shares many immune evasion-associated genes with Mtb.

We previously reported that the Mtb protease, Hip1 (Rv2224c), promotes sub-optimal host immune responses, including suppression of dendritic cells (DCs), which play a key role in the generation of CD4 T cell responses. As BCG is closely related to Mtb and expresses an identical Hip1 protein, we tested the hypothesis that BCG Hip1 modulates DC functions, thereby limiting BCG immunogenicity. I generated a strain of BCG lacking *hip1* (BCG $\Delta$ *hip1*), and show that it more effectively induces DC maturation and cytokine production than the parent BCG strain. Further we report that BCG $\Delta$ *hip1* infected DCs are better able to activate CD4 T cells and drive their differentiation into antigen-specific IFN- $\gamma$  or IL-17 producing cells *in vitro*. Mucosal transfer of BCG $\Delta$ *hip1*-infected DCs into mouse lungs induced robust CD4 T cell activation *in vivo* and generated antigen-specific polyfunctional CD4 T cell responses in the lungs. Importantly, BCG $\Delta$ *hip1*-infected DCs enhanced control of pulmonary bacterial burden following Mtb aerosol challenge compared to transfer of BCG-infected DCs. These findings illustrate that BCG utilizes Hip1 to dampen DC responses and subsequent CD4 T cell responses, leading to limited capacity to control Mtb burden after challenge. Thus, vaccination with BCG $\Delta$ *hip1* is likely to be more efficacious than BCG and has the potential to improve protective immunity to Mtb infection.

In this dissertation work, I also characterized the relationship between Hip1 and a closely related mycobacterial protease, Rv2223c. I show that Hip1 and Rv2223c are highly conserved across both pathogenic and non-pathogenic mycobacterial strains. Furthermore, my observation that Rv2223c interacts with the Hip1 substrate, GroEL2, suggests that Rv2223c may cooperate with Hip1. These findings, along with data suggesting that deletion of both proteases is lethal for Mtb growth, support the hypothesis that they work in conjunction with one another to perform essential virulence functions in Mtb pathogenesis.

Mycobacterial serine proteases and modulation of host immunity

By

Erica Denise Bizzell  
B.S., Towson University, 2008

Advisor: Jyothi Rengarajan, Ph.D.

A dissertation submitted to the Faculty of the  
James T. Laney School of Graduate Studies of Emory University  
in partial fulfillment of the requirements for the degree of  
Doctor of Philosophy

Graduate Division of Biological and Biomedical Sciences  
Microbiology and Molecular Genetics

2017

## ACKNOWLEDGEMENTS

I would like to express my deep appreciation and gratitude to my advisor, Dr. Jyothi Rengarajan, for your patient mentorship during my time in your lab. You are an exceptional scientist and a great person. Thank you for challenging me to push beyond my perceived limits in order to become an even better scientist. Thank you so much for encouraging my career exploration and supporting my goals throughout. After my having to switch projects a year into my dissertation work, your ability to seamlessly regroup all while calmly helping me to do so as well, was inspiring and admirable. You have been a wonderful mentor, and I will be forever grateful that you took a chance on me!

Next, I would like to thank my committee members, Dr. Charles Moran, Dr. Daniel Kalman, Dr. Bill Shafer, and Dr. David Weiss. I truly appreciate every meeting, recommendation and suggestion that you all provided me. Thank you, Charlie for allowing me to get my first taste of graduate school through my first rotation in your lab. I greatly appreciate your door always being open. Thank you, Dan for always stimulating me and making me think outside of the box during our scientific discussions, both during my graduate school interview and as my committee member. Thank you, Bill for the wisdom and knowledge that you have consistently provided me with both in science as well as in my career search. You were always willing to meet with me and offer your advice whenever I needed it, and I truly appreciate that. Thank you, David for your beneficial insight in committee meetings as well as during our short-lived joint lab

meetings. Each of you managed to make me come out of my committee meetings more optimistic and much less stressed than when I came in.

Thanks to my lab mates, both past and present. You have all helped to keep me sane throughout my years here. To Amita, Ana, Becky, Kevin, Marcos, Maria, Melanie, Ranjna, and Uma, working with you has been such a rich and rewarding experience. I will be forever grateful for all of the friendship, support, collaboration, laughs, cries, celebrations, and late-night dancing/singing sessions that you have shared with me.

I would like to thank our collaborators in the lab of Dr. Gregory Petsko and Dr. Dagmar Ringe at Brandeis University. Thanks to Dagmar for your advice and for allowing me to work in the lab, and thank you to all of the lab members who were so welcoming each time that I visited. Thank you to Dr. Andrew Daab for his work, which helped to set the stage for me. Thank you in particular to Dr. Jackie Naffin-Olivos for your patience while teaching me all of the biochemistry techniques that I know and for selflessly offering up your home whenever I visited. I am glad to say that in you, I gained not only a colleague, but also a great friend!

Thanks to Dr. Miriam Braunstein of the University of North Carolina and to her lab members, Ellen, Jenny, and Kate for advising me in my mycobacterial genetics techniques, and for your constant willingness to talk or to send a reagent.

Finally, I would like to thank my family and loved ones. To Edward, thank you for your love, laughter, and motivation over these last 2 years. Thanks to my sisters, Crystal and ZaToya for your friendship throughout my life and for inspiring me through your lives everyday. Also thanks for my nieces and nephews who have added even more joy to my world! To my Father, Eric, I have always known that you will be there for me if I need you. I thank you for your love, advice, jokes, and support throughout my life, and thank you for always believing in me. To my mother, Michelle, I would not be here today if it weren't for your sacrifice and tireless efforts to ensure that I received the best education possible. You have always supported my dreams no matter what, and have been my biggest cheerleader and critic (always constructive) throughout my life. I love you so much, and thank you for your unconditional love. Mom and Dad, I know that I could never repay you for all that you've done, but I will try! To my Uncle Ronnie, you were at every graduation and you always encouraged and invested in me. I wish that you could be here for this final graduation. To my Grandma Juanita, I wish that you could see that your advice to "make your books your boyfriend" paid off. I so wish that you could have witnessed it yourself, but I thank you for all of the love and support that you gave me.

## TABLE OF CONTENTS

CHAPTER 1:	Introduction.....	1
CHAPTER 2:	Deletion of the Hip1 protease in BCG enhances dendritic cell functions and augments lung CD4 T cell responses .....	22
	Chapter 2 Tables and Figures .....	43
CHAPTER 3:	Molecular characterization of the secreted <i>Mycobacterium tuberculosis</i> protease, Rv2223c .....	51
	Chapter 3 Tables and Figures .....	70
CHAPTER 4:	Unpublished data .....	78
	Chapter 4 Tables and Figures .....	91
CHAPTER 5:	Discussion.....	102
CHAPTER 6:	Bibliography .....	110
CHAPTER 7:	Appendix – Other publications and unpublished citations .....	149
	Chapter 2 citation.....	150
	Engaging the CD40-CD40L pathway augments T-helper cell responses and improves control of <i>Mycobacterium tuberculosis</i> infection .....	151
	<i>Mycobacterium tuberculosis</i> GroEL2 modulates dendritic cell responses.....	174

## LIST OF TABLES AND FIGURES

### CHAPTER 2

Figure 1:	Deletion of <i>hip1</i> from BCG does not affect growth of BCG in broth or in dendritic cells.....	43
Figure 2:	BCG $\Delta$ <i>hip1</i> induces stronger pro-inflammatory cytokine production from innate immune cells.....	44
Figure 3:	BCG $\Delta$ <i>hip1</i> enhances expression of costimulatory molecules on infected DCs .....	46
Figure 4:	DCs infected with BCG $\Delta$ <i>hip1</i> induce higher levels of IFN- $\gamma$ and IL-17 production from CD4 T cells compared to BCG .....	47
Figure 5:	Intratracheal instillation of DCs infected with BCG $\Delta$ <i>hip1</i> enhances mucosal CD4 T cell responses and improves control of Mtb burden after aerosol challenge .....	48
Figure S1:	Southern blot and PCR analysis of BCG $\Delta$ <i>hip1</i> .....	50

### CHAPTER 3

Table 1:	Primer list.....	70
Table 2:	Plasmid list.....	70
Table 3:	Mycobacterial intergenic regions.....	70
Figure 1:	The predicted serine protease, Rv2223c is closely related to Mtb serine protease, Hip1 .....	72
Figure 2:	<i>Rv2223c</i> and <i>hip1/Rv2224c</i> are both highly conserved across mycobacterial species .....	73
Figure 3:	Rv2223c is secreted from cells in a signal sequence-dependent manner.....	74
Figure 4:	Rv2223c undergoes S <sub>232</sub> -dependent autoproteolytic processing upon secretion between residues G <sub>41</sub> and Q <sub>42</sub> .....	75
Figure 5:	Rv2223c interacts with GroEL2 in vitro, but fails to complement GroEL2 cleavage in vivo .....	76
Figure S1:	Pathogenic mycobacteria have tightly-conserved <i>Rv2223c-hip1</i>	

intergenic region .....	77
-------------------------	----

#### CHAPTER 4

Table 1: Primer list.....	91
Table 2: Plasmid list.....	92
Table 3: Purification experiments .....	92
Figure 1: Purification of Rv2223c from Msm supernatants.....	93
Figure 2: Expression of N-terminal 6X His-tagged Rv2223c $\Delta$ 34 and $\Delta$ 41 in C43 and BL21 star <i>E. coli</i> .....	94
Figure 3: L-arginine does not stabilize purified Rv2223c in solution.....	95
Figure 4: Absorbance based analysis of stabilizing capabilities of the indicated buffers on Rv2223c $\Delta$ 34 .....	96
Figure 5: Hexamine cobalt trichloride does not stabilize Rv2223c in solution .....	97
Figure 6: Expression of C-terminally tagged Rv2223c $\Delta$ 34 and $\Delta$ 41 in C41 and BL21 star <i>E. coli</i> .....	98
Figure 7: Thermal fluorescence screen of the effect of detergents on Rv2223c protein stability .....	99
Figure 8: Southern blot and PCR analysis of Mtb $\Delta$ Rv2223c $\Delta$ hip1 .....	100
Figure 9: Verification of Rv223c and <i>hip1</i> recombination.....	101

## **Chapter 1**

### **Introduction**

## **Part 1 – History of bacterial infectious disease research**

Whether through hieroglyphics or investigations of mummified remains, evidence of pestilence in the human race can be dated as far back as our history can reach. Despite the prolonged presence of these diseases, it has only within the last half millennium that we have been able to visualize and definitively determine their causes. Anton van Leeuwenhoek's invention of the microscope in the 17<sup>th</sup> century, provided researchers with the ability to take a peek into the microbial world surrounding, yet continuously eluding us. Even with this early invention, not until the 19<sup>th</sup> century did scientists begin to empirically show that some of the microorganisms thus seen were the cause of a host of ailments. These observations further led to the development of a set of rules by Dr. Jakob Henle and his pupil Dr. Robert Koch to definitively determine whether a microbe was the causative agent of a disease (1). Dr. Koch presented these guidelines, called the Henle-Koch's Postulates to the public in 1884 (1). These rules generally stated that in order to determine whether a microbe causes a given disease one must be able to identify the microbe in every case of the disease, and that the microbe, once isolated and used to infect test organisms, must cause the same disease (2). One of Koch's first discoveries based on these guidelines was that of the tubercule bacillus, which he showed to be the causative agent of tuberculosis (TB) disease in humans. The discovery of this and other disease-causing agents not only provided us with brand new insights into pathogenesis, but also allowed for direct targeting of the pathogens themselves. By learning more about the nature of microbes and their interaction with the world surrounding them, remarkable advances were achieved, such as the discovery of penicillin, the first commercially used

antibiotic by Alexander Fleming in 1928. Microbial research in conjunction with medical and immunological advances remains the driving force in developing our arsenal against infectious diseases today.

## **Part 2 – Background on tuberculosis**

### 2.1 – History

TB is one of the oldest diseases to plague the human population, with evidence of human infections dating back 9000 years (3). In the millennia since, there have been multiple recorded TB epidemics throughout the world, and the disease has been referred to by several different names. In classical Greece, TB was known as phthisis, while during the European epidemics of the 18<sup>th</sup> and 19<sup>th</sup> centuries, consumption or the White Plague were common terms for the disease (4). Poor nutrition, overcrowding, and the lack of knowledge of the underlying microbial cause of the disease contributed to the many lives claimed by TB during these epidemic periods. Despite the longstanding history of TB with its human host, Robert Koch would not discover the causative agent until 1882 (5). The rod-shaped bacillus that Koch observed under his microscope in samples from both human specimens and from the animals that he had infected was what we now know as *Mycobacterium tuberculosis* (Mtb). The successful evolution of Mtb with mankind over many centuries has made it one of the most well adapted bacterial pathogens to the human host environment. This adaptation has resulted in a great deal of difficulty in eradicating TB and contributes to the current success in infection of about one-third of the world's population (6).

## 2.2 – Tuberculosis symptoms, diagnoses, and treatments

The primary manifestation of TB disease is as pulmonary Mtb infection, which can be established by inhalation of as few as one bacterium into the lungs (7). Due to the hardy and host-adapted nature of Mtb, the bacteria are able to persist within alveolar macrophages, which serve as the first-responding innate immune cells in the alveolar spaces of the lungs. These infectious bacilli, through expression of several effector proteins, successfully delay the onset of adaptive immune responses that would normally be deleterious to less host-adapted pathogens (8). This delayed and inadequate immune response, coupled with the resiliency of Mtb, results in formation of lesions known as granulomas, where Mtb persists within the lungs of infected individuals. Granulomas consist of Mtb-infected macrophages at their core surrounded by other innate immune cells, including macrophages, neutrophils, and dendritic cells, which are ineffective at killing the bacteria (8). These innate cells are further surrounded by T and B cells of the adaptive immune response, which arrive late to the site of infection due to Mtb-elicited delays in response (9). These granulomas, while ineffective at eliminating the bacteria, can be effective at containing mycobacterial infection by sequestering Mtb within the infected lung.

When the bacteria are successfully contained within the lung, presumably within macrophages, an asymptomatic infection known as latent TB infection (LTBI) occurs. 90% of healthy, HIV-uninfected people infected with Mtb develop LTBI state, while

approximately 10% develop the symptomatic pulmonary disease known as active TB. However latently infected individuals can progress to active TB when perturbations in immune control occur, leading to increased bacterial replication and reactivation to active TB disease (10, 11). Symptoms of active TB disease include weight loss, fatigue, and fever, with the most profound symptom being a productive, painful cough. This characteristic cough leads to aerosolization of bacteria which results in effective spread of Mtb from an infected person to multiple others through inhalation of Mtb-containing aerosol particles.

The primary method by which individuals suspected of having active TB can be diagnosed is through detection of the presence of Mtb bacilli from a sample of their sputum. As sputum can be difficult to obtain, alternative diagnoses are often required. Diagnosis of people suspected of either LTBI or active TB usually begins with administration of the Mantoux tuberculin skin test (TST) (12). This test requires inoculation of purified tuberculin proteins intradermally; an individual who has a memory immune response to prior mycobacterial infection will locally respond in the form of inflammation. However, due to proteins shared between Mtb and other mycobacterial species, including the vaccine strain *Mycobacterium bovis* BCG, a positive response to this test is not always indicative of infection with Mtb. Another family of tests that is often used for TB diagnosis is the interferon-gamma (IFN- $\gamma$ ) release assay (IGRA) (13). For these assays, patient blood samples are tested for the presence of T cells that respond to stimulation with the Mtb-specific proteins, ESAT6 and CFP10, and the response is measured by assaying for the cytokine, IFN- $\gamma$ . IGRAs are more specific

as they indicate infection with Mtb, however they do not distinguish LTBI and active TB. Until more definitive blood-based tests for TB disease are developed, diagnosis of TB disease requires a combination of clinical assessments, including symptom screens and lung x-rays in order to visualize any active granulomas that may be present.

Upon diagnosis of an individual with TB, treatment varies between LTBI and active TB. Prior to the advent of antibiotics, the treatment recommended for active TB was generally fresh air and rest. Facilities where individuals could spend time recovering from tuberculosis were called sanatoria, the first of which, founded in Austria by Herman Brehmer, opened in 1859 (14). Here, patients were able to get the rest, healthy diet, fresh air, sunlight, and moderate exercise that served as the “cure” for TB at the time. Adirondack Cottage Sanatorium, founded by Edward Livingston Trudeau in 1884, was America’s longest run sanatorium, and served ailing TB patients until it finally closed in 1954 (14).

The seminal event that brought about the eventual demise in sanatorium care for TB was the discovery of the first antibiotic effective against Mtb, streptomycin, which was isolated by Dr. Albert Schatz et al. in 1944 (15). Together with improved sanitation and public health measures, antibiotics were responsible for controlling TB in much of the developed world. Today, there are four frontline drugs used to treat TB. These are rifampicin (RIF), isoniazid (INH), pyzinamide (PZA), and ethambutol (ETH), collectively known as RIPE and active TB patients are prescribed all 4 drugs for 2 months, followed by 4 months of Rif and Inh alone (16). Preventive treatment for LTBI

consists of a 9-month regimen of INH or a newer 3-month regimen of Rifapentine and INH combined (17). Evolutionary pressure stemming from inadequate adherence to the long treatment regimens for TB, has contributed to development of a number of antibiotic resistance-causing mutations within Mtb genome, leading to more frequent use of second-line drugs to treat the disease (18, 19). There are now multiple classifications for resistant Mtb based on the treatment regimens necessary to eradicate the disease. Mtb that is resistant to both RIF and INH is classified as multi-drug resistant (MDR), while bacteria that are both MDR and resistant to a second-line drug are considered extensively drug resistant (XDR) (19). The increasing incidence of MDR and XDR TB disease throughout the world is an indication of the urgent need for new drugs and novel strategies to treat TB.

### 2.3 – Mtb classification and the Mtb complex

Actinomycetales, the order under which Mtb falls, generally consists of Gram-positive, GC rich bacteria. The complex cell wall of Mtb, however, renders it incapable of being stained via typical Gram staining. The Mtb cell wall consists of a phospholipid bilayer as its innermost cell membrane, followed by peptidoglycan without an outer phospholipid layer, much like a Gram-positive bacterial wall. However, unlike a Gram-positive organism, the Mtb peptidoglycan is covalently linked to what is called the arabinogalactan (AG) layer, consisting of arabinan and galactan (20). Finally, covalently linked to the arabinogalactan are mycolic acids (MAs), which make up the outermost layer of the Mtb cell wall (20). Interspersed throughout the outer layers of the cell wall

are lipid-linked polysaccharides known as lipoarabinomannan (LAM) capped with mannose (ManLAM) (21).

The complexity of this cell wall along with the hydrophobic nature of the mycolic acids gives Mtb a waxy coating, which is quite difficult to penetrate with the typical Gram staining dyes. To overcome these challenges, in 1883, Franz Ziehl and Friedrich Neelsen developed a new method of bacterial classification via staining known as Ziehl-Neelsen, or acid-fast staining (22). This method is comprised of staining the bacteria with carbol-fuchsin, a phenolic stain which is able to penetrate the waxy Mtb cell wall, followed by treatment with an acid, which will wash away the stain only from standard Gram-positive or Gram-negative bacteria, and finally a counter stain, which will only be taken up by those bacteria that have had the carbol-fuchsin washed away. Therefore, Mtb and other bacteria within the genus are classified as acid-fast instead of Gram-positive, referring to the fact that they are able to retain the carbol-fuchsin even after acidic treatment.

The full group of mycobacterial species that cause TB in humans and/or animals is called the *Mycobacterium tuberculosis* complex (MTBC). This complex consists of *M. tuberculosis*, *M. bovis*, *M. canetti*, *M. africanum*, *M. caprae*, *M. pinnipedii*, *M. microti*, *M. mungi*, and most recently, *M. orygis*. These species are all slow growing, and take about 3 weeks for colony formation on a solid medium. In the past, species within this group were generally differentiated by their differing growth phenotypes, their epidemiology, and later through spoligotyping and restriction fragment length polymorphism (RSLP) analysis. However, advances in genomic sequencing leading to

the publication and annotation of each of these genomes have allowed researchers to even further delineate between them (23-26). Analysis of various SNPs within each of these genomes has given the field a clearer picture of the evolution of the MTBC.

#### 2.4 – Mouse model of TB

There are multiple animal models for TB research including primates, guinea pigs, rabbits and even zebrafish, however the most widely used is the mouse model. Using mice as model organisms provides researchers with a genetically tractable system with a relatively short lifespan. The many years of TB research on mice has revealed many insights about crucial host-pathogen interactions during Mtb infection. Seminal research by Medina et al. found the susceptibility of a variety of common mouse strains, which harbored different genetic mutations (27). The authors discovered that the most commonly used mouse strains, Balb/C and C57BL/6, were relatively resistant to Mtb infection. From these studies, it was also revealed that the C3HeB/FeJ (C3H) mouse strain was highly susceptible to Mtb infection (27). Later studies found that the C3HeB/FeJ mouse strain, which is a derivative of the C3H mouse, serves as an effective model of granuloma formation in mice as Mtb infection of these mice results in formation of necrotic lesions in their lungs (28). Overall, studying the response of mice to Mtb infection has provided the TB field with many immunological insights, one of the earliest being the importance of IFN- $\gamma$  producing T cell responses in the control of Mtb infection (29).

Aside from studying mouse strains already available, directed genetic mutation of mice has allowed researchers to investigate the role of specific genes in host responses to Mtb infection. The dissemination of bacteria in Mtb-infected mice that are deficient in IFN- $\gamma$  production revealed the important role of this T cell cytokine on Mtb infection (30). Similar studies of knockout mice showed the critical roles of IL-12 and TNF- $\alpha$  in protection against Mtb infection (31, 32). Another advantage of the mouse model of Mtb is the availability of reagents within this system. As mice are used to model a plethora of diseases, many antibodies or drugs that specifically target mouse proteins of interest are available for use in TB research. For example, researchers observed by utilizing an antibody blockade of the mouse IL-10 receptor, that IL-10 production promotes Mtb growth in mice (33). Overall, the mouse model serves as an affordable, genetically tractable, system in which to study Mtb infection.

### **Part 3 – Mtb and host interactions**

#### **3.1 – Recognition of Mtb by host immune cells**

Upon inhalation of Mtb by a host organism, the bacteria enter into the lung alveoli, where a number of innate immune cells reside. One of the key innate immune cell types that Mtb encounters within the alveolar spaces is the macrophage. Macrophages, which serve as the first line of defense against microbial infections, provide protection by first phagocytosing the infectious microbes. Within the phagosome of the macrophage, microbes encounter a harsh environment that consists of stressors such as low pH, antimicrobial peptides, and reactive oxygen and/or nitrogen species. Finally, secretion

of cytokines from infected macrophages leads to further activation of both the innate and adaptive branches of the immune system. Multiple studies have demonstrated the critical role of alveolar macrophages (AMs) in early immune responses to Mtb infection (34).

Macrophages first recognize Mtb via engagement of various surface ligands and pattern recognition receptors (PRRs) including mannose receptors (MRs), toll-like receptors (TLRs), and NOD receptors. MRs, which are highly expressed on AMs, recognize components of various glycolipids of Mtb including ManLAM found in the mycobacterial cell wall, and their engagement has been shown to induce phagocytosis (35). Toll-like receptors (TLRs), which recognize pathogen-associated molecular patterns (PAMPS) that are expressed by infectious agents, are another group of key PRRs that have been shown to function in macrophage recognition of Mtb. TLR-2 recognizes the various Mtb cell wall components, including lipoproteins LprG and LprA, as well as ManLAM (36, 37). TLR-4, while classically defined as the LPS receptor in gram-negative bacterial infections, has been found to also recognize Mtb heat shock proteins Hsp65 (GroEL2) and Hsp70 (38). NOD2, a receptor found in the cytoplasm of macrophages and dendritic cells, recognizes peptidoglycan and muramyl dipeptide (MDP) of Mtb and other bacteria (39). NOD2 engagement by Mtb leads to increased production of pro-inflammatory cytokines TNF $\alpha$ , IL-6 and IL-1 $\beta$  (40). While crucial for the initial immune response to Mtb, human AMs have been shown to be inefficient at presenting antigen to T cells, a process that is necessary for an effective adaptive immune response (41).

Along with AMs, another important innate immune cell infected by Mtb within the lungs is the dendritic cell (DC) (42). DCs are critical for the crosstalk between innate and adaptive immunity, as they serve as professional antigen presenting cells (APCs). The receptors on DCs that have been shown to recognize Mtb include MR, Dendritic cell-specific intercellular adhesion molecule-3 grabbing nonintegrin (DC-SIGN), Dectin-2, TLR2, TLR4, and TLR9 (34). DC-SIGN engages with ManLAM on the surface of mycobacterial cells (43), and recognition of Mtb via TLR9 significantly contributes to DC IL-12 production (44, 45). Upon recognition and uptake of bacterial pathogens, DCs process the antigens into peptides, which are then loaded onto MHC class I or class II molecules. MHC-peptide complexes are then displayed on the surface of the infected DC, which T cells are then able to recognize via their T cell receptors (TCRs). DCs also display co-stimulatory markers, such as CD40, CD80, and CD86 on their cell surface, which are recognized by corresponding receptors on T cells. These interactions provide optimal T cell activation. The final signals to the T cell provided by DCs are various cytokines, including IL-12p40, IL-6, and IL-1 $\beta$ , which help to polarize CD4 T cells to different functional subsets. Extensive research studies have identified IFN- $\gamma$  production by CD4 T cells known as T-helper 1 (Th1) as playing a crucial role in Mtb control during infection (30, 46, 47). More recently, IL-17-producing Th17 cells have been shown to play an important role in Mtb control (48-51).

### 3.2 – Immune evasion and immunomodulation by Mtb

The co-evolution of Mtb and humans over thousands of years has allowed the TB-causing bacterium to develop various methods to subvert and manipulate the host immune system. These evasive techniques include modifications by the bacterium of its complex cell wall, secretion of effector and decoy proteins, and overall prevention of normal host immune responses in order to provide a favorable environment for Mtb growth and survival.

The first interactions of Mtb with its host are between the bacterial cell wall and host innate immune cells. Upon recognition by various receptors on macrophages and DCs, components of the Mtb cell wall have been shown to suppress different aspects of the host immune response to infection with the bacteria. For example, Mtb ManLAM is recognized by multiple macrophage and DC receptors; interaction of ManLAM with DC-SIGN or Dectin-2 on DCs has been shown to induce increased production of the anti-inflammatory cytokine, IL-10, which may counteract the pro-inflammatory cytokines that ManLAMs also induce (43, 52). IL-10 production has been implicated in dampened production of pro-inflammatory cytokine such as IL-12 and IL-1 $\beta$  and has been found to contribute to disease progression in Mtb infected mice (33). Recognition of Mtb lipoproteins such as LprG and 19-kDa by TLR-2 on macrophages, results in inhibition of antigen MHC class II antigen processing and MHC class II expression respectively (36, 53). Muramyl dipeptide (MDP) derived from Mtb peptidoglycan is recognized by NOD2 in macrophages (40).

Some of the most crucial strategies used by *Mtb* to modulate the host immune response lie in the proteins encoded by genes within its region of deletion 1 (RD1). The RD1 region is a genetic locus consisting of 9 genes, which are required for virulence of pathogenic mycobacterial strains (54, 55). Notably, the RD1 region is thought to be the key deletion during attenuation of *M. bovis* attributing to the avirulence of BCG (56-58). Deletion of the RD1 region from *Mtb* results in attenuation of the bacteria in mice, even after a high dose of infection, while re-introduction of the locus of genes into the attenuated *M. bovis* BCG increases virulence of the vaccine strain (55, 56). This locus contains the genetic information for the ESX-1 type VII secretion system and the ESAT-6/CFP-10 protein complex (54, 59-61). ESAT-6 and CFP-10 are two of the most extensively studied effector proteins of *Mtb*. They have been implicated in inhibition of ROS production by *Mtb* infected macrophages, pore formation for *Mtb* phagosomal escape, and induction of apoptosis (62-64). Further, ESAT-6 and CFP-10 are highly antigenic, and are potent stimulators of early IFN- $\gamma$  production from T cells (65, 66).

Upon phagocytosis by macrophages, bacteria temporarily reside in the phagosomal compartment of the innate immune cell. Normally, this compartment then matures and forms the phagolysosome via fusion with a lysosomal compartment, which harbors various antimicrobial peptides, proteases, and provides an acidic environment conducive to antigen processing. This, along with the reactive oxygen and nitrogen species produced within the mature phagolysosome compartment, then leads to the eventual killing of susceptible intracellular bacteria. *Mtb*, however, is capable of blocking this maturation of the phagosome into the phagolysosomal compartment thereby maintaining

a microenvironment that is more conducive to the bacterium's survival (67). Mtb produces multiple effector proteins that are involved in blocking phagolysosome fusion. For example, PtpA, an Mtb tyrosine phosphatase, blocks phagosome maturation through interaction with a host vacuolar ATPase required for phagosome acidification (68). The Mtb serine-threonine kinase, PknG, has been implicated in inhibition of phagosome maturation, in that deletion of *pknG* results in *M. bovis* BCG localizing with macrophage lysosomal compartments (69).

Mtb employs the help of a multitude of other effector proteins in order to subvert and modulate host immune responses. Antigen 85b (Ag85b) is a highly antigenic protein secreted by Mtb early in infection (70, 71). The strong T cell responses elicited by this protein, however, do not result in eradication of the bacteria from the host (71). Instead, Ag85b is thought to function as a decoy protein antigen, stimulating a strong memory response that recognizes antigen that is no longer expressed after establishment of infection (72, 73). Another Mtb immunomodulatory protein of interest is the serine protease Hip1, which has been shown to be necessary for optimal survival of the bacteria in macrophages, and to be involved in blunting the early innate immune response to Mtb (74, 75). One mechanism underlying Hip1 immune modulation appears to be its cleavage of the chaperonin-like protein, GroEL2, which has potent immunostimulatory functions its full length form but is poorly stimulatory when cleaved into a shorter protein (76). The effects of Hip1 on Mtb virulence and immunogenicity will be discussed in more detail later.

#### Part 4 – BCG vaccine

Bacille Calmette-Guérin (BCG) is currently the only vaccine used to prevent TB. The scientists Albert Calmette and Camille Guérin, for whom the BCG vaccine is named, initiated development of a tuberculosis vaccine in 1908 with the bovine TB-causing bacterium *Mycobacterium bovis* (77). Efforts to vaccinate against TB prior to the development of BCG included inoculation of animals and/or humans with Mtb that had undergone heat inactivation, attenuation through culturing, or even small doses of live Mtb (78). As killed bacteria had proven unsuccessful, and with full awareness of the risks that the other two approaches entailed, Calmette and Guerin ventured to create a live vaccine by deliberately attenuating *M. bovis* to the point of little to no chance of its regaining virulence. The process consisted of serial passaging of *M. bovis* on medium including potatoes cooked in ox bile (78). In 1919, 11 years and 230 sub-cultures later, the BCG vaccine was completed, and in 1921, the first BCG human vaccine trial was conducted(78). With confirmation of the safety of the vaccine, BCG was soon widely distributed and used throughout the world.

90 years since its initial development, BCG is still one of the most widely used vaccines today, and has maintained its status as the sole vaccine against TB. Shortly after the first human trials of BCG, the vaccine was distributed to countries around the world where physicians and scientists continued to validate the safety of the vaccine, and further passaged the live vaccine (77). Today, BCG is incorporated into the vaccination programs of nearly every county worldwide (79). However, none of these strains are

identical to that of Calmette and Guerin's original strain, which was lost during World War I (80). Separate propagation of the BCG vaccine by individual countries has resulted in wide genetic variation of the strains of BCG used, and may contribute to the wide variation in protective capabilities of the various strains (80).

Despite its widespread use, BCG does not provide lasting protection against TB. The vaccine is currently given to infants shortly after birth in TB endemic areas. BCG vaccination protects children under the age of five against disseminated forms of TB such as TB meningitis, but fails to effectively protect against pulmonary TB or to reliably provide protection into adulthood (81, 82). In fact, a longitudinal study in infants vaccinated with BCG revealed that antigen-specific memory CD4 T cell responses peak around 10 weeks post-vaccination and gradually decline back to pre-vaccination levels (83). Vaccine trials conducted in newborns between 1948 and 1961 reported an average of 73% efficacy against TB disease, while meta-analyses of BCG vaccination studies concluded that BCG provides an average of 50% protection from disease in adults (84-86). There are a variety of factors that likely contribute to the limited efficacy of BCG, including prior exposure to environmental mycobacterial species (81), and the bacteria's expression of genes involved in immune evasion and immunomodulation (87-89). Some studies have shown that the diversity of BCG strains used around the world also may affect the efficacy of the vaccine (90).

Currently many efforts are aimed at improving the ability of BCG to stimulate a stronger and more protective immune response, mainly through modification of the BCG genome.

These modifications to BCG have largely focused on expression of non-endogenous genes from Mtb, and a limited number of studies have explored deleting genes from BCG that suppress host immune responses (89, 91). One such modified BCG strain, which expresses listeriolysin from *Listeria monocytogenes* and harbors a deletion of the urease-producing gene, *ureC* has recently progressed to clinical trials (92-94). The only clinical TB vaccine trial to have advanced to the final stages of testing since the development of BCG comprised an MVA-based vaccine expressing the immunodominant Mtb protein, Ag85a, however this vaccine failed to provide any more protection than BCG against TB (95). With this in mind, coupled with the fact that BCG has a long record of safety in children and already widely used, the approach of modifying BCG in an effort to make it more protective may prove to be the best approach to creating an improved TB vaccine.

### **Part 5 – Role of Mtb proteases during infection**

Proteases are enzymes present in all organisms, which cleave peptide bonds of proteins at specific peptide sequences. Many bacterial pathogens are known to utilize secreted proteases to mediate pathogenesis and use proteolytic processing as a virulence mechanism to evade host immunity. Importantly, protease inhibitors have been successful in treating many bacterial pathogen-related diseases (96). Mtb encodes over 100 predicted proteases and it is increasingly appreciated that proteases play an important role in Mtb pathogenesis. However, insight into the molecular and biochemical mechanisms underlying Mtb proteases is quite limited and very few proteases have been characterized with regard to their physiological substrates. Thus, compared to other

bacterial pathogens, relatively little was known about proteases in Mtb. However, in the past decade, several proteases have been implicated in the ability of Mtb to adapt to host cells. For instance, PepD, a secreted serine protease that promotes Mtb virulence was shown to hydrolyze the general protease substrate casein but its physiological substrates remain unknown (97). The cell wall-associated serine protease, MycP1 plays an important role in secretion of substrates of the Mtb ESX-1 Type VII secretion system, which is important for Mtb virulence (98). Notably, recent studies of Mtb proteases that have been the most extensively studied have revealed potential benefits of inhibiting their action during infection (99-101). Importantly many Mtb proteases belong to novel, previously uncharacterized protease families, which further highlights the need for their detailed molecular biochemical characterization.

#### **Part 6 – Hip1 and Rv2223c serine proteases of Mtb**

The Mtb serine protease, Hip1 (Rv2224c), has been implicated in modification of the bacterial cell wall, intracellular survival of Mtb, and dampening of the host immune response. Multiple studies, largely from the Rengarajan group, have highlighted the role of Hip1 in modulating host innate responses through DCs and macrophages. Transposon disruption of Hip1 in Mtb results in increased survival of infected mice, increased pro-inflammatory cytokine production and decreased lung pathology. These effects are partially attributed to the proteolytic activity of Hip1 on the essential Mtb protein, GroEL2 (74, 76). Rv2223c, which encodes a predicted secreted serine protease, lies downstream of *hip1* in the Mtb genome, within a predicted operon. We have shown that

hip1 encodes a cell wall associated serine protease, which shares 47% amino acid identity and 60% similarity with Rv2223c. Both Hip1 and Rv2223c are  $\alpha/\beta$  hydrolase family members and share limited amino acid similarity to tripeptidyl peptidases (TPPs), TppA, SlpD and SlpE from *Streptomyces lividans*, which are mycelium-associated serine peptidases involved in cell growth (102). Excitingly, the 3-dimensional structure of Hip1 was recently solved by X-ray crystallography and revealed that Hip1 belongs to a novel protease family (103). This analysis found that, while similar to TPP endopeptidases, the active site of Hip1 can accommodate much larger substrates, which suggests that Hip1 has endopeptidase activity (103). Although the 3-dimensional structure of Rv2223c remains unsolved, predictive models based on Hip1 structure show that Rv2223c has similar characteristics to Hip1, and is classified as an alpha/beta hydrolase family protein similar to Hip1.

While several studies from the Rengarajan laboratory have shown that Hip1 is involved in dampening the host immune response to Mtb infection thereby leading to increased bacterial virulence, the role for Rv2223c is less well understood. Preliminary data suggest that Hip1 and Rv2223c share substrates and may work in conjunction to regulate Mtb pathogenesis. However the extracellular localization of Rv2223c suggests that the secreted protease likely also has independent functions from Hip1 in Mtb pathogenesis.

## **Part 7 – Thesis overview**

Despite the availability of treatments and a vaccine against tuberculosis, the disease continues to have a high global burden and persists as one of the deadliest infectious

diseases worldwide. The limited protection provided by the BCG vaccine against TB along with the continuous rise in drug resistant *Mycobacterium tuberculosis* infections highlight the need for better treatments and vaccines. Recent efforts within the TB field have focused on gaining a better understanding of the mechanisms used by Mtb to modulate and evade host immune responses. Previous studies in our laboratory have added to these efforts, revealing that the Mtb serine protease, Hip1 is one of the immunomodulatory factors used for Mtb pathogenesis. These studies have helped to lay the groundwork for the research presented in this dissertation. In chapter 2, we reveal that Hip1 acts as an immune evasion protein even in the vaccine strain, BCG. Importantly, we find that we can enhance the immunogenicity of BCG through deletion of *hip1*. Additionally, in chapters 3 and 4, we characterize the predicted serine protease Rv2223c and its relationship to its close relative, Hip1. We also provide some insight that two proteases may work in conjunction with one another.

## Chapter 2

### **Deletion of BCG Hip1 protease enhances dendritic cell and CD4 T cell responses and improves control of *Mycobacterium tuberculosis***

Chapter adapted from:

Erica Bizzell\*, Kevin Sia\* *et al* (2017)

Deletion of the Hip1 protease in BCG enhances dendritic cell functions and augments lung CD4 T cell responses.

\*These authors contributed equally to this work

**ABSTRACT**

Dendritic cells (DCs) play a key role in the generation of CD4 T cell responses to pathogens. *Mycobacterium tuberculosis* (Mtb) harbors immune evasion mechanisms that impair DC responses and prevent optimal CD4 T cell immunity. The vaccine strain *Mycobacterium bovis* Bacille Calmette-Guérin (BCG) shares many of the immune evasion proteins utilized by Mtb, but the role of these proteins in DC and T cell responses elicited by BCG is poorly understood. We previously reported that the Mtb serine protease, Hip1, promotes sub-optimal DC responses during infection. Here, we tested the hypothesis that BCG Hip1 modulates DC functions and prevents optimal antigen-specific CD4 T cell responses that limit the immunogenicity of BCG. We generated a strain of BCG lacking *hip1* (BCG $\Delta$ *hip1*) and show that it has superior capacity to induce DC maturation and cytokine production compared to parental BCG. Furthermore, BCG $\Delta$ *hip1*-infected DCs were more effective at driving the production of IFN- $\gamma$  and IL-17 from antigen-specific CD4 T cells *in vitro*. Mucosal transfer of BCG $\Delta$ *hip1*-infected DCs into mouse lungs induced robust CD4 T cell activation *in vivo* and generated antigen-specific polyfunctional CD4 T cell responses in the lungs. Importantly, BCG $\Delta$ *hip1*-infected DCs enhanced control of pulmonary bacterial burden following Mtb aerosol challenge compared to transfer of BCG-infected DCs. These results reveal that BCG employs Hip1 to impair DC activation, leading to attenuated lung CD4 T cell responses with limited capacity to control Mtb burden after challenge.

## INTRODUCTION

Critical to the success of *Mycobacterium tuberculosis* (Mtb) as a pathogen is its ability to evade host innate and adaptive immunity. Mtb dampens macrophage functions and impairs the ability of dendritic cells (DCs) to induce optimal antigen-specific CD4 T cell responses. As the major antigen-presenting cell (APC) in the immune system, DCs are central to the generation of CD4 T cell responses after infection and vaccination. However, immunomodulatory factors expressed by Mtb promote sub-optimal DC maturation, cytokine production and antigen presentation to CD4 T cells, which adversely affects T cell immunity and impedes control of Mtb infection (34, 104). BCG is an attenuated strain of *Mycobacterium bovis* and the only licensed vaccine for tuberculosis (TB) in humans. While BCG vaccination protects children under the age of five from disseminated forms of TB disease, BCG has limited efficacy against pulmonary TB in children and adults (81, 82). However, the immunological basis for sub-optimal immunity induced by BCG remains unclear. The genome of the BCG parent strain, *M. bovis* shares over 99.95% sequence identity with the Mtb genome (24) and BCG retains many of the genes shown to encode immune evasion proteins in Mtb. We therefore reasoned that retention of immune evasion strategies that are present in virulent mycobacteria by BCG may impede generation of effective innate and adaptive immune responses induced by the vaccine. Thus, we hypothesized that deleting immune evasion genes in BCG that impair DC functions has the potential to improve innate and adaptive immune responses induced by BCG.

We have previously demonstrated that an Mtb cell wall-associated serine protease, Hip1 (Hydrolase important for pathogenesis 1, Rv2224c), is involved in impairing DC functions (105). Since Hip1 from BCG and Mtb are 100% identical, we hypothesized that BCG Hip1 may contribute to sub-optimal DC and CD4 T cell responses and that deletion of *hip1* from BCG would augment innate and adaptive immune responses. In this study, we generated a BCG (Danish) strain lacking *hip1* (BCG $\Delta$ *hip1*) to investigate whether deletion of *hip1* in BCG enhances DC functions and improves CD4 T cell responses *in vitro* and *in vivo*. We show that DCs infected with BCG $\Delta$ *hip1* produce significantly enhanced levels of pro-inflammatory cytokines and express higher levels of major histocompatibility complex (MHC) class II and costimulatory molecules compared to DCs infected with the parent BCG strain. Additionally, deletion of *hip1* from BCG augmented DC antigen presentation to CD4 T cells *in vitro*. Moreover, mucosal priming of immune responses via intratracheal instillation of BCG $\Delta$ *hip1*-infected DCs improved antigen-specific CD4 T cell responses in the lungs and enhanced control of Mtb burden following aerosol challenge, compared to transfer of BCG-infected DCs. Our results demonstrate that BCG subversion of DC functions through Hip1 impedes the generation of robust CD4 T cell responses and provides a rationale for targeting *hip1* to improve BCG immunogenicity.

## MATERIALS AND METHODS

### Bacterial strains and culture conditions

BCG (Danish), BCG $\Delta$ *hip1*, and BCG $\Delta$ *hip1* complemented with *hip1* (BCG $\Delta$ *hip1* comp) were grown at 37°C in Middlebrook 7H9 broth supplemented with 10% oleic acid-albumin-dextrose-catalase (OADC), 0.2% glycerol and 0.05% Tween 80 or on Middlebrook 7H10 agar supplemented with 10% OADC, 0.5% glycerol, and 0.2% Tween 80. Media for complemented BCG $\Delta$ *hip1* was supplemented with 20 $\mu$ g/ml of streptomycin (Sigma-Aldrich, St. Louis, MO), and media for BCG $\Delta$ *hip1* was supplemented with 50 $\mu$ g/ml of hygromycin (Roche Diagnostics, Indianapolis, IN). For growth curves, bacterial strains were inoculated into supplemented 7H9 medium at OD<sub>600</sub> 0.05, and the OD<sub>600</sub> measurements were taken daily.

### Construction of BCG $\Delta$ *hip1* and complemented strains

BCG was transformed via electroporation with 3 $\mu$ g of pEBOP-2 (pYUB657 suicide vector containing a  $\Delta$ *hip1* allele, a selectable hygromycin resistance marker, and a counter selectable *sacB* marker). Resulting transformants that were resistant to hygromycin were then patched onto 7H10 plates containing 2% sucrose. Colonies that displayed hygromycin resistance and sucrose sensitivity were considered to have undergone a single crossover event resulting in incorporation of pEBOP-2 into the BCG genome. These colonies were then grown to saturation for a week in 5ml of 7H9 broth, and then serial dilutions were plated in duplicate onto 7H10 plates supplemented with 2% sucrose. Colonies arising on these plates were patched onto hygromycin-containing

plates. Colonies that were both hygromycin sensitive and sucrose resistant were grown in 7H9 broth, and genomic DNA was extracted using the protocol adapted from Belisle and Sonnenberg (106). Genomic DNA was then subjected to Southern blot analysis. DNA was digested with *NcoI*, and then probed with a DIG-labeled DNA amplicon corresponding to a 1kb region present in both the genome and pEBOP-02. Deletion of *hip1* was also confirmed via amplification of the deleted region using primers upstream (forward primer 5'-CGGCCACCCGCTCACCGCCCTCG-3') and downstream (reverse primer 5'-GCACGGCGAATGTCAGATAGGG-3') of the 1kb regions of homologous recombination, resulting in a 4.5kb amplicon from the *BCGΔhip1* genome, and a 6kb amplicon from the wild-type BCG genome (Fig. S1C). These amplicons were then sequenced for further confirmation of gene deletion. *BCGΔhip1* was complemented via electroporation with *hip1*, which was cloned with the 300bp region upstream of its start codon for expression from its natural promoter into the integrating, streptomycin resistance-conferring plasmid, pTC.

## **Mice**

All mice were housed under specific pathogen-free conditions in filter-top cages within the vivarium at the Yerkes National Primate Center, Emory University, and provided with sterile water and food ad libitum. C57BL/6J mice were purchased from The Jackson Laboratory (Bar Harbor, ME). OT-II TCR transgenic mice specific for OVA<sub>323-339</sub> peptide were obtained from Dr. Bali Pulendran (originally generated in the laboratory of Dr. F. Carbone, University of Melbourne), and bred at the Yerkes animal facility.

**BMDM and BMDC generation and infection**

Bone marrow-derived macrophages (BMDMs) were generated as previously described (107). Bone marrow cells were isolated from C57BL/6J mice and differentiated for 7 days at 37°C with 5% CO<sub>2</sub> in Dulbecco's modified Eagle's medium (DMEM)/F-12 medium (Lonza, Walkersville, MD) containing 10% fetal bovine serum (FBS; HyClone, Logan, UT), 2mM L-glutamine, and 10% L-cell conditioned medium (LCM). Adherent cells were collected, and macrophages were plated onto 24-well plates at 3x10<sup>5</sup> per well and rested overnight. For heat-killed BCG infections, bacteria suspended in DMEM/F-12 medium containing 10% FBS, 2mM L-glutamine, and 5% LCM were added to differentiated BMDMs in 24 well plates at indicated MOIs. Murine bone marrow derived dendritic cells (BMDCs) were generated as previously described (108). Bone marrow cells isolated from C57BL/6J mice were grown and differentiated for 8 days in Roswell Park Memorial Institute (RPMI) medium (Lonza, Walkersville, MD) supplemented with 10% FBS (HyClone, Logan, UT), 2mM L-glutamine (Gibco, Grand Island, NY), 20ng/ml recombinant murine granulocyte-macrophage colony-stimulating factor (rmGM-CSF) (R&D systems, Minneapolis, MN), 50 µM beta-mercaptoethanol (Gibco, Grand Island, NY), 1X non-essential amino acids (Gibco, Grand Island, NY), 10mM HEPES buffer (Lonza, Walkersville, MD), 1mM sodium pyruvate (Lonza, Walkersville, MD). Non-adherent cells were harvested after 8 days and purified using CD11c microbeads (Miltenyi, Gladbach, Germany), plated at 3x10<sup>5</sup> per well, and rested overnight. For heat-killed BCG infections, bacteria were suspended in DC media without rmGM-CSF and added to differentiated BMDCs in 24 well plates at indicated MOIs and incubated at 37°C. For live infections, BCG strains suspended in DC media without rmGM-CSF,

were added to BMDCs at indicated MOIs and allowed to incubate at 37°C for 4 hours. Monolayers were then treated with 200µg/ml amikacin for 45 minutes. Cells were then washed thrice with PBS, and DC media without rmGM-CSF was then added to infected cells. To determine the CFU of bacteria within infected cells, one set of BMDCs was first washed with PBS then lysed using PBS containing 0.5% TritonX, and serial dilutions of the lysate were plated onto 7H10 plates. To assess BCG growth within BMDCs, cell lysates were plated on days 1, 3 and 5 after initial infection. CFU were enumerated after 21 days of incubation. Supernatants from infected BMDCs or BMDMs were collected at indicated timepoints and analyzed via ELISA for cytokine levels according to the manufacturers' instructions: BD OptEIA kits for IL-6, IL-1β, and IL-12p40 (BD Biosciences, San Jose, CA) and IL-23 (Biolegend, San Diego, CA) per manufacturer's instructions.

### **BMDC-T cell co-cultures**

BMDCs were co-cultured with CD4 T cells 24 hours after infection with BCG strains. Briefly, CD4 T cells were isolated from splenocytes collected from OT-II TCR transgenic mice and purified using CD4 magnetic microbeads (Miltenyi, Gladbach, Germany). Purified CD4 T cells were suspended at  $1 \times 10^6$ /ml in supplemented RPMI and co-cultured with BMDCs to achieve a 1:4 DC:T cell ratio. Supernatants from co-cultures were collected after 72 hours, spun down to remove cells, and frozen. Cytokine levels were analyzed via ELISA according to manufacturers' instructions: IFN-γ (Mabtech, Cincinnati, OH), IL-2 (BD Biosciences, San Jose, CA), and IL-17 (eBioscience, San Diego, CA)

**Intratracheal instillation of BMDCs**

BMDCs were generated as described, purified using CD11c microbeads (Miltenyi), and stimulated as indicated or left unstimulated in media for 24 hours. BMDCs were then washed, resuspended in PBS and intratracheally instilled ( $1 \times 10^6$  per mouse in 50 $\mu$ l PBS) into isoflurane-anesthetized C57BL/6J hosts.

**Assessment of antigen-specific responses**

6 days after intratracheal BMDC transfer, lungs were harvested and processed for further analysis. Briefly, organs were minced and placed in harvest medium consisting of HBSS containing 10mM HEPES, 2% FBS, 0.1% collagenase type IV (Worthington, Lakewood, NJ), and 0.01% DNase I (Worthington, Lakewood, NJ) for 30 minutes at 37°C.

Following incubation, organs were processed into single cell suspension utilizing the gentleMACs tissue dissociator (Miltenyi, Gladbach, Germany). Cells were thoroughly washed, counted, and  $1 \times 10^6$  cells were plated for phenotypic analysis or antigen restimulation. Cells were exposed to media (unstimulated), PMA/ionomycin (80ng/ml and 500ng/ml, respectively), or 10ug/ml whole cell lysate (WCL). Cells were then incubated at 37°C for 1.5 hours before addition of BFA (5ug/ml) and monensin (1:1500) followed by a further incubation at 37°C for 4.5 hours (for media and PMA/ionomycin stimulations) or overnight (for WCL stimulations). Cells were then spun down, washed, and stained with the following fluorophore conjugated antibodies purchased from BD Biosciences, Biolegend, or eBioscience for flow cytometric analysis: anti-CD8 PerCP (clone 53-6.7, BD), anti-CD44 APC-Cy7 (clone IM7, BD), anti-TCR  $\gamma\delta$  BV605 (clone

GL3, Biolegend), anti-CD3e V450 (clone 500A2, BD), anti-CD4 Alexa700 (clone RM4-5, BD), anti-TNF- $\alpha$  PE-Cy7 (clone MP6-XT22, BD), anti-IL-2 FITC (clone JES6-5H4, BD), anti-IL-17 PECF594 (clone TC11-18H10, BD), and anti-IFN- $\gamma$  APC (clone XMG1.2, eBioscience). Live cells were determined by exclusion of amine-reactive dye (Live/Dead Fixable Aqua Dead Cell Stain kit, Life Technologies, Carlsbad, CA). Samples were acquired using an LSRII flow cytometer and analyzed by FlowJo (FlowJo, LLC).

### **Mtb aerosol challenge and enumeration of bacteria**

Groups of mice were intratracheally instilled with  $1 \times 10^6$  BMDCs, rested for 14 days, and then challenged with a low dose ( $\sim 100$  CFU) of Mtb H37Rv using an Intox aerosol apparatus. Lungs from infected mice were harvested 28 days post-challenge, homogenized, plated on 7H10 agar plates, and incubated for 21 days in  $37^\circ\text{C}$  prior to CFU enumeration.

## RESULTS

### **Construction of a BCG $\Delta hip1$ strain**

To determine the role of *hip1* in BCG-induced DC responses, we generated an in-frame, unmarked deletion of *hip1* in the BCG Danish strain. We utilized the suicide vector, pYUB657, which expresses a hygromycin resistance cassette and a counter-selectable marker, to introduce an allelic exchange-based deletion of *hip1* (Fig. S1A). The resulting BCG $\Delta hip1$  strain harbored a complete deletion of *hip1* from its genome, which we verified via PCR amplification of the genomic region as well as through Southern blot analysis (Fig. S1B and S1C). Next, we sought to determine the effect of deleting *hip1* on BCG growth kinetics. We observed no significant differences between BCG, BCG $\Delta hip1$ , and BCG $\Delta hip1$  complemented with *hip1* (BCG $\Delta hip1$  comp) on growth in 7H9 broth (Fig. 1A). Additionally, these strains, grew comparably in bone marrow-derived dendritic cells (BMDCs) over 5 days of culture (Fig. 1B).

### **BCG $\Delta hip1$ elicits robust DC cytokine responses compared to BCG**

DC cytokine production is a canonical signal driving differentiation of naïve CD4 T cells to specific CD4 T-helper (Th) subsets. We therefore sought to compare cytokine responses from DCs infected with BCG or BCG $\Delta hip1$ . We infected BMDCs from C57BL/6J mice with BCG, BCG $\Delta hip1$  or BCG $\Delta hip1$  comp and measured DC cytokine production by ELISA. DCs infected with BCG $\Delta hip1$  produced significantly higher levels of IL-6 and IL-12p40 than DCs infected with BCG. Importantly, cytokine levels induced by BCG $\Delta hip1$  were restored to BCG levels after infection with the complemented strain (Fig. 2A), indicating that BCG limits DC cytokine production through *hip1*. We next

infected DCs with BCG or BCG $\Delta$ *hip1* at multiplicities of infection (MOI) of 10 and 20 and assessed cytokine levels in the supernatant at 24, 48 and 72 hours after infection by ELISA. DCs infected with BCG $\Delta$ *hip1* produced significantly higher levels of IL-6 and IL-12p40 relative to BCG infection at all MOIs and time points tested (Fig. 2B). Notably, incubation of DCs with heat-killed BCG $\Delta$ *hip1* also resulted in significantly higher levels of cytokines compared to heat-killed BCG, indicating that enhanced cytokine production by DCs infected with BCG $\Delta$ *hip1* was not dependent on viability of the bacteria (Fig. 2C). Further, we found that bone marrow-derived macrophages (BMDMs) infected with BCG $\Delta$ *hip1* produced higher levels of IL-6 and IL-1 $\beta$  compared to BCG-infected BMDMs at all MOIs tested (Fig. 2D). These data demonstrate that deletion of *hip1* in BCG results in significantly augmented pro-inflammatory cytokine production from both infected DCs and macrophages.

### **BCG $\Delta$ *hip1* enhances expression of costimulatory molecules on infected DCs**

Following infection, DCs undergo maturation, which is required for optimal antigen presentation and initiation of antigen-specific CD4 T cell responses. DCs present antigens via MHC class II complexes and provide critical costimulatory signals to CD4 T cells through upregulation of molecules such as CD40 and CD86. We determined the expression levels of MHC class II and the costimulatory molecules CD40 and CD86 on DCs infected with BCG or BCG $\Delta$ *hip1* by flow cytometry. DCs infected with BCG $\Delta$ *hip1* expressed higher levels of MHC class II, CD40, and CD86 when compared to BCG-infected DCs (Fig. 3). These data suggest that deletion of *hip1* in BCG enhances DC maturation and expression of costimulatory molecules.

### **Enhanced polarization of IFN- $\gamma$ and IL-17- producing antigen-specific CD4 T cells by DCs infected with BCG $\Delta$ *hip1***

IL-12 is known to drive the polarization of IFN- $\gamma$ -producing Th<sub>1</sub> subsets while IL-6, IL-1 $\beta$ , and IL-23 can drive the polarization and expansion of IL-17-producing Th<sub>17</sub> subsets (109). Since DCs infected with BCG $\Delta$ *hip1* induced higher levels of pro-inflammatory cytokines (Fig. 2) and displayed an enhanced maturation profile (Fig. 3) compared to BCG infection, we hypothesized that BCG $\Delta$ *hip1*-infected DCs would more effectively polarize antigen-specific CD4 T cells towards Th<sub>1</sub> and Th<sub>17</sub> subsets compared to BCG-infected DCs. To test this, we co-cultured DCs infected with BCG or BCG $\Delta$ *hip1* with naïve ovalbumin-specific TCR transgenic CD4 T cells (OT-II) for 3 days in the presence of cognate peptide (OVA<sub>323-339</sub>). Levels of IFN- $\gamma$ , IL-17, and IL-2 were measured via ELISA (Fig. 4A). DCs infected with BCG $\Delta$ *hip1* promoted significantly higher levels of IFN- $\gamma$  and IL-17 from antigen-specific CD4 T cells after co-culture (Fig. 4A). This was consistent with the higher levels of the Th<sub>1</sub>-polarizing cytokine IL-12p40 induced by BCG $\Delta$ *hip1*-infected DCs as well as higher levels of Th<sub>17</sub>-polarizing cytokines IL-6, IL-1 $\beta$ , and IL-23 compared to BCG-infected DCs (Fig. 4B). These data demonstrate that BCG $\Delta$ *hip1*-infected DCs have an enhanced capacity to induce antigen-specific IFN- $\gamma$  and IL-17 responses compared to BCG-infected DCs.

**Intratracheal instillation of DCs infected with BCG $\Delta$ *hip1* enhances lung CD4 T cell responses *in vivo* and improves control of Mtb burden following aerosol challenge.**

Mucosal administration of DCs has been utilized to assess early antigen-specific T cell responses to mycobacteria in the lungs of mice (110), and antigen-loaded DCs have previously been shown to confer protection against Mtb challenge (108, 111-113). Therefore, we used a tractable DC intratracheal instillation model to assess antigen-specific CD4 T cell responses *in vivo* following transfer of BCG or BCG $\Delta$ *hip1*-infected DCs, or control uninfected DCs, into the lungs of mice. After 6 days, we harvested lungs and assessed, by flow cytometry, antigen-specific CD4 T cell responses upon *ex vivo* stimulation of lung cells with Mtb whole cell lysate (WCL). We measured the number of activated CD44<sup>+</sup> CD4 T cells in the lungs following intratracheal instillation of BCG or BCG $\Delta$ *hip1*-infected DCs, which reflects levels of CD4 T cell activation. We found higher numbers of CD44<sup>+</sup> CD4 T cells in the lungs of mice that received DCs infected with BCG $\Delta$ *hip1* compared to mice that received BCG (Fig. 5B), indicating that BCG $\Delta$ *hip1*-infected DCs induced better activation of CD4 T cells *in vivo*. Next, we assessed the functionality of antigen-specific CD4 T cells in the lungs by measuring cytokine responses by intracellular cytokine staining (ICS) and flow cytometry following restimulation with WCL. We found higher numbers of antigen-specific CD4 T cells producing IL-2, IFN- $\gamma$ , TNF- $\alpha$ , and IL-17 in the lungs of mice that received BCG $\Delta$ *hip1* DCs compared to BCG DCs (Fig. 5C). Moreover, the proportion of CD4 T cells producing at least three cytokines expanded in the lungs of animals that received BCG $\Delta$ *hip1* DCs compared to those that received BCG DCs (Fig. 5D). Interestingly, we observed a higher frequency of CD4 T cells producing IFN- $\gamma$ , IL-2, and TNF- $\alpha$  in animals that received BCG $\Delta$ *hip1* DCs compared to BCG DCs (Fig. 5D). Triple cytokine-producing CD4 T cells, conventionally termed polyfunctional CD4 T cells, are thought to

be indicative of a more protective adaptive immune response (114). To investigate whether mucosal administration of DCs exposed to BCG $\Delta$ *hip1* would provide enhanced bacterial control compared to BCG after low dose aerosol Mtb challenge, we intratracheally instilled BCG DCs or BCG $\Delta$ *hip1* DCs, rested mice for 2 weeks prior to aerogenic challenge with low-dose Mtb H37Rv, and determined lung Mtb bacterial burden 4 weeks post-challenge. As shown in Fig. 5E, mice that received BCG $\Delta$ *hip1*-infected DCs harbored significantly less Mtb CFU post-challenge compared to mice that received BCG-infected DCs (Fig. 5E). These results demonstrate that mucosal-targeted approaches using BCG $\Delta$ *hip1* can augment antigen-specific CD4 T cell responses compared to BCG and lead to enhanced control of Mtb burden.

## DISCUSSION

The interplay between mycobacteria and DCs is a critical consideration for rational development of efficacious vaccines for TB. In this study, we demonstrate that deletion of the BCG serine protease, Hip1, promotes robust DC activation and enhances antigen-specific lung CD4 T cell responses. We have shown that BCG $\Delta$ *hip1*-infected DCs produce higher levels of cytokines, express elevated levels of costimulatory molecules, and enhance CD4 T cell responses both *in vitro* and *in vivo* compared to DCs infected with BCG. These data provide insight into the sub-optimal immunogenicity of BCG and demonstrate that deletion of the immune evasion gene, *hip1*, in BCG promotes enhanced DC-T cell crosstalk that leads to better control of Mtb burden.

The underlying reasons for the variable efficacy of BCG as a TB vaccine are unclear. Since DCs are the key cells linking innate and adaptive immunity, the interaction between DCs and BCG is a critical factor in generating anti-mycobacterial T cell responses. Our results are consistent with a growing body of literature suggesting that BCG impairs innate and adaptive immune responses. BCG has been shown to adversely impact antigen-specific CD4 T cell activation through the upregulation of PD-L1 and PD-L2 (115), and diminish activation of antigen-specific CD8 T cells by inducing DC death (116). Furthermore, BCG-infected DCs produce significantly lower levels of IL-23, IL-1 $\beta$ , TNF- $\alpha$ , and IL-12 than Mtb-infected DCs (117), indicating that BCG stimulates weaker innate immune responses than Mtb. Interestingly, a study by Satchidanandam *et al* showed that overexpression of an Mtb glycosylated protein, Rv1860, in BCG impaired

DC maturation, attenuated Th<sub>1</sub> and Th<sub>17</sub> polarization, and led to subsequent loss of protection against Mtb challenge conferred by BCG vaccination (118), suggesting that Mtb proteins that negatively impact DC responses can attenuate the protective effect of BCG vaccination. Conversely, relatively little is known about BCG genes that retain immunomodulatory properties and thus promote impaired DC responses and sub-optimal T cell immunity. Our data showing that BCG Hip1 contributes to impaired DC cytokine production and maturation demonstrates that BCG retains immunomodulatory factors that negatively impact DC and T cell responses, leading to impaired control of Mtb after challenge.

Several avenues have been explored for improving BCG immunogenicity and efficacy, including introduction of immunodominant proteins from Mtb (118-121), and expression of host proteins (122-128). The majority of studies utilizing recombinant or mutant strains of BCG are primarily focused on enhancing macrophage driven responses and functions, such as phagosomal maturation, apoptosis of infected macrophages, and bacterial escape from phagosomal compartments (129-134). For instance, a recombinant strain of BCG lacking urease production and expressing listeriolysin from *Listeria monocytogenes* (BCG $\Delta$ ureC::*hly*) was shown to enhance apoptosis of infected macrophages (131), leading to increased central memory T cell responses (135), enhanced Th<sub>1</sub> and Th<sub>17</sub> immunity (136), and cross-presentation to CD8 T cells (132). Interestingly, deletion of anti-apoptotic gene *nuoG* in BCG $\Delta$ ureC::*hly* showed enhanced efficacy over BCG $\Delta$ ureC::*hly* (137). Notably, we show evidence that BCG $\Delta$ hip1-infected macrophages display enhanced cytokine production relative to BCG-infected

macrophages (Fig. 2). Since we utilized a mucosal transfer approach that exclusively utilized DCs, it will be important to address the role that macrophages may play at priming antigen-specific CD4 and CD8 T cell responses after vaccination with *BCG $\Delta$ hip1*.

Relatively few studies have elaborated on BCG factors that can be targeted to improve DC responses. However, targeting DCs has proven to be a viable approach to improve Mtb-specific CD4 T cell responses after vaccination. H56, a subunit vaccine incorporating Ag85B, ESAT-6, and Rv2660, was shown to provide enhanced protection relative to BCG (138), and utilizes a liposome-based adjuvant (CAF01) that targets DCs (139). Furthermore, improving DC antigen-presentation by induction of autophagy has been shown to improve BCG immunogenicity and improve control of Mtb burden after challenge (140). Our data show that transfer of *BCG $\Delta$ hip1*-DCs leads to enhanced lung CD4 T cell responses compared to transfer of BCG-DCs, including higher frequencies of antigen-specific, polyfunctional CD4 T cells contributing to better control of Mtb burden after challenge (Fig. 5). Thus, our studies suggest that deleting BCG *hip1* alone, or in concert with deleting additional immune evasion genes, is a feasible approach to enhance DC functions for the rational improvement of BCG as a vaccine. A growing number of studies indicate that vaccination through the mucosal route induces robust antigen-specific responses that confer better protection at mucosal surfaces, such as the lung, relative to parenteral routes (108, 111, 112, 141-146). Using an intratracheal DC installation model, we observed that transfer of DCs infected with *BCG $\Delta$ hip1* into mouse lungs more effectively activated CD4 T cells, induced higher numbers of antigen-specific

mucosal CD4 T cells secreting IFN- $\gamma$ , IL-2, TNF- $\alpha$ , and IL-17 *in vivo*, and led to enhanced Mtb control after challenge compared to transfer of BCG-DCs. These studies provide proof of principle data and reveal insights into BCG interactions with DCs, but may not mirror mucosal vaccination using bacteria alone. Bacteria encounter a wider variety of myeloid cells in the lungs, including alveolar macrophages and lung DC subsets, that may differ from BMDCs. Therefore, further studies examining the effects of BCG $\Delta$ *hip1* utilizing more traditional vaccination approaches are of interest.

In summary, our work supports a growing body of evidence that enhancing DC functions will improve BCG-induced immunity. Deletion of *hip1* in BCG augmented DC functions, improved antigen-specific CD4 T cell responses in the lungs, and promoted enhanced control of Mtb burden after challenge. These data indicate that strategies targeting BCG immune evasion genes, such as *hip1*, are a viable avenue for improving innate and adaptive immunity to provide enhanced control of Mtb.

**AUTHORSHIP**

Experimental design and conception: JR EB JKS.

Experimentation: EB, JKS, MQ, AE, MG.

Data analysis: JR, EB, JKS.

Writing: JR, EB, JKS.

Review and editing: JR, EB, JKS, AE.

## ACKNOWLEDGEMENTS

We would like to thank Dr. Miriam Braunstein (University of North Carolina, Chapel Hill), and her current and former lab members, Dr. Jennifer Hayden, Dr. Ellen Perkowski and Kate Zulauf, for providing the pYUB657 plasmid, and for their helpful advice for generating the BCG $\Delta$ *hip1* strain. We would also like to thank past and present members of the Rengarajan lab for helpful discussions.

This study was supported by grants from the National Institute of Allergy and Infectious Diseases, National Institutes of Health grants: 5R01AI083366-05 and 2R56AI083366-06A1 (to JR), a Yerkes National Primate Center base grant: RR000165, an Immunoengineering Seed Grant from the Georgia Research Alliance and Georgia CTSA, the Emory Integrated Genomics Core (EIGC), which is subsidized by the Emory University School of Medicine. EIGC is one of the Emory Integrated Core Facilities, which is in part supported by the National Center for Advancing Translational Sciences of the National Institutes of Health under Award Number UL1TR000454. The funders had no role in the study.

**Figure 1. Deletion of *hip1* from BCG does not affect growth of BCG in broth or in dendritic cells.** (A) BCG Danish, BCG $\Delta$ *hip1*, or complemented BCG $\Delta$ *hip1* (comp) were inoculated into 7H9 liquid medium supplemented with OADC and glycerol at a starting OD<sub>600</sub> of 0.05, were incubated at 37°C shaking, and the absorbance of the cultures at OD<sub>600</sub>, was recorded daily. (B) BMDCs from C57BL/6J mice were infected with BCG, BCG $\Delta$ *hip1*, or comp and grown at 37°C. DCs were collected and lysed at the indicated time points, and bacteria were plated on 7H10 plates for CFU determination. Values are presented as means  $\pm$ SD.

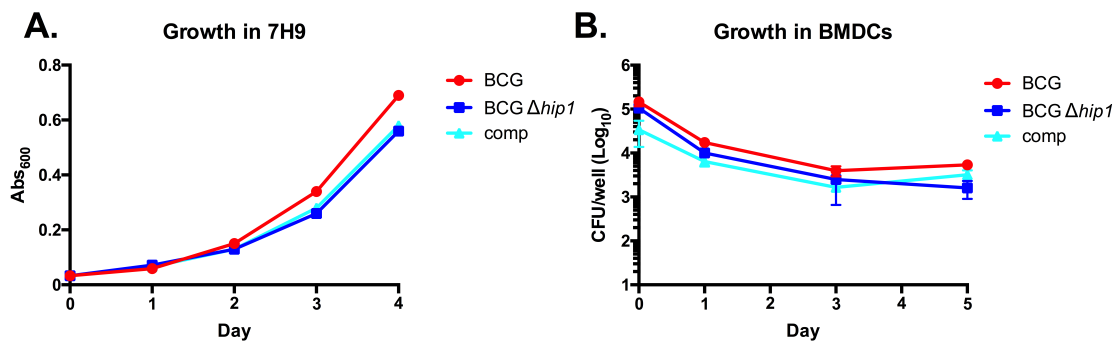


**Figure 2. BCG $\Delta$ *hip1* induces stronger pro-inflammatory cytokine production from innate immune cells.** (A) BMDCs from C57BL/6J mice were infected with BCG, BCG $\Delta$ *hip1*, or BCG $\Delta$ *hip1* complemented with *hip1* (BCG comp) at a multiplicity of infection (MOI) of 10 and incubated at 37°C. After 24 hours, the culture supernatants were assessed for levels of IL-6 and IL-12p40 via ELISA. (B) BMDCs were infected with varying MOIs (10 and 20) of BCG or BCG $\Delta$ *hip1*, and culture supernatants were assayed for IL-6 and IL-12p40 at 24, 48, and 72 hours post-infection. Heat-killed BCG or BCG $\Delta$ *hip1* were exposed to BMDCs (C) or BMDMs (D) at MOIs of 5, 10, and 20 for 24 hours at 37°C. Culture supernatants were tested for IL-6 and IL-12p40 (C) or IL-6 and IL-1 $\beta$  (D) via ELISA. Statistical significance was determined by unpaired two-tailed student's t-test. Values are presented as mean  $\pm$ SD. \* $p$ <0.05, \*\* $p$ <0.01, \*\*\* $p$ <0.001 \*\*\*\* $p$ <0.0001, ns= no significance, ui= uninfected

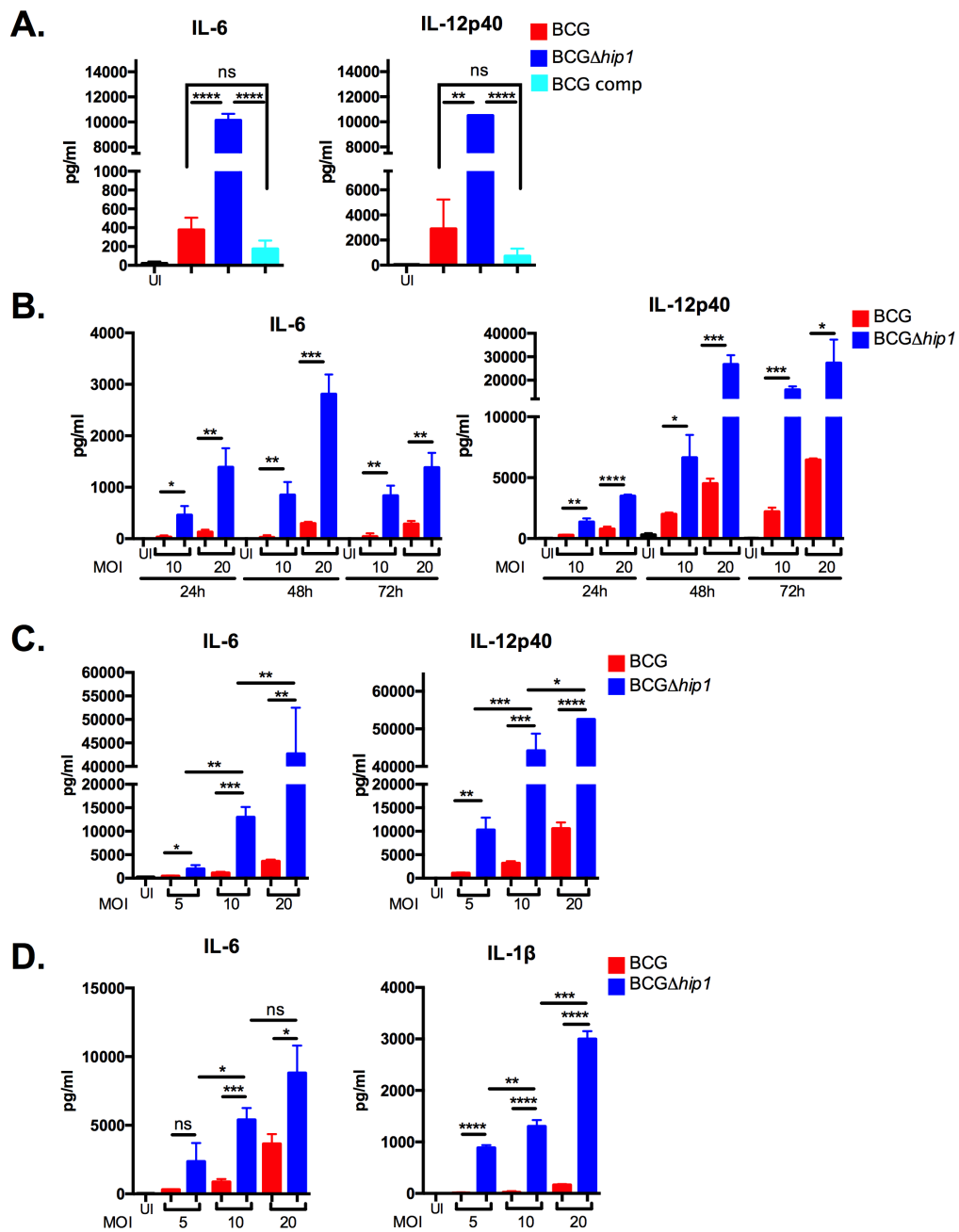


**Figure 3. BCG $\Delta$ hip1 enhances expression of costimulatory molecules on infected DCs.**

BMDCs from C57BL/6J mice were either uninfected, infected with BCG or BCG $\Delta$ hip1 (MOI 10), or stimulated with LPS (1  $\mu$ g/ml) for 24 hours. BMDCs were then stained for maturation markers CD86 (top), CD40 (middle), and MHC class II (bottom). Representative histograms (left) and summary graphs (right) of median fluorescence intensities of each marker is shown. Cells were pre-gated on live, CD11c<sup>+</sup>CD11b<sup>+</sup> singlets. Statistical significance was determined by unpaired two-tailed student's t-test. Values are presented as mean  $\pm$ SD. \*p<0.05, \*\*p<0.01, \*\*\*\*p<0.0001, ns= no significance.

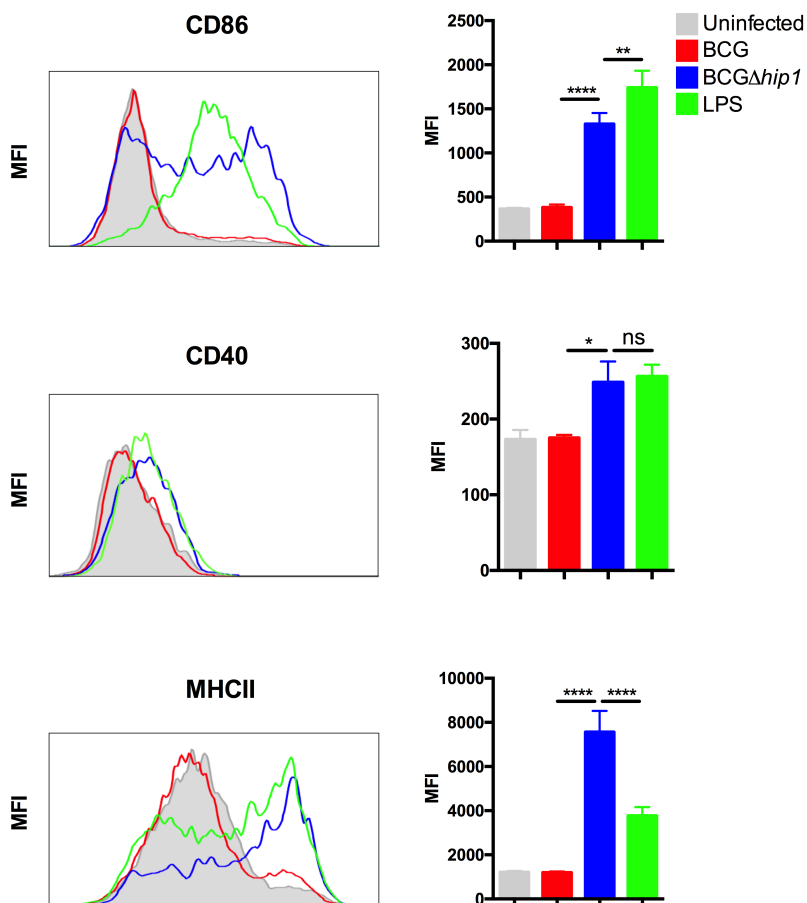


**Figure 4. DCs infected with *BCG $\Delta$ hip1* induce higher levels of IFN- $\gamma$  and IL-17 production from CD4 T cells compared to BCG.** BMDCs from C57BL/6J mice were pulsed with OVA<sub>323-339</sub> peptide, and 6hrs later, infected with BCG or *BCG $\Delta$ hip1*. After 24 hours, culture supernatants were removed and purified OT-II CD4 T cells were added to the adherent BMDC monolayer at a 4:1 T cell to DC ratio. 3 days after addition of CD4 T cells, culture supernatants were collected and IL-2, IFN- $\gamma$ , and IL-17 levels were assessed via ELISA (A). Levels of IL-6, IL-1 $\beta$ , IL-12p40, and IL-23 from culture supernatants containing solely BMDCs were assessed via ELISA (B). Statistical significance was determined by unpaired two-tailed student's t-test. Values are presented as mean  $\pm$ SD. \* $p$ <0.05, \*\* $p$ <0.01, ns= no significance.

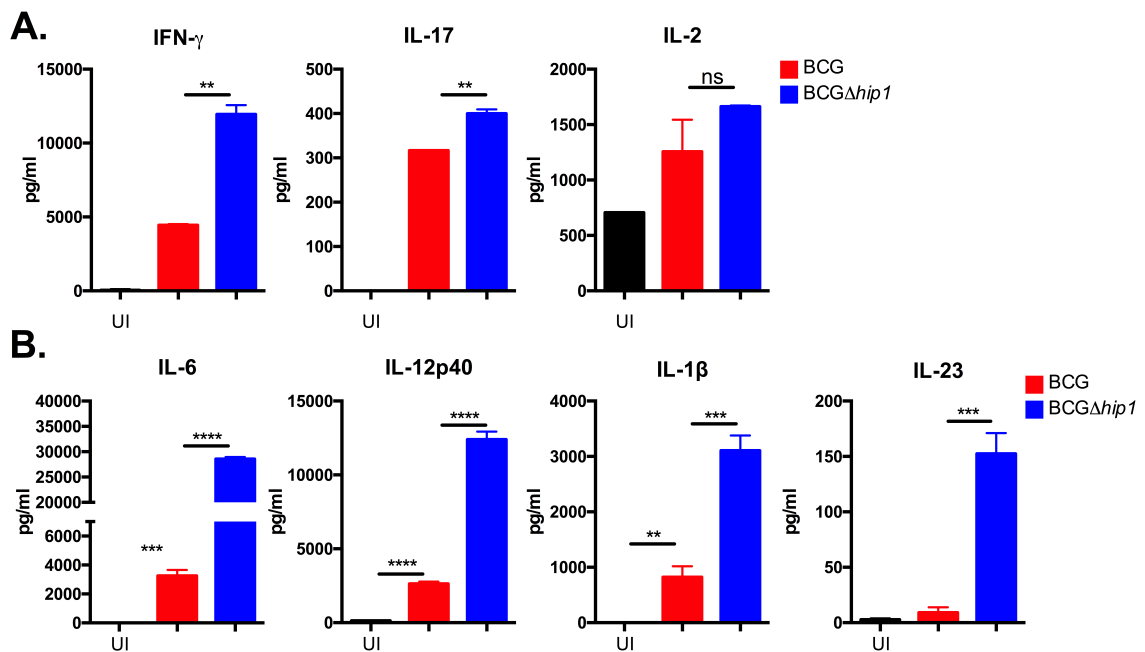


**Figure 5. Intratracheal instillation of DCs infected with BCG $\Delta$ *hip1* enhances mucosal CD4 T cell responses and improves control of Mtb burden after aerosol challenge.** (A) Diagram of experimental design. BMDCs were exposed to BCG or BCG $\Delta$ *hip1* or were left uninfected for 24 hours prior to being intratracheally instilled ( $1 \times 10^6$  per mouse). Mice that did not receive any DCs were used as no transfer (NT) controls. Lung immune responses were assessed 1-week post-intratracheal instillation. Remaining animals were challenged 2 weeks post-intratracheal instillation with low dose aerosolized Mtb (H37Rv) and lung bacterial burden was assessed 4 weeks post-challenge. (B) Representative plots of the frequencies (left) and summary graph of the absolute counts (right) of CD4<sup>+</sup>CD44<sup>+</sup> cells in the lungs 1-week post-intratracheal instillation. (C) Lung IFN- $\gamma$ <sup>+</sup> CD4<sup>+</sup> cells (top) and IL-2<sup>+</sup>, TNF- $\alpha$ <sup>+</sup>, IL-17<sup>+</sup> CD4<sup>+</sup> cells (bottom) responding to whole cell lysate restimulation 1 week post-intratracheal instillation. (D) Pie chart depicting lung CD4<sup>+</sup> cells secreting 1 (red), 2 (green), 3 (blue), or 4 (yellow) cytokines after whole cell lysate restimulation 1 week post-intratracheal instillation (left). Summary graph of the frequency of lung polyfunctional (IFN- $\gamma$ +IL-2<sup>+</sup>TNF- $\alpha$ <sup>+</sup>) CD4<sup>+</sup> cells responding to whole cell lysate restimulation 1 week post-intratracheal instillation (right). Cells were pre-gated on live, CD3<sup>+</sup>CD8<sup>-</sup>TCR  $\gamma\delta$ <sup>-</sup> singlets. (E) Lung bacterial burden at 4 weeks post-challenge from animals that received uninfected BMDCs or BMDCs stimulated with BCG or BCG $\Delta$ *hip1*. Statistical significance was determined by unpaired two-tailed student's t-test. Values are presented as mean  $\pm$ SD. \* $p < 0.05$ , \*\* $p < 0.01$ , \*\*\* $p < 0.001$ , ns= no significance.

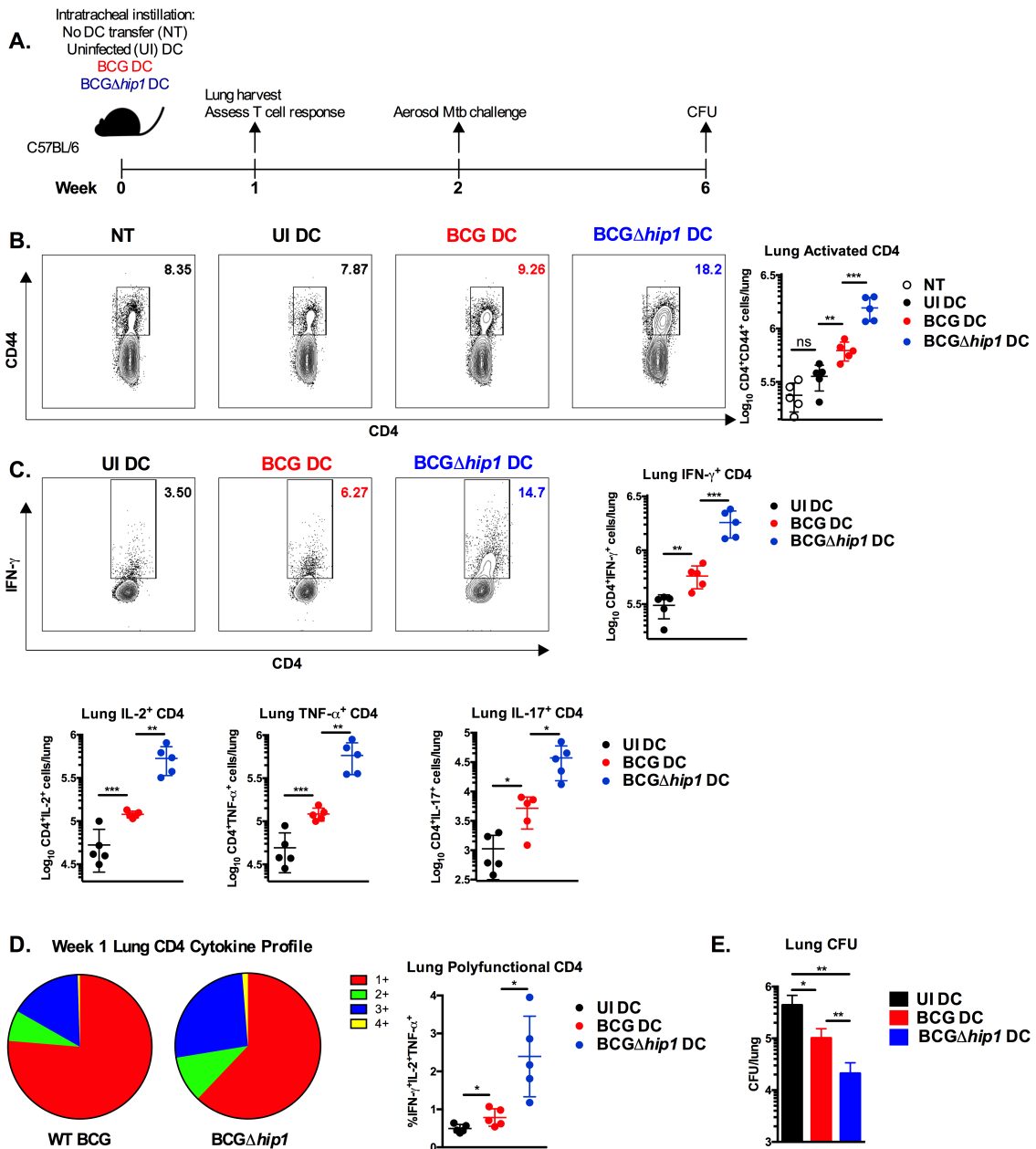
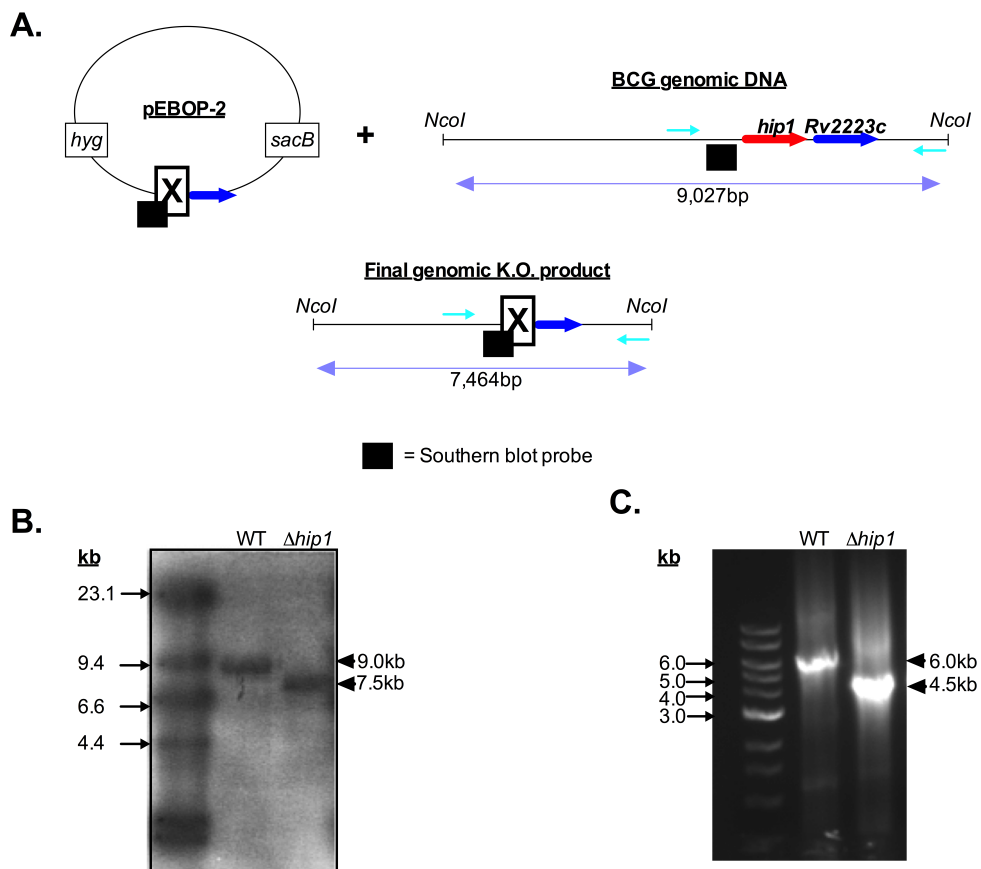


**Figure S1. Southern blot and PCR analysis of BCG $\Delta$ *hip1*.** (A) pEBOP-2 suicide vector schematic, chromosomal locus for *hip1*, and schematic of  $\Delta$ *hip1* allele. *NcoI* restriction endonuclease sites are denoted. The Southern probe used is represented by a black box, while cyan arrows indicate PCR amplification primers. (B) Southern blot of *NcoI* digested genomic DNA purified from WT BCG or BCG $\Delta$ *hip1* probed with digoxigenin (DIG)-labeled amplicon of the 1kb region upstream of *hip1*. Black arrows denote molecular weight marker values, while black arrowheads indicate DNA detected by probe. (C) PCR amplification of the genomic region surrounding *hip1* using primers 1.6kb upstream and 2.8kb downstream of *hip1*. Black arrows denote molecular weight marker values, while black arrowheads indicate amplified DNA. The contrast and brightness of the Southern blot and DNA gel were adjusted for clarity.



### Chapter 3

#### **Molecular characterization of the secreted *Mycobacterium tuberculosis* protease, Rv2223c**

Note: Chapter 3 is adapted from a manuscript currently under preparation with the following authorship:

**Erica Bizzell**, Maria Georgieva, Vaibhav Vindal, Jaqueline Naffin-Olivos, Gregory Petsko, Dagmar Ringe, and Jyothi Rengarajan

**ABSTRACT**

*Mycobacterium tuberculosis* (*Mtb*) has evolved multiple strategies to evade host immune defenses and replicate within immune cells. These include alteration of its complex cell wall during intracellular growth, and secretion of effectors that modulate immune responses and enhance pathogen survival. Several pathogenic bacteria use extracellularly secreted proteases to regulate processes ranging from repression of cytokine production to degradation of surface-associated host proteins. While *Mtb* encodes several putative secreted proteases, their functions are poorly understood. One such protease, Rv2223c, is transcribed from a predicted operon with a cell wall-associated serine protease, Hip1 (Rv2224c) with which it shares 47% amino acid identity. Here, we show that *Rv2223c* and *hip1* are highly conserved in close genomic proximity across pathogenic and non-pathogenic mycobacterial strains. We have observed that unlike Hip1, Rv2223c is secreted from mycobacterial cells and undergoes further autoproteolytic cleavage upon secretion. We have previously reported that Hip1 contributes to dampening of immune responses during *Mtb* infection, partly through its cleavage of the *Mtb* GroEL2 protein. Here, we have found that Rv2223c interacts with GroEL2, but is unable to complement the *hip1* mutant *Mtb* GroEL2 cleavage defect. We provide insights into the molecular functions of Rv2223c and support to the hypothesis that Rv2223c and Hip1 likely cooperatively play a crucial role in mycobacterial survival.

## INTRODUCTION

With over 10 million new cases reported in 2015 alone, tuberculosis (TB) continues to plague the human population despite its emergence over 8,000 years ago. The apparent success of the causative agent TB, *Mycobacterium tuberculosis* (Mtb), can be attributed in part to its employment of a multitude of strategies that modulate host responses. These evasion tactics include, but are not limited to, modification of the complex Mtb cell wall and secretion of effector proteins and/or cell wall components, which act directly on host cells to modulate immune responses and enhance pathogen survival. The current treatment for TB involves a 6-month daily multi-drug regimen, to which non-adherence is a continued issue. Thus there is a pressing need for new anti-tubercular drugs and therapies that shorten treatment, and vaccines that protect against TB. To identify new drug targets and vaccine candidates for TB, we need a better understanding of Mtb genes involved in pathogenesis and their underlying molecular and biochemical mechanisms. Several genome-wide mutagenesis screens, including our own, have highlighted many Mtb gene products that are critical for Mtb virulence, but the precise molecular functions of most of these factors remain poorly defined.

Many pathogenic bacteria species utilize proteases to regulate a diverse range of host processes. Pathogenic bacterial proteases exported to the cell wall or secreted extracellularly are optimally localized for direct interactions with host cells, and have been shown to assist in bacterial evasion of host responses through methods such as suppression of cytokine production (147), degradation of surface-associated host

receptors (148), and cleavage of molecules of the host complement pathway (149). Notably, protease inhibitors have been successful in treating a number of infectious diseases, while multiple studies have revealed promising effects of targeting Mtb virulence-associated proteases (150-153). Over 100 predicted proteases are encoded in the Mtb genome, of which very few have been extensively studied. The Mtb gene, *Rv2223c*, encodes for a predicted extracellularly secreted serine protease. *Rv2223c* lies directly downstream of the gene for the Mtb immune evasion serine protease, Hip1 (hydrolase important for pathogenesis)/ *Rv2224c*. Recent work solving the 3D crystal structure of Hip1 has shown the enzyme to belong to a novel family of proteases, of which *Rv2223c* also appears to belong.

Hip1 is an Mtb cell wall-associated serine protease, which we have previously shown to play an important role in Mtb modulation and evasion of host innate and adaptive immune responses. Several studies have revealed that Hip1 is involved in blunting early innate immune responses such as cytokine production from infected macrophages and dendritic cells (DCs), leading to suboptimal T cell immunity and attenuated Mtb virulence. Further, we have previously shown that the effects of Hip1 on Mtb immunogenicity are due in part to Hip1-mediated proteolytic cleavage of Mtb GroEL2. The close genomic proximity of *Rv2223c* and *Rv2224c* (*hip1*) suggest that the two proteins may work in conjunction with one another. However, the prediction that *Rv2223c* may be secreted from bacterial cells suggests that the protein may have independent and unique functions apart from those of Hip1.

The aim of this study was to define the molecular characteristics of Rv2223c and to explore the relationship between Rv2223c and Hip1. Here we show that Rv2223c and Hip1 are both highly conserved across a wide range of mycobacterial species with little to no variability across pathogenic species. We also show that while Rv2223c shares many similarities with Hip1, it is secreted extracellularly, displays unique autoproteolytic characteristics, and appears to have a separate, yet unknown function from Hip1 in Mtb pathogenesis.

## RESULTS

### **Mtb Rv2223c is closely related to the cell wall-associated protease, Hip1(Rv2224c).**

In order to gain insight into the structural features of the previously uncharacterized Mtb protein, Rv2223c, we first utilized a bioinformatics approach. Running the Rv2223c amino acid sequence through BLASTp revealed that the protein, which is classified as a member of the novel CaeA (Hip1) alpha-beta hydrolase family, is comprised of two alpha-beta hydrolase domains, one of which corresponded to a tripeptidyl aminopeptidase (TAP) like family of bacterial peptidases, and an N-terminal region likely corresponding to a signal peptide (Fig1A). *Rv2223c* is transcribed directly downstream of *Rv2224c* (*hip1*), the gene for the Mtb serine protease, Hip1, which has previously been shown to display serine protease activity (74, 76). Using the EMBOSS Needle pairwise sequence alignment tool, we found that Rv2223c and Hip1 share 47% amino acid sequence identity and 60% similarity (Fig 1B). Importantly, the residues comprising the known catalytic active site for Hip1 are conserved in Rv2223c, forming the catalytic triad S<sub>232</sub>, D<sub>461</sub>, and H<sub>488</sub> (Fig. 1C). As the Hip1 crystal structure was recently solved (103), using the SWISS-MODEL online software, we were able to develop a predicted 3D model of the Rv2223c tertiary structure based on the known Hip1 structure (Fig 1C). Highlighted in red are the predicted catalytic active site residues within this model.

### ***Rv2223c* and *hip1* are highly conserved across mycobacterial species**

We next analyzed 59 mycobacterial species, including 20 Mtb strains, and found that both genes are conserved across both non-pathogenic and pathogenic species, including

within the highly niche-adapted *M. leprae* genome. Phylogenetic analysis revealed very little sequence divergence among pathogenic mycobacterial strains for both Rv2223c and Hip1 as indicated by the tree branch lengths (Fig 2). Conservation of both genes across such a wide range of species suggests that Rv2223c and Hip1 may be involved in functions essential for survival of all mycobacteria. Short (<100bp) intergenic regions within a bacterial genome can be an indicator of co-transcription of two given genes, which often suggests protein involvement in similar cellular processes. We therefore investigated the conservation of the intergenic region length between *Rv2223c* and *hip1*. We found that a mean intergenic length of 62bp was conserved throughout all pathogenic mycobacterial genomes assessed (Table 3, Fig. S1). We observed much more variability within the *Rv2223c-hip1* intergenic regions of non-pathogenic mycobacteria, with a mean intergenic length of 103.5bp (Fig. S1). These findings further suggest that Hip1 and Rv2223c may work in conjunction with one another.

### **Rv2223c is secreted from mycobacterial cells in a secretion signal sequence-dependent manner**

Rv2223c is annotated as a probable exported protease of Mtb. In order to determine whether Rv2223c is secreted from mycobacterial cells we expressed Rv2223c containing a C-terminal FLAG epitope tag, in *Mycobacterium smegmatis* (Msm). Anti-FLAG Western blotting showed that Rv2223c was found in both the cellular lysates/pellet protein fraction and the secreted supernatant protein fraction of Msm (Fig 3A). Using the Sig-PRED online signal sequence predictive software, we determined the predicted secretion signal sequence to be comprised of the first 34 amino acids of Rv2223c (Fig

3A). To test this prediction we next expressed C-terminally FLAG-tagged Mtb Rv2223c lacking its first 34 amino acids ( $\Delta$ 1-34 Rv2223c) in Msm and Mtb. We found that  $\Delta$ 1-34 Rv2223c was detected in the pellet protein fraction of but not in the supernatants of both Msm and Mtb (Fig 3A and 3B), indicating that Rv2223c secretion from mycobacterial cells is dependent on its 34 amino acid signal peptide sequence. Further, this secretion appears to be neither SecA2 nor twin arginine transport (TAT) dependent, as we observed secretion of Rv2223c expressed in Msm strains deficient in these pathways (data not shown).

**Rv2223c undergoes cleavage that is dependent on its serine residue S<sub>232</sub>, between residues G<sub>41</sub> and Q<sub>42</sub>.**

We observed two forms of Rv2223c present in the pellet protein fractions of Msm prior to secretion from bacterial cells and upon secretion into the bacterial culture supernatants, we detected further cleavage of Rv2223c to an even shorter form (Fig. 4A). Based on these observations, we hypothesized that Rv2223c is expressed as a pro-enzyme, requiring further processing to reach its final mature form. The three forms of Rv2223c that we observe in the pellet and supernatant fractions of *Msm* are thus predicted to represent (1) the pre-proenzyme, consisting of the full Rv2223c protein construct, (2) the proenzyme, which is made up of Rv2223c lacking its signal sequence and is present in both the pellet and the supernatant, and (3) the fully processed mature enzyme, which is the shortest form of the protein (Fig. 4A). Several well-studied bacterial proenzymes, undergo the process of self-cleavage, or autoproteolysis, to transition from their proenzyme state to their mature active state (154-156). We therefore sought to determine

whether Rv2223c autoproteolytically cleaves itself from its proenzyme state to its final mature form. In order to test this, we mutated the serine residue S<sub>232</sub> within the catalytic triad of the predicted active site within Rv2223c, to an alanine residue, and expressed this FLAG-tagged construct in both Msm and Mtb. This mutated Rv2223c S<sub>232</sub>A protein did not undergo the final cleavage to the predicted mature form upon secretion (Fig. 4A). The observation that Rv2223c cleavage in mycobacterial supernatants is dependent on S<sub>232</sub> is consistent with the possibility that processing of Rv2223c to its mature form is a result of autoproteolysis. We next sought to determine where the final cleavage of the Rv2223c proenzyme to the mature enzyme occurs. Based on the sizes of the cleaved forms of the proenzyme and mature form of Rv2223c (~70 and 65kDa respectively), we hypothesized that the cleavage site would lie within the amino acid residues 39-43 of Rv2223c (Fig 4B). We used site-directed mutagenesis to map the cleavage site by first mutating two consecutive residues at a time to prolines, then assessing the processing of Rv2223c in mycobacterial supernatants. This allowed us to hone in on the site of cleavage, as the Rv2223c G<sub>41</sub>P-Q<sub>42</sub>P mutant was unable to be cleaved to its final mature form (Fig 4C). We then assessed the introduction of single mutations into the Rv2223c residues A<sub>40</sub>, G<sub>41</sub>, and Q<sub>42</sub> to prolines, and found that we were unable to detect cleavage of the Rv2223c proenzyme in supernatants of both the G<sub>41</sub>P and the Q<sub>42</sub>P mutant expressing strains (Fig 4D). These data suggest that the site at which the apparent Rv2223c autoproteolysis occurs is between residues G<sub>41</sub> and Q<sub>42</sub>.

**Rv2223c interacts with Hip1 substrate, GroEL2, but is unable to complement cleavage in the *hip1* Mtb mutant**

Due to the similarities between the Mtb cell wall-associated protein, Hip1 and Rv2223c, we hypothesized that the two proteins may share common substrates. Publications from our laboratory have shown that the Mtb chaperonin-like protein, GroEL2, is a physiological substrate of Hip1, and a *hip1* mutant strain displays aberrant cleavage of GroEL2 (74, 76). As a first step towards determining whether Rv2223c is able to cleave GroEL2, we investigated the interaction between the two proteins. Using a FLAG tag-based co-immunoprecipitation approach, we looked for the interaction of either FLAG-tagged wild type Rv2223c or the catalytically inactive S<sub>232</sub>A Rv2223c mutant with endogenous GroEL2 protein. We observed that GroEL2 co-immunoprecipitated with both Rv2223c and S<sub>232</sub>A Rv2223c (Fig 5A). We hypothesize that the apparent stronger interaction observed between S<sub>232</sub>A Rv2223c and GroEL2 may be due to the inability of the catalytically inactive enzyme to release its potential substrate, GroEL2. Given the interaction of Rv2223c with GroEL2, we next chose ascertain whether Rv2223c was capable of complementing the defective GroEL2 cleavage seen in the *hip1* mutant Mtb. While GroEL2 cleavage was partially restored via complementation of the *hip1* mutant strain with Hip1, both from its natural promoter and from the constitutive GroEL2 promoter, we were unable to detect any GroEL2 cleavage in the supernatants when Rv2223c was expressed within the *hip1* mutant (Fig. 5B). In contrast, expression of both Rv2223c and Hip1 appeared to restore GroEL2 cleavage. These results, together with the interaction studies suggest that while Rv2223c may work in conjunction with Hip1 to cleave GroEL2 and potentially other substrates.

## Discussion

In this study we provide insight into the previously uncharacterized predicted protease, Rv2223c, which is closely related to the virulence associated Mtb protease, Hip1. Here, we show evolutionary evidence that Hip1 and Rv2223c likely serve a critical role in mycobacterial survival as they are conserved across a wide range of mycobacterial species. Our study also reveals that Rv2223c is secreted extracellularly and displays autoproteolytic activity upon secretion from mycobacterial cells. Moreover, Rv2223c and is able to interact with the Hip1 substrate, GroEL2. While Rv2223c is unable to complement the GroEL2 cleavage defect of and Mtb *hip1* mutant, we hypothesize that the two proteins may work in conjunction with one another in processes essential for mycobacterial pathogenesis.

While over 100 predicted proteases are annotated in the Mtb genome (23), the majority of them have yet to be studied. Our study is focused on the Mtb protease, Rv2223c and the closely related, serine protease, Hip1. These proteases are of particular interest, as the genes for both proteins are conserved within the genome of both pathogenic and non-pathogenic mycobacterial species. Conservation of mycobacterial genes in the highly niche-adapted *M. leprae* strain, which contains ~1,600 coding genes compared to ~3,900 in Mtb (23, 157), is thought to be a predictor of the core essential genes for mycobacterial pathogenesis. Interestingly, both *hip1* and *Rv2223c* are conserved in the *M. leprae* genome (158). In this study, we have shown that these genes are not only conserved in slow-growing pathogenic mycobacteria, but in non-pathogenic strains such as the fast-

growing Msm as well (Fig. 2). Hip1 and Rv2223c are both individually predicted to be non-essential for *in vitro* growth of Mtb (159-161), while Hip1 has been shown to play an essential role in Mtb survival in macrophages and mice (107, 162, 163). However, the broad mycobacterial conservation of both Hip1 and Rv2223c (Fig 2), along with their high similarity (Fig 1B), suggests that they may both be involved in essential cellular functions and may work in conjunction with one another. Further supporting this hypothesis is our observation that Mtb appears to be resistant to deletion of the *Rv2223c-hip1* genomic region. Attempts to delete both *Rv2223c* and *hip1* together from Mtb via suicide vector allelic exchange resulted in compensatory mutations resulting in non-specific recombination of the genes in another genetic locus in all strains harboring a confirmed knockout (data not shown), suggesting that deletion of both proteases is detrimental to Mtb survival.

Microbial proteases have served as successful targets for a number of infectious diseases. Recently, more efforts have been taken to investigate potential protease inhibitors to combat TB (99, 100, 151). One of the most promising targets for protease inhibitors is the ClpP protease complex, against which studies of several inhibitors have recently been directed (100, 101, 164, 165). The Mtb ClpP protease complex, consists of two ClpP protease subunits, ClpP1 and ClpP2, neither of which display much activity alone, partnered with an ATPase to function (164). Interestingly, we have reported that Rv2223c interacts with GroEL2, which we have previously shown to be a Hip1 substrate, but that it is unable to complement the *hip1* mutant GroEL2 cleavage defect. This observation leads us to hypothesize that Hip1 and Rv2223c may form a complex with

GroEL2. GroEL2 is a chaperonin-like protein of Mtb, which is essential for Mtb growth *in vitro*, however studies of GroEL2 to date have not demonstrated its chaperone activity (166). Although it has not yet been determined whether GroEL2 displays chaperone activity, we cannot rule out the possibility that if it does indeed function as a chaperone, its binding to Rv2223c to may be a result of this potential activity. However, due to previous findings showing that complementation *hip1* and *Rv2223c* together are better able to complement the *hip1* mutant Mtb GroEL2 cleavage than *hip1* complementation alone (74), we hypothesize that Hip1 and Rv2223c may form a complex that allows for optimal cleavage of their substrates (Fig 5C). Further studies into this hypothesis are of great interest.

Both Rv2223c and Hip1 share similar catalytic active sites consisting of Ser-Asp-His catalytic triad (Fig 1). We have shown that Rv2223c undergoes autoproteolytic cleavage that is dependent on the S<sub>232</sub> residue within its catalytic triad (Fig 4A). Proteases from a number of bacterial pathogenesis have been shown to undergo autoproteolysis. Within Mtb, the well-studied serine protease, MycP1 is expressed as pro-enzyme, requiring further autoproteolysis before activation of its mature enzyme (98, 167, 168). While the Hip1-based crystal structure model of Rv2223c provides some insight into the potential activity of the enzyme (Fig 1C), further studies are currently underway to purify Rv2223c in order to determine its proteolytic activity and actual crystal structure.

Both Rv2223c and Hip1 contain protease domains similar to TAP proteins originally isolated from *Streptomyces lividans* (102, 169-171), which are the closest relatives to

these Mtb proteases. Additionally, the recently solved crystal structure of Hip1 revealed that the protease belongs to a novel family, defined in part by the larger active site allowing for its likely additional function as an endopeptidase (103). Through BlastP analysis of the Rv2223c amino acid sequence, we found that the protein belongs to the same novel family as Hip1. Given their unique classification and their high conservation Hip1 and Rv2223c may provide a completely pathogen-specific drug target, which the homology of some of the current potential protease targets to host proteins does not allow for.

A recent study of the periplasmically localized protease, MarP, which is necessary for Mtb establishment of infection as well as resistance to acid and oxidative stresses (172, 173), showed selective inhibition of MarP to be capable of killing Mtb under acidic conditions (99). We have previously shown that Hip1 is associated with the cell wall and cell membrane fractions of Mtb (74), and we have now shown that Rv2223c is secreted from mycobacterial cells (Fig. 3), making both proteases uniquely situated at the host-pathogen interface. In view of their localization and the potentially vital roles that both proteases may play in mycobacterial survival, Hip1 and Rv2223c would make excellent candidates for future drug targeting studies.

## Materials and Methods

### *In silico* analysis tools

The amino acid sequence of Rv2223c and Hip1 were obtained from the NCBI protein database. Rv2223c and Hip1 amino acid sequences were aligned and percent identity and similarity was determined via EMBOSS Needle pairwise alignment tool. Functional domain predictions were determined using NCBI BLASTP. The amino acid signal sequence was predicted using both SignalP and the Sig-Pred online signal sequence prediction tools. The complete genome sequences of mycobacterial species analyzed were downloaded from NCBI FTP genomes server (<ftp://ftp.ncbi.nlm.nih.gov/>).

Reciprocal Best BLAST Hit (RBBH) method was used to predict orthologous proteins in mycobacterial proteomes. Pairs of proteins, from two mycobacterium species, covering at least 50% sequence length of both the proteins in alignment and E-values lower than  $10^{-10}$  for both directions using BLASTP program, with all other parameters at default values, were selected as RBBHs (174-176). The stretch of DNA sequence located between genes was extracted as the intergenic sequence corresponding to the downstream gene. In the case of overlapping genes, an intergenic region with negative value was reported. ClustalW sequence alignments between orthologs and maximum parsimony phylogenetic trees were generated using Mega7 software. In order to generate the model crystal structure of Rv2223c, the amino acid sequences of Rv2223c and Hip1 were aligned via Clustal Omega, and this result was then entered into the SWISS-MODEL software (<https://swissmodel.expasy.org/>).

### **Bacterial strains and culture conditions**

*Mycobacterium tuberculosis* (H37Rv), *hip1* mutant, *hip1* mutant complemented (with *hip1*, *Rv2223c*, or *hip1+Rv2223c*), were grown at 37°C in Middlebrook 7H9 (Difco) broth supplemented with 10% oleic acid-albumin-dextrose-catalase (OADC), 0.2% glycerol and 0.05% Tween 80 or on Middlebrook 7H10 agar supplemented with 10% OADC, 0.5% glycerol, and 0.2% Tween 80. *Mycobacterium smegmatis* (mc<sup>2</sup>155) was grown under the same conditions in broth or on agar supplemented with 10% albumin-dextrose-catalase (ADC) instead of OADC. Media for the *hip1* mutant strain contained 20µg/ml of kanamycin. Media for complemented  $\Delta hip1 \Delta Rv2223c$  Mtb was supplemented with 50µg/ml of hygromycin or 20µg/ml of kanamycin.

### **Cloning of constructs and site-directed mutagenesis**

WT Mtb *Rv2223c* was amplified from H37Rv genomic DNA using forward primer, JR376 – 5'-GCAAGATCTCGGTGAGACGATGGCGGCC-3' and reverse primer, JR338 – 5'-GTAGTCCCATATGGAGCCGCCGGGCGCGCACCGCAGAC-3'.  $\Delta 1-34$  *Rv2223c* was amplified using forward primer, JR377 – 5'-GCAAGATCTCGGTGAGACGATGACTGAAGAACCCGGCG-3' and reverse primer, JR338. Both amplicons were digested with *BglIII* and *NdeI*, and ligated into *BamHI* and *NdeI*-digested plasmid, pEB03 (pMV762 containing a C-terminal FLAG tag with an upstream linker containing an *NdeI* restriction site) in order to make the plasmids pEB08 (WT *Rv2223c*) and pEB12 ( $\Delta 1-34$  *Rv2223c*). Site-directed mutagenesis was performed on WT *Rv2223c* according to the MEGAWHOP site-directed mutagenesis technique (177). An alanine mutation was introduced into the S<sub>232</sub> amino acid residue of WT

*Rv2223c* within pEB08 using forward primer, JR501 – 5'-CAATCCACCGCTGTACTAGTGCAATTGGGGAGC-3', which introduced a *SpeI* cleavage site into the plasmid for later confirmation and reverse primer, JR390 – 5'-TGCCCAACTCGGTGCCGTAGGCGTATCCGAGGTAGTTG-3', which contained the S<sub>232</sub>A mutation. This amplicon was then used as a “megaprimer” to amplify the full pEB08 plasmid, and to introduce both mutations, resulting in the plasmid pEB26. A<sub>40</sub>P, G<sub>41</sub>P, and Q<sub>42</sub>P point mutations were introduced into pEB08 using the following reverse primers in conjunction with forward primer, JR501 respectively, JR502 – 5'CCCGGGGTTTGGCCGGGGCCGGGTTCTTCAG-3', JR503 – 5'CCCGGGGTTTGGGGGGCGCCGGGTTCTTCAG-3', and JR504 – 5'-CGCACCCGGGGTTGGGCGGCGCCGGGTT-3', resulting in plasmids pEB39, pEB40, and pEB41.

### **Preparation of mycobacterial supernatant and pellet protein fractions**

For pellet and supernatant fractions of *M. tuberculosis* or *M. smegmatis*, 50ml bacterial cultures were grown to an OD<sub>600</sub> of 0.4-0.5, then centrifuged at 4000xg for 10 minutes. Pellets were washed twice, resuspended in 100ml Sauton's medium supplemented with 0.05% Tween 20 along with appropriate antibiotic, and grown to OD<sub>600</sub> 0.4-0.6. Cultures were then centrifuged, washed twice, and resuspended in 50ml Sauton's medium and allowed to grow for 3 hours (*M. smegmatis*) or overnight (Mtb). Cultures were centrifuged and the supernatants were concentrated using Centricon Plus-70 centrifugal units (Millipore), and Mtb were filtered with 0.22µm Steriflip filtration device (Millipore) prior to concentration. Pellets were resuspended in lysis buffer (25mM Tris, 50mM

NaCl, with or without 34mM BME, and Roche protease inhibition cocktail), transferred to lysing matrix B bead-beating tubes (MP Biomedicals) and subjected to bead beating (3X one minute each with five-minute rests on ice). They were then centrifuged at 12,000xg for 20 minutes and supernatants were saved for later analysis via Western blot.

### **Co-Immunoprecipitation**

To obtain protein extracts from *M. smegmatis* or *M. tuberculosis*, cultures were grown to an OD<sub>600</sub> of 0.4-0.6. Bacterial cultures were then pelleted at 4,000xg for 10 minutes and the bacterial cells were resuspended in lysis buffer (50mM tris, 150mM NaCl, 0.5% Triton X-100) at 3ml/1mg of pellet. Pellet slurries were placed in lysing matrix B tubes (MP Biomedicals Inc.) and bacterial cells were lysed via bead beating for one minute three times with five minute incubations on ice in between. 200-800µg of bacterial lysate protein extracts were then added to 25µl of prewashed, chilled anti-FLAG magnetic beads (Sigma). This suspension was brought to a total volume of 1ml with lysis buffer and incubated at 4°C under constant rotation. After 10-16h of incubation, suspension tubes were placed on a magnetic stand, the unbound protein fraction was collected, beads were washed twice with TBS buffer (50mM Tris, 150mM NaCl, pH 7.4), and bound proteins were finally eluted from magnetic beads using 300ug/ml 3X-FLAG peptide (Sigma) in TBS buffer.

### **Western blotting**

Protein samples were denatured by boiling for 5 minutes with Unpaged 1X LDS buffer, and then centrifuged at 12,000xg for 2 minutes. Protein samples were separated via

electrophoresis on a NuPAGE 10% Bis-Tris gel, and were then transferred to a nitrocellulose membrane using the NuPAGE blotting system. Membranes were blocked with 3% Biotin in TBST (150mM NaCl, 25mM Tris-HCl pH 7.4, 0.1% Tween 20) for 1hr at room temperature or overnight at 4°C, then incubated with primary antiserum at 4°C overnight. Primary antisera included anti-FLAG (1:1000 in TBST, Sigma-Aldrich, St. Louis, MO), anti-sigma 70 (1:2000 dilution in 3% Biotin, NeoClone, Madison, WI), anti-His tag (1:2000 dilution in 3% Biotin, Abcam, Cambridge, MA), and anti-Hsp65 monoclonal antibody (1:2000 dilution in 3% Biotin, Enzo Life Sciences, Farmingdale, NY). Membranes were washed in TBST for 10 minutes and incubated for 1hr at room temperature with goat anti-mouse IgG peroxidase conjugated secondary antibody (Thermo Fisher Scientific, Waltham, MA) (for anti-His, anti-Hsp65, and anti-sigma 70). Blots were developed using the SuperSignal West Pico Chemiluminescent Substrate kit (Thermo Fisher Scientific, Waltham, MA) and visualized using UVP Biospectrum imaging system (Upland, CA).

**Table 1:** Primer list

Primer	Sequence	Details
JR376	GCAAGATCTCGGTGAGACGATGG CGGCC	F Rv2223 w/ <i>Bgl</i> III site
JR377	GCAAGATCTCGGTGAGACGATGA CTGAAGAACCCGGCG	F Rv2223 w/out signal w/ <i>Bgl</i> III site
JR338	GTAGTCCCATATGGAGCCGCCGG GCGCGCACCCGACAGAC	R Rv2223 (w/ <i>Nde</i> I site)
JR501	CAATCCACCGCTGTACTAGTGCA ATTGGGGAGC	F-megawhop primer w/ <i>Spe</i> I site for site-directed mutagenesis
JR390	TGCCCAACTCGGTGCCGTAGGCG TATCCGAGGTAGTTG	R Site-directed mutagenesis S232A
JR502	CCCGGGGTTTGGCCGGGGCCGGG TTCTTCAG	R Site-directed mutagenesis A40P
JR503	CCCGGGGTTTGGGGGGCGCCGGG TTCTTCAG	R Site-directed mutagenesis G41P
JR504	CGCACCCGGGGTTGGGCCGGCGC CGGGTT	R Site-directed mutagenesis Q42P

**Table 2:** Plasmid list

	Description
pEB08	pMV762-PgroEL-Rv2223-FLAG
pEB12	pMV762-PgroEL-*Rv2223-FLAG (w/out signal seq)
pEB26	pMV762-PgroEL-Rv2223 (S232A)-FLAG
pEB39	pMV762-PgroEL-Rv2223c (A40P)-FLAG
pEB40	pMV762-PgroEL-Rv2223c (G41P)-FLAG
pEB41	pMV762-PgroEL-Rv2223c (Q42P)-FLAG

**Table 3:** Mycobacterial intergenic regions

Species name	NCBI Ref Seq ID#	Intergenic region (bp)	Pathogen (P)/Non- pathogen (NP)
M. sp. MCS	NC_008146.1	-10	NP
M. abscessus-Bolletii	NC_021278.1	26	NP
M. abscessus	NC_010394.1	35	NP
Mtb-H37Rv	NC_000962.3	61	P
M. africanum	NC_015758.1	61	P
M. bovis AF2122/97	NC_002945.3	61	P
M. bovis BCG-Korea	NC_020245.2	61	NP
M. bovis BCG-Mexico	NC_016804.1	61	NP

M. bovis BCG-Pasteur	NC_008769.1	61	NP
M. bovis BCG-Tokyo	NC_012207.1	61	NP
M. canettii	NC_019950.1	61	P
M. canettii	NC_019965.1	61	P
M. canettii	NC_019951.1	61	P
M. canettii	NC_019952.1	61	P
Mtb-Beijing/NITR203	NC_021054.1	61	P
Mtb-CCDC5079	NC_021251.1	61	P
Mtb-CCDC5180	NC_017522.1	61	P
Mtb-CDC1551	NC_002755.2	61	P
Mtb-CTRI	NC_017524.1	61	P
Mtb-EAI5/NITR206	NC_021194.1	61	P
Mtb-EAI5	NC_021740.1	61	P
Mtb-Erdman	NC_020559.1	61	P
Mtb-F11	NC_009565.1	61	P
Mtb-H37Ra	NC_009525.1	61	P
Mtb-H37Rv	NC_018143.2	61	P
Mtb-Haarlem	NC_022350.1	61	P
Mtb KZN-1435	NC_012943.1	61	P
Mtb KZN-4207	NC_016768.1	61	P
Mtb KZN_605	NC_018078.1	61	P
Mtb UT205	NC_016934.1	61	P
Mtb 7199-99	NC_020089.1	61	P
M.sp. JLS	NC_009077.1	65	NP
M.sp. KMS	NC_008703.1	65	NP
M. leprae Br4923	NC_011896.1	74	P
M. leprae TN	NC_002677.1	74	P
M. vanbaalenii	NC_008726.1	78	NP
M. smegmatis MC2-155	NC_018289.1	80	NP
M. neoaurum VKM	NC_023036.2	93	NP
M. smegmatis MC2-155	NC_008596.1	128	NP
M. sp. MOTT36Y	NC_017904.1	146	NP
M. indicus pranii	NC_018612.1	146	NP
M. yongonense	NC_020275.1	146	NP
M. avium-ptb K10	NC_002944.2	150	NP
M. avium-ptb MAP4	NC_021200.1	150	NP
M. intracellulare ATCC13950	NC_016946.1	164	NP
M. intracellulare MOTT2	NC_016947.1	164	NP
M. intracellulare MOTT64	NC_016948.1	164	NP

**Figure 1. The predicted serine protease, Rv2223c is closely related to Mtb serine protease, Hip1.** (A) Schematic of predicted domains of Rv2223c. Catalytic triad residues are highlighted in red. (B) Pairwise amino acid sequence alignment of Rv2223c with Hip1 (left). Catalytic triad sites are highlighted in yellow. Dot-plot depicting amino acid sequence similarity between Rv2223c and Hip1 (right). (C) Model crystal structure of Rv2223c with catalytic triad amino acid residues highlighted in red.

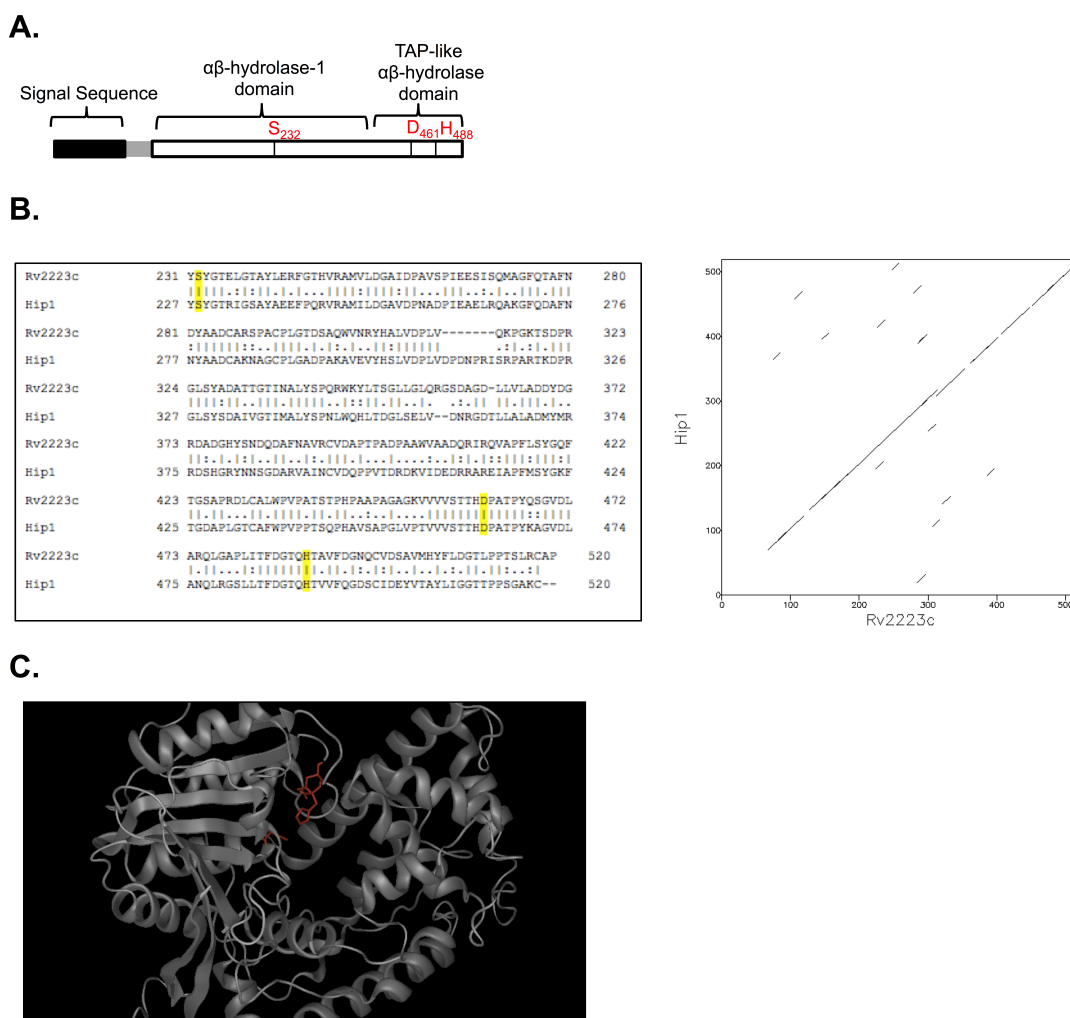
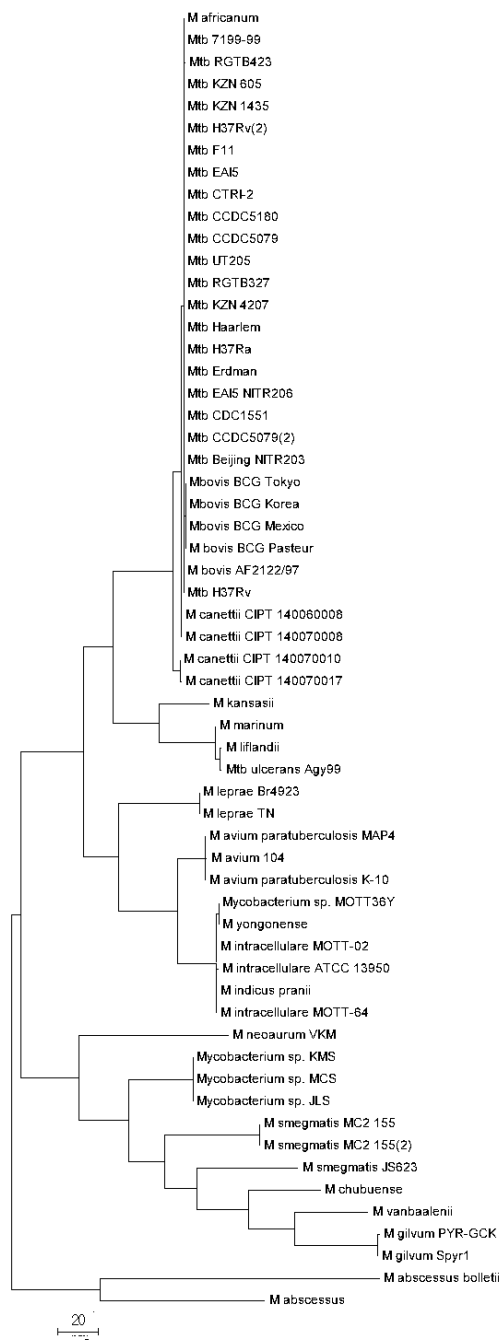


**Figure 2. Rv2223c and Hip1/Rv2224c are both highly conserved across mycobacterial species.** Phylogenetic trees of Rv2223c and Hip1 across 59 mycobacterial species.

Rv2223c



Hip1/Rv2224c

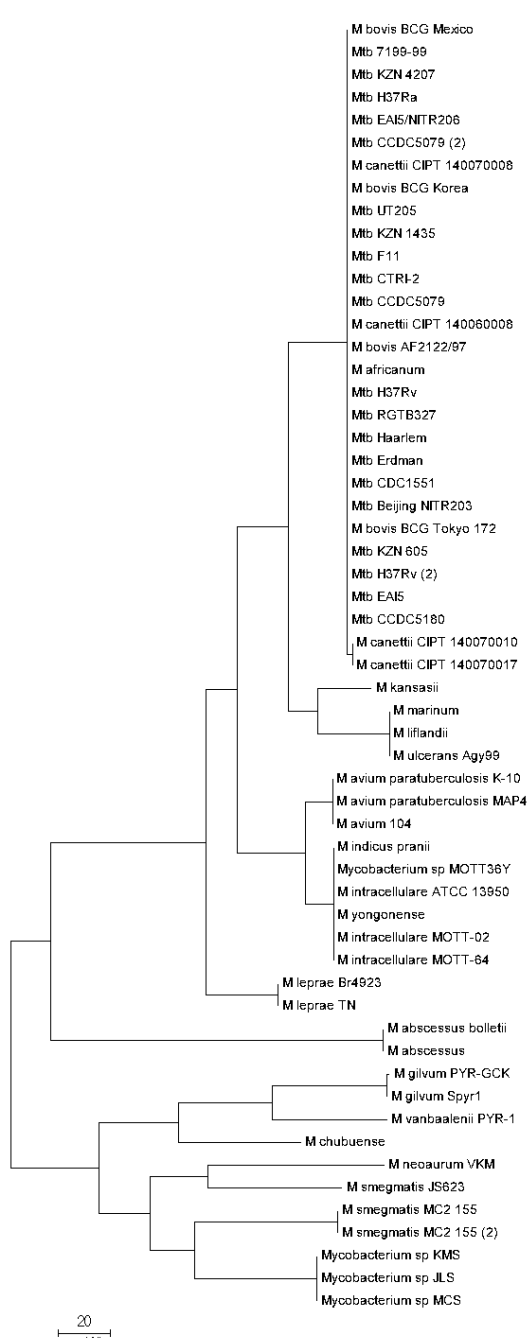


**Figure 3. Rv2223c is secreted from cells in a signal sequence dependent manner.**

(A) Schematic of predicted signal sequence of Rv2223c (right). Western blot of pellet and supernatant protein fractions from Msm expressing FLAG-tagged Rv2223c or  $\Delta 34$  Rv2223c (B) Western blot of pellet and supernatant protein fractions from Mtb expressing FLAG-tagged Rv2223c or  $\Delta 34$  Rv2223c. SigA serves as a pellet fraction control.

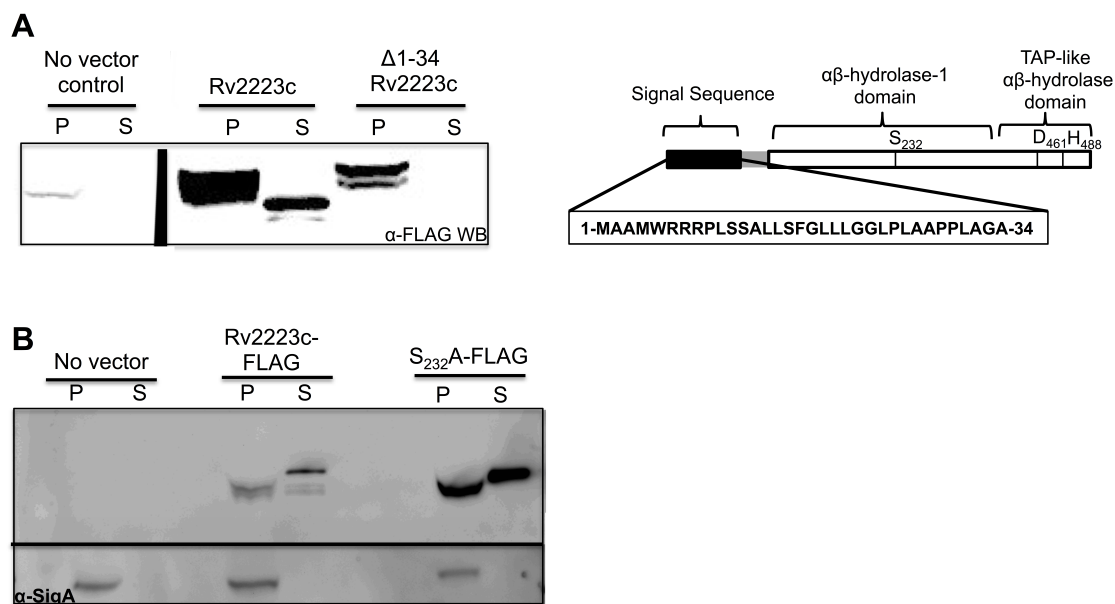


**Figure 4. Rv2223c undergoes S<sub>232</sub>-dependent autoproteolytic processing upon secretion between residues G<sub>41</sub> and Q<sub>42</sub>.** (A) Western blot of *M. smegmatis* expressing Rv2223c or S<sub>232</sub>A Rv2223c (left), and schematic of predicted enzyme forms (right). Arrows with numbers indicate the predicted enzyme forms on the Western blot. (B) schematic of cleavage site. Mutated residues are depicted in red. (C and D) Western blots of supernatants from Msm expressing FLAG-tagged Rv2223c with the indicated mutations.

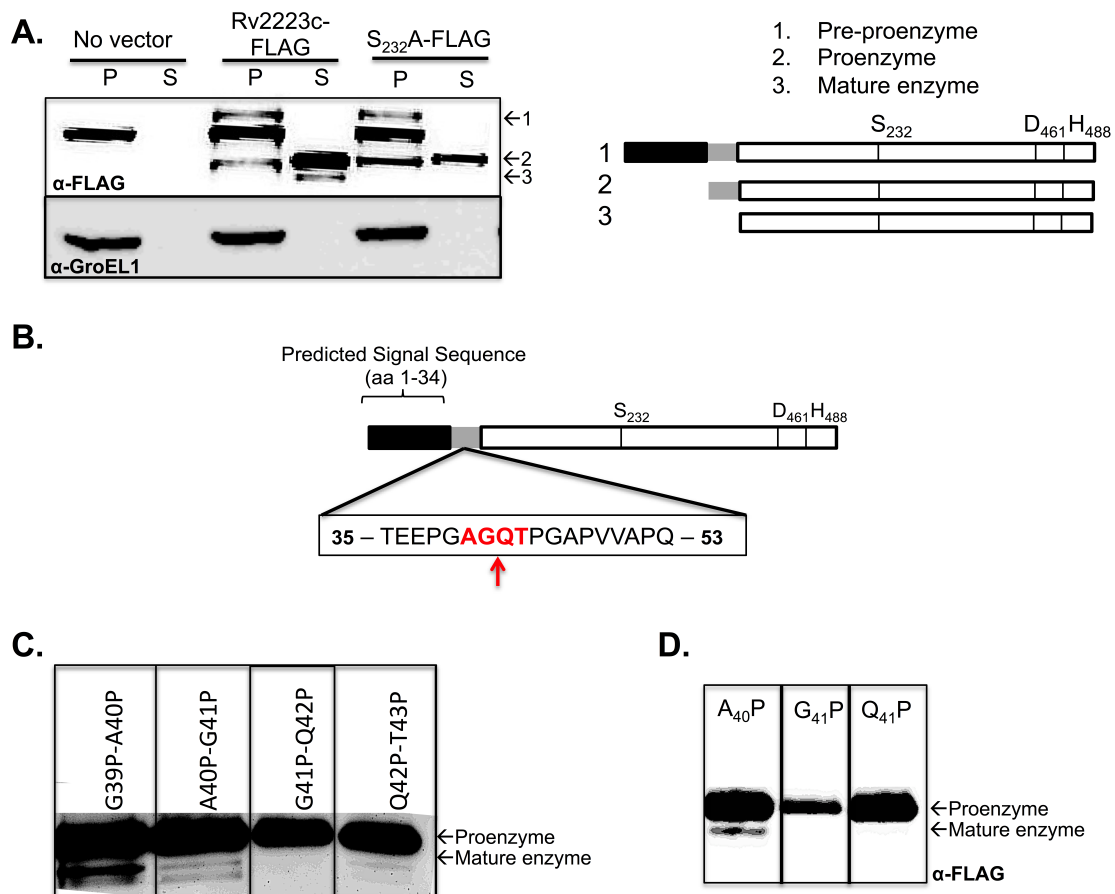
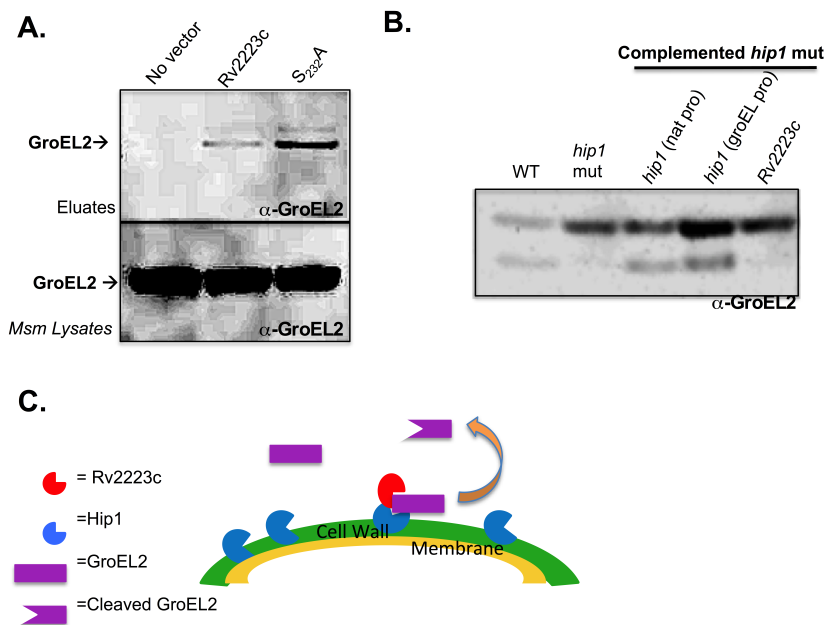


**Figure 5. Rv2223c interacts with GroEL2 in vitro, but fails to complement GroEL2 cleavage in vivo.** (A) (Top panel) Western blot of GroEL2 co-immunoprecipitated with FLAG-tagged Rv2223c or S<sub>232</sub>A Rv2223c from Msm . (Bottom panel) GroEL2 Western blot of Msm lysates. (B) GroEL2 Western blot of supernatants from the indicated Mtb strains. (C) Predictive model of Rv2223c and Hip1 action.





## **Chapter 4**

### **Unpublished Data**

## **Attempts to Purify Rv2223c for biochemical studies**

### **Expression and purification of Rv2223c from *Mycobacterium smegmatis* (Msm)**

Unlike the cell wall-anchored Hip1 protease of Mtb, Rv2223c, in its pro-enzyme and mature enzyme forms, is secreted into the culture supernatants of both Mtb and Msm (Chapter 3 Fig 3). We therefore decided to take advantage of the presence of this soluble Rv2223c protein by purifying it from mycobacterial supernatants in its native form (Table 3, Exp 1). We expressed either wild type Rv2223c (pMG-EB1) or S<sub>232</sub>A Rv2223c (pEB38), which was shown in Chapter 3 to be catalytically inactive, with a C-terminal 6X-histidine tag from an exogenous plasmid in Msm. While we were able to detect the resulting purified protein via Western blot analysis and silver staining (Fig. 1), the levels of secreted protein were low and we were unable to purify sufficient quantities of protein for enzymatic studies, even from up to 6L of culture. In order to obtain higher yields of purified protein, we therefore decided to purify recombinant Rv2223c from *E. coli*.

### **Expression and purification of Rv2223c from *E. coli* cells (conducted in collaboration with Drs. Jackie Naffin-Olivos and Dagmar Ringe, Brandeis University)**

Previous studies of Mtb Hip1, with which Rv2223c shares 47% amino acid sequence identity and 60% similarity, revealed that when expressed in BL21star *E. coli*, the protein localized to inclusion bodies (76). We cloned Rv2223c with deletions of either the first 34 amino acids (Rv2223c $\Delta$ 34) or the first 41 amino acids (Rv2223c $\Delta$ 41), to represent the pro-enzyme and mature forms of the protein respectively (see Chapter 3 Fig. 4), into expression plasmid pET28a with an N-terminal 6X-histidine tag. We hypothesized that,

due to the fact that both of these shorter forms of Rv2223c are secreted into culture supernatants of mycobacterial cells (Chapter 3 Fig 4) that they may localize to soluble fractions of *E. coli* protein preparations. However, similarly to Hip1, both of these proteins localized to the insoluble inclusion bodies of BL21 star cells (data not shown). Due to the high percentage of amino acid sequence identity and similarity of Rv2223c to Hip1 as well as the insolubility of Rv2223c in *E. coli* protein preparations, our collaborators conducted an initial purification attempt of Rv2223c (Table 3, Exp 2) using the purification methods optimized for Hip1 and detailed previously (76). Circular dichroism (CD) analysis of the purified Rv2223c protein revealed the soluble protein, resulted in improper folding and ultimately aggregation. In order to determine optimal Rv2223c refolding conditions, we conducted a high-throughput absorbance-based inclusion body protein solubility screen (Table 3, Exp 3), which was first described by Vincentelli et al. (178). This assay requires monitoring the turbidity at Abs<sub>340</sub> of different buffers containing a protein of interest over time, where increased absorbance over a time zero baseline reading indicates increased protein stability. The results of this screen revealed that stability of the aggregated Rv2223c could be increased in a buffer containing 0.8M L-arginine.

### **Second round of purification attempts**

Subsequent attempts to purify Rv2223c focused on increasing the stability of Rv2223c during purification and refolding. Alongside the pET28a Rv2223c constructs, Rv2223c $\Delta$ 34 and Rv2223c $\Delta$ 41 were also cloned into the pET22b expression vector, as well as the full length Rv2223c (Table 3 Exp 4). The pET22b expression vector harbors

a *pelB* signal sequence upstream of the cloned in DNA sequence for potential localization of recombinant proteins into the *E. coli* periplasm. As Rv2223c is normally secreted from mycobacterial cells, we hypothesized that the periplasm of *E. coli* would provide a more favorable environment for proper folding of the protein. In order to address the potential that expression of soluble Rv2223c could be toxic to *E. coli*, we also tested expression and localization of the protein from a BL21 mutant strain, C43. A mutation in the T7 RNA polymerase in the C43 *E. coli* expression strain allows for more time for expression and lower levels of potentially toxic proteins in order to obtain soluble protein (179, 180). We found optimal expression of the Rv2223c proteins from the pET28a plasmid in the insoluble protein fractions of BL21 star cells, and no Rv2223c in the soluble fractions of BL21 star or C43 cells (Fig. 2A). Although there appeared to be expression of a band slightly lower than expected in the periplasm of BL21 star cells expressing pET22b $\Delta$ 34 and induced at 18°C, we decided not to use this strain at the time as protein expression was low (Fig. 2B). This is an avenue that could possibly be explored later. We therefore continued subsequent purification attempts with the pET28a expression plasmid constructs in BL21 star cells.

In order to utilize 0.8M L-arginine during refolding of purified Rv2223c, we needed to address the fact that L-arginine strips nickel from Ni-NTA agarose columns. To bypass this complication, we opted to refold the Rv2223c proteins only after eluting the protein from the nickel column. Upon purification, both Rv2223c $\Delta$ 34 and Rv2223c $\Delta$ 41 were refolded via dialysis in buffers containing 0.8M L-arginine and step-wise reductions in urea concentrations. We then subjected the resulting protein to a fluorescence thermal

shift assay through which we determined that both purified Rv2223c proteins were aggregated and mis-folded (Fig. 3).

### **Detergent/additive screens and histidine tag rearrangement**

Since the addition of L-arginine was unable to fully stabilize Rv2223c in solution, we set out to find additional compounds to aid in stabilization. To do so we used a fluorescence thermal shift-based assay to screen a total of 99 detergents and additives that have been known to help in protein solubilization and/or stability. (Table 3 Exp 5). The most promising compounds were then re-tested, this time in the absorbance based assay that we had previously utilized in Exp 2 from Table 3 (Fig 4). These screens revealed that addition of hexamine cobalt trichloride to the purified Rv2223c $\Delta$ 34 and Rv2223c $\Delta$ 41 aggregates led to increased protein stability in solution (Table 3 Exp 6). However, addition of hexamine cobalt trichloride, while providing some additional stability during refolding of Rv2223c, failed to fully stabilize the protein (Fig. 5). It should be noted that while Hip1 normally produces one peak in thermal fluorescence shift assays, addition of L-arginine in the assay buffer resulted in two peaks. We hypothesize that L-arginine may bind to Hip1 and have some stabilizing affect as well.

Because our studies in Msm where properly folded, soluble Rv2223c was expressed were done with C-terminally tagged protein, we decided to investigate the affect of changing the terminal of the Rv2223c 6XHis tag on solubility and refolding of Rv2223c in *E. coli*. We created new pET28a Rv2223c $\Delta$ 34 and Rv2223c $\Delta$ 41 plasmid constructs with C-terminal 6X-histidine tags (Table 3 Exp 7). We then examined protein expression in

BL21 star cells as well as C41 cells, which are similar to C43 expression cells, except with a different mutation in the T7 RNA polymerase (179), and we again found optimal protein expression in the insoluble protein fractions of BL21 star cells, and saw no expression of either construct in C41 cells under any induction temperature (Fig 6). We then purified and refolded Rv2223c on the NiNTA column in the presence of various stabilizing detergents or via dialysis in the presence L-arginine. All refolding conditions resulted in aggregation of the Rv2223c proteins (Fig 5A), and although some fluorescence shifts seemed stable, this was due to the background detergent fluorescence (Fig 5B).

Due to these observations along with the inherent affinity of cobalt to histidine, we hypothesized that aggregation of purified Rv2223c may be a result of the presence of the 6X-polyhistidine tag, and that cobalt binding to the tag stabilizes the protein. Therefore, it may be productive for future attempts to purify Rv2223c to include either untagged expression constructs or the use of another small tag that would not chelate a metal ion.

### **Deletion of *Rv2223c* and *hip1***

As reported in Chapter 3, we utilized a suicide vector allelic exchange approach to delete both *Rv2223c* and *hip1* in one strain (Fig. 8A). We were able to successfully confirm deletion of both genes from their endogenous locus via Southern blot, PCR (Fig 8B and 8C) and sequencing. However, upon further investigation, we found that from each of the 17 PCR-verified knockouts, both *Rv2223c* and *hip1* could be amplified from the genome (Fig9). These results indicate that a non-specific, compensatory recombination

event occurred at some point during generation of the mutant strain. These data suggest that while neither *Rv2223c* nor *hip1* are predicted to be essential singularly, the two proteins together may play a vital more essential role and thus deleting both genes is likely lethal to Mtb growth. To definitively verify this hypothesis, it would be necessary investigate the growth phenotype of Mtb strains containing conditional knockdowns of *Rv2223c* and *hip1* when expression of one or both genes is knocked down.

## Materials And Methods

### Cloning of recombinant proteins for expression in Msm

Mtb *Rv2223c* was amplified from H37Rv genomic DNA with forward primer JR264 – 5'-ACGAGATCTATGGCGGCCATGTGG-3' and reverse primer JR265 – 5'-AGTAAGCTTTCAGTGGTGATGATGGTGATGTCCGCTTCCGCTTCCGGGCGCGC ACCGCAGACTCGTCGG-3', yielding an *Rv2223c* construct with an in frame C-terminal 6X-histidine tag. This amplicon was digested with restriction enzymes *BglII* and *HindIII* and ligated into a *BamHI* and *HindIII* digested pMV762 vector downstream of the constitutive PgroEL mycobacterial promoter, resulting in pMG-EB1. An alanine mutation was introduced into the S<sub>232</sub> amino acid residue of WT *Rv2223c* within pMG-EB1 using forward primer, JR501 – 5'-CAATCCACCGCTGTACTAGTGCAATTGGGGAGC-3', which introduced a *SpeI* cleavage site into the plasmid for later confirmation and reverse primer, JR390 – 5'-TGCCCAACTCGGTGCCGTAGGCGTATCCGAGGTAGTTG-3', which contained the S<sub>232</sub>A mutation. This amplicon was then used as a “megaprimer” to amplify the full pMG-EB1 plasmid, and to introduce both mutations, resulting in the plasmid pEB38.

### Expression and purification of recombinant protein in Msm

Msm expressing C-terminally 6X-His-tagged Rv2223c from an episomal plasmid was grown at 37°C in 1L Middlebrook 7H9 (Difco) broth supplemented with 10% oleic acid-albumin-dextrose-catalase (OADC), 0.2% glycerol, 0.05% Tween 80, and 50µg/ml Hygromycin. Cultures were then transferred to 6L of Sauton's medium supplemented with 0.05% Tween 80 and 50µg/ml Hygromycin, and grown for 3 days to an OD<sub>600</sub> of 0.5-0.7. Cells were centrifuged at 4000g x 10 minutes at 4°C, and resuspended in 300ml of Sauton's medium without Tween overnight. Cells were centrifuged at 4000g x 10 minutes at 4°C, then resuspended in 1ml of binding buffer (5mM imidazole). Protein was then incubated with Ni<sup>+</sup> charged agarose beads at 4°C for 30 minutes with slow rotation. The bead protein slurry was then added to a column and the beads were washed with x1 with 5mM imidazole, x1 with 20mM imidazole, and then eluted with 240mM imidazole. The eluates were then dialyzed and concentrated. Resulting purified protein along with the supernatant, unbound sample, washes, and eluate were subjected to SDS-PAGE and silver staining analysis.

### Cloning of recombinant proteins for expression in *E. coli*

Mtb Rv2223c lacking either the first 34 amino acids (which removes its N-terminal secretion signal sequence), or the first 41 amino acids (which results in the mature enzyme form of Rv2223c) was cloned into pET28a or pET22b. For cloning into pET28a, Rv2223cΔ34 was amplified from H37Rv genomic DNA using forward primer 5'-CGGCCTGGTGCCGCGCGGCAGCCATATGACTGAAGAACCCGGCGCCGGCCAA



**With L-arginine stabilization.** The plasmids pET28a-His-Rv2223cΔ34 and pET28a-His-Rv2223cΔ41 were transformed into BL21 star cells. LB (1L) containing 50μg/ml of kanamycin (for pET28a plasmid containing strains) were inoculated with 5ml of overnight cultures, and grown at 37°C to OD<sub>600</sub> 0.6-0.8. The cells were then cooled to room temperature and 1mM IPTG was added to induce expression. Incubated overnight 25°C. *E. coli* pellets were harvested via centrifugation at 10,000 rpm for 1h. Cell pellets were resuspended in 1X PBS buffer, and sonicated. The sonicated solutions were then centrifuged at 11,000 RPM for 1h in order to separate soluble from the insoluble, inclusion body-containing fractions. The insoluble pellet fraction was washed twice by resuspending in 50mM Tris-HCl pH8.0, 100mM NaCl, 0.5% Triton X with a dounce homogenizer and centrifugation at 10,000 RPM for 1h. To reduce and denature the inclusion body proteins, washed pellets were resuspended in 50mM Tris-HCl, pH8.0, 100mM NaCl, 5mM BME, and 8M urea with a dounce homogenizer and the solution was allowed to incubate overnight at 4°C while slowly stirring. Denatured protein solutions were centrifuged at 10,000 rpm for 1h, and the supernatants were added to nickel (Ni<sup>2+</sup>) resin and slowly rotated at 4°C for 1h for equilibration before transferring to gravity columns. All of the following steps were performed at 4°C. Following two washes with 50mM Tris-HCl, pH8.0, 100mM NaCl, 8M Urea, 10mM imidazole, and 5% glycerol the immobilized protein was eluted from the nickel resin with 50mM Tris-HCl, pH8.0, 100mM NaCl, 8M Urea, 250mM imidazole, 5% glycerol in 1ml aliquots. For protein folding, protein-rich aliquots were pooled then subjected via dialysis to a step-wise reduction in urea concentration in the presence of a redox pair, reduced and oxidized glutathione, as well as 0.8M L-arginine. The purified protein pool was first dialyzed

against 50mM Tris-HCl, pH8.0, 100mM NaCl, 5% glycerol, and 8M Urea in order to eliminate imidazole from the protein solution. Subsequent dialysis buffers consisted of 50mM Tris-HCl, pH8.0, 100mM NaCl, 5% glycerol, 1mM reduced glutathione, 0.2mM oxidized glutathione, 0.8M L-arginine, with varying concentrations of 6M, 3M, 1M, and no urea. In the case of protein refolding with a cobalt stabilizer, the refolding buffers were supplemented with 10mM hexamine cobalt trichloride. The expressed proteins under all conditions were present as single bands on an SDS-PAGE gel.

#### Absorbance based protein stability assay

Buffers containing either 0.8M L-arginine HCl, 3% 1,8-Diaminooctane, 3% 1,6-Diaminohexane, 4% Tert-Butanol, 10mM Hexamine cobalt trichloride, 100mM Ammonium sulfate, combinations of additives (indicated in Fig 4), or no additives were made in a base buffer (50mM Tris HCl pH8, 100mM NaCl). 95 $\mu$ l of each buffer was then placed into two 96 well plates, and 5 $\mu$ l of purified Rv2223c $\Delta$ 34 1mg/ml solution was added to each well for a final concentration of 0.1mg/ml in 100 $\mu$ l per well. The baseline absorbance of each plate was assessed at OD of 340nm, after which one plate was left to incubate at 25°C and the other at 37°C. After 11 hours, the OD<sub>340</sub> of each well was measured, and the baseline measurement was subtracted in order to determine the change in absorbance. Buffers resulting in positive changes in absorbance over the cutoff of OD<sub>340</sub> 0.05 were considered to be Rv2223c $\Delta$ 34-stabilizing buffers. Buffers resulting in OD<sub>340</sub> change of -0.05 or lower were considered to be destabilizing.

### Thermal fluorescence shift assay

Thermal fluorescence shift assays were conducted using SYPRO orange protein gel stain (Invitrogen) and results were acquired using the Applied Biosystems Step1 Plus Real-time PCR system. Samples were prepared with equal concentrations of the purified protein across conditions assessed (1-20 $\mu$ M final concentration) and 10X final concentration of SYPRO Orange dye. In order to measure the thermodynamic stability of Rv2223c recombinant proteins after purification and refolding, the final purification dialysis buffer (50mM Tris-HCl, pH8.0, 100mM NaCl, 5% glycerol, 1mM reduced glutathione, 0.2mM oxidized glutathione, 0.8M L-arginine) was utilized for thermal shift analysis samples. In subsequent screens to determine the effect of various detergents and additives on protein stability, different buffer compositions were used with the final dialysis buffer serving as the base buffer. Samples were incrementally heated from 25°C to 95°C in increments of 0.3°C. Fluorescence at each temperature was recorded at 480nm following excitation at 568nm. In order to cancel out inherent buffer fluorescence, emission intensity of each sample was normalized against fluorescence of samples without protein. The normalized fluorescence was then plotted as a function of temperature. In screening experiments, buffers containing detergents or additives with inherent fluorescence above that of samples containing protein were rejected for potential use in subsequent purification since we would be unable to determine if these reagents had any effect.

### **Construction of $\Delta hip1$ - $\Delta Rv2223c$ mutant *M. tuberculosis***

H37Rv was transformed via electroporation with 3µg of pEBOP-01 (a suicide vector containing a  $\Delta hip1-\Delta Rv2223c$  allele, a selectable hygromycin resistance marker, and a counter selectable *sacB* marker). Resultant transformants that were resistant to hygromycin were then patched onto 7H10 plates containing 2% sucrose. Colonies that displayed hygromycin resistance and sucrose sensitivity were considered to have undergone a single crossover event resulting in incorporation of pEBOP-01 into the Mtb genome. These colonies were then grown to saturation for a week in 5ml of 7H9 broth, and then serial dilutions were plated in duplicate onto 7H10 plates supplemented with 2% sucrose. Colonies arising on these plates were patched onto hygromycin. Those that were hygromycin sensitive and sucrose resistant were grown in 7H9 broth, and genomic DNA was extracted using the protocol adapted from Belisle and Sonnenberg (106). Genomic DNA was then subjected to Southern blot analysis. DNA was digested with *NcoI*, and then probed with a DIG-labeled amplicon corresponding to a 1kb region present in the both the genome and pEBOP-01. Deletion of the *Rv2223c-hip1* locus was also confirmed via amplification of the deleted region using primers upstream (forward primer 5'-CGGCCACCCGCTCACCGCCCTCG-3') and downstream (reverse primer 5'-GCACGGCGAATGTCAGATAGGG-3') of the 1kb regions of homologous recombination, resulting in a 3kb amplicon from the BCG $\Delta hip1$  genome, and a 6kb amplicon from the wild-type BCG genome (Figure 8). These amplicons were then sequenced for further confirmation of gene deletion.



**Table 2:** Plasmid list

Plasmid	Description
pMG-EB1	pMV762-PgroEL-Rv2223-c-term 6XHis
pEB38	pMV762-PgroEL- Rv2223 (S232A)-c-term 6XHis
pEBOP-03	pET22b-n-term 6xHis-Rv2223c (Full length)
pEBOP-04	pET22b-n-term 6xHis Rv2223c $\Delta$ 34
pEBOP-05	pET22b-n-term 6xHis Rv2223c $\Delta$ 41
pEBOP-06	pET28a-n-term 6xHis Rv2223c $\Delta$ 34
pEBOP-07	pET28a-n-term 6xHis Rv2223c $\Delta$ 41
pEB34	pET28a-Rv2223c $\Delta$ 34-c-term 6XHis
pEB35	pET28a-Rv2223c $\Delta$ 34-c-term 6XHis
pEBOP-01	$\Delta$ <i>hip1</i> - $\Delta$ Rv2223c construct

**Table 3:** Purification experiments

Exp #	Experimenter	Constructs	Approach	Expressed	Soluble protein?	Findings
1	Erica Bizzell	pMG-EB1 pEB38	Purification from <i>M. smegmatis</i> supernatant	Yes	In supernatant	Low yield
2	Andrew Daab	pEBOP-06 pEBOP-07	Hip1 purification method (Naffin-Olivos et al. 2014 PLOS Path.)	Yes	From inclusion bodies	Aggregated (CD)
3	Andrew Daab	pEBOP-06 pEBOP-07	Absorbance-based inclusion body protein solubility screen (Vincentelli et al. 2004 Protein Sci)	Protein from Exp 2	From inclusion bodies	0.8M L-arginine stabilizes Rv2223c
4	Erica Bizzell	pEBOP-03 pEBOP-04 pEBOP-05 pEBOP-06 pEBOP-07	Tested BL21 and C43 expression lines; Tested induction temperatures; Purified with refolding in the presence of 0.8M L-arginine	Yes	From inclusion bodies	Aggregated (Thermo)
5	Erica Bizzell	pEBOP-06	Screened 99 additives and detergents (see Table 4)	Protein from Exp 4	From inclusion bodies	Hexamine Cobalt Trichloride
6	Erica Bizzell	pEBOP-06 pEBOP-07	Purification with 0.8M L-arginine and Hexamine Cobalt Trichloride		From inclusion bodies	Aggregated
7	Erica Bizzell	pEB34 pEB35	Used C-terminally 6XHis-tagged Rv2223c constructs and purified with or without detergents		From inclusion bodies	Aggregated

CD = Circular dichroism

Thermo = Thermo Fluorescence Shift Assay

**Figure 1. Purification of Rv2223c from Msm supernatant** (A) Anti-His tag Western blot of pellet and supernatant fractions from Msm expressing 6X-histidine tagged Rv2223c. The enzyme forms detected are indicated by arrows and numbers; 1. Pre-proenzyme, 2. Pro-enzyme, 3. Mature enzyme. (B) Silver stained SDS-PAGE of purification protein fractions. Purified Rv2223c is boxed in blue. M-marker, S-supernatant fraction, U-unbound protein, W1/W2-washes 1 and 2, CE-concentrated eluate.

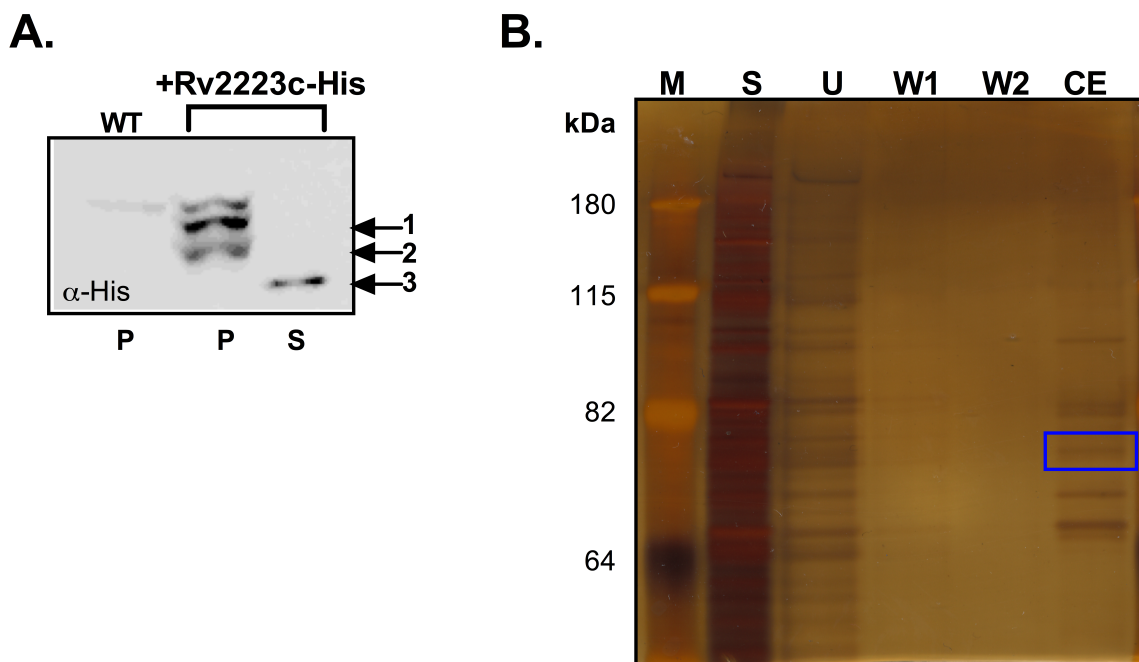


**Figure 2. Expression of N-terminal 6X His-tagged Rv2223c $\Delta$ 34 and  $\Delta$ 41 in C43 and BL21 star *E. coli*.** (A) SDS-PAGE analysis of soluble (left) and insoluble inclusion body (right) fractions of C43 and BL21 star cells harboring pET28a-6XHis-Rv2223c $\Delta$ 34 or pET28a-6XHis-Rv2223c $\Delta$ 41. (B) SDS-PAGE analysis of periplasmic and insoluble (right) fractions of pET22b-6XHis-Rv2223c $\Delta$ 34 or pET22b-6XHis-Rv2223c $\Delta$ 41 containing C43 and BL21 star cells. Induction of Rv2223c expression was tested at 18°C and 25°C, with the expressed Rv2223c protein is boxed in red.

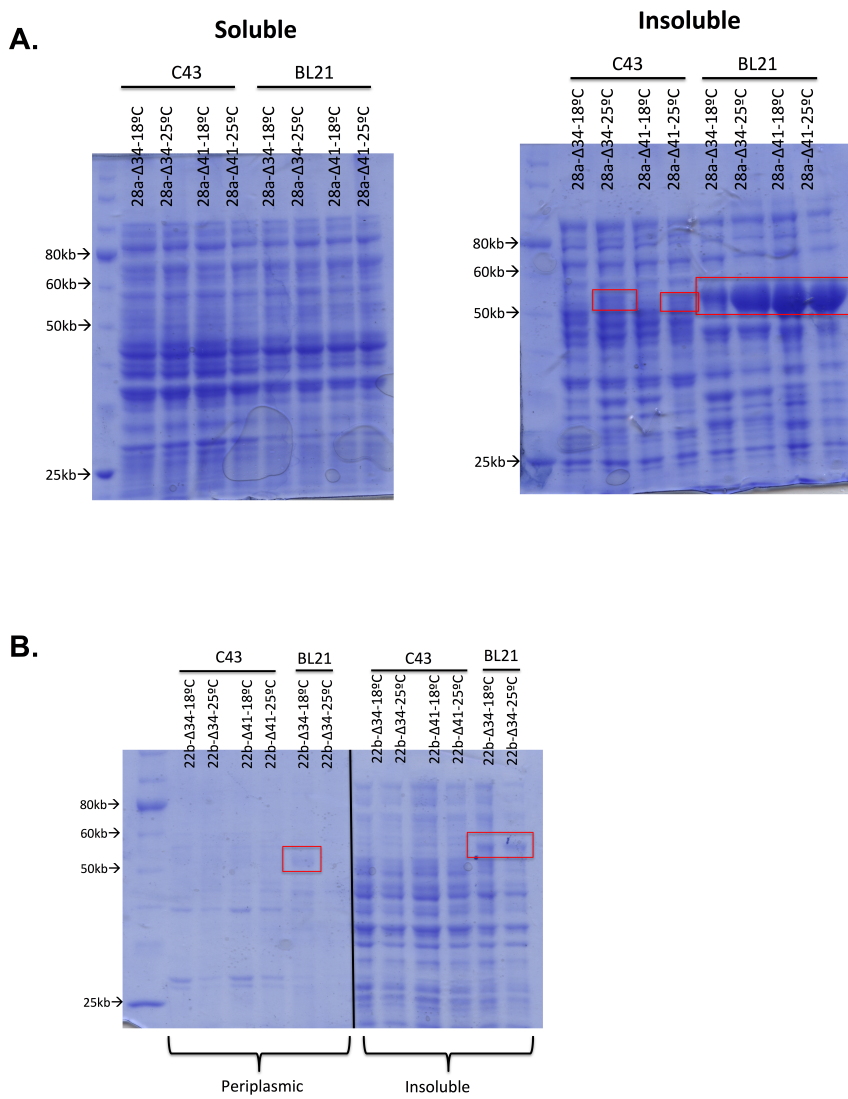


**Figure 3. L-arginine does not stabilize purified Rv2223c in solution.** Thermal fluorescence shift analysis to check the stability of purified N-terminal 6X-His-tagged Rv2223c $\Delta$ 34 (A) and Rv2223c $\Delta$ 41 (B) in solution with and without L-arginine.

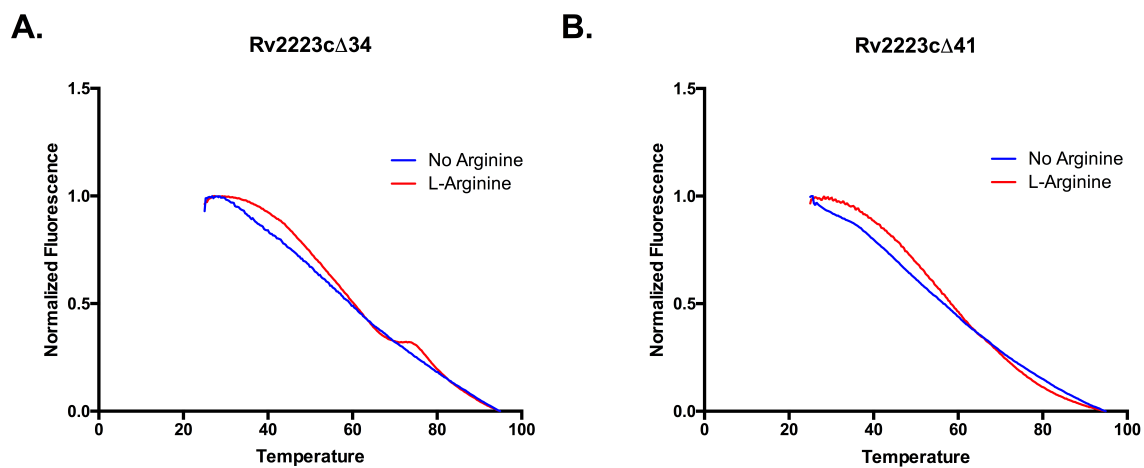


**Figure 4. Absorbance based analysis of stabilizing capabilities of the indicated buffers on Rv2223cΔ34.** Aggregated protein was incubated for 11h in the indicated buffers at either 25°C (A) or 37°C (B). The change in OD<sub>340</sub> from 0hrs is graphed and a minimum cutoff of 0.05, which is denoted by a dotted line, serves as the readout for enhanced protein stabilization. Stabilizing conditions are boxed in red.

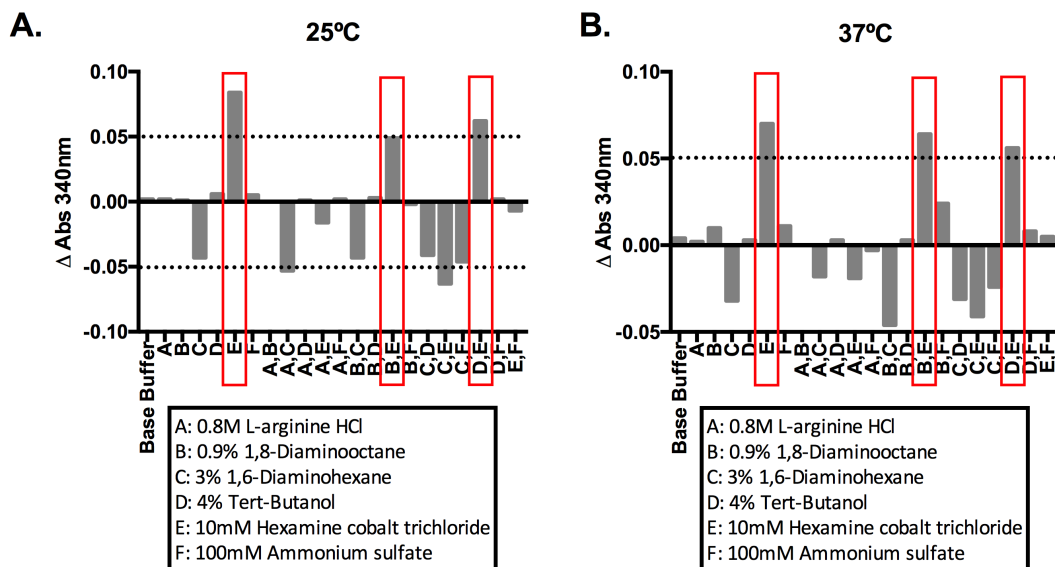


**Figure 5. Hexamine cobalt trichloride does not stabilize Rv2223c in solution.**

Thermal fluorescence shift analysis of N-terminally 6X-His-tagged Rv2223c $\Delta$ 34 and  $\Delta$ 41 purified and refolded in the presence of L-arginine with or without hexamine cobalt trichloride (+Co). Purified Hip1 is included as a control stable protein control.

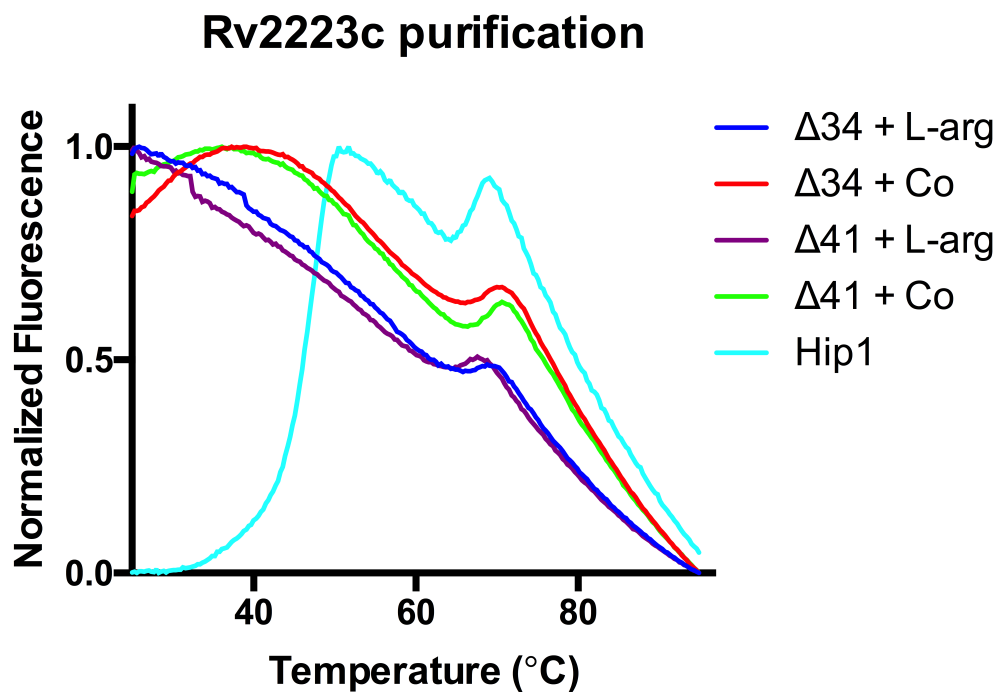


**Figure 6. Expression of C-terminally tagged Rv2223c $\Delta$ 34 and  $\Delta$ 41 in C41 and BL21 star *E. coli*.** SDS-PAGE analysis of soluble (left) and insoluble inclusion body (right) fractions of C41 and BL21 star cells harboring pET28a-Rv2223c $\Delta$ 34-6XHis or pET28a-Rv2223c $\Delta$ 41-6XHis. Induction of Rv2223c expression was tested at 18°C, 25°C, and 37°C with the expressed protein denoted by red boxes.

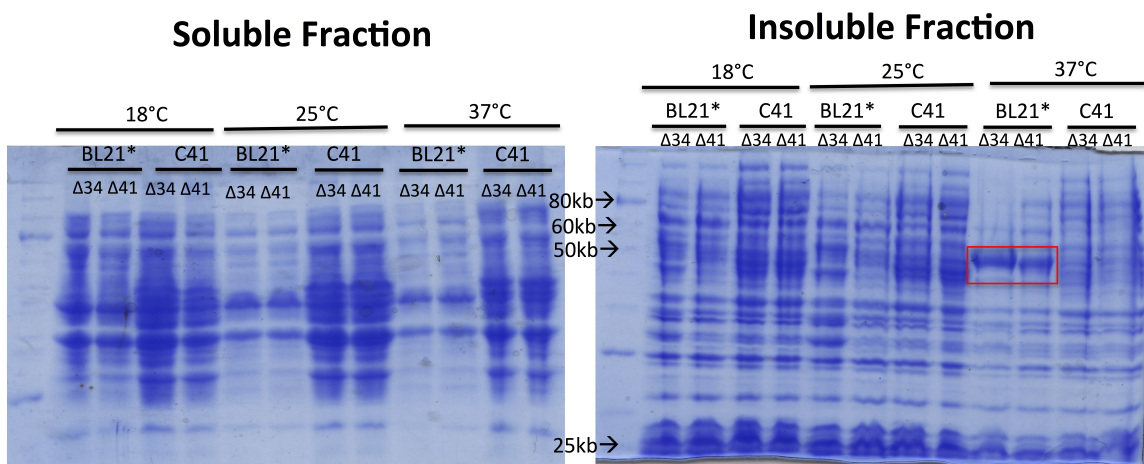


**Figure 7. Thermal fluorescence screen of the effect of detergents on Rv2223c protein stability.** (A) Thermal fluorescence shift assessment of solubility of C-terminally tagged Rv2223c $\Delta$ 34 (top panel) and  $\Delta$ 41 (lower panel) purified in the presence of the indicated detergents. (B) Assessment of inherent detergent fluorescence (solid lines) and fluorescence of detergent with protein present (dashed lines) of C-terminally tagged Rv2223c $\Delta$ 34 (top panel) and  $\Delta$ 41 (lower panel).

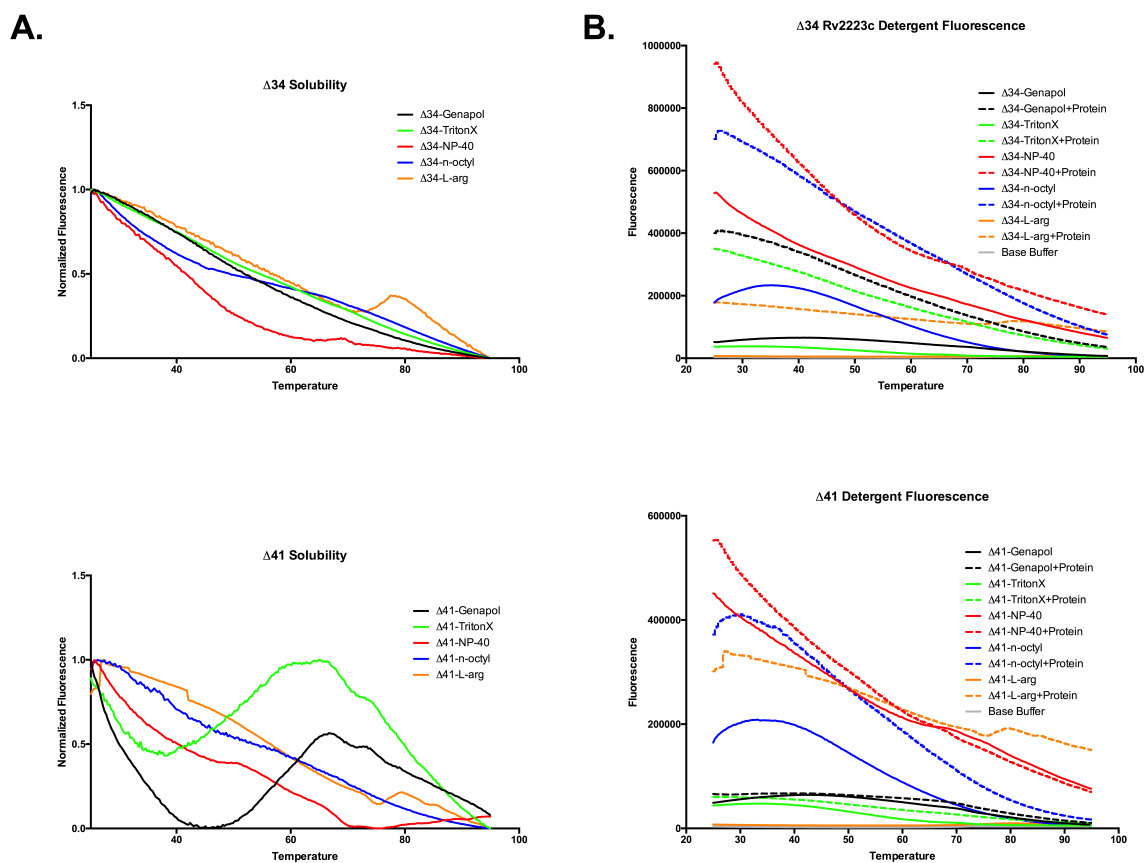


**Figure 8. Southern blot and PCR analysis of *Mtb* $\Delta$ *Rv2223c* $\Delta$ *hip1*.** (A) pEBOP-01 suicide vector schematic, chromosomal locus for *hip1*-*Rv2223c* locus, and schematic of  $\Delta$ *Rv2223c* $\Delta$ *hip1* allele. *NcoI* restriction endonuclease sites are denoted. The Southern probe used is represented by a black box, while green arrows indicate PCR amplification primers. (B) Southern blot of *NcoI* digested genomic DNA purified from WT *Mtb* or *Mtb* $\Delta$ *Rv2223c* $\Delta$ *hip1* probed with digoxigenin (DIG)-labeled amplicon of the 1kb region downstream of *Rv2223c*. Black arrows denote DNA detected by the probe. (C) PCR amplification of the genomic region surrounding *hip1* using primers 1.6kb upstream and 2.8kb downstream of *hip1*. Black arrows indicate amplified DNA. The contrast and brightness of the Southern blot and DNA gel were adjusted for clarity.

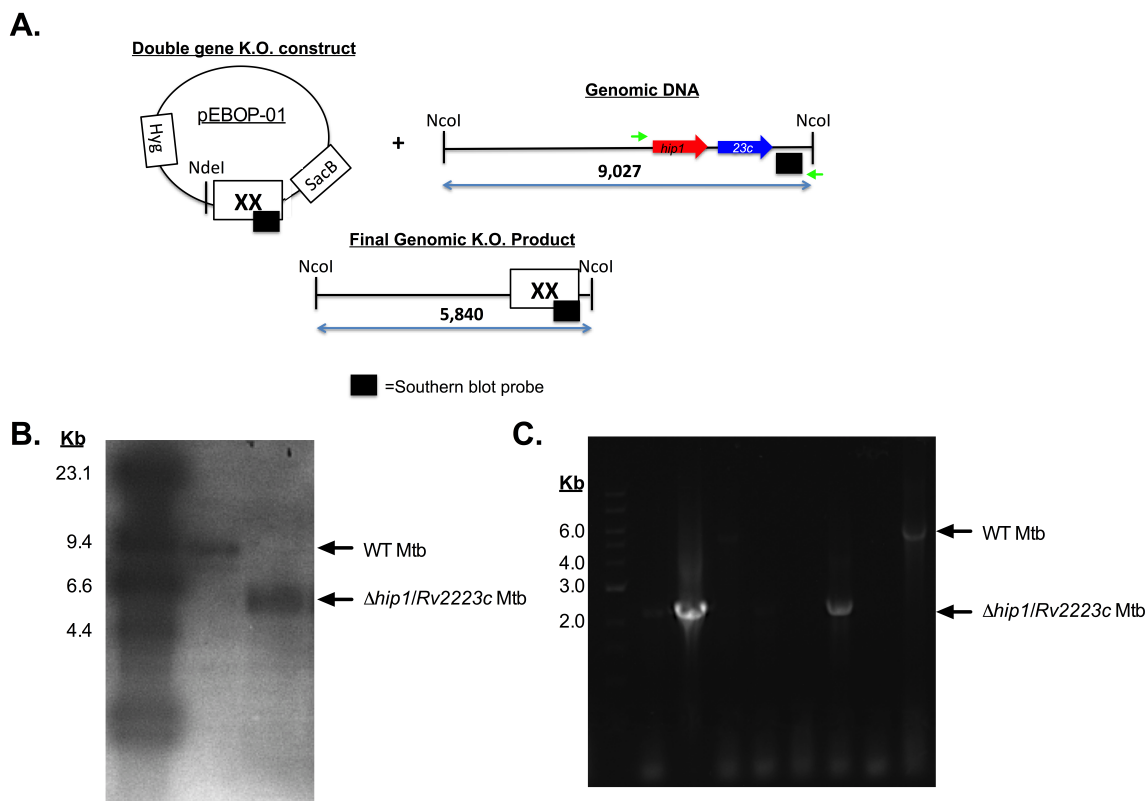
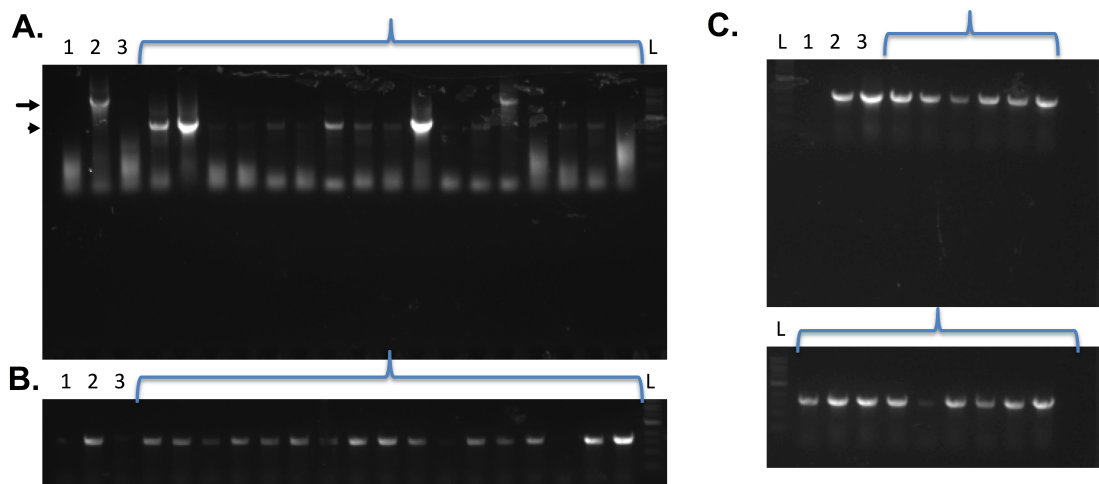


**Figure 9. Verification of *Rv2223c* and *hip1* recombination.** (A) PCR amplification of the *Rv2223c-hip1* locus from the DNA of *MtbΔRv2223cΔhip1* secondary recombinants with primers JR505 and JR506. A black arrowhead indicates the expected size of the double *Mtb* knockout amplicon, while a black arrow denotes the expected size of a WT *Mtb* amplicon. (B) PCR amplification of *hip1* from *MtbΔRv2223cΔhip1* secondary recombinants from panel A. (C) PCR amplification of *Rv2223c* from *MtbΔRv2223cΔhip1* secondary recombinants from panel A. Blue brackets indicated *MtbΔRv2223cΔhip1* secondary recombinants. L-ladder, 1-No DNA, 2-WT *Mtb*, 3-*Mtb hip1*-mutant.



**Chapter 5**

**Discussion**

Throughout several millennia of co-evolution with the human population, *Mycobacterium tuberculosis* (Mtb) has developed multiple mechanisms to evade host immune responses and cause disease. Only within the last century have we begun to understand some of these strategies, which have more recently aided in efforts to develop better vaccines and drugs to combat them. Despite major advances, there is still much work to be done in this arena that relies heavily on gaining a better understanding of how Mtb modulates host immune responses.

We highlighted some of our current knowledge of the immune evasion strategies employed by Mtb in the introduction of this dissertation. The immunosuppressive capabilities of Mtb are due in part to proteins that are situated at the host-pathogen interface either through association with the bacterial cell wall or through extracellular release from the bacteria. Within this dissertation, we discuss two such factors, one of which, Hip1, is associated with the mycobacterial cell wall, and the other, Rv2223c, we have shown is secreted from mycobacterial cells.

In chapter 2 of this dissertation, we provide insights into the role of the immune evasion associated serine protease, Hip1, on the development of BCG induced immunity to Mtb. Our introduction outlined some of the shortcomings of BCG that may contribute to its limited protective capabilities, including utilization of immune evasion mechanisms employed by pathogenic mycobacterial strains. Using the BCG $\Delta$ *hip1* strain, we reveal that BCG uses Hip1 to suppress and evade the immune responses elicited by the vaccine. We provide key insights into the relationship between BCG and dendritic cells (DCs),

showing that BCG $\Delta$ *hip1* is better able to stimulate DC maturation and functions including pro-inflammatory cytokine production and activation of T-cells. We report that BCG $\Delta$ *hip1* infected DCs are able to drive differentiation of T cells to Th1 and Th17 types both in vitro and within mouse lungs, and to stimulate production of more polyfunctional T-cells in vivo. Notably, we found that the enhanced immune responses stimulated by BCG $\Delta$ *hip1* results in better protection of mice against Mtb challenge. In summary, our findings identify the mycobacterial immune evasion protease, Hip1, as a key player in the suboptimal immune responses elicited by BCG.

Our findings on the role of Hip1 in BCG extend previous findings published from our laboratory in Mtb, which revealed that Mtb Hip1 dampens DC functions and subsequently T cell response during Mtb infection (105). Importantly, our findings significantly contributing to a growing body of work implicating genes previously characterized as Mtb immune evasion genes in dampened BCG induced immunity (88, 91, 129, 130, 137, 181, 182). For instance, a BCG study found that the secreted acid phosphatase, SapM, which was previously shown to be necessary for Mtb-driven arrest of phagosomal maturation and overall virulence (183, 184), also contributed to BCG immune evasion (91). Similar to our BCG $\Delta$ *hip1* strain, a BCG strain lacking SapM was able to induce enhanced maturation and cytokine production from DCs, and vaccination with the strain provided better protection from Mtb challenge than WT BCG (91).

In this dissertation, we utilized a DC intratracheal administration vaccination model for our BCG $\Delta$ *hip1* vaccination studies, which allowed us to highlight the important role of

the enhanced DC functions stimulated by the mutant strain. Ideally, we would like to investigate the protective capabilities of BCG $\Delta$ *hip1* in a traditional vaccination model, however very preliminary data from one trial suggests that the mutant strain is cleared from mouse lungs quicker than the parental BCG strain. These findings are not completely surprising, when we consider that several screens have implicated Hip1 as being necessary for survival of Mtb in mice (162, 163) as well as in macrophages (107). While the Mtb *hip1* mutant is capable of persisting within mouse lungs (74), unlike Mtb, BCG is cleared from host organisms. BCG lacks many immune evasion mechanisms that Mtb uses, which allow the pathogen to persist within host lungs. Deletion of one immune evasion gene, such as *hip1*, from BCG may have a significant effect on bacterial survival in vivo. Further studies (by Kevin Sia and Ana Enriquez) are ongoing to determine the survival of intratracheally instilled BCG $\Delta$ *hip1* compared to wild-type BCG in mouse lungs.

Aside from the use of BCG $\Delta$ *hip1* as a replacement to the current BCG vaccine, it may be of interest to investigate the use of our novel strain as a potential boost to BCG. As mentioned in the introduction of this dissertation, BCG offers limited protection, mainly to children against disseminated TB (81, 82), and that evidence suggests that peak memory responses elicited by the vaccine occur about 10 weeks after vaccination (83). There are a number of trials currently underway with vaccines that are aimed to either serve as BCG boosts or post-exposure vaccinations (185). While further studies would need to be conducted to investigate the strategy, it would be of great interest to

investigate whether the *BCG $\Delta$ hip1* strain would better serve as a boost to BCG vaccination.

In chapter 3 of this dissertation work, we provided insight into the relationship of the predicted secreted protease, Rv2223c, with its homolog, Hip1. We highlighted the high amino acid similarity between both proteins along with their high conservation across both pathogenic and nonpathogenic mycobacterial species. Further, through our characterization studies, we discovered that Rv2223c is secreted from mycobacterial cells in signal sequence dependent manner and revealed that the enzyme is autoproteolytically cleaved upon its secretion. We found that Rv2223c interacts with the chaperonin-like protein GroEL2, which we have previously identified as a physiological substrate of Hip1 (74, 76). However, Rv2223c was unable to complement the GroEL2 cleavage defect of a *hip1* mutant strain of Mtb when overexpressed in this strain.

We hypothesize, due to their high mycobacterial conservation, genomic proximity, and high similarity that Rv2223c and Hip1 may work in conjunction with one another to perform a critical function within mycobacterial cells. Further evidence supporting this hypothesis is the fact that Mtb appears to be resistant to a double deletion of *hip1* and *Rv2223c*, as all attempts to knockout this region resulted in recombination of the genes elsewhere in the genome (Chapter 4). If Rv2223c and Hip1 are truly essential for Mtb survival, their localization at the host pathogen makes them ideal targets for therapeutic drugs agents against TB. In fact, recent findings from and investigation of a cyclopiostin

and cyclophostin analog found to display strong activity against extracellular Mtb revealed Hip1 as one of the targets of the drug (186).

Bacterial pathogens often utilize proteases for their virulence-specific functions, and exported proteases have the unique opportunity to cleave both bacterial proteins or directly targeted host substrates (187). With Hip1 associated with the cell wall (74) and Rv2223c secreted from mycobacterial cells as shown in Chapter 3 of this dissertation, both proteins are situated at the host-pathogen interface. While we have only shown that Rv2223c is able to interact with GroEL2 of Mtb, it is possible that since Rv2223c is released from Mtb, that it may target some host proteins for proteolysis. Secreted proteases from a number of bacterial pathogens have been shown to cleave host proteins in order to evade host immunity. For instance, *Staphylococcus aureus* is known to secrete many proteases during infection, including staphopain A, which directly cleaves the host chemokine receptor, CXCR2 in order to block neutrophil migration to the site of infection (148). An interesting avenue to pursue for further studies of Rv2223c would be to identify potential host substrates through pull-down studies with purified Rv2223c.

Our efforts to purify Rv2223c were unsuccessful, but did provide some insight into more optimal conditions under which the protein may be purified, which were reported in chapter 4. We showed in chapter 3 that Rv2223c undergoes autoproteolytic processing upon its secretion from mycobacterial cells, which is reflective of the fact that many secreted bacterial proteases are expressed as pro-enzymes that require processing for full activation. Further, the cleaved pro-peptide of autoproteolytically cleaved bacterial

proteases can be required for their stability. For example, the cell membrane-associated Mtb serine protease, MycP1 is stabilized by its cleaved pro-peptide, and displays enhanced activity against its protein substrate in the presence of the peptide (168). While our attempts to detect expression of the full-length Rv2223c protein in *E. coli* were unsuccessful (data not shown), future efforts revisiting this approach may be worthwhile.

Along with autoproteolytic processing, we discovered that Rv2223c is also able to interact with the Hip1 protein substrate, GroEL2. While researchers have not yet demonstrated whether GroEL2 is capable of chaperone activity, the essential protein is annotated as a chaperonin-like protein. A recent study reported interaction of the Mtb protease, RipA with the chaperone, MoxR1 (188). Interestingly, co-expression of the two proteins in *E. coli* resulted in enhanced solubility of RipA and resulted in some localization of properly folded RipA in supernatants as opposed to localization in inclusion bodies (188). Studies by our collaborators are ongoing to explore GroEL2 activity along with potentially purifying Rv2223c in the presence of GroEL2. Upon successful purification of Rv2223c, we envision conducting interaction studies to investigate whether the protein forms a complex with GroEL2 and Hip1, which have both previously been successfully purified, will be of great interest.

There is a crucial need to develop more efficacious therapeutics and vaccines to combat tuberculosis. Overall, the findings presented in this dissertation highlight the benefits of studying the various immune evasion mechanisms of Mtb in addressing this necessity. Gaining a better understanding of the mycobacterial genes necessary for modulation or

suppression of host immune responses, can unlock the door to a host of potential new treatment drug targets and vaccine candidates for effective immunity to tuberculosis.

**Chapter 6**  
**Bibliography**

1. Evans AS. Causation and disease: the Henle-Koch postulates revisited. *The Yale journal of biology and medicine*. 1976;49(2):175-95. Epub 1976/05/01. PubMed PMID: 782050; PMCID: PMC2595276.
2. Falkow S. Molecular Koch's postulates applied to bacterial pathogenicity--a personal recollection 15 years later. *Nature reviews Microbiology*. 2004;2(1):67-72. Epub 2004/03/24. doi: 10.1038/nrmicro799. PubMed PMID: 15035010.
3. Hershkovitz I, Donoghue HD, Minnikin DE, Besra GS, Lee OY, Gernaey AM, Galili E, Eshed V, Greenblatt CL, Lemma E, Bar-Gal GK, Spigelman M. Detection and molecular characterization of 9,000-year-old *Mycobacterium tuberculosis* from a Neolithic settlement in the Eastern Mediterranean. *PloS one*. 2008;3(10):e3426. Epub 2008/10/17. doi: 10.1371/journal.pone.0003426. PubMed PMID: 18923677; PMCID: PMC2565837.
4. Donoghue HD. Paleomicrobiology of Human Tuberculosis. *Microbiology spectrum*. 2016;4(4). Epub 2016/10/12. doi: 10.1128/microbiolspec.PoH-0003-2014. PubMed PMID: 27726782.
5. Cambau E, Drancourt M. Steps towards the discovery of *Mycobacterium tuberculosis* by Robert Koch, 1882. *Clinical microbiology and infection : the official publication of the European Society of Clinical Microbiology and Infectious Diseases*. 2014;20(3):196-201. Epub 2014/01/24. doi: 10.1111/1469-0691.12555. PubMed PMID: 24450600.

6. WHO. World Health Organization-Tuberculosis Fact Sheet  
<http://www.who.int/mediacentre/factsheets/fs104/en/2017> [updated March 2017; cited 2017 05-10-2017].
7. Wells WF, Ratcliffe HL, Grumb C. On the mechanics of droplet nuclei infection; quantitative experimental air-borne tuberculosis in rabbits. *American journal of hygiene*. 1948;47(1):11-28. Epub 1948/01/01. PubMed PMID: 18921435.
8. Pieters J. Mycobacterium tuberculosis and the macrophage: maintaining a balance. *Cell host & microbe*. 2008;3(6):399-407. Epub 2008/06/11. doi: 10.1016/j.chom.2008.05.006. PubMed PMID: 18541216.
9. Reiley WW, Calayag MD, Wittmer ST, Huntington JL, Pearl JE, Fountain JJ, Martino CA, Roberts AD, Cooper AM, Winslow GM, Woodland DL. ESAT-6-specific CD4 T cell responses to aerosol Mycobacterium tuberculosis infection are initiated in the mediastinal lymph nodes. *Proceedings of the National Academy of Sciences of the United States of America*. 2008;105(31):10961-6. Epub 2008/08/01. doi: 10.1073/pnas.0801496105. PubMed PMID: 18667699; PMCID: PMC2504808.
10. Keane J, Gershon S, Wise RP, Mirabile-Levens E, Kasznica J, Schwieterman WD, Siegel JN, Braun MM. Tuberculosis associated with infliximab, a tumor necrosis factor alpha-neutralizing agent. *The New England journal of medicine*. 2001;345(15):1098-104. Epub 2001/10/13. doi: 10.1056/NEJMoa011110. PubMed PMID: 11596589.
11. Kwan CK, Ernst JD. HIV and tuberculosis: a deadly human syndemic. *Clinical microbiology reviews*. 2011;24(2):351-76. Epub 2011/04/13. doi: 10.1128/cmr.00042-10. PubMed PMID: 21482729; PMCID: PMC3122491.

12. Tuberculin Skin Testing. Fact Sheet. CDC, Elimination DoT; 2016.
13. Interferon-Gamma Release Assays (IGRAs) - Blood Tests for TB Infection. CDC, Elimination DoT; 2015.
14. Daniel TM. The history of tuberculosis. *Respiratory medicine*. 2006;100(11):1862-70. Epub 2006/09/05. doi: 10.1016/j.rmed.2006.08.006. PubMed PMID: 16949809.
15. Schatz A, Bugie E, Waksman SA. Streptomycin, a substance exhibiting antibiotic activity against gram-positive and gram-negative bacteria. . *Proc Exp Biol Med*. 1944(55):66-9. Epub 2005/08/02. PubMed PMID: 16056018.
16. Nahid P, Dorman SE, Alipanah N, Barry PM, Brozek JL, Cattamanchi A, Chaisson LH, Chaisson RE, Daley CL, Grzemska M, Higashi JM, Ho CS, Hopewell PC, Keshavjee SA, Lienhardt C, Menzies R, Merrifield C, Narita M, O'Brien R, Peloquin CA, Raftery A, Saukkonen J, Schaaf HS, Sotgiu G, Starke JR, Migliori GB, Vernon A. Executive Summary: Official American Thoracic Society/Centers for Disease Control and Prevention/Infectious Diseases Society of America Clinical Practice Guidelines: Treatment of Drug-Susceptible Tuberculosis. *Clinical infectious diseases : an official publication of the Infectious Diseases Society of America*. 2016;63(7):853-67. Epub 2016/09/14. doi: 10.1093/cid/ciw566. PubMed PMID: 27621353.
17. Recommendations for use of an isoniazid-rifapentine regimen with direct observation to treat latent *Mycobacterium tuberculosis* infection. *MMWR Morbidity and mortality weekly report*. 2011;60(48):1650-3. Epub 2011/12/14. PubMed PMID: 22157884.

18. Smith T, Wolff KA, Nguyen L. Molecular biology of drug resistance in *Mycobacterium tuberculosis*. *Current topics in microbiology and immunology*. 2013;374:53-80. Epub 2012/11/28. doi: 10.1007/82\_2012\_279. PubMed PMID: 23179675; PMCID: PMC3982203.
19. Marks SM, Flood J, Seaworth B, Hirsch-Moverman Y, Armstrong L, Mase S, Salcedo K, Oh P, Graviss EA, Colson PW, Armitige L, Revuelta M, Sheeran K. Treatment practices, outcomes, and costs of multidrug-resistant and extensively drug-resistant tuberculosis, United States, 2005-2007. *Emerging infectious diseases*. 2014;20(5):812-21. Epub 2014/04/23. doi: 10.3201/eid2005.131037. PubMed PMID: 24751166; PMCID: PMC4012799.
20. Hett EC, Rubin EJ. Bacterial growth and cell division: a mycobacterial perspective. *Microbiology and molecular biology reviews : MMBR*. 2008;72(1):126-56, table of contents. Epub 2008/03/07. doi: 10.1128/mmbr.00028-07. PubMed PMID: 18322037; PMCID: PMC2268284.
21. Chatterjee D, Lowell K, Rivoire B, McNeil MR, Brennan PJ. Lipoarabinomannan of *Mycobacterium tuberculosis*. Capping with mannosyl residues in some strains. *The Journal of biological chemistry*. 1992;267(9):6234-9. Epub 1992/03/25. PubMed PMID: 1556132.
22. Madkour MMA-O, K. E.; Swailem R.A. Historical aspects of tuberculosis. In: Madkour MM, editor. *Tuberculosis*. Germany Springer; 2004. p. 23.
23. Cole ST, Brosch R, Parkhill J, Garnier T, Churcher C, Harris D, Gordon SV, Eiglmeier K, Gas S, Barry CE, 3rd, Tekaia F, Badcock K, Basham D, Brown D, Chillingworth T, Connor R, Davies R, Devlin K, Feltwell T, Gentles S, Hamlin N,

Holroyd S, Hornsby T, Jagels K, Krogh A, McLean J, Moule S, Murphy L, Oliver K, Osborne J, Quail MA, Rajandream MA, Rogers J, Rutter S, Seeger K, Skelton J, Squares R, Squares S, Sulston JE, Taylor K, Whitehead S, Barrell BG. Deciphering the biology of *Mycobacterium tuberculosis* from the complete genome sequence. *Nature*. 1998;393(6685):537-44. Epub 1998/06/20. doi: 10.1038/31159. PubMed PMID: 9634230.

24. Garnier T, Eiglmeier K, Camus JC, Medina N, Mansoor H, Pryor M, Duthoy S, Grondin S, Lacroix C, Monsempe C, Simon S, Harris B, Atkin R, Doggett J, Mayes R, Keating L, Wheeler PR, Parkhill J, Barrell BG, Cole ST, Gordon SV, Hewinson RG. The complete genome sequence of *Mycobacterium bovis*. *Proceedings of the National Academy of Sciences of the United States of America*. 2003;100(13):7877-82. Epub 2003/06/06. doi: 10.1073/pnas.1130426100. PubMed PMID: 12788972; PMCID: PMC164681.

25. Bentley SD, Comas I, Bryant JM, Walker D, Smith NH, Harris SR, Thurston S, Gagneux S, Wood J, Antonio M, Quail MA, Gehre F, Adegbola RA, Parkhill J, de Jong BC. The genome of *Mycobacterium africanum* West African 2 reveals a lineage-specific locus and genome erosion common to the *M. tuberculosis* complex. *PLoS neglected tropical diseases*. 2012;6(2):e1552. Epub 2012/03/06. doi: 10.1371/journal.pntd.0001552. PubMed PMID: 22389744; PMCID: PMC3289620.

26. Zhu L, Zhong J, Jia X, Liu G, Kang Y, Dong M, Zhang X, Li Q, Yue L, Li C, Fu J, Xiao J, Yan J, Zhang B, Lei M, Chen S, Lv L, Zhu B, Huang H, Chen F. Precision methylome characterization of *Mycobacterium tuberculosis* complex (MTBC) using PacBio single-molecule real-time (SMRT) technology. *Nucleic acids research*.

2016;44(2):730-43. Epub 2015/12/26. doi: 10.1093/nar/gkv1498. PubMed PMID: 26704977; PMCID: PMC4737169.

27. Medina E, North RJ. Resistance ranking of some common inbred mouse strains to *Mycobacterium tuberculosis* and relationship to major histocompatibility complex haplotype and *Nramp1* genotype. *Immunology*. 1998;93(2):270-4. Epub 1998/06/09. PubMed PMID: 9616378; PMCID: PMC1364188.

28. Harper J, Skerry C, Davis SL, Tasneen R, Weir M, Kramnik I, Bishai WR, Pomper MG, Nuernberger EL, Jain SK. Mouse model of necrotic tuberculosis granulomas develops hypoxic lesions. *The Journal of infectious diseases*. 2012;205(4):595-602. Epub 2011/12/27. doi: 10.1093/infdis/jir786. PubMed PMID: 22198962; PMCID: PMC3266133.

29. Chackerian AA, Perera TV, Behar SM. Gamma interferon-producing CD4+ T lymphocytes in the lung correlate with resistance to infection with *Mycobacterium tuberculosis*. *Infection and immunity*. 2001;69(4):2666-74. Epub 2001/03/20. doi: 10.1128/iai.69.4.2666-2674.2001. PubMed PMID: 11254633; PMCID: PMC98205.

30. Cooper AM, Dalton DK, Stewart TA, Griffin JP, Russell DG, Orme IM. Disseminated tuberculosis in interferon gamma gene-disrupted mice. *The Journal of experimental medicine*. 1993;178(6):2243-7. Epub 1993/12/01. PubMed PMID: 8245795; PMCID: PMC2191280.

31. Cooper AM, Magram J, Ferrante J, Orme IM. Interleukin 12 (IL-12) is crucial to the development of protective immunity in mice intravenously infected with *mycobacterium tuberculosis*. *The Journal of experimental medicine*. 1997;186(1):39-45. Epub 1997/07/07. PubMed PMID: 9206995; PMCID: PMC2198958.

32. Flynn JL, Goldstein MM, Chan J, Triebold KJ, Pfeffer K, Lowenstein CJ, Schreiber R, Mak TW, Bloom BR. Tumor necrosis factor-alpha is required in the protective immune response against *Mycobacterium tuberculosis* in mice. *Immunity*. 1995;2(6):561-72. Epub 1995/06/01. PubMed PMID: 7540941.
33. Beamer GL, Flaherty DK, Assogba BD, Stromberg P, Gonzalez-Juarrero M, de Waal Malefyt R, Vesosky B, Turner J. Interleukin-10 promotes *Mycobacterium tuberculosis* disease progression in CBA/J mice. *Journal of immunology (Baltimore, Md : 1950)*. 2008;181(8):5545-50. Epub 2008/10/04. PubMed PMID: 18832712; PMCID: PMC2728584.
34. Sia JK, Georgieva M, Rengarajan J. Innate Immune Defenses in Human Tuberculosis: An Overview of the Interactions between *Mycobacterium tuberculosis* and Innate Immune Cells. *Journal of immunology research*. 2015;2015:747543. Epub 2015/08/11. doi: 10.1155/2015/747543. PubMed PMID: 26258152; PMCID: PMC4516846.
35. Schlesinger LS, Hull SR, Kaufman TM. Binding of the terminal mannosyl units of lipoarabinomannan from a virulent strain of *Mycobacterium tuberculosis* to human macrophages. *Journal of immunology (Baltimore, Md : 1950)*. 1994;152(8):4070-9. Epub 1994/04/15. PubMed PMID: 8144972.
36. Gehring AJ, Dobos KM, Belisle JT, Harding CV, Boom WH. *Mycobacterium tuberculosis* LprG (Rv1411c): a novel TLR-2 ligand that inhibits human macrophage class II MHC antigen processing. *Journal of immunology (Baltimore, Md : 1950)*. 2004;173(4):2660-8. Epub 2004/08/06. PubMed PMID: 15294983.

37. Pecora ND, Gehring AJ, Canaday DH, Boom WH, Harding CV. Mycobacterium tuberculosis LprA is a lipoprotein agonist of TLR2 that regulates innate immunity and APC function. *Journal of immunology (Baltimore, Md : 1950)*. 2006;177(1):422-9. Epub 2006/06/21. PubMed PMID: 16785538.
38. Bulut Y, Michelsen KS, Hayrapetian L, Naiki Y, Spallek R, Singh M, Arditi M. Mycobacterium tuberculosis heat shock proteins use diverse Toll-like receptor pathways to activate pro-inflammatory signals. *The Journal of biological chemistry*. 2005;280(22):20961-7. Epub 2005/04/06. doi: 10.1074/jbc.M411379200. PubMed PMID: 15809303.
39. Coulombe F, Divangahi M, Veyrier F, de Leseleuc L, Gleason JL, Yang Y, Kelliher MA, Pandey AK, Sasseti CM, Reed MB, Behr MA. Increased NOD2-mediated recognition of N-glycolyl muramyl dipeptide. *The Journal of experimental medicine*. 2009;206(8):1709-16. Epub 2009/07/08. doi: 10.1084/jem.20081779. PubMed PMID: 19581406; PMCID: PMC2722178.
40. Juarez E, Carranza C, Hernandez-Sanchez F, Leon-Contreras JC, Hernandez-Pando R, Escobedo D, Torres M, Sada E. NOD2 enhances the innate response of alveolar macrophages to Mycobacterium tuberculosis in humans. *European journal of immunology*. 2012;42(4):880-9. Epub 2012/04/26. doi: 10.1002/eji.201142105. PubMed PMID: 22531915.
41. Lyons CR, Ball EJ, Toews GB, Weissler JC, Stastny P, Lipscomb MF. Inability of human alveolar macrophages to stimulate resting T cells correlates with decreased antigen-specific T cell-macrophage binding. *Journal of immunology (Baltimore, Md : 1950)*. 1986;137(4):1173-80. Epub 1986/08/15. PubMed PMID: 2426354.

42. Wolf AJ, Linas B, Trevejo-Nunez GJ, Kincaid E, Tamura T, Takatsu K, Ernst JD. Mycobacterium tuberculosis infects dendritic cells with high frequency and impairs their function in vivo. *Journal of immunology (Baltimore, Md : 1950)*. 2007;179(4):2509-19. Epub 2007/08/07. PubMed PMID: 17675513.
43. Geijtenbeek TB, Van Vliet SJ, Koppel EA, Sanchez-Hernandez M, Vandenbroucke-Grauls CM, Appelmek B, Van Kooyk Y. Mycobacteria target DC-SIGN to suppress dendritic cell function. *The Journal of experimental medicine*. 2003;197(1):7-17. Epub 2003/01/08. PubMed PMID: 12515809; PMCID: PMC2193797.
44. Bafica A, Scanga CA, Feng CG, Leifer C, Cheever A, Sher A. TLR9 regulates Th1 responses and cooperates with TLR2 in mediating optimal resistance to Mycobacterium tuberculosis. *The Journal of experimental medicine*. 2005;202(12):1715-24. Epub 2005/12/21. doi: 10.1084/jem.20051782. PubMed PMID: 16365150; PMCID: PMC2212963.
45. Pompei L, Jang S, Zamlynny B, Ravikumar S, McBride A, Hickman SP, Salgame P. Disparity in IL-12 release in dendritic cells and macrophages in response to Mycobacterium tuberculosis is due to use of distinct TLRs. *Journal of immunology (Baltimore, Md : 1950)*. 2007;178(8):5192-9. Epub 2007/04/04. PubMed PMID: 17404302.
46. Newport MJ, Huxley CM, Huston S, Hawrylowicz CM, Oostra BA, Williamson R, Levin M. A mutation in the interferon-gamma-receptor gene and susceptibility to mycobacterial infection. *The New England journal of medicine*. 1996;335(26):1941-9. Epub 1996/12/26. doi: 10.1056/nejm199612263352602. PubMed PMID: 8960473.

47. Jouanguy E, Altare F, Lamhamedi S, Revy P, Emile JF, Newport M, Levin M, Blanche S, Seboun E, Fischer A, Casanova JL. Interferon-gamma-receptor deficiency in an infant with fatal bacille Calmette-Guerin infection. *The New England journal of medicine*. 1996;335(26):1956-61. Epub 1996/12/26. doi: 10.1056/nejm199612263352604. PubMed PMID: 8960475.
48. Wozniak TM, Saunders BM, Ryan AA, Britton WJ. Mycobacterium bovis BCG-specific Th17 cells confer partial protection against Mycobacterium tuberculosis infection in the absence of gamma interferon. *Infection and immunity*. 2010;78(10):4187-94. Epub 2010/08/04. doi: 10.1128/iai.01392-09. PubMed PMID: 20679438; PMCID: PMC2950338.
49. Scriba TJ, Kalsdorf B, Abrahams DA, Isaacs F, Hofmeister J, Black G, Hassan HY, Wilkinson RJ, Walzl G, Gelderbloem SJ, Mahomed H, Hussey GD, Hanekom WA. Distinct, specific IL-17- and IL-22-producing CD4+ T cell subsets contribute to the human anti-mycobacterial immune response. *Journal of immunology (Baltimore, Md : 1950)*. 2008;180(3):1962-70. Epub 2008/01/23. PubMed PMID: 18209095; PMCID: PMC2219462.
50. Freches D, Korf H, Denis O, Havaux X, Huygen K, Romano M. Mice genetically inactivated in interleukin-17A receptor are defective in long-term control of Mycobacterium tuberculosis infection. *Immunology*. 2013;140(2):220-31. Epub 2013/06/01. doi: 10.1111/imm.12130. PubMed PMID: 23721367; PMCID: PMC3784168.
51. Khader SA, Bell GK, Pearl JE, Fountain JJ, Rangel-Moreno J, Cilley GE, Shen F, Eaton SM, Gaffen SL, Swain SL, Locksley RM, Haynes L, Randall TD, Cooper AM. IL-

23 and IL-17 in the establishment of protective pulmonary CD4<sup>+</sup> T cell responses after vaccination and during *Mycobacterium tuberculosis* challenge. *Nature immunology*.

2007;8(4):369-77. Epub 2007/03/14. doi: 10.1038/ni1449. PubMed PMID: 17351619.

52. Yonekawa A, Saijo S, Hoshino Y, Miyake Y, Ishikawa E, Suzukawa M, Inoue H, Tanaka M, Yoneyama M, Oh-Hora M, Akashi K, Yamasaki S. Dectin-2 is a direct receptor for mannose-capped lipoarabinomannan of mycobacteria. *Immunity*.

2014;41(3):402-13. Epub 2014/09/02. doi: 10.1016/j.immuni.2014.08.005. PubMed PMID: 25176311.

53. Noss EH, Pai RK, Sellati TJ, Radolf JD, Belisle J, Golenbock DT, Boom WH, Harding CV. Toll-like receptor 2-dependent inhibition of macrophage class II MHC expression and antigen processing by 19-kDa lipoprotein of *Mycobacterium tuberculosis*.

*Journal of immunology (Baltimore, Md : 1950)*. 2001;167(2):910-8. Epub 2001/07/07. PubMed PMID: 11441098.

54. Guinn KM, Hickey MJ, Mathur SK, Zakel KL, Grotzke JE, Lewinsohn DM, Smith S, Sherman DR. Individual RD1-region genes are required for export of ESAT-6/CFP-10 and for virulence of *Mycobacterium tuberculosis*. *Molecular microbiology*.

2004;51(2):359-70. Epub 2004/02/06. doi: 10.1046/j.1365-2958.2003.03844.x. PubMed PMID: 14756778; PMCID: PMC1458497.

55. Lewis KN, Liao R, Guinn KM, Hickey MJ, Smith S, Behr MA, Sherman DR.

Deletion of RD1 from *Mycobacterium tuberculosis* mimics bacille Calmette-Guerin attenuation. *The Journal of infectious diseases*. 2003;187(1):117-23. Epub 2003/01/01.

doi: 10.1086/345862. PubMed PMID: 12508154; PMCID: PMC1458498.

56. Pym AS, Brodin P, Brosch R, Huerre M, Cole ST. Loss of RD1 contributed to the attenuation of the live tuberculosis vaccines *Mycobacterium bovis* BCG and *Mycobacterium microti*. *Molecular microbiology*. 2002;46(3):709-17. Epub 2002/11/02. PubMed PMID: 12410828.
57. Mahairas GG, Sabo PJ, Hickey MJ, Singh DC, Stover CK. Molecular analysis of genetic differences between *Mycobacterium bovis* BCG and virulent *M. bovis*. *Journal of bacteriology*. 1996;178(5):1274-82. Epub 1996/03/01. PubMed PMID: 8631702; PMCID: PMC177799.
58. Gey Van Pittius NC, Gamielien J, Hide W, Brown GD, Siezen RJ, Beyers AD. The ESAT-6 gene cluster of *Mycobacterium tuberculosis* and other high G+C Gram-positive bacteria. *Genome biology*. 2001;2(10):Research0044. Epub 2001/10/13. PubMed PMID: 11597336; PMCID: PMC57799.
59. Stanley SA, Raghavan S, Hwang WW, Cox JS. Acute infection and macrophage subversion by *Mycobacterium tuberculosis* require a specialized secretion system. *Proceedings of the National Academy of Sciences of the United States of America*. 2003;100(22):13001-6. Epub 2003/10/15. doi: 10.1073/pnas.2235593100. PubMed PMID: 14557536; PMCID: PMC240734.
60. Simeone R, Bottai D, Brosch R. ESX/type VII secretion systems and their role in host-pathogen interaction. *Current opinion in microbiology*. 2009;12(1):4-10. Epub 2009/01/22. doi: 10.1016/j.mib.2008.11.003. PubMed PMID: 19155186.
61. Stoop EJ, Bitter W, van der Sar AM. Tubercle bacilli rely on a type VII army for pathogenicity. *Trends in microbiology*. 2012;20(10):477-84. Epub 2012/08/04. doi: 10.1016/j.tim.2012.07.001. PubMed PMID: 22858229.

62. Basu SK, Kumar D, Singh DK, Ganguly N, Siddiqui Z, Rao KV, Sharma P. Mycobacterium tuberculosis secreted antigen (MTSA-10) modulates macrophage function by redox regulation of phosphatases. *The FEBS journal*. 2006;273(24):5517-34. Epub 2007/01/11. doi: 10.1111/j.1742-4658.2006.05543.x. PubMed PMID: 17212774.
63. Smith J, Manoranjan J, Pan M, Bohsali A, Xu J, Liu J, McDonald KL, Szyk A, LaRonde-LeBlanc N, Gao LY. Evidence for pore formation in host cell membranes by ESX-1-secreted ESAT-6 and its role in Mycobacterium marinum escape from the vacuole. *Infection and immunity*. 2008;76(12):5478-87. Epub 2008/10/15. doi: 10.1128/iai.00614-08. PubMed PMID: 18852239; PMCID: PMC2583575.
64. Derrick SC, Morris SL. The ESAT6 protein of Mycobacterium tuberculosis induces apoptosis of macrophages by activating caspase expression. *Cellular microbiology*. 2007;9(6):1547-55. Epub 2007/02/15. doi: 10.1111/j.1462-5822.2007.00892.x. PubMed PMID: 17298391.
65. Sorensen AL, Nagai S, Houen G, Andersen P, Andersen AB. Purification and characterization of a low-molecular-mass T-cell antigen secreted by Mycobacterium tuberculosis. *Infection and immunity*. 1995;63(5):1710-7. Epub 1995/05/01. PubMed PMID: 7729876; PMCID: PMC173214.
66. Andersen P, Andersen AB, Sorensen AL, Nagai S. Recall of long-lived immunity to Mycobacterium tuberculosis infection in mice. *Journal of immunology (Baltimore, Md : 1950)*. 1995;154(7):3359-72. Epub 1995/04/01. PubMed PMID: 7897219.
67. Rohde K, Yates RM, Purdy GE, Russell DG. Mycobacterium tuberculosis and the environment within the phagosome. *Immunological reviews*. 2007;219:37-54. Epub 2007/09/14. doi: 10.1111/j.1600-065X.2007.00547.x. PubMed PMID: 17850480.

68. Wong D, Bach H, Sun J, Hmama Z, Av-Gay Y. Mycobacterium tuberculosis protein tyrosine phosphatase (PtpA) excludes host vacuolar-H<sup>+</sup>-ATPase to inhibit phagosome acidification. *Proceedings of the National Academy of Sciences of the United States of America*. 2011;108(48):19371-6. Epub 2011/11/17. doi: 10.1073/pnas.1109201108. PubMed PMID: 22087003; PMCID: PMC3228452.
69. Walburger A, Koul A, Ferrari G, Nguyen L, Prescianotto-Baschong C, Huygen K, Klebl B, Thompson C, Bacher G, Pieters J. Protein kinase G from pathogenic mycobacteria promotes survival within macrophages. *Science (New York, NY)*. 2004;304(5678):1800-4. Epub 2004/05/25. doi: 10.1126/science.1099384. PubMed PMID: 15155913.
70. Pais TF, Silva RA, Smedegaard B, Appelberg R, Andersen P. Analysis of T cells recruited during delayed-type hypersensitivity to purified protein derivative (PPD) versus challenge with tuberculosis infection. *Immunology*. 1998;95(1):69-75. Epub 1998/10/10. PubMed PMID: 9767459; PMCID: PMC1364378.
71. Rogerson BJ, Jung YJ, LaCourse R, Ryan L, Enright N, North RJ. Expression levels of Mycobacterium tuberculosis antigen-encoding genes versus production levels of antigen-specific T cells during stationary level lung infection in mice. *Immunology*. 2006;118(2):195-201. Epub 2006/06/15. doi: 10.1111/j.1365-2567.2006.02355.x. PubMed PMID: 16771854; PMCID: PMC1782281.
72. Winslow GM, Cooper A, Reiley W, Chatterjee M, Woodland DL. Early T-cell responses in tuberculosis immunity. *Immunological reviews*. 2008;225:284-99. Epub 2008/10/08. doi: 10.1111/j.1600-065X.2008.00693.x. PubMed PMID: 18837789; PMCID: PMC3827678.

73. Baena A, Porcelli SA. Evasion and subversion of antigen presentation by *Mycobacterium tuberculosis*. *Tissue antigens*. 2009;74(3):189-204. Epub 2009/07/01. doi: 10.1111/j.1399-0039.2009.01301.x. PubMed PMID: 19563525; PMCID: PMC2753606.
74. Rengarajan J, Murphy E, Park A, Krone CL, Hett EC, Bloom BR, Glimcher LH, Rubin EJ. *Mycobacterium tuberculosis* Rv2224c modulates innate immune responses. *Proceedings of the National Academy of Sciences of the United States of America*. 2008;105(1):264-9. Epub 2008/01/04. doi: 10.1073/pnas.0710601105. PubMed PMID: 18172199; PMCID: PMC2224198.
75. Madan-Lala R, Peixoto KV, Re F, Rengarajan J. *Mycobacterium tuberculosis* Hip1 dampens macrophage proinflammatory responses by limiting toll-like receptor 2 activation. *Infection and immunity*. 2011;79(12):4828-38. Epub 2011/09/29. doi: 10.1128/iai.05574-11. PubMed PMID: 21947769; PMCID: PMC3232659.
76. Naffin-Olivos JL, Georgieva M, Goldfarb N, Madan-Lala R, Dong L, Bizzell E, Valinetz E, Brandt GS, Yu S, Shabashvili DE, Ringe D, Dunn BM, Petsko GA, Rengarajan J. *Mycobacterium tuberculosis* Hip1 modulates macrophage responses through proteolysis of GroEL2. *PLoS pathogens*. 2014;10(5):e1004132. Epub 2014/05/17. doi: 10.1371/journal.ppat.1004132. PubMed PMID: 24830429; PMCID: PMC4022732.
77. Tran V, Liu J, Behr MA. BCG Vaccines. *Microbiology spectrum*. 2014;2(1):Mgm2-0028-2013. Epub 2014/02/01. doi: 10.1128/microbiolspec.MGM2-0028-2013. PubMed PMID: 26082111.

78. Calmette A. Preventive Vaccination Against Tuberculosis with BCG. Proceedings of the Royal Society of Medicine. 1931;24(11):1481-90. Epub 1931/09/01. PubMed PMID: 19988326; PMCID: PMC2182232.
79. Zwerling A, Behr MA, Verma A, Brewer TF, Menzies D, Pai M. The BCG World Atlas: a database of global BCG vaccination policies and practices. PLoS medicine. 2011;8(3):e1001012. Epub 2011/03/30. doi: 10.1371/journal.pmed.1001012. PubMed PMID: 21445325; PMCID: PMC3062527.
80. Behr MA, Wilson MA, Gill WP, Salamon H, Schoolnik GK, Rane S, Small PM. Comparative genomics of BCG vaccines by whole-genome DNA microarray. Science (New York, NY). 1999;284(5419):1520-3. Epub 1999/05/29. PubMed PMID: 10348738.
81. Mangtani P, Abubakar I, Ariti C, Beynon R, Pimpin L, Fine PE, Rodrigues LC, Smith PG, Lipman M, Whiting PF, Sterne JA. Protection by BCG vaccine against tuberculosis: a systematic review of randomized controlled trials. Clinical infectious diseases : an official publication of the Infectious Diseases Society of America. 2014;58(4):470-80. Epub 2013/12/18. doi: 10.1093/cid/cit790. PubMed PMID: 24336911.
82. Trunz BB, Fine P, Dye C. Effect of BCG vaccination on childhood tuberculous meningitis and miliary tuberculosis worldwide: a meta-analysis and assessment of cost-effectiveness. Lancet (London, England). 2006;367(9517):1173-80. Epub 2006/04/18. doi: 10.1016/s0140-6736(06)68507-3. PubMed PMID: 16616560.
83. Soares AP, Kwong Chung CK, Choice T, Hughes EJ, Jacobs G, van Rensburg EJ, Khomba G, de Kock M, Lerumo L, Makhetha L, Maneli MH, Pienaar B, Smit E, Tena-Coki NG, van Wyk L, Boom WH, Kaplan G, Scriba TJ, Hanekom WA. Longitudinal

changes in CD4(+) T-cell memory responses induced by BCG vaccination of newborns.

The Journal of infectious diseases. 2013;207(7):1084-94. Epub 2013/01/08. doi:

10.1093/infdis/jis941. PubMed PMID: 23293360; PMCID: PMC3583271.

84. Lahey T, von Reyn CF. Mycobacterium bovis BCG and New Vaccines for the Prevention of Tuberculosis. Microbiology spectrum. 2016;4(5). Epub 2016/10/21. doi:

10.1128/microbiolspec.TNMI7-0003-2016. PubMed PMID: 27763257.

85. Colditz GA, Brewer TF, Berkey CS, Wilson ME, Burdick E, Fineberg HV, Mosteller F. Efficacy of BCG vaccine in the prevention of tuberculosis. Meta-analysis of the published literature. Jama. 1994;271(9):698-702. Epub 1994/03/02. PubMed PMID: 8309034.

86. Brewer TF. Preventing tuberculosis with bacillus Calmette-Guerin vaccine: a meta-analysis of the literature. Clinical infectious diseases : an official publication of the Infectious Diseases Society of America. 2000;31 Suppl 3:S64-7. Epub 2000/09/30. doi: 10.1086/314072. PubMed PMID: 11010824.

87. Kernodle DS. Decrease in the effectiveness of Bacille Calmette-Guerin vaccine against pulmonary tuberculosis: a consequence of increased immune suppression by microbial antioxidants, not overattenuation. Clinical infectious diseases : an official publication of the Infectious Diseases Society of America. 2010;51(2):177-84. Epub 2010/06/08. doi: 10.1086/653533. PubMed PMID: 20524854.

88. Sadagopal S, Braunstein M, Hager CC, Wei J, Daniel AK, Bochan MR, Crozier I, Smith NE, Gates HO, Barnett L, Van Kaer L, Price JO, Blackwell TS, Kalams SA, Kernodle DS. Reducing the activity and secretion of microbial antioxidants enhances the

- immunogenicity of BCG. *PloS one*. 2009;4(5):e5531. Epub 2009/05/14. doi: 10.1371/journal.pone.0005531. PubMed PMID: 19436730; PMCID: PMC2677452.
89. Gengenbacher M, Nieuwenhuizen NE, Kaufmann S. BCG - old workhorse, new skills. *Current opinion in immunology*. 2017;47:8-16. Epub 2017/07/19. doi: 10.1016/j.coi.2017.06.007. PubMed PMID: 28719821.
90. Moliva JI, Turner J, Torrelles JB. Prospects in *Mycobacterium bovis* Bacille Calmette et Guerin (BCG) vaccine diversity and delivery: why does BCG fail to protect against tuberculosis? *Vaccine*. 2015;33(39):5035-41. Epub 2015/09/01. doi: 10.1016/j.vaccine.2015.08.033. PubMed PMID: 26319069; PMCID: PMC4577463.
91. Festjens N, Bogaert P, Batni A, Houthuys E, Plets E, Vanderschaeghe D, Laukens B, Asselbergh B, Parthoens E, De Rycke R, Willart MA, Jacques P, Elewaut D, Brouckaert P, Lambrecht BN, Huygen K, Callewaert N. Disruption of the SapM locus in *Mycobacterium bovis* BCG improves its protective efficacy as a vaccine against *M. tuberculosis*. *EMBO molecular medicine*. 2011;3(4):222-34. Epub 2011/02/18. doi: 10.1002/emmm.201000125. PubMed PMID: 21328541; PMCID: PMC3377067.
92. Grode L, Ganoza CA, Brohm C, Weiner J, 3rd, Eisele B, Kaufmann SH. Safety and immunogenicity of the recombinant BCG vaccine VPM1002 in a phase 1 open-label randomized clinical trial. *Vaccine*. 2013;31(9):1340-8. Epub 2013/01/08. doi: 10.1016/j.vaccine.2012.12.053. PubMed PMID: 23290835.
93. Loxton AG, Knaul JK, Grode L, Gutschmidt A, Meller C, Eisele B, Johnstone H, van der Spuy G, Maertzdorf J, Kaufmann SH, Hesselring AC, Walzl G, Cotton MF. Safety and Immunogenicity of the Recombinant *Mycobacterium bovis* BCG Vaccine VPM1002 in HIV-Unexposed Newborn Infants in South Africa. *Clinical and vaccine*

immunology : CVI. 2017;24(2). Epub 2016/12/16. doi: 10.1128/cvi.00439-16. PubMed PMID: 27974398; PMCID: PMC5299117.

94. Kaufmann SH, Cotton MF, Eisele B, Gengenbacher M, Grode L, Hesselting AC, Walzl G. The BCG replacement vaccine VPM1002: from drawing board to clinical trial. *Expert review of vaccines*. 2014;13(5):619-30. Epub 2014/04/08. doi: 10.1586/14760584.2014.905746. PubMed PMID: 24702486.

95. Tameris MD, Hatherill M, Landry BS, Scriba TJ, Snowden MA, Lockhart S, Shea JE, McClain JB, Hussey GD, Hanekom WA, Mahomed H, McShane H. Safety and efficacy of MVA85A, a new tuberculosis vaccine, in infants previously vaccinated with BCG: a randomised, placebo-controlled phase 2b trial. *Lancet (London, England)*. 2013;381(9871):1021-8. Epub 2013/02/09. doi: 10.1016/s0140-6736(13)60177-4. PubMed PMID: 23391465.

96. Supuran CT, Scozzafava A, Clare BW. Bacterial protease inhibitors. *Medicinal research reviews*. 2002;22(4):329-72. Epub 2002/07/12. doi: 10.1002/med.10007. PubMed PMID: 12111749.

97. White MJ, He H, Penoske RM, Twining SS, Zahrt TC. PepD participates in the mycobacterial stress response mediated through MprAB and SigE. *Journal of bacteriology*. 2010;192(6):1498-510. Epub 2010/01/12. doi: 10.1128/jb.01167-09. PubMed PMID: 20061478; PMCID: PMC2832534.

98. Ohol YM, Goetz DH, Chan K, Shiloh MU, Craik CS, Cox JS. Mycobacterium tuberculosis MycP1 protease plays a dual role in regulation of ESX-1 secretion and virulence. *Cell host & microbe*. 2010;7(3):210-20. Epub 2010/03/17. doi: 10.1016/j.chom.2010.02.006. PubMed PMID: 20227664; PMCID: PMC3121311.

99. Zhao N, Darby CM, Small J, Bachovchin DA, Jiang X, Burns-Huang KE, Botella H, Ehrh S, Boger DL, Anderson ED, Cravatt BF, Speers AE, Fernandez-Vega V, Hodder PS, Eberhart C, Rosen H, Spicer TP, Nathan CF. Target-based screen against a periplasmic serine protease that regulates intrabacterial pH homeostasis in *Mycobacterium tuberculosis*. *ACS chemical biology*. 2015;10(2):364-71. Epub 2014/12/03. doi: 10.1021/cb500746z. PubMed PMID: 25457457; PMCID: PMC4340348.
100. Gavriš E, Sit CS, Cao S, Kandror O, Spoering A, Peoples A, Ling L, Fetterman A, Hughes D, Bissell A, Torrey H, Akopian T, Mueller A, Epstein S, Goldberg A, Clardy J, Lewis K. Lassomycin, a ribosomally synthesized cyclic peptide, kills *Mycobacterium tuberculosis* by targeting the ATP-dependent protease ClpC1P1P2. *Chemistry & biology*. 2014;21(4):509-18. Epub 2014/04/02. doi: 10.1016/j.chembiol.2014.01.014. PubMed PMID: 24684906; PMCID: PMC4060151.
101. Gao W, Kim JY, Anderson JR, Akopian T, Hong S, Jin YY, Kandror O, Kim JW, Lee IA, Lee SY, McAlpine JB, Mulugeta S, Sunoqrot S, Wang Y, Yang SH, Yoon TM, Goldberg AL, Pauli GF, Suh JW, Franzblau SG, Cho S. The cyclic peptide ecumicin targeting ClpC1 is active against *Mycobacterium tuberculosis* in vivo. *Antimicrobial agents and chemotherapy*. 2015;59(2):880-9. Epub 2014/11/26. doi: 10.1128/aac.04054-14. PubMed PMID: 25421483; PMCID: PMC4335914.
102. Binnie C, Butler MJ, Aphale JS, Bourgault R, DiZonno MA, Krygsmann P, Liao L, Walczyk E, Malek LT. Isolation and characterization of two genes encoding proteases associated with the mycelium of *Streptomyces lividans* 66. *Journal of bacteriology*.

1995;177(21):6033-40. Epub 1995/11/01. PubMed PMID: 7592364; PMCID: PMC177439.

103. Naffin-Olivos JL, Daab A, White A, Goldfarb NE, Milne AC, Liu D, Baikovitz J, Dunn BM, Rengarajan J, Petsko GA, Ringe D. Structure Determination of Mycobacterium tuberculosis Serine Protease Hip1 (Rv2224c). *Biochemistry*. 2017;56(17):2304-14. Epub 2017/03/28. doi: 10.1021/acs.biochem.6b01066. PubMed PMID: 28346784.

104. Goldberg MF, Saini NK, Porcelli SA. Evasion of Innate and Adaptive Immunity by Mycobacterium tuberculosis. *Microbiology spectrum*. 2014;2(5). Epub 2015/06/25. doi: 10.1128/microbiolspec.MGM2-0005-2013. PubMed PMID: 26104343.

105. Madan-Lala R, Sia JK, King R, Adekambi T, Monin L, Khader SA, Pulendran B, Rengarajan J. Mycobacterium tuberculosis impairs dendritic cell functions through the serine hydrolase Hip1. *Journal of immunology (Baltimore, Md : 1950)*. 2014;192(9):4263-72. Epub 2014/03/25. doi: 10.4049/jimmunol.1303185. PubMed PMID: 24659689; PMCID: PMC3995873.

106. Belisle JT, Sonnenberg MG. Isolation of genomic DNA from mycobacteria. *Methods in molecular biology (Clifton, NJ)*. 1998;101:31-44. Epub 1999/01/28. doi: 10.1385/0-89603-471-2:31. PubMed PMID: 9921467.

107. Rengarajan J, Bloom BR, Rubin EJ. Genome-wide requirements for Mycobacterium tuberculosis adaptation and survival in macrophages. *Proceedings of the National Academy of Sciences of the United States of America*. 2005;102(23):8327-32. Epub 2005/06/02. doi: 10.1073/pnas.0503272102. PubMed PMID: 15928073; PMCID: PMC1142121.

108. Sia JK, Bizzell E, Madan-Lala R, Rengarajan J. Engaging the CD40-CD40L pathway augments T-helper cell responses and improves control of Mycobacterium tuberculosis infection. *PLoS pathogens*. 2017;13(8):e1006530. Epub 2017/08/03. doi: 10.1371/journal.ppat.1006530. PubMed PMID: 28767735; PMCID: PMC5540402.
109. Zhu J, Yamane H, Paul WE. Differentiation of effector CD4 T cell populations (\*). *Annual review of immunology*. 2010;28:445-89. Epub 2010/03/03. doi: 10.1146/annurev-immunol-030409-101212. PubMed PMID: 20192806; PMCID: PMC3502616.
110. Srivastava S, Ernst JD. Cell-to-cell transfer of M. tuberculosis antigens optimizes CD4 T cell priming. *Cell host & microbe*. 2014;15(6):741-52. Epub 2014/06/13. doi: 10.1016/j.chom.2014.05.007. PubMed PMID: 24922576; PMCID: PMC4098643.
111. McShane H, Behboudi S, Goonetilleke N, Brookes R, Hill AV. Protective immunity against Mycobacterium tuberculosis induced by dendritic cells pulsed with both CD8(+)- and CD4(+)-T-cell epitopes from antigen 85A. *Infection and immunity*. 2002;70(3):1623-6. Epub 2002/02/21. PubMed PMID: 11854254; PMCID: PMC127749.
112. Griffiths KL, Ahmed M, Das S, Gopal R, Horne W, Connell TD, Moynihan KD, Kolls JK, Irvine DJ, Artyomov MN, Rangel-Moreno J, Khader SA. Targeting dendritic cells to accelerate T-cell activation overcomes a bottleneck in tuberculosis vaccine efficacy. *Nature communications*. 2016;7:13894. Epub 2016/12/23. doi: 10.1038/ncomms13894. PubMed PMID: 28004802; PMCID: PMC5192216.
113. Tascon RE, Soares CS, Ragno S, Stavropoulos E, Hirst EM, Colston MJ. Mycobacterium tuberculosis-activated dendritic cells induce protective immunity in

mice. *Immunology*. 2000;99(3):473-80. Epub 2000/03/11. PubMed PMID: 10712679; PMCID: PMC2327172.

114. Beveridge NE, Price DA, Casazza JP, Pathan AA, Sander CR, Asher TE, Ambrozak DR, Precopio ML, Scheinberg P, Alder NC, Roederer M, Koup RA, Douek DC, Hill AV, McShane H. Immunisation with BCG and recombinant MVA85A induces long-lasting, polyfunctional *Mycobacterium tuberculosis*-specific CD4<sup>+</sup> memory T lymphocyte populations. *European journal of immunology*. 2007;37(11):3089-100. Epub 2007/10/20. doi: 10.1002/eji.200737504. PubMed PMID: 17948267; PMCID: PMC2365909.

115. Schreiber HA, Hulseberg PD, Lee J, Prechl J, Barta P, Szlavik N, Harding JS, Fabry Z, Sandor M. Dendritic cells in chronic mycobacterial granulomas restrict local anti-bacterial T cell response in a murine model. *PloS one*. 2010;5(7):e11453. Epub 2010/07/14. doi: 10.1371/journal.pone.0011453. PubMed PMID: 20625513; PMCID: PMC2897891.

116. van Faassen H, Dudani R, Krishnan L, Sad S. Prolonged antigen presentation, APC-, and CD8<sup>+</sup> T cell turnover during mycobacterial infection: comparison with *Listeria monocytogenes*. *Journal of immunology (Baltimore, Md : 1950)*. 2004;172(6):3491-500. Epub 2004/03/09. PubMed PMID: 15004149.

117. Etna MP, Giacomini E, Pardini M, Severa M, Bottai D, Cruciani M, Rizzo F, Calogero R, Brosch R, Coccia EM. Impact of *Mycobacterium tuberculosis* RD1-locus on human primary dendritic cell immune functions. *Scientific reports*. 2015;5:17078. Epub 2015/11/26. doi: 10.1038/srep17078. PubMed PMID: 26602835; PMCID: PMC4658526.

118. Satchidanandam V, Kumar N, Jumani RS, Challu V, Elangovan S, Khan NA. The glycosylated Rv1860 protein of *Mycobacterium tuberculosis* inhibits dendritic cell mediated TH1 and TH17 polarization of T cells and abrogates protective immunity conferred by BCG. *PLoS pathogens*. 2014;10(6):e1004176. Epub 2014/06/20. doi: 10.1371/journal.ppat.1004176. PubMed PMID: 24945624; PMCID: PMC4055742.
119. Pym AS, Brodin P, Majlessi L, Brosch R, Demangel C, Williams A, Griffiths KE, Marchal G, Leclerc C, Cole ST. Recombinant BCG exporting ESAT-6 confers enhanced protection against tuberculosis. *Nature medicine*. 2003;9(5):533-9. Epub 2003/04/15. doi: 10.1038/nm859. PubMed PMID: 12692540.
120. Hoft DF, Blazevic A, Selimovic A, Turan A, Tennant J, Abate G, Fulkerson J, Zak DE, Walker R, McClain B, Sadoff J, Scott J, Shepherd B, Ishmukhamedov J, Hokey DA, Dheenadhayalan V, Shankar S, Amon L, Navarro G, Podyminogin R, Aderem A, Barker L, Brennan M, Wallis RS, Gershon AA, Gershon MD, Steinberg S. Safety and Immunogenicity of the Recombinant BCG Vaccine AERAS-422 in Healthy BCG-naive Adults: A Randomized, Active-controlled, First-in-human Phase 1 Trial. *EBioMedicine*. 2016;7:278-86. Epub 2016/06/21. doi: 10.1016/j.ebiom.2016.04.010. PubMed PMID: 27322481; PMCID: PMC4909487.
121. Horwitz MA, Harth G, Dillon BJ, Maslesa-Galic S. Enhancing the protective efficacy of *Mycobacterium bovis* BCG vaccination against tuberculosis by boosting with the *Mycobacterium tuberculosis* major secretory protein. *Infection and immunity*. 2005;73(8):4676-83. Epub 2005/07/26. doi: 10.1128/iai.73.8.4676-4683.2005. PubMed PMID: 16040980; PMCID: PMC1201189.

122. Hatano S, Tamura T, Umemura M, Matsuzaki G, Ohara N, Yoshikai Y. Recombinant *Mycobacterium bovis* bacillus Calmette-Guerin expressing Ag85B-IL-7 fusion protein enhances IL-17A-producing innate gammadelta T cells. *Vaccine*. 2016;34(22):2490-5. Epub 2016/04/16. doi: 10.1016/j.vaccine.2016.03.096. PubMed PMID: 27079930.
123. Wangoo A, Brown IN, Marshall BG, Cook HT, Young DB, Shaw RJ. Bacille Calmette-Guerin (BCG)-associated inflammation and fibrosis: modulation by recombinant BCG expressing interferon-gamma (IFN-gamma). *Clinical and experimental immunology*. 2000;119(1):92-8. Epub 1999/12/22. PubMed PMID: 10606969; PMCID: PMC1905541.
124. Rao M, Vogelzang A, Kaiser P, Schuerer S, Kaufmann SH, Gengenbacher M. The tuberculosis vaccine candidate *Bacillus Calmette-Guerin* DeltaureC::hly coexpressing human interleukin-7 or -18 enhances antigen-specific T cell responses in mice. *PloS one*. 2013;8(11):e78966. Epub 2013/11/16. doi: 10.1371/journal.pone.0078966. PubMed PMID: 24236077; PMCID: PMC3827306.
125. Murray PJ, Aldovini A, Young RA. Manipulation and potentiation of antimycobacterial immunity using recombinant bacille Calmette-Guerin strains that secrete cytokines. *Proceedings of the National Academy of Sciences of the United States of America*. 1996;93(2):934-9. Epub 1996/01/23. PubMed PMID: 8570663; PMCID: PMC40162.
126. Yang X, Bao L, Deng Y. A novel recombinant *Mycobacterium bovis* bacillus Calmette-Guerin strain expressing human granulocyte macrophage colony-stimulating factor and *Mycobacterium tuberculosis* early secretory antigenic target 6 complex

augments Th1 immunity. *Acta biochimica et biophysica Sinica*. 2011;43(7):511-8. Epub 2011/06/17. doi: 10.1093/abbs/gmr045. PubMed PMID: 21676888.

127. Luo Y, Yamada H, Chen X, Ryan AA, Evanoff DP, Triccas JA, O'Donnell MA. Recombinant *Mycobacterium bovis* bacillus Calmette-Guerin (BCG) expressing mouse IL-18 augments Th1 immunity and macrophage cytotoxicity. *Clinical and experimental immunology*. 2004;137(1):24-34. Epub 2004/06/16. doi: 10.1111/j.1365-2249.2004.02522.x. PubMed PMID: 15196240; PMCID: PMC1809079.

128. O'Donnell MA, Aldovini A, Duda RB, Yang H, Szilvasi A, Young RA, DeWolf WC. Recombinant *Mycobacterium bovis* BCG secreting functional interleukin-2 enhances gamma interferon production by splenocytes. *Infection and immunity*. 1994;62(6):2508-14. Epub 1994/06/01. PubMed PMID: 8188376; PMCID: PMC186538.

129. Master SS, Rampini SK, Davis AS, Keller C, Ehlers S, Springer B, Timmins GS, Sander P, Deretic V. *Mycobacterium tuberculosis* prevents inflammasome activation. *Cell host & microbe*. 2008;3(4):224-32. Epub 2008/04/15. doi: 10.1016/j.chom.2008.03.003. PubMed PMID: 18407066; PMCID: PMC3657562.

130. Johansen P, Fettelschoss A, Amstutz B, Selchow P, Waeckerle-Men Y, Keller P, Deretic V, Held L, Kundig TM, Bottger EC, Sander P. Relief from Zmp1-mediated arrest of phagosome maturation is associated with facilitated presentation and enhanced immunogenicity of mycobacterial antigens. *Clinical and vaccine immunology : CVI*. 2011;18(6):907-13. Epub 2011/04/08. doi: 10.1128/cvi.00015-11. PubMed PMID: 21471301; PMCID: PMC3122614.

131. Grode L, Seiler P, Baumann S, Hess J, Brinkmann V, Nasser Eddine A, Mann P, Goosmann C, Bandermann S, Smith D, Bancroft GJ, Reyrat JM, van Soolingen D,

Raupach B, Kaufmann SH. Increased vaccine efficacy against tuberculosis of recombinant *Mycobacterium bovis* bacille Calmette-Guerin mutants that secrete listeriolysin. *The Journal of clinical investigation*. 2005;115(9):2472-9. Epub 2005/08/20. doi: 10.1172/jci24617. PubMed PMID: 16110326; PMCID: PMC1187936.

132. Farinacci M, Weber S, Kaufmann SH. The recombinant tuberculosis vaccine rBCG DeltaureC::hly(+) induces apoptotic vesicles for improved priming of CD4(+) and CD8(+) T cells. *Vaccine*. 2012;30(52):7608-14. Epub 2012/10/24. doi: 10.1016/j.vaccine.2012.10.031. PubMed PMID: 23088886.

133. Saiga H, Nieuwenhuizen N, Gengenbacher M, Koehler AB, Schuerer S, Moura-Alves P, Wagner I, Mollenkopf HJ, Dorhoi A, Kaufmann SH. The Recombinant BCG DeltaureC::hly Vaccine Targets the AIM2 Inflammasome to Induce Autophagy and Inflammation. *The Journal of infectious diseases*. 2015;211(11):1831-41. Epub 2014/12/17. doi: 10.1093/infdis/jiu675. PubMed PMID: 25505299.

134. Hess J, Miko D, Catic A, Lehmsiek V, Russell DG, Kaufmann SH. *Mycobacterium bovis* Bacille Calmette-Guerin strains secreting listeriolysin of *Listeria monocytogenes*. *Proceedings of the National Academy of Sciences of the United States of America*. 1998;95(9):5299-304. Epub 1998/06/06. PubMed PMID: 9560270; PMCID: PMC20255.

135. Vogelzang A, Perdomo C, Zedler U, Kuhlmann S, Hurwitz R, Gengenbacher M, Kaufmann SH. Central memory CD4+ T cells are responsible for the recombinant *Bacillus Calmette-Guerin* DeltaureC::hly vaccine's superior protection against tuberculosis. *The Journal of infectious diseases*. 2014;210(12):1928-37. Epub

2014/06/20. doi: 10.1093/infdis/jiu347. PubMed PMID: 24943726; PMCID: PMC4241943.

136. Desel C, Dorhoi A, Bandermann S, Grode L, Eisele B, Kaufmann SH. Recombinant BCG DeltaureC hly+ induces superior protection over parental BCG by stimulating a balanced combination of type 1 and type 17 cytokine responses. *The Journal of infectious diseases*. 2011;204(10):1573-84. Epub 2011/09/22. doi: 10.1093/infdis/jir592. PubMed PMID: 21933877; PMCID: PMC3192191.

137. Gengenbacher M, Nieuwenhuizen N, Vogelzang A, Liu H, Kaiser P, Schuerer S, Lazar D, Wagner I, Mollenkopf HJ, Kaufmann SH. Deletion of nuoG from the Vaccine Candidate *Mycobacterium bovis* BCG DeltaureC::hly Improves Protection against Tuberculosis. *mBio*. 2016;7(3). Epub 2016/05/26. doi: 10.1128/mBio.00679-16. PubMed PMID: 27222470; PMCID: PMC4895111.

138. Aagaard C, Hoang T, Dietrich J, Cardona PJ, Izzo A, Dolganov G, Schoolnik GK, Cassidy JP, Billeskov R, Andersen P. A multistage tuberculosis vaccine that confers efficient protection before and after exposure. *Nature medicine*. 2011;17(2):189-94. Epub 2011/01/25. doi: 10.1038/nm.2285. PubMed PMID: 21258338.

139. Kamath AT, Rochat AF, Christensen D, Agger EM, Andersen P, Lambert PH, Siegrist CA. A liposome-based mycobacterial vaccine induces potent adult and neonatal multifunctional T cells through the exquisite targeting of dendritic cells. *PloS one*. 2009;4(6):e5771. Epub 2009/06/06. doi: 10.1371/journal.pone.0005771. PubMed PMID: 19492047; PMCID: PMC2685976.

140. Jagannath C, Lindsey DR, Dhandayuthapani S, Xu Y, Hunter RL, Jr., Eissa NT. Autophagy enhances the efficacy of BCG vaccine by increasing peptide presentation in

mouse dendritic cells. *Nature medicine*. 2009;15(3):267-76. Epub 2009/03/03. doi: 10.1038/nm.1928. PubMed PMID: 19252503.

141. Dong H, Stanek O, Salvador FR, Langer U, Morillon E, Ung C, Sebo P, Leclerc C, Majlessi L. Induction of protective immunity against *Mycobacterium tuberculosis* by delivery of ESX antigens into airway dendritic cells. *Mucosal immunology*. 2013;6(3):522-34. Epub 2012/10/04. doi: 10.1038/mi.2012.92. PubMed PMID: 23032790.

142. Ahmed M, Jiao H, Domingo-Gonzalez R, Das S, Griffiths KL, Rangel-Moreno J, Nagarajan UM, Khader SA. Rationalized design of a mucosal vaccine protects against *Mycobacterium tuberculosis* challenge in mice. *Journal of leukocyte biology*. 2017;101(6):1373-81. Epub 2017/03/05. doi: 10.1189/jlb.4A0616-270R. PubMed PMID: 28258153; PMCID: PMC5433857.

143. Perdomo C, Zedler U, Kuhl AA, Lozza L, Saikali P, Sander LE, Vogelzang A, Kaufmann SH, Kupz A. Mucosal BCG Vaccination Induces Protective Lung-Resident Memory T Cell Populations against Tuberculosis. *mBio*. 2016;7(6). Epub 2016/11/24. doi: 10.1128/mBio.01686-16. PubMed PMID: 27879332; PMCID: PMC5120139.

144. Aguilo N, Toledo AM, Lopez-Roman EM, Perez-Herran E, Gormley E, Rullas-Trincado J, Angulo-Barturen I, Martin C. Pulmonary *Mycobacterium bovis* BCG vaccination confers dose-dependent superior protection compared to that of subcutaneous vaccination. *Clinical and vaccine immunology : CVI*. 2014;21(4):594-7. Epub 2014/02/07. doi: 10.1128/cvi.00700-13. PubMed PMID: 24501340; PMCID: PMC3993116.

145. Aguilo N, Alvarez-Arguedas S, Uranga S, Marinova D, Monzon M, Badiola J, Martin C. Pulmonary but Not Subcutaneous Delivery of BCG Vaccine Confers Protection to Tuberculosis-Susceptible Mice by an Interleukin 17-Dependent Mechanism. *The Journal of infectious diseases*. 2016;213(5):831-9. Epub 2015/10/24. doi: 10.1093/infdis/jiv503. PubMed PMID: 26494773.
146. Chen L, Wang J, Zganiacz A, Xing Z. Single intranasal mucosal *Mycobacterium bovis* BCG vaccination confers improved protection compared to subcutaneous vaccination against pulmonary tuberculosis. *Infection and immunity*. 2004;72(1):238-46. Epub 2003/12/23. PubMed PMID: 14688101; PMCID: PMC344011.
147. Caulfield AJ, Walker ME, Giolda LM, Lathem WW. The Pla protease of *Yersinia pestis* degrades fas ligand to manipulate host cell death and inflammation. *Cell host & microbe*. 2014;15(4):424-34. Epub 2014/04/12. doi: 10.1016/j.chom.2014.03.005. PubMed PMID: 24721571; PMCID: PMC4020149.
148. Laarman AJ, Mijnheer G, Mootz JM, van Rooijen WJ, Ruyken M, Malone CL, Heezius EC, Ward R, Milligan G, van Strijp JA, de Haas CJ, Horswill AR, van Kessel KP, Rooijackers SH. *Staphylococcus aureus* Staphopain A inhibits CXCR2-dependent neutrophil activation and chemotaxis. *The EMBO journal*. 2012;31(17):3607-19. Epub 2012/08/02. doi: 10.1038/emboj.2012.212. PubMed PMID: 22850671; PMCID: PMC3433787.
149. Fraga TR, Courrol Ddos S, Castiblanco-Valencia MM, Hirata IY, Vasconcellos SA, Juliano L, Barbosa AS, Isaac L. Immune evasion by pathogenic *Leptospira* strains: the secretion of proteases that directly cleave complement proteins. *The Journal of*

infectious diseases. 2014;209(6):876-86. Epub 2013/10/29. doi: 10.1093/infdis/jit569. PubMed PMID: 24163418.

150. Upadhye V, Majumdar A, Gomashe A, Joshi D, Gangane N, Thamke D, Mendiratta D, Harinath BC. Inhibition of Mycobacterium tuberculosis secretory serine protease blocks bacterial multiplication both in axenic culture and in human macrophages. Scandinavian journal of infectious diseases. 2009;41(8):569-76. Epub 2009/05/30. doi: 10.1080/00365540903015109. PubMed PMID: 19479636.

151. Roberts DM, Personne Y, Ollinger J, Parish T. Proteases in Mycobacterium tuberculosis pathogenesis: potential as drug targets. Future microbiology. 2013;8(5):621-31. Epub 2013/05/07. doi: 10.2217/fmb.13.25. PubMed PMID: 23642117.

152. Moreira W, Ngan GJ, Low JL, Poulsen A, Chia BC, Ang MJ, Yap A, Fulwood J, Lakshmanan U, Lim J, Khoo AY, Flotow H, Hill J, Raju RM, Rubin EJ, Dick T. Target mechanism-based whole-cell screening identifies bortezomib as an inhibitor of caseinolytic protease in mycobacteria. mBio. 2015;6(3):e00253-15. Epub 2015/05/07. doi: 10.1128/mBio.00253-15. PubMed PMID: 25944857; PMCID: PMC4436076.

153. Famulla K, Sass P, Malik I, Akopian T, Kandror O, Alber M, Hinzen B, Ruebsamen-Schaeff H, Kalscheuer R, Goldberg AL, Brotz-Oesterhelt H. Acyldepsipeptide antibiotics kill mycobacteria by preventing the physiological functions of the ClpP1P2 protease. Molecular microbiology. 2016;101(2):194-209. Epub 2016/02/27. doi: 10.1111/mmi.13362. PubMed PMID: 26919556; PMCID: PMC5469208.

154. Power SD, Adams RM, Wells JA. Secretion and autoproteolytic maturation of subtilisin. Proceedings of the National Academy of Sciences of the United States of

America. 1986;83(10):3096-100. Epub 1986/05/01. PubMed PMID: 3517850; PMCID: PMC323459.

155. Kessler E, Safrin M. Synthesis, processing, and transport of *Pseudomonas aeruginosa* elastase. *Journal of bacteriology*. 1988;170(11):5241-7. Epub 1988/11/01. PubMed PMID: 3141383; PMCID: PMC211597.

156. Luo Y, Pfuetzner RA, Mosimann S, Paetzel M, Frey EA, Cherney M, Kim B, Little JW, Strynadka NC. Crystal structure of LexA: a conformational switch for regulation of self-cleavage. *Cell*. 2001;106(5):585-94. Epub 2001/09/12. PubMed PMID: 11551506.

157. Cole ST, Eiglmeier K, Parkhill J, James KD, Thomson NR, Wheeler PR, Honore N, Garnier T, Churcher C, Harris D, Mungall K, Basham D, Brown D, Chillingworth T, Connor R, Davies RM, Devlin K, Duthoy S, Feltwell T, Fraser A, Hamlin N, Holroyd S, Hornsby T, Jagels K, Lacroix C, Maclean J, Moule S, Murphy L, Oliver K, Quail MA, Rajandream MA, Rutherford KM, Rutter S, Seeger K, Simon S, Simmonds M, Skelton J, Squares R, Squares S, Stevens K, Taylor K, Whitehead S, Woodward JR, Barrell BG. Massive gene decay in the leprosy bacillus. *Nature*. 2001;409(6823):1007-11. Epub 2001/03/10. doi: 10.1038/35059006. PubMed PMID: 11234002.

158. Ribeiro-Guimaraes ML, Pessolani MC. Comparative genomics of mycobacterial proteases. *Microbial pathogenesis*. 2007;43(5-6):173-8. Epub 2007/07/06. doi: 10.1016/j.micpath.2007.05.010. PubMed PMID: 17611072.

159. Lamichhane G, Zignol M, Blades NJ, Geiman DE, Dougherty A, Grosset J, Broman KW, Bishai WR. A postgenomic method for predicting essential genes at subsaturation levels of mutagenesis: application to *Mycobacterium tuberculosis*.

- Proceedings of the National Academy of Sciences of the United States of America. 2003;100(12):7213-8. Epub 2003/05/31. doi: 10.1073/pnas.1231432100. PubMed PMID: 12775759; PMCID: PMC165855.
160. Zhang YJ, Ioerger TR, Huttenhower C, Long JE, Sasseti CM, Sacchettini JC, Rubin EJ. Global assessment of genomic regions required for growth in *Mycobacterium tuberculosis*. PLoS pathogens. 2012;8(9):e1002946. Epub 2012/10/03. doi: 10.1371/journal.ppat.1002946. PubMed PMID: 23028335; PMCID: PMC3460630.
161. Griffin JE, Gawronski JD, Dejesus MA, Ioerger TR, Akerley BJ, Sasseti CM. High-resolution phenotypic profiling defines genes essential for mycobacterial growth and cholesterol catabolism. PLoS pathogens. 2011;7(9):e1002251. Epub 2011/10/08. doi: 10.1371/journal.ppat.1002251. PubMed PMID: 21980284; PMCID: PMC3182942.
162. Sasseti CM, Rubin EJ. Genetic requirements for mycobacterial survival during infection. Proceedings of the National Academy of Sciences of the United States of America. 2003;100(22):12989-94. Epub 2003/10/22. doi: 10.1073/pnas.2134250100. PubMed PMID: 14569030; PMCID: PMC240732.
163. Lamichhane G, Tyagi S, Bishai WR. Designer arrays for defined mutant analysis to detect genes essential for survival of *Mycobacterium tuberculosis* in mouse lungs. Infection and immunity. 2005;73(4):2533-40. Epub 2005/03/24. doi: 10.1128/iai.73.4.2533-2540.2005. PubMed PMID: 15784600; PMCID: PMC1087429.
164. Ollinger J, O'Malley T, Ahn J, Odingo J, Parish T. Inhibition of the sole type I signal peptidase of *Mycobacterium tuberculosis* is bactericidal under replicating and nonreplicating conditions. Journal of bacteriology. 2012;194(10):2614-9. Epub

2012/03/20. doi: 10.1128/jb.00224-12. PubMed PMID: 22427625; PMCID: PMC3347204.

165. Akopian T, Kandror O, Tsu C, Lai JH, Wu W, Liu Y, Zhao P, Park A, Wolf L, Dick LR, Rubin EJ, Bachovchin W, Goldberg AL. Cleavage Specificity of Mycobacterium tuberculosis ClpP1P2 Protease and Identification of Novel Peptide Substrates and Boronate Inhibitors with Anti-bacterial Activity. *The Journal of biological chemistry*. 2015;290(17):11008-20. Epub 2015/03/12. doi: 10.1074/jbc.M114.625640. PubMed PMID: 25759383; PMCID: PMC4409261.

166. Chilukoti N, Kumar CM, Mande SC. GroEL2 of Mycobacterium tuberculosis Reveals the Importance of Structural Pliability in Chaperonin Function. *Journal of bacteriology*. 2015;198(3):486-97. Epub 2015/11/11. doi: 10.1128/jb.00844-15. PubMed PMID: 26553853; PMCID: PMC4719451.

167. Dave JA, Gey van Pittius NC, Beyers AD, Ehlers MR, Brown GD. Mycosin-1, a subtilisin-like serine protease of Mycobacterium tuberculosis, is cell wall-associated and expressed during infection of macrophages. *BMC microbiology*. 2002;2:30. Epub 2002/10/09. PubMed PMID: 12366866; PMCID: PMC131053.

168. Sun D, Liu Q, He Y, Wang C, Wu F, Tian C, Zang J. The putative propeptide of MycP1 in mycobacterial type VII secretion system does not inhibit protease activity but improves protein stability. *Protein & cell*. 2013;4(12):921-31. Epub 2013/11/20. doi: 10.1007/s13238-013-3089-7. PubMed PMID: 24248472; PMCID: PMC4875400.

169. Krieger TJ, Bartfeld D, Jenish DL, Hadary D. Purification and characterization of a novel tripeptidyl aminopeptidase from *Streptomyces lividans* 66. *FEBS letters*. 1994;352(3):385-8. Epub 1994/10/03. PubMed PMID: 7926006.

170. Butler MJ, Aphale JS, Binnie C, DiZonno MA, Krygsman P, Soltes G, Walczyk E, Malek LT. Cloning and analysis of a gene from *Streptomyces lividans* 66 encoding a novel secreted protease exhibiting homology to subtilisin BPN'. *Applied microbiology and biotechnology*. 1996;45(1-2):141-7. Epub 1996/03/01. PubMed PMID: 8920189.
171. Butler MJ, Binnie C, DiZonno MA, Krygsman P, Soltes GA, Soostmeyer G, Walczyk E, Malek LT. Cloning and characterization of a gene encoding a secreted tripeptidyl aminopeptidase from *Streptomyces lividans* 66. *Applied and environmental microbiology*. 1995;61(8):3145-50. Epub 1995/08/01. PubMed PMID: 7487044; PMCID: PMC167588.
172. Levitte S, Adams KN, Berg RD, Cosma CL, Urdahl KB, Ramakrishnan L. Mycobacterial Acid Tolerance Enables Phagolysosomal Survival and Establishment of Tuberculous Infection In Vivo. *Cell host & microbe*. 2016;20(2):250-8. Epub 2016/08/12. doi: 10.1016/j.chom.2016.07.007. PubMed PMID: 27512905; PMCID: PMC4985559.
173. Small JL, O'Donoghue AJ, Boritsch EC, Tsodikov OV, Knudsen GM, Vandal O, Craik CS, Ehrt S. Substrate specificity of MarP, a periplasmic protease required for resistance to acid and oxidative stress in *Mycobacterium tuberculosis*. *The Journal of biological chemistry*. 2013;288(18):12489-99. Epub 2013/03/19. doi: 10.1074/jbc.M113.456541. PubMed PMID: 23504313; PMCID: PMC3642297.
174. Altschul SF, Gish W, Miller W, Myers EW, Lipman DJ. Basic local alignment search tool. *Journal of molecular biology*. 1990;215(3):403-10. Epub 1990/10/05. doi: 10.1016/s0022-2836(05)80360-2. PubMed PMID: 2231712.

175. Moreno-Hagelsieb G, Latimer K. Choosing BLAST options for better detection of orthologs as reciprocal best hits. *Bioinformatics (Oxford, England)*. 2008;24(3):319-24. Epub 2007/11/29. doi: 10.1093/bioinformatics/btm585. PubMed PMID: 18042555.
176. Midha M, Polavarapu R, Meetei PA, Krishnan H, Mohareer K, Vindal V. OrFin: A web tool for detection of putative orthologs. *Bioinformation*. 2012;8(15):738-9. Epub 2012/10/12. doi: 10.6026/97320630008738. PubMed PMID: 23055622; PMCID: PMC3449379.
177. Miyazaki K. MEGAWHOP cloning: a method of creating random mutagenesis libraries via megaprimer PCR of whole plasmids. *Methods in enzymology*. 2011;498:399-406. Epub 2011/05/24. doi: 10.1016/b978-0-12-385120-8.00017-6. PubMed PMID: 21601687.
178. Vincentelli R, Canaan S, Campanacci V, Valencia C, Maurin D, Frassinetti F, Scappucini-Calvo L, Bourne Y, Cambillau C, Bignon C. High-throughput automated refolding screening of inclusion bodies. *Protein science : a publication of the Protein Society*. 2004;13(10):2782-92. Epub 2004/09/25. doi: 10.1110/ps.04806004. PubMed PMID: 15388864; PMCID: PMC2286565.
179. Kwon SK, Kim SK, Lee DH, Kim JF. Comparative genomics and experimental evolution of *Escherichia coli* BL21(DE3) strains reveal the landscape of toxicity escape from membrane protein overproduction. *Scientific reports*. 2015;5:16076. Epub 2015/11/05. doi: 10.1038/srep16076. PubMed PMID: 26531007; PMCID: PMC4632034.
180. Miroux B, Walker JE. Over-production of proteins in *Escherichia coli*: mutant hosts that allow synthesis of some membrane proteins and globular proteins at high

- levels. *Journal of molecular biology*. 1996;260(3):289-98. Epub 1996/07/19. doi: 10.1006/jmbi.1996.0399. PubMed PMID: 8757792.
181. Kozak R, Behr MA. Divergence of immunologic and protective responses of different BCG strains in a murine model. *Vaccine*. 2011;29(7):1519-26. Epub 2010/12/28. doi: 10.1016/j.vaccine.2010.12.012. PubMed PMID: 21184855.
182. Pedroza-Roldan C, Guapillo C, Barrios-Payan J, Mata-Espinosa D, Aceves-Sanchez Mde J, Marquina-Castillo B, Hernandez-Pando R, Flores-Valdez MA. The BCGDeltaBCG1419c strain, which produces more pellicle in vitro, improves control of chronic tuberculosis in vivo. *Vaccine*. 2016;34(40):4763-70. Epub 2016/08/23. doi: 10.1016/j.vaccine.2016.08.035. PubMed PMID: 27546876.
183. Vergne I, Chua J, Lee HH, Lucas M, Belisle J, Deretic V. Mechanism of phagolysosome biogenesis block by viable *Mycobacterium tuberculosis*. *Proceedings of the National Academy of Sciences of the United States of America*. 2005;102(11):4033-8. Epub 2005/03/09. doi: 10.1073/pnas.0409716102. PubMed PMID: 15753315; PMCID: PMC554822.
184. Puri RV, Reddy PV, Tyagi AK. Secreted acid phosphatase (SapM) of *Mycobacterium tuberculosis* is indispensable for arresting phagosomal maturation and growth of the pathogen in guinea pig tissues. *PloS one*. 2013;8(7):e70514. Epub 2013/08/08. doi: 10.1371/journal.pone.0070514. PubMed PMID: 23923000; PMCID: PMC3724783.
185. Pitt JM, Blankley S, McShane H, O'Garra A. Vaccination against tuberculosis: how can we better BCG? *Microbial pathogenesis*. 2013;58:2-16. Epub 2012/12/22. doi: 10.1016/j.micpath.2012.12.002. PubMed PMID: 23257069.

186. Nguyen PC, Delorme V, Benarouche A, Martin BP, Paudel R, Gnawali GR, Madani A, Puppo R, Landry V, Kremer L, Brodin P, Spilling CD, Cavalier JF, Canaan S. Cyclopostins and Cyclophostin analogs as promising compounds in the fight against tuberculosis. *Scientific reports*. 2017;7(1):11751. Epub 2017/09/20. doi: 10.1038/s41598-017-11843-4. PubMed PMID: 28924204; PMCID: PMC5603573.
187. Frees D, Brondsted L, Ingmer H. Bacterial proteases and virulence. *Sub-cellular biochemistry*. 2013;66:161-92. Epub 2013/03/13. doi: 10.1007/978-94-007-5940-4\_7. PubMed PMID: 23479441.
188. Bhuwan M, Arora N, Sharma A, Khubaib M, Pandey S, Chaudhuri TK, Hasnain SE, Ehtesham NZ. Interaction of Mycobacterium tuberculosis Virulence Factor RipA with Chaperone MoxR1 Is Required for Transport through the TAT Secretion System. *mBio*. 2016;7(2):e02259. Epub 2016/03/05. doi: 10.1128/mBio.02259-15. PubMed PMID: 26933057; PMCID: PMC4810496.

**CHAPTER 7****Appendix****Other publications and unpublished citations**

Chapter 2 citation:

**Bizzell E\***, Sia JK\*, Quezada M, Enriquez A, Georgieva M, and Rengarajan J. Deletion of the Hip1 protease in BCG enhances dendritic cell functions and augments lung CD4 T cell responses, Manuscript in revision, Journal of Leukocyte Biology

\*Authors contributed equally

PDF of:

Jonathan Kevin Sia, Erica Bizzell, *et al.* (2017)

Engaging the CD40-CD40L pathway augments T-helper cell responses and improves control of *Mycobacterium tuberculosis* infection

PLoS Pathog. 2017; 13(8):e1006530; doi: 10.1371/journal.ppat.1006530

Contribution(s):

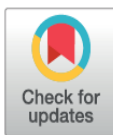
I was involved in the experimentation related to figure 4 (pg. 158). Specifically, I participated in animal harvests, tissue processing, and staining for flow cytometry at all timepoints.

## RESEARCH ARTICLE

# Engaging the CD40-CD40L pathway augments T-helper cell responses and improves control of *Mycobacterium tuberculosis* infection

Jonathan Kevin Sia<sup>1</sup>, Erica Bizzell<sup>1</sup>, Ranjna Madan-Lala<sup>1</sup>, Jyothi Rengarajan<sup>1,2\*</sup>

<sup>1</sup> Emory Vaccine Center, Emory University, Atlanta, GA, United States of America, <sup>2</sup> Department of Medicine, Division of Infectious Diseases, Emory University School of Medicine, Atlanta, GA, United States of America

\* [jrengar@emory.edu](mailto:jrengar@emory.edu)

## Abstract

*Mycobacterium tuberculosis* (Mtb) impairs dendritic cell (DC) functions and induces suboptimal antigen-specific CD4 T cell immune responses that are poorly protective. Mucosal T-helper cells producing IFN- $\gamma$  (Th<sub>1</sub>) and IL-17 (Th<sub>17</sub>) are important for protecting against tuberculosis (TB), but the mechanisms by which DCs generate antigen-specific T-helper responses during Mtb infection are not well defined. We previously reported that Mtb impairs CD40 expression on DCs and restricts Th<sub>1</sub> and Th<sub>17</sub> responses. We now demonstrate that CD40-dependent costimulation is required to generate IL-17 responses to Mtb. CD40-deficient DCs were unable to induce antigen-specific IL-17 responses after Mtb infection despite the production of Th<sub>17</sub>-polarizing innate cytokines. Disrupting the interaction between CD40 on DCs and its ligand CD40L on antigen-specific CD4 T cells, genetically or via antibody blockade, significantly reduced antigen-specific IL-17 responses. Importantly, engaging CD40 on DCs with a multimeric CD40 agonist (CD40LT) enhanced antigen-specific IL-17 generation in *ex vivo* DC-T cell co-culture assays. Further, intratracheal instillation of Mtb-infected DCs treated with CD40LT significantly augmented antigen-specific Th<sub>17</sub> responses *in vivo* in the lungs and lung-draining lymph nodes of mice. Finally, we show that boosting CD40-CD40L interactions promoted balanced Th<sub>1</sub>/Th<sub>17</sub> responses in a setting of mucosal DC transfer, and conferred enhanced control of lung bacterial burdens following aerosol challenge with Mtb. Our results demonstrate that CD40 costimulation by DCs plays an important role in generating antigen-specific Th<sub>17</sub> cells and targeting the CD40-CD40L pathway represents a novel strategy to improve adaptive immunity to TB.

 OPEN ACCESS

**Citation:** Sia JK, Bizzell E, Madan-Lala R, Rengarajan J (2017) Engaging the CD40-CD40L pathway augments T-helper cell responses and improves control of *Mycobacterium tuberculosis* infection. PLoS Pathog 13(8): e1006530. <https://doi.org/10.1371/journal.ppat.1006530>

**Editor:** Padmini Salgame, New Jersey Medical School, UNITED STATES

**Received:** May 17, 2017

**Accepted:** July 13, 2017

**Published:** August 2, 2017

**Copyright:** © 2017 Sia et al. This is an open access article distributed under the terms of the [Creative Commons Attribution License](https://creativecommons.org/licenses/by/4.0/), which permits unrestricted use, distribution, and reproduction in any medium, provided the original author and source are credited.

**Data Availability Statement:** All relevant data are within the paper and its Supporting Information files.

**Funding:** This work was supported by grants from the National Institute of Allergy and Infectious Diseases, National Institutes of Health: 5R01AI083366-05 and 2R56AI083366-06A1 (to JR), a Yerkes National Primate Center base grant: RR000165 and a Center for AIDS research (CFAR) Immunology Core grant (to Emory University): P30AI050409. The funders had no role in study

## Author summary

Tuberculosis (TB) remains a serious global health problem and understanding how to induce protective immunity to *M. tuberculosis* (Mtb) remains a major challenge. While antigen-specific CD4 T cells and IFN- $\gamma$  are important for controlling Mtb infection, they are not sufficient for protecting against TB. We need insights into host pathways that can be targeted to overcome suboptimal antigen-specific immunity induced by Mtb. Dendritic

design, data collection and analysis, decision to publish, or preparation of the manuscript.

**Competing interests:** The authors have declared that no competing interests exist.

cells (DCs) are antigen presenting cells that orchestrate the adaptive immune response to infection, but Mtb subverts DC-T cell interactions. Therefore, improving the crosstalk between DCs and T cells during Mtb infection has the potential to enhance anti-mycobacterial immunity. Here we identify interaction between CD40 on DCs and CD40L on T cells as a critical mechanism for generating lung Th<sub>17</sub> cells. By engaging CD40 on DCs using a multimeric reagent, we significantly augmented early Mtb-specific Th<sub>17</sub> responses in lungs. Intratracheal DC instillation in conjunction with CD40 engagement provided a balanced Th<sub>1</sub>/Th<sub>17</sub> response and improved control of bacterial burden after aerosol challenge with Mtb. Our studies show that the CD40-CD40L pathway is important for the generation of Mtb-specific Th<sub>17</sub> responses and targeting CD40-CD40L interactions is a promising avenue for improving adaptive immunity to TB.

## Introduction

Critical to the success of *Mycobacterium tuberculosis* (Mtb) as a pathogen is its ability to manipulate host innate and adaptive immune responses to its benefit. Despite the development of antigen-specific T cell responses following infection, Mtb is able to persist within the host, indicating that Mtb-specific T cell immunity is suboptimal and ineffective at eliminating the pathogen [1, 2]. Indeed, several studies have shown that mice infected with Mtb exhibit delayed initiation of antigen-specific CD4 T cell responses, which is preceded by delayed migration of Mtb-containing dendritic cells (DCs) from the lung to draining lymph nodes [3–5]. Moreover, although IFN- $\gamma$  and T-helper 1 (Th<sub>1</sub>) responses are important for controlling infection, they are not sufficient to eradicate bacteria and do not protect against developing tuberculosis (TB) [6–8]. Recently, IL-17 and Th<sub>17</sub> responses have emerged as important for protective immunity to TB [9–16]. Studies in mice suggest that early induction of IL-17 in the lung promotes control of mycobacterial growth, and balanced Th<sub>1</sub>/Th<sub>17</sub> responses in the lung have been reported to be more effective [17–19]. We previously reported that an avirulent *hip1* (Hydrolase important for pathogenesis 1; Rv2224c) mutant Mtb strain induced significantly higher IL-17 and IFN- $\gamma$  responses compared to infection with wild type Mtb due to enhanced functions of infected DCs [20, 21]. Together, these studies suggest that wild type Mtb subverts DCs to prevent optimal T-helper responses and that augmenting DC functions during infection may be beneficial for improving protective immunity. While several studies have reported that Mtb manipulation of DC functions leads to suboptimal Th<sub>1</sub> responses [21–24], we lack insights into Th<sub>17</sub> generation during Mtb infection. To gain insight into host pathways involved in generating Th<sub>17</sub> responses during Mtb infection, we sought to define the molecular mechanisms underlying Th<sub>17</sub> responses following Mtb infection of DCs.

As the primary antigen-presenting cells in the immune system, DCs are instrumental in shaping adaptive immunity and determining the types of antigen-specific T-helper subsets that are generated in response to infection. Upon phagocytosis of the pathogen, DCs present pathogen-derived antigens to naïve CD4 T cells, provide critical costimulatory signals and produce cytokines; these signals initiate antigen-specific T-helper cell activation and polarization towards specific subsets [25–27]. However, beyond the role of cytokines such as IL-1 $\beta$ , IL-6, and IL-23 in polarizing and committing antigen-specific CD4 T cells towards a Th<sub>17</sub> phenotype, the DC-T cell interactions underlying Th<sub>17</sub> polarization during Mtb infection are poorly defined. We previously showed that eliminating Hip1-dependent immune evasion mechanisms in Mtb enhanced the capacity of DCs to induce Th<sub>17</sub> responses and was accompanied by significantly higher expression of the costimulatory molecule, CD40, on infected DCs [21]. Because costimulation of naïve T cells in the context of cognate interactions between DCs and

T cells is critical for optimal activation and differentiation of antigen-specific T cells, these data suggested that impaired CD40-dependent costimulation during wild type Mtb infection may lead to suboptimal Th<sub>17</sub> responses in TB. CD40 has previously been implicated in generating Th<sub>1</sub> responses during Mtb infection [28], but its role in the polarization of the Th<sub>17</sub> subset during infection is not defined. We therefore sought to investigate the contribution of the CD40 costimulatory pathway in Th<sub>17</sub> generation during Mtb infection and determine the effects of augmenting CD40 costimulation on bacterial control. In this study, we show that CD40 expression on DCs is required for the generation of IL-17 responses to Mtb infection and that interaction between CD40 on DCs and CD40L on CD4 T cells is critical for generating antigen-specific IL-17 responses. Importantly, we found that engaging CD40 on DCs via crosslinking with a multimeric CD40 agonist reagent (CD40LT) significantly enhanced antigen-specific IL-17 responses to Mtb. Further, intratracheal instillation of Mtb-infected DCs treated with CD40LT led to significant enhancement of antigen-specific Th<sub>17</sub> responses in the lungs and mediastinal lymph nodes (MLN) of mice, showing that engaging the CD40-CD40L pathway can overcome suboptimal Th<sub>17</sub> responses to Mtb *in vivo*. Finally, we show that CD40 engagement in the setting of a DC transfer model enhances control of Mtb following aerosol challenge. Our results demonstrate that the CD40-CD40L pathway is critical for generating IL-17 responses and that targeting this costimulatory pathway represents a novel strategy to potentially improve protection against TB.

## Results

### CD40 on DCs is required for the generation of antigen-specific IL-17 responses during Mtb infection

To test whether CD40 expression is required for differentiation of naïve CD4 T cells into IL-17-producing cells in response to Mtb infection, we used DC-T cell co-culture assays as previously described [21]. We infected bone marrow derived DCs from wild type C57BL/6 mice (B6) or from *CD40*<sup>-/-</sup> mice for 24 hours, followed by co-culture with purified naïve TCR-transgenic (Tg) CD4 T cells isolated from OT-II mice in the presence of OVA<sub>323–339</sub> peptide (Fig 1A). Supernatants were harvested 72 hours after co-culture and assayed for IL-17, IL-2 and IFN- $\gamma$  by ELISA. Mtb-infected DCs from B6 mice induced increasing levels of IL-17, IL-2 and IFN- $\gamma$  cytokines with increasing concentrations of peptide. In contrast, *CD40*<sup>-/-</sup> DCs were significantly impaired in their ability to induce IL-17-producing cells in response to Mtb, but retained the capacity to induce IFN- $\gamma$  and IL-2 (Fig 1A). These data indicate that CD40 is specifically required to generate antigen-specific IL-17 responses.

To assess whether the defect in IL-17 production was specific for CD40 deficiency, we examined the contribution of the costimulatory molecules CD80 and CD86, which are known to be essential for IL-2 production and are required for optimal T cell proliferation [29, 30]. While DCs that were doubly-deficient in CD80 and CD86 were severely impaired in IL-2 production, their ability to induce antigen-specific IL-17 responses were comparable to DCs from B6 mice (Fig 1B) and did not exhibit the defective IL-17 responses observed in *CD40*<sup>-/-</sup> DCs. These data indicate that CD40-dependent costimulation plays an essential and specific role in the generation of IL-17 responses to Mtb.

Cytokines produced by infected DCs are known to be critical for polarizing antigen-specific CD4 T cell subsets [17, 31]. Since IL-6, IL-1 $\beta$ , and TGF- $\beta$  have been shown to induce Th<sub>17</sub> polarization, we sought to assess whether defective IL-17 responses seen in Mtb-infected *CD40*<sup>-/-</sup> DCs was due to defects in their ability to produce innate cytokines following Mtb infection. However, levels of IL-6, IL-1 $\beta$ , and IL-12 produced by DCs from *CD40*<sup>-/-</sup> mice were comparable to the levels seen in DCs from B6 mice (Fig 1C) and bioactive TGF- $\beta$  was

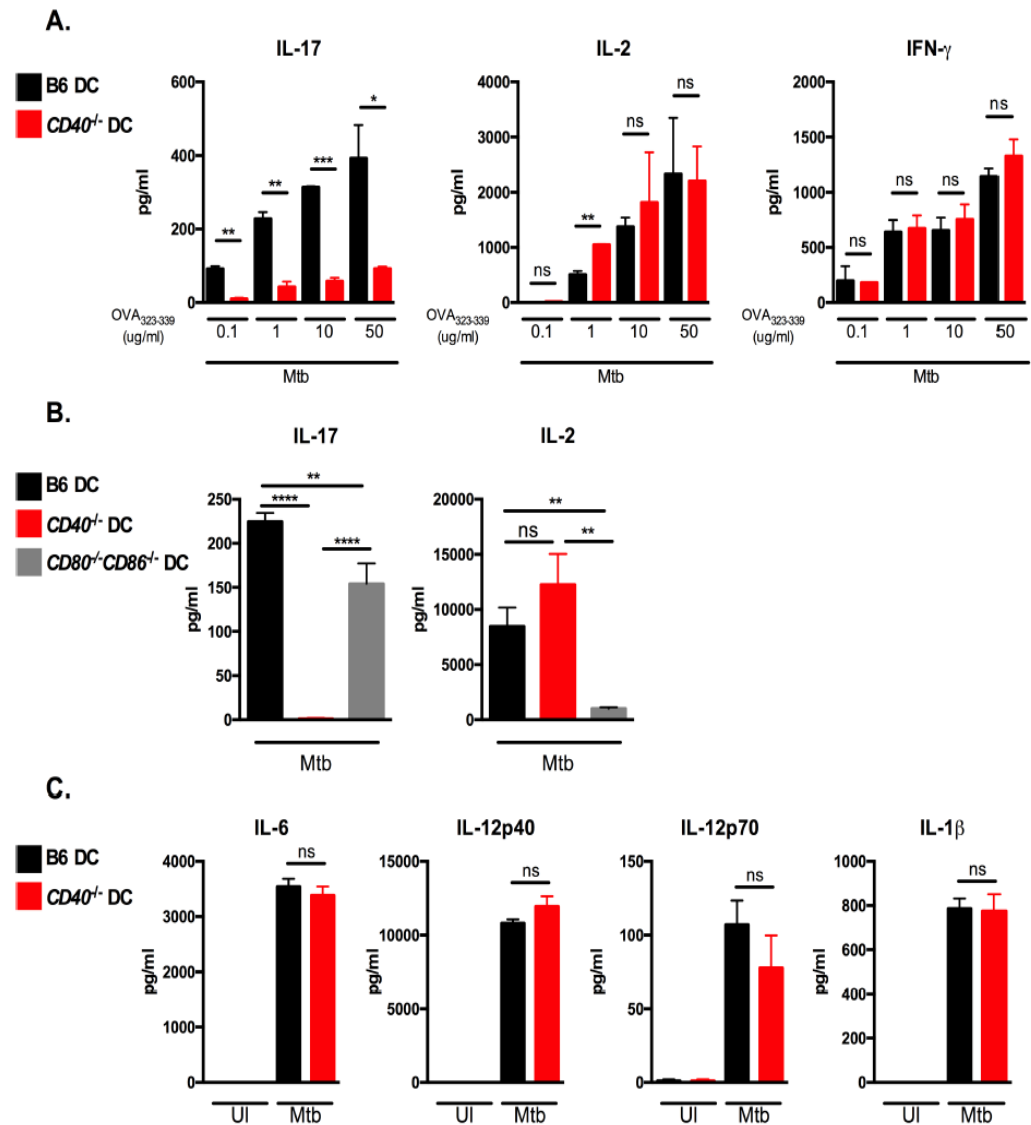


**Fig 1. CD40 on DCs is required for the generation of antigen-specific IL-17 responses during Mtb infection.** (A) DCs derived from B6 or *CD40*<sup>-/-</sup> mice were pulsed with OVA<sub>323-339</sub> at the indicated concentrations and infected with Mtb for 24 hours followed by co-culture with purified OT-II TCR-Tg CD4 T cells for 72 hours. Supernatants were assayed for the indicated cytokines by ELISA. (B) DCs from B6, *CD40*<sup>-/-</sup>, or *CD80*<sup>-/-</sup>*CD86*<sup>-/-</sup> mice were pulsed with 10 μg/ml OVA<sub>323-339</sub>, infected with Mtb and co-cultured with OT-II TCR-Tg CD4 T cells. Cell-free supernatants were harvested after 72 hours and assessed for the indicated cytokines by ELISA. (C) B6 or *CD40*<sup>-/-</sup> DCs were left uninfected (UI) or infected with Mtb. After 24 hours, cell-free supernatants were collected and assessed for the indicated cytokines by ELISA. Data are representative of 3–4 independent experiments. Values are presented as mean ± SD. Statistical significance was determined using a 2-tailed unpaired T-test. \* p<0.05; \*\* p<0.005; \*\*\* p<0.0005; \*\*\*\* p<0.0001, ns = not significant.

<https://doi.org/10.1371/journal.ppat.1006530.g001>

undetectable in all culture conditions. Thus, the inability of *CD40*<sup>-/-</sup> DCs to induce IL-17 responses is not due to impaired innate cytokine responses, suggesting that interaction of CD40 expressed on DCs with its ligand, CD40L (CD154), may be necessary for production of IL-17 by CD4 T cells following Mtb infection.

## CD40-CD40L interaction is critical for inducing antigen-specific IL-17 responses to Mtb infection

CD40L is expressed on antigen-activated T cells and binding of CD40 with CD40L provides accessory costimulatory signals that are necessary for optimal activation and differentiation of antigen-specific T cells. In order to determine whether interaction of CD40 with CD40L was required for IL-17 generation, we carried out co-culture assays using antigen-specific CD4 T cells isolated from OT-II mice crossed to mice lacking CD40L ( $CD40lg^{-/-}$  x OT-II). This allowed us to test whether CD40L on T cells was required for IL-17 generation in a setting where CD40 expression on DCs remained intact. We found that  $CD40lg^{-/-}$  CD4 T cells were attenuated in their ability to generate IL-17 responses after co-culture with Mtb-infected DCs (Fig 2A), concordant with the defective IL-17 response seen with  $CD40^{-/-}$  DCs (Fig 1). Interestingly,  $CD40lg^{-/-}$  T cells also displayed attenuated IFN- $\gamma$  and IL-2 responses (S1 Fig), which suggests that lack of CD40L leads to broader defects in T cell responses compared to the absence of CD40. These results show that both CD40 and CD40L are required for optimal IL-17 generation. To further extend our genetic knockouts studies, we carried out co-culture assays in which we blocked CD40-CD40L interactions using saturating doses of a non-agonistic, anti-CD40L monoclonal antibody (clone MR1). This antibody has been shown to successfully block CD40-CD40L interactions *in vitro* (S2 Fig) and *in vivo* [32]. Blockade of CD40-CD40L interaction between Mtb-infected DCs and CD40L-replete antigen-specific CD4 T cells significantly reduced antigen-specific IL-17 responses (Fig 2B). Together, these data show that interaction between CD40 and CD40L is critical for production of IL-17 by CD4 T cells during Mtb infection.

## Engaging CD40 on DCs enhances antigen-specific IL-17 responses

The requirement for the CD40-CD40L pathway in IL-17 generation suggested that boosting interactions between CD40 and CD40L could serve as a tool to augment IL-17 responses. To exogenously engage CD40 on Mtb-infected DCs, we utilized a multimeric CD40 agonist in which two trimeric CD40L constructs are artificially linked (CD40L trimers; CD40LT). The CD40LT reagent effectively aggregates and activates CD40 independently of T cells. Addition

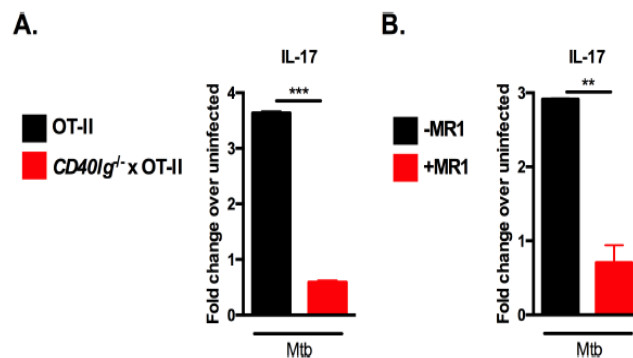


**Fig 2. CD40-CD40L interaction is critical for inducing antigen-specific IL-17 responses to Mtb infection.** (A) B6 DCs were pulsed with OVA<sub>323-339</sub> at 10  $\mu$ g/ml and infected with Mtb for 24 hours followed by co-culture with purified CD4 T cells from OT-II or  $CD40lg^{-/-}$  x OT-II TCR-Tg mice or (B) with purified OT-II TCR-Tg T cells in the presence or absence of 20  $\mu$ g/ml anti-CD40L blocking antibody (clone MR1). Cell-free supernatants were collected after 72 hours and IL-17 assessed by ELISA. Data are representative of two independent experiments. Values are presented as mean fold change over uninfected  $\pm$  SD. Statistical significance was determined using a 2-tailed unpaired T-test. \*\*  $p < 0.005$ , \*\*\*  $p < 0.0005$ .

<https://doi.org/10.1371/journal.ppat.1006530.g002>

of CD40LT to Mtb-infected B6 DCs produced enhanced levels of IL-12 (Fig 3A), consistent with previous reports showing IL-12 induction after CD40 engagement [33]. Importantly, treatment with CD40LT significantly enhanced production of IL-6 and IL-23, which are key cytokines for Th<sub>17</sub> polarization and expansion (Fig 3A). IL-1 $\beta$ , which also promotes Th<sub>17</sub> differentiation in combination with IL-6 and IL-23, was not altered by treatment with CD40LT (Fig 3A). Moreover, CD40LT-treated Mtb-infected DCs induced significantly higher levels of IL-17 from co-cultured ESAT-6 TCR-Tg CD4 T cells compared to Mtb-infected DCs lacking CD40 engagement (Fig 3B). In contrast, CD40LT-treatment did not alter production of IFN- $\gamma$  from antigen-specific CD4 T cells *in vitro* (Fig 3B). These data show that CD40 engagement augments antigen-specific IL-17 generation.

Costimulatory signals synergize with antigen-specific signals downstream of T cell receptor (TCR) ligation to promote full activation of T cells. Absence of signaling through the CD80/86-CD28 costimulatory pathway, for example, results in suboptimal T cell activation and anergic responses [29, 30, 34, 35]. CD28 signaling is thought to function by lowering the T cell activation threshold, thus facilitating optimal T cell activation and IL-2 production. To investigate whether CD40 engagement on DCs similarly impacts the activation threshold of Mtb-specific T cells and whether this, in turn, influences IL-17 production, Mtb-infected DCs were either treated with CD40LT or left untreated, pulsed with increasing concentrations of ESAT-6<sub>1-20</sub> peptide, and co-cultured with ESAT-6 TCR-Tg CD4 T cells. We found that CD40LT-treated DCs displayed an enhanced capacity to induce IL-17 responses at all antigen doses compared to untreated conditions (Fig 3C). The ability of Mtb-infected DCs to induce IL-17 at lower

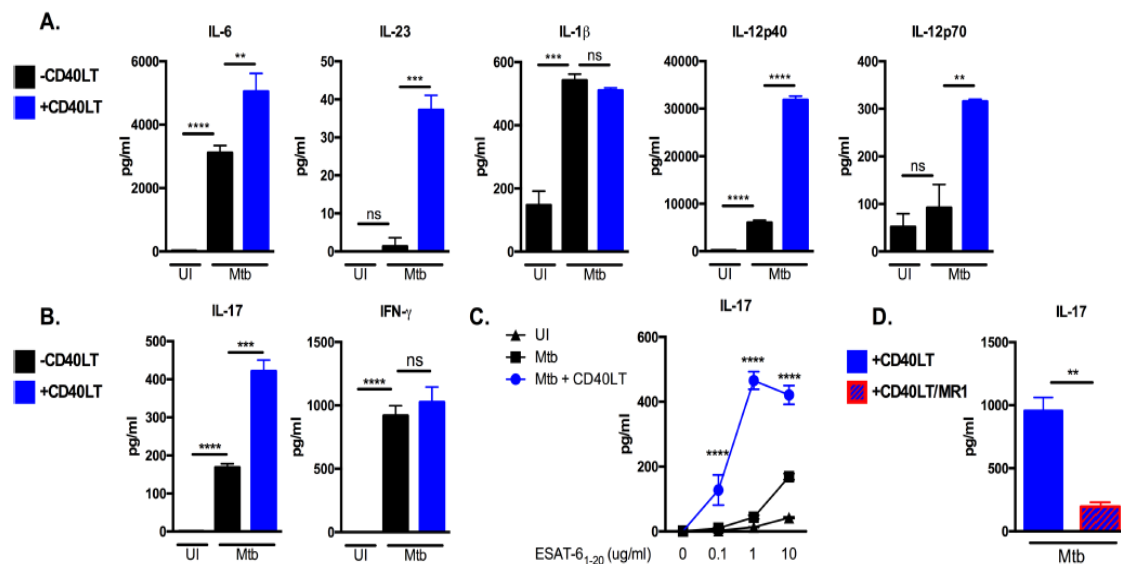


**Fig 3. Engaging CD40 on DCs enhances antigen-specific IL-17 responses.** (A) B6 DCs were left uninfected or infected with Mtb in the presence or absence of 1  $\mu$ g/ml multimeric CD40LT reagent (CD40LT) for 24 hours. Cell-free supernatants were collected after 24 hours and the indicated innate cytokines were measured by ELISA. (B) DCs from (A) were pulsed with ESAT-6<sub>1-20</sub> at 10  $\mu$ g/ml in the presence or absence of CD40LT and co-cultured with ESAT-6 TCR-Tg T cells for 72 hours. Supernatants were assayed for IL-17 and IFN- $\gamma$  by ELISA. (C) B6 DCs were pulsed with increasing concentrations of ESAT-6<sub>1-20</sub> peptide (0, 0.1, 1.0 and 10  $\mu$ g/ml) either left uninfected (UI) or infected with Mtb in the presence or absence of 1  $\mu$ g/ml CD40LT for 24 hours followed by co-culture with purified ESAT-6 TCR-Tg CD4 T cells for 72 hours. Supernatants were assayed for IL-17 by ELISA. (D) B6 DCs were pulsed with ESAT-6<sub>1-20</sub> peptide at 10  $\mu$ g/ml and infected with Mtb in the presence or absence of 1  $\mu$ g/ml CD40LT for 24 hours. Co-culture with ESAT-6 TCR-Tg CD4 T cells was done in the presence or absence of 20  $\mu$ g/ml anti-CD40L blocking antibody (clone MR1). Cell-free supernatants were collected after 72 hours and IL-17 levels determined by ELISA. Data are representative of 3–4 independent experiments. Values are presented as mean  $\pm$  SD. Statistical significance was determined using a 2-tailed unpaired T-test. \*\*  $p < 0.005$ , \*\*\*  $p < 0.0005$ , \*\*\*\*  $p < 0.0001$ , ns = not significant.

<https://doi.org/10.1371/journal.ppat.1006530.g003>

concentrations of peptide after CD40LT treatment suggests that signals induced by CD40 engagement lowers the threshold for antigen-specific production of IL-17. Thus, CD40-dependent costimulation may serve to overcome suboptimal generation of IL-17 responses elicited early in Mtb infection when antigen levels are low.

In order to dissect the relative contributions of Th<sub>17</sub>-polarizing cytokines and CD40-CD40L interaction on IL-17 responses, Mtb-infected DCs were treated with or without CD40LT and then co-cultured with ESAT-6 TCR-Tg CD4 T cells in the presence of the MRI CD40L-blocking antibody as described in Fig 2B. Interestingly, antibody blockade of CD40-CD40L interaction significantly decreased antigen-specific IL-17 responses even in the presence of CD40LT (Fig 3D). These data suggest that exogenous engagement of CD40 on DCs that results in enhanced production of Th<sub>17</sub>-polarizing cytokines is not sufficient for generating antigen-specific IL-17 responses in a setting where CD40 cannot interact with CD40L on antigen-specific CD4 T cells.

### CD40 engagement of Mtb-infected DCs induces antigen-specific Th<sub>17</sub> *in vivo*

Induction of early IL-17 responses on mucosal surfaces of the lung is thought to be important for immunity to Mtb and inducing balanced Mtb-specific Th<sub>1</sub>/Th<sub>17</sub> responses may enhance protective immunity. To determine whether CD40 engagement on DCs can enhance the induction of Mtb-specific lung Th<sub>17</sub> responses *in vivo*, we utilized a mucosal transfer approach via intratracheal instillation of DCs. This approach allows for targeted manipulation of Mtb-infected DCs without potential confounding from off-target effects such as CD40 engagement of alveolar macrophages. Transferred DCs have been shown to prime adoptively transferred Mtb-antigen-specific T cells in lymph nodes and lungs of mice by 3 days post-intratracheal instillation [23].

We adoptively transferred naïve CD45.2<sup>+</sup> ESAT-6 TCR-Tg CD4 T cells into CD45.1<sup>+</sup> congenic hosts. The next day, we transferred DCs infected with Mtb in the presence or absence of CD40LT by intratracheal instillation (Fig 4A). At 6 and 12 days after DC transfer, we assessed Th<sub>17</sub> responses in the lungs and MLN by determining the expression of IL-17 and RORγt in CD45.2<sup>+</sup> ESAT-6-specific CD4 T cells by intracellular cytokine staining (ICS) and flow cytometry. Engaging CD40 on Mtb-infected DCs using CD40LT enhanced the frequency of ESAT-6-specific RORγt<sup>+</sup>IL-17<sup>+</sup> T cells in the lungs (Fig 4B) and MLN (Fig 4C). Notably, the majority of IL-17<sup>+</sup> cells expressed RORγt, the transcription factor that determines Th<sub>17</sub> lineage commitment [36], indicating that CD40LT-treated Mtb-infected DCs polarized CD4 T cells into Th<sub>17</sub> cells.

### Enhanced antigen-specific Th<sub>17</sub> responses in the lungs and MLN of mice following transfer of CD40LT-engaged Mtb-infected DCs or *hip1* mutant Mtb-infected DCs

To determine Th<sub>1</sub> and Th<sub>17</sub> responses in the lungs and MLN of mice at 6 and 12 days after intratracheal instillation of DCs, we assessed IFN-γ and IL-17 production in CD45.2<sup>+</sup> ESAT-6 TCR-Tg T cells by flow cytometry (Fig 5A). Transfer of Mtb-infected DCs that were treated with CD40LT resulted in a greater expansion of ESAT-6 TCR-Tg CD4 T cells compared to Mtb DCs that did not receive exogenous CD40LT, and was comparable to the expansion of ESAT-6 TCR-Tg CD4 T cells in response to *hip1* mutant Mtb-infected DCs (Fig 5B). Moreover, transfer of CD40LT-treated, Mtb-infected DCs significantly enhanced the frequencies of antigen-specific Th<sub>17</sub> cells in lungs and MLN compared to Mtb-infected DCs alone and was comparable to the Th<sub>17</sub> frequencies elicited by *hip1* mutant Mtb-infected DCs (Fig 5C). We

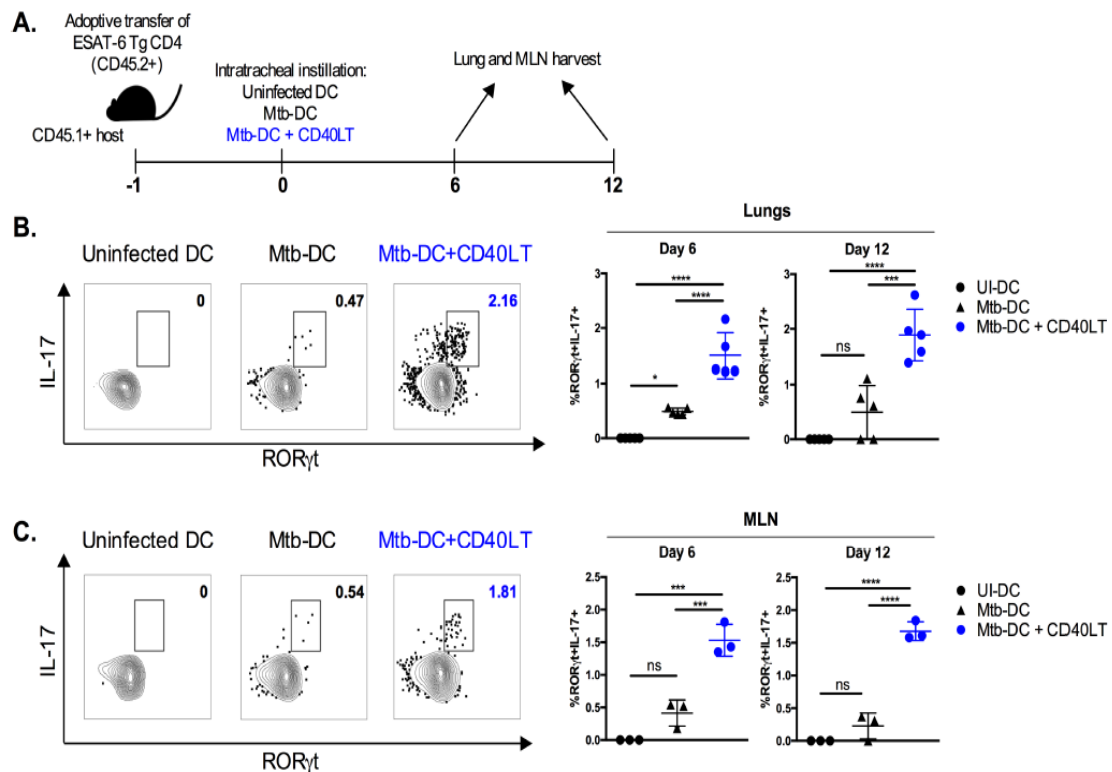


**Fig 4. CD40 engagement of Mtb-infected DCs induces antigen-specific Th<sub>17</sub> *in vivo*.** (A) Diagram of experimental design. CD45.2<sup>+</sup> ESAT-6 TCR Tg CD4 T cells were purified from spleen and lymph nodes and intravenously transferred ( $1 \times 10^6$  per mouse) into congenic (CD45.1<sup>+</sup>) hosts. Animals were rested for 1 day after which DCs ( $1 \times 10^6$  per condition) were transferred into recipient hosts by intratracheal instillation: uninfected DCs (UI-DC), Mtb-infected DCs (Mtb-DC) or Mtb-infected DCs with CD40L trimer treatment (Mtb-DC + CD40LT). Lungs and MLN were harvested 6 and 12 days post-intratracheal instillation and CD4 T cell responses assessed. MLN were pooled to attain sufficient cells for restimulation. Representative flow plots (left; day 6 values) and summary graph (right) of the lung (B) and pooled MLN (C) frequencies of ROR $\gamma$ t<sup>+</sup>IL-17<sup>+</sup> cells after ESAT-6<sub>1-20</sub> restimulation 6 and 12 days after DC transfer. Populations shown have been pre-gated on live CD3<sup>+</sup>CD8 $\gamma$  $\delta$  TCR<sup>+</sup>CD45.2<sup>+</sup> singlets. 5 mice were used for each group. Statistical significance was determined using one-way analysis of variance (ANOVA) correcting for multiple comparisons. \*  $p < 0.05$ , \*\*\*  $p < 0.0005$ , \*\*\*\*  $p < 0.0001$ , ns = not significant.

<https://doi.org/10.1371/journal.ppat.1006530.g004>

also observed higher frequencies of antigen-specific IFN- $\gamma$ <sup>+</sup> CD4 T cells in the lung, but not MLN, on day 6 post-intratracheal transfer of either Mtb-infected CD40LT-treated DCs or *hip1* mutant Mtb-infected DCs compared to their untreated counterpart (Fig 5D). 12 days after intratracheal instillation of DCs, CD45.2<sup>+</sup> ESAT-6-specific IFN- $\gamma$  responses in the lungs were comparable, suggesting that DCs that did not receive CD40LT were delayed in inducing Th<sub>1</sub> responses relative to Mtb-infected CD40LT-treated and *hip1* mutant Mtb-infected DCs. Interestingly, antigen-specific CD4 T cells producing IL-17 and IFN- $\gamma$  were mutually exclusive populations and double producing cells were not detected. These data demonstrate that engagement of the CD40 pathway can overcome deficits in Th<sub>17</sub> generation during Mtb infection and leads to enhanced antigen-specific Th<sub>1</sub> and Th<sub>17</sub> responses *in vivo*.

### CD40 engagement of DCs enhances control of Mtb infection

DCs loaded with Mtb antigens have been previously shown to confer better anti-mycobacterial immunity than BCG (Bacillus Calmette-Guérin) vaccination in mouse models [37, 38].

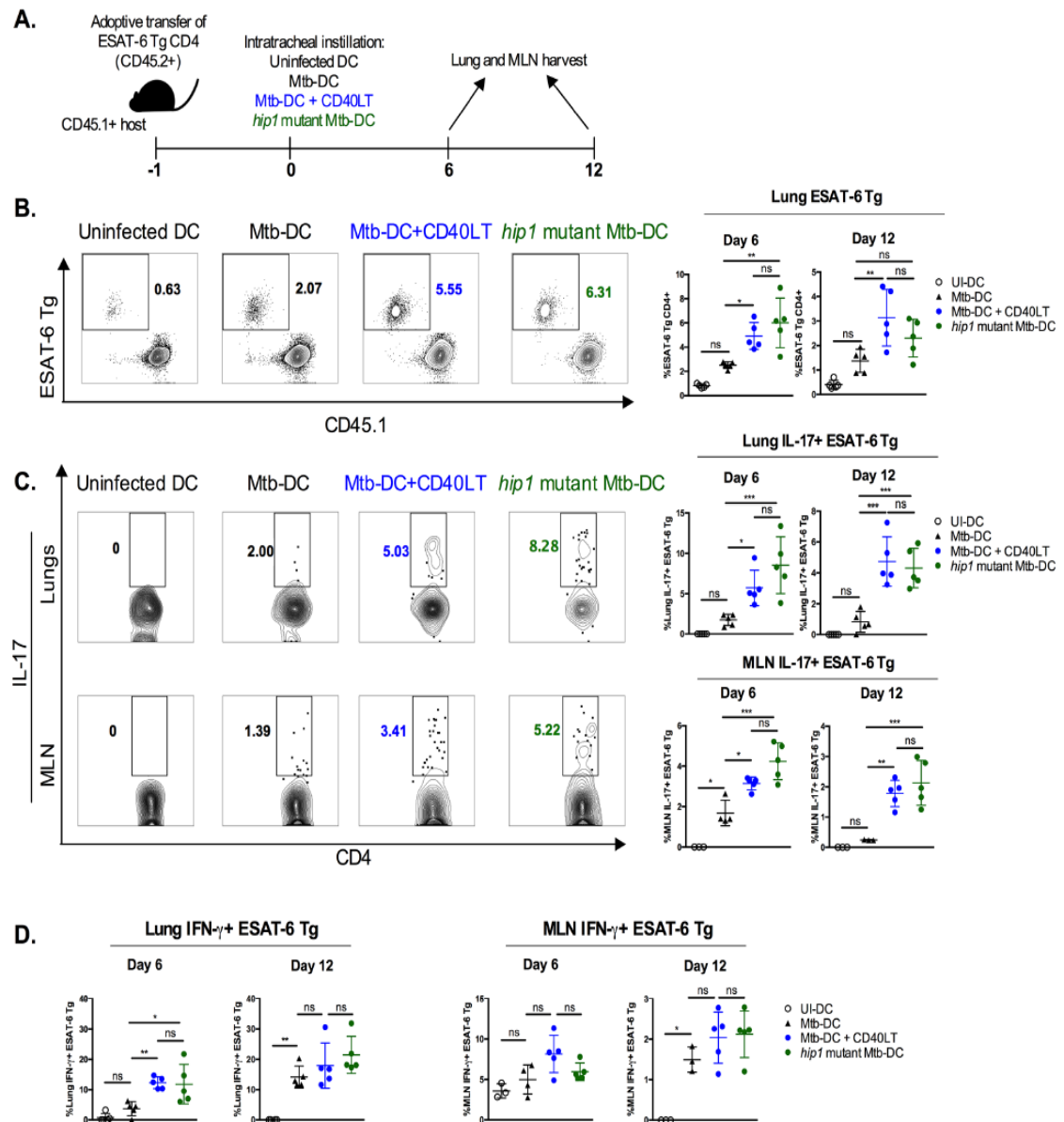


**Fig 5. Enhanced antigen-specific Th<sub>17</sub> responses in the lungs and MLN of mice following transfer of CD40LT-engaged Mtb-infected DCs or *hip1* mutant Mtb-infected DCs.** (A) Diagram of experimental design. As before, purified CD45.2<sup>+</sup> ESAT-6 TCR Tg CD4 T cells were adoptively transferred 1 day before intratracheal instillation of DCs: uninfected DCs (UI-DC), Mtb-infected DCs (Mtb-DC), Mtb-infected DCs with CD40L trimer treatment (Mtb-DC + CD40LT), or *hip1* mutant Mtb-infected DC (*hip1* mutant-DC). Lungs and MLN were harvested 6 and 12 days post-intratracheal instillation and CD4 T cell responses assessed. (B) Representative flow plots (left; day 6 values) and summary graph (right) of the frequencies of CD45.2<sup>+</sup> ESAT-6 TCR-Tg CD4 T cells in the lungs 6 and 12 days post-instillation. (C) Representative flow plots (left; day 6 values) and summary graphs (right) of the frequencies of IL-17<sup>+</sup> ESAT-6 TCR-Tg CD4 T cells in the lungs (top) and MLN (bottom) after stimulation with ESAT-6<sub>1-20</sub> peptide (10  $\mu$ g/ml). (D) Summary graphs of the frequencies of IFN- $\gamma$ <sup>+</sup> ESAT-6 TCR-Tg CD4 T cells in the lungs (left) and MLN (right) after ESAT-6<sub>1-20</sub> restimulation (10  $\mu$ g/ml). Populations shown have been pre-gated on live CD3<sup>+</sup>CD8<sup>-</sup> $\gamma$  $\delta$  TCR<sup>+</sup>CD45.2<sup>+</sup> singlets. 5 mice were used for each group. Statistical significance was determined using one-way analysis of variance (ANOVA) correcting for multiple comparisons. \*  $p < 0.05$ ; \*\*  $p < 0.005$ , \*\*\*  $p < 0.0005$ , ns = not significant.

<https://doi.org/10.1371/journal.ppat.1006530.g005>

Therefore, DC-based vaccination provides a useful model to study the impact of boosting CD40-engagement on priming of antigen-specific T cell pools and on the control of Mtb infection *in vivo*. We exposed DCs to heat-killed (HK) Mtb followed by treatment with CD40LT. DCs stimulated with HK Mtb and CD40LT were equivalent to *ex vivo* assays using live Mtb (S3 Fig). Comparison groups included transfer of uninfected DCs, DCs stimulated with HK wild type Mtb or with HK *hip1* mutant Mtb. Upon transfer of antigen-loaded DCs into mouse lungs by intratracheal instillation, we assessed immune responses generated by transferred DCs by measuring the activation of endogenous CD4 T cell responses and frequencies of Th<sub>17</sub> and Th<sub>1</sub> cells in the lungs of mice 6 and 12 days after DC transfer. 15 days after DC transfer, we challenged mice with low-dose aerosolized Mtb. At 5 weeks post-challenge (day 50), we determined lung bacterial burden and Mtb-specific Th<sub>1</sub> and Th<sub>17</sub> responses (Fig 6A).

CD40LT treatment induced significantly higher frequencies of activated CD44<sup>+</sup> CD4 T cells (Fig 6B) and higher frequencies of lung IL-17<sup>+</sup> CD4 T cells 6 and 12 days after DC transfer (Fig 6C). IFN- $\gamma$ <sup>+</sup> CD4 T cell frequencies were higher on day 6 in mice receiving CD40LT-treated DCs compared to untreated Mtb-DCs, but were comparable by day 12. As expected, transfer of *hip1* mutant Mtb-stimulated DCs induced robust Th<sub>17</sub> and Th<sub>1</sub> responses in the lungs of mice on day 6 and day 12 post-DC transfer. Following aerosol challenge with low dose Mtb 15 days after intratracheal transfer of DCs, we assessed bacterial burden in the lungs of mice 5 weeks after challenge by plating for CFU. As shown in Fig 6D, transfer of DCs stimulated with HK Mtb resulted in significant reductions in lung bacterial burden at day 50 compared to transfer of DCs alone. Interestingly, CD40LT treatment reduced bacterial burden even further, showing that boosting CD40-CD40L interactions could overcome pathogen-mediated impairment of CD40 costimulation and promote enhanced anti-mycobacterial immunity. Notably, transfer of DCs exposed to *hip1* mutant Mtb also showed comparable reductions in bacterial burden. These results are consistent with our previous report showing that *hip1* mutant Mtb inherently induces superior DC responses compared to wild type Mtb, i.e., significantly higher induction of Th<sub>1</sub>- and Th<sub>17</sub>-polarizing cytokines, higher expression of CD40, enhanced antigen presentation and balanced Th<sub>1</sub>/Th<sub>17</sub> responses [21]. To assess Mtb-specific Th<sub>1</sub> and Th<sub>17</sub> responses in the lungs of mice post-challenge, we stimulated lung cells *ex vivo* with Mtb whole cell lysate (WCL) and determined IFN- $\gamma$ <sup>+</sup> and IL-17<sup>+</sup> CD4 T cell frequencies by flow cytometry. We found significantly enhanced Th<sub>17</sub> responses in mice that intratracheally received CD40LT-treated DCs or *hip1* mutant Mtb-stimulated DCs compared to those that received Mtb-stimulated DCs. However, there was no discernible difference between the groups in terms of lung CD4 IFN- $\gamma$  responses (Fig 6E). Importantly, lung IL-17 responses inversely correlated with bacterial burden, while there was no significant correlation between IFN- $\gamma$  responses and lung bacterial burden (Fig 6F). Our data show that we can improve protection against Mtb challenge by overcoming Mtb-mediated impairments in CD40 costimulation.

## Discussion

The findings in this study identify the CD40-CD40L pathway as a critical mechanism for the generation of antigen-specific Th<sub>17</sub> responses and highlight the importance of DC-T cell cross-talk in immunity to Mtb infection. Importantly, we provide insights into improving adaptive immunity to TB by augmenting the functions of DCs and show that exogenously engaging CD40 on DCs significantly enhances control of Mtb burden in the lungs of infected mice.

Costimulatory signals provided by antigen presenting cells such as macrophages and DCs are critical for full activation of naive antigen-specific CD4 T cells and promote their rapid expansion into cytokine-producing effector cells, which exert their antimicrobial functions at

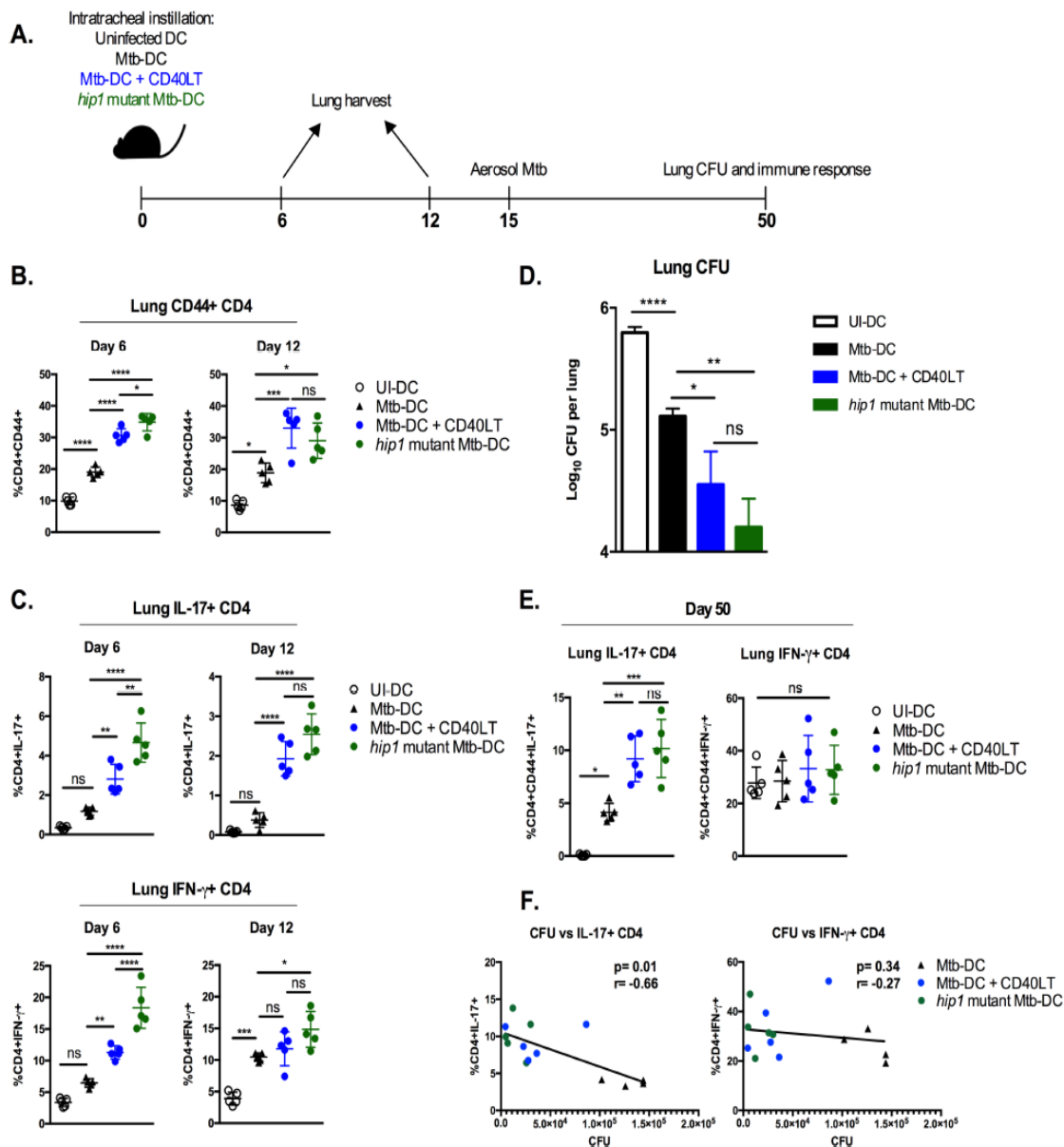


**Fig 6. CD40 engagement of DCs enhances control of Mtb infection.** B6 DCs were left uninfected or infected with heat-killed Mtb in the presence or absence of CD40LT treatment (1  $\mu$ g/ml), or infected with heat-killed *hip1* mutant Mtb, each for 24 hours. Cells were washed twice and reconstituted in PBS to deliver  $1 \times 10^6$  DC per mouse intratracheally. (A) Diagram of experimental design. Lung responses were assessed 6 and 12 days post-instillation. Mice were infected through the aerosol route with  $\sim 100$  CFU Mtb 15 days post-instillation and bacterial burden was assessed 35 days (5 weeks) post-challenge. (B) Frequencies of CD44<sup>+</sup> CD4<sup>+</sup> T cells in the lungs 6 and 12 days after intratracheal instillation of DCs. (C) Frequencies of IL-17<sup>+</sup> (top) and IFN- $\gamma$ <sup>+</sup> (bottom) CD4<sup>+</sup> cells in the lungs 6 and 12 days after intratracheal instillation of DCs. Cells were stimulated with PMA (80 ng/ml) and ionomycin (500 ng/ml). (D) Lung bacterial burden 35 days post-challenge (overall day 50 post-DC intratracheal instillation). Bacterial burden was assessed by plating homogenized lungs on 7H10 agar plates and counting CFU. (E) Lung CD4<sup>+</sup> IL-17<sup>+</sup> and IFN- $\gamma$ <sup>+</sup> frequencies at day 50 following Mtb whole cell lysate (10  $\mu$ g/ml) restimulation. (F) Correlation plots showing association between lung bacterial burden and IL-17 (left) or IFN- $\gamma$  (right) responses to WCL restimulation. A linear regression was utilized to generate a best-fit line and Spearman's correlation coefficient calculated. 4–5 mice were used for each group. Statistical significance (B–E) was determined using one-way analysis of variance correcting for multiple comparisons. \*  $p < 0.05$ , \*\*  $p < 0.005$ , \*\*\*  $p < 0.0005$ , \*\*\*\*  $p < 0.0001$ , ns = not significant.

<https://doi.org/10.1371/journal.ppat.1006530.g006>

the site of infection. While differentiation of activated CD4 T cells into IFN- $\gamma$ <sup>+</sup> Th<sub>1</sub> subsets is relatively well understood, the molecular mechanisms underlying the generation of Th<sub>17</sub> cells, particularly during Mtb infection, are less clear. Moreover, the mechanisms by which Mtb induces delayed, suboptimal T cell immunity, which enables the pathogen to successfully evade adaptive immunity and persist within the host, remain poorly understood. Several studies, including our own, have shown that Mtb impairs antigen presentation in infected DCs and dampens production of Th<sub>17</sub>-polarizing cytokines, such as IL-6, IL-23 and IL-1 $\beta$  [21, 22, 24, 39–41]. However, very little was known about the role of costimulatory pathways in driving Th<sub>17</sub> development in TB prior to our study. Our work shows that innate cytokines are important for the generation of IL-17 responses (Figs 1 and 3) and is consistent with other studies showing a critical role for CD40-dependent IL-6 and IL-23 in the induction and expansion of Th<sub>17</sub> cells [42–44]. Interestingly, our results show that blocking CD40-CD40L interaction with MR1 attenuates IL-17 responses to Mtb-infected DCs despite treatment of DCs with CD40LT, which suggests that optimal induction of IL-17 to Mtb infection requires CD40-CD40L interaction (Fig 3D). However, studies have shown that exogenous addition of supraphysiological levels of Th<sub>17</sub>-polarizing cytokines can drive CD40<sup>-/-</sup> DCs to induce IL-17 [42]. Our data suggest that costimulatory interactions between Mtb-infected DCs and T cells are required for optimal generation of IL-17 responses. In addition, localization of CD4 T cells in close proximity to infected DCs is likely to be an important determinant of the type of antigen-specific CD4 T cells mobilized after infection. Recent work has demonstrated that uninfected MLN-resident DCs acquire antigen from infected lung DCs and can prime Mtb-specific CD4 T cells to produce IFN- $\gamma$  [23]. It is possible that while MLN-resident DCs acquire antigen, their maturation status and costimulatory capacity may be suboptimal without Mtb infection and, thus, not amenable to generating CD4 T cell responses beyond IFN- $\gamma$ . Moreover, within the Th<sub>1</sub> subset, studies have shown distinct IFN- $\gamma$ -producing CD4 T cells in the vasculature and parenchyma of Mtb-infected mice [45]. However, localization of Th<sub>17</sub> cells within lung compartments and the role of lung-specific DC subsets in driving the polarization of Th<sub>1</sub> and Th<sub>17</sub> during Mtb infection are poorly understood. Our study uses bone marrow derived DCs and therefore the extent to which our experiments model *in vivo*-generated lung DCs needs to be investigated further. Overall, our data showing that CD40-CD40L interaction is required for optimal Th<sub>17</sub> generation in response to Mtb and that boosting CD40-CD40L interactions augments Th<sub>1</sub> and Th<sub>17</sub> responses suggests that restriction of costimulatory pathways is an important virulence mechanism used by Mtb for inducing suboptimal T-helper responses that benefits the pathogen.

Our finding that exogenous induction of CD40-mediated costimulation, via CD40LT treatment, is able to elicit IL-17 production at lower concentrations of peptide stimulation (Fig 3) than by Mtb-infected DCs alone leads to an interesting speculation. In early stages of Mtb infection, low levels of antigen in the lung, combined with impaired CD40 induction on Mtb-infected DCs, likely results in suboptimal costimulation of naïve CD4 T cells and therefore suboptimal and delayed induction of Th<sub>17</sub> responses. However, engaging the CD40-CD40L pathway and promoting interactions between these two molecules likely facilitates better Th<sub>17</sub> generation, even when lung antigen levels are low during early stages of infection. It has been reported that higher peptide concentrations are required for inducing Th<sub>17</sub> polarization compared to Th<sub>1</sub> in a study that examined activation of Smar2-Tg T cells [42]. Efficient CD40-mediated costimulation may serve to lower the threshold for T cell activation and Th<sub>17</sub> polarization, and overcome the need for high antigen loads. Interestingly, *hip1* mutant Mtb-loaded DCs induced higher Th<sub>17</sub> responses compared to wild type Mtb, even without CD40LT treatment (Fig 5), and enhanced protection (Fig 6). We have previously shown that *hip1* mutant Mtb induces high levels of CD40 and Th<sub>17</sub> responses [21]. Therefore, it is likely that

elimination of Hip1 results in efficient CD40-dependent costimulation, and bypasses the need for exogenous engagement of the CD40-CD40L pathway. However, we do not rule out the possibility that *hip1* mutant Mtb activates alternate DC pathways that promote robust T cell immunity and further investigation into the common and exclusive immune pathways activated by CD40LT and *hip1* mutant Mtb is of interest.

Previous work by Demangel et al demonstrated that lung Th<sub>1</sub> responses can be augmented by transferring BCG-infected DCs in conjunction with agonistic anti-CD40 mAb [33]. However, this approach did not significantly restrict Mtb lung burdens following challenge compared to BCG-infected DCs alone. We speculate that the use of heat killed Mtb in our study as well as the timing of the aerosol challenge at 2 weeks after intratracheal instillation of DCs (in contrast to 2 days post-DC transfer in the Demangel et al study) likely established higher frequencies of antigen-specific Th<sub>17</sub> and Th<sub>1</sub> precursors, leading to better control of Mtb. Additionally, recent work by Griffiths et al showed that mice vaccinated with BCG followed by intratracheal delivery of Ag85B peptide loaded DCs, one day before and four days after challenge with Mtb HN878, had enhanced bacterial control [46]. Interestingly, they achieved similar reductions in bacterial burden after administration of TLR-9 and CD40 agonists together with Ag85B peptide and also showed higher levels of lung IFN- $\gamma$  and IL-17 responses. The study by Griffiths et al complements our results, which provide mechanistic evidence that the CD40-CD40L pathway is critical for the generation of Mtb-specific lung Th<sub>17</sub> responses. While IL-17 responses appear to be required for resistance against infection with the hypervirulent Mtb HN878 strain, IL-17 may also be important for generating efficacious vaccine-induced immunity. Our data show an association between enhanced IL-17 responses and lower bacterial burden after aerosol Mtb challenge (Fig 6F), but do not directly link Th<sub>17</sub> responses with increased protection. While we have demonstrated that engaging CD40 on DCs confers enhanced Th<sub>17</sub> responses in the lungs in a setting of mucosal DC transfer, we also observed augmented Th<sub>1</sub> responses *in vivo* prior to challenge (Figs 5 and 6). Therefore, our data demonstrate that CD40 engagement on DCs improves adaptive immunity to TB, likely due to induction of a balanced Th<sub>1</sub>/Th<sub>17</sub> response. Although we have not shown that the Th<sub>17</sub> cells generated in the lung following transfer of DCs stimulated with HK Mtb + CD40LT or HK *hip1* mutant Mtb are directly responsible for the increased protection seen in Fig 6, our studies provide a platform to further investigate the potential of designing vaccination strategies that overcome Mtb immune evasion, either by augmenting CD40 costimulation and/or deletion of immunomodulatory factors such as *hip1* (in BCG or other live attenuated Mtb vaccine strains) that impair DC functions.

Our studies on understanding the role of CD40 costimulation in Th<sub>17</sub> responses significantly extend our understanding of the CD40-CD40L pathway during infection, as previous investigations studying this pathway in TB as well as in other infections have focused on Th<sub>1</sub> responses. CD40 has been shown to promote Th<sub>1</sub> responses by synergizing with TLR signaling to induce high levels of IL-12 production from antigen presenting cells in several infections [33, 47, 48]. While our own data show that *CD40*<sup>-/-</sup> DCs and CD40LT-treated DCs infected with Mtb do not affect IFN- $\gamma$  responses in a closed system *in vitro* (Figs 1 and 3), treatment of Mtb-infected DCs with CD40LT does augment IFN- $\gamma$  responses in the lungs 6 days after intratracheal instillation of DCs (Figs 5 and 6), suggesting that engaging the CD40-CD40L pathway enhances both Th<sub>1</sub> and Th<sub>17</sub> responses *in vivo* and may lead to a more balanced Th<sub>1</sub>/Th<sub>17</sub> immunity to TB. Engagement of CD40 is not uniquely important for Th<sub>17</sub> generation, as previous investigations on the role of CD40 in mycobacterial diseases have supported the importance of CD40 in the amplification of Th<sub>1</sub> responses. *CD40*<sup>-/-</sup> mice were shown to be susceptible to aerosol infection with Mtb due to a defective Th<sub>1</sub> response [28], but *CD40lg*<sup>-/-</sup> mice were reported to be resistant to Mtb infection and capable of establishing Th<sub>1</sub> immunity [28,

49]. Together with our data showing that Mtb poorly induces CD40 expression on infected DCs [21], these studies suggest that, while CD40L may be dispensable for generating Th<sub>1</sub> responses that control bacterial burden, engaging the CD40-CD40L pathway may be important for generating balanced Th<sub>1</sub>/Th<sub>17</sub> responses that may better control Mtb infection. Moreover, while IL-17 responses were not examined in those studies, mucosal Th<sub>17</sub> cells are also likely to contribute to controlling Mtb in *CD40*<sup>-/-</sup> mice *in vivo*; this may be dependent on antigen load as the reported susceptibility of *CD40*<sup>-/-</sup> mice disappeared after high dose aerosol challenge [28]. Our work showing that promoting CD40-CD40L interaction augments early Th<sub>17</sub> responses in the lung (Figs 5 and 6) is consistent with several previous reports showing an important role for Th<sub>17</sub> cells in protection at mucosal surfaces such as in the lung and intestine [18, 19, 50, 51]. In TB, it has been suggested that Th<sub>17</sub> cells in the lung may act directly on infected cells or by recruiting additional immune cells, such as IFN- $\gamma$ <sup>+</sup> Th<sub>1</sub>, to combat infection. Notably, in Figs 5 and 6, we show that intratracheal instillation of Mtb-infected DCs treated with CD40LT is associated with an earlier IFN- $\gamma$  response in the lungs compared to Mtb-DC, which supports the idea that induction of early antigen-specific Th<sub>17</sub> can serve to recruit antigen-specific Th<sub>1</sub> cells. Our work highlights the importance of augmenting DC costimulation in order to improve adaptive immunity to TB and provides evidence that specifically augmenting DCs through CD40 can enhance antigen-specific mucosal immunity.

The generation of robust antigen-specific immunity that goes beyond IFN- $\gamma$ -producing Th<sub>1</sub> responses is an important consideration for vaccines and host-directed therapeutics for TB. The IL-12/STAT-1/IFN- $\gamma$  axis is important for the control of Mtb, but robust induction of IFN- $\gamma$  alone does not correlate with enhanced protection against developing TB disease in a variety of vaccine trials [6, 7], and there is mounting evidence for IFN- $\gamma$  independent and Th<sub>17</sub>-mediated mechanisms of Mtb control [9, 52, 53]. In fact, recent work in mice has demonstrated that IFN- $\gamma$  plays a more important role in control of bacterial burden at extra-pulmonary sites such as the spleen and must be restrained to prevent lung pathology [54]. In humans, bi-allelic mutations in *RORC*, leading to abrogated IL-17 responses, is associated with susceptibility to mycobacteria, suggesting a role for IL-17 responses in human TB [55]. In addition, the emerging importance of mucosal Th<sub>17</sub> responses in protective and vaccine-induced immunity to Mtb [18, 19, 51] highlights the need to design and evaluate candidate vaccines that induce robust early Th<sub>17</sub> responses. It is important to keep in mind, however, that unbalanced production of IL-17 can be pathogenic [56]. Over-exuberant induction of IL-17 at non-mucosal sites via repeated subcutaneous BCG exposure can lead to worsening of disease [57] and damaging neutrophilia, while IFN- $\gamma$  receptor signaling limits excessive Th<sub>17</sub>-mediated neutrophilia [58]. In this context, future studies aimed at augmenting CD40 costimulation would benefit from studying how augmenting this pathway impacts neutrophil responses.

In summary, our studies demonstrate a novel role for CD40 costimulation in generating Th<sub>17</sub> responses in TB and show that augmenting the CD40-CD40L pathway, either through DC-targeted strategies or deletion of immune-evasion genes in the pathogen, can bolster adaptive immunity in TB. Our results indicate that targeting DC costimulatory pathways in the context of subunit vaccines or live attenuated vaccines represents a novel strategy to induce balanced Th<sub>1</sub>/Th<sub>17</sub> immunity and improve control of Mtb infection.

## Material and methods

### Ethics statement

All experiments using animals or tissue derived from animals were approved by the Institutional Animal Care and Use Committee (IACUC) at Emory University (Protocol number

YER-2003476-060919GN). Experiments were carried out in strict accordance with the recommendations in the Guide for the Care and Use of Laboratory Animals of the National Institutes of Health.

### Bacterial strains

*Mtb* H37Rv was grown as described previously [21, 40]. Briefly, bacteria were grown at 37°C in Middlebrook 7H9 broth or 7H10 agar supplemented with 10% oleic acid-albumin-dextrose-catalase (OADC) (Becton Dickinson, Franklin Lakes, NJ), 0.5% glycerol, and 0.05% Tween 80 (for broth), with the addition of 25 µg/ml kanamycin (Sigma-Aldrich, St. Louis, MO) for *hip1* mutant *Mtb*. For heat inactivation, bacterial stocks in 7H9 were grown to midlog phase, sonicated, washed twice with PBS and inactivated at 80°C for 2 hours.

### Mice

All mice were housed under specific pathogen-free conditions in filter-top cages within the vivarium at the Yerkes National Primate Center, Emory University, and provided with sterile water and food ad libitum. C57BL/6, and C57BL/6 CD45.1<sup>+</sup> congenic mice, *CD80*<sup>-/-</sup>/*CD86*<sup>-/-</sup>, and *CD40*<sup>-/-</sup> mice were purchased from The Jackson Laboratory. OT-II TCR Tg mice specific for OVA<sub>323–339</sub> peptide were obtained from Dr. Bali Pulendran (originally generated in the laboratory of Dr. F. Carbone, University of Melbourne), and TCR-Tg mice specific for early secreted antigenic target 6 (ESAT-6)<sub>1–20</sub>/I-A<sup>b</sup> epitope were obtained from Dr. Andrea Cooper (Trudeau Institute) and were bred at the Yerkes animal facility. *CD40lg*<sup>-/-</sup> x OT-II Tg mice were obtained from Dr. Mandy Ford (Emory University) and bred at the Yerkes animal facility.

### Generation of bone marrow derived dendritic cells

For generating murine bone marrow derived DCs, bone marrow cells from indicated strains of mice were flushed from excised femurs and tibias and grown in RPMI 1640 medium (Lonza, Walkersville, MD) supplemented with 10% heat-inactivated FBS (HyClone, Logan, UT), 2 mM glutamine, 1x β-mercaptoethanol, 10 mM HEPES, 1 mM sodium pyruvate, 1x nonessential amino acids, and 20 ng/ml murine recombinant GM-CSF (R&D Systems, Minneapolis, MN). Incubations were carried out at 37°C with 5% CO<sub>2</sub>. Fresh medium with GM-CSF (20ng/ml) was added on days 3 and 6, and cells were used on day 8 for all experiments. We routinely obtained >85% CD11c<sup>+</sup> CD11b<sup>+</sup> MHCII<sup>+</sup> cell purity by flow cytometry. DCs were further purified using CD11c microbead kits as per the manufacturer's instructions (Miltenyi Biotec, Auburn, CA).

### Mtb infection of DCs

3x10<sup>5</sup> CD11c-purified bone marrow derived DCs were plated onto 24-well plates overnight prior to infection. For live infections, bacteria were filtered through 5 µm filters, resuspended in complete medium, and sonicated twice for 5 seconds before addition to the adherent monolayers. Bacteria were used for infection (in triplicate) at a multiplicity of infection (MOI) of 10 or as indicated. Infection of DCs was carried out for 4 hours, after which monolayers were incubated with amikacin (200 µg/ml; Sigma-Aldrich) for 45 minutes to kill extracellular bacteria and then washed four times with PBS before incubating in complete medium. To determine bacterial input, a set of wells was lysed in PBS containing 0.5% Triton X-100 and plated onto 7H10 agar plates for CFU enumeration after 21 days. For stimulation of DCs with heat killed *Mtb*, DC were exposed to heat-killed *Mtb* at an MOI of 10 in complete medium as

determined by CFU enumerated from bacterial stocks prior to heat killing. Uninfected DCs were used as controls for each experiment. For some experiments, DCs were treated with multimeric CD40LT reagent (Adipogen) concurrent with infection or stimulation. Cell free supernatants were collected after 24 hours to assay for cytokines: IL-12p40, IL-12p70, IL-6, IL-1 $\beta$  (BD OptEIA, San Jose, CA) and IL-23 (Biolegend, San Diego, CA) by ELISA according to manufacturers' instructions.

### DC-T cell co-culture assays

CD4 T cells were purified from single-cell suspensions of spleen and lymph nodes from 6–8 week old transgenic mice (Naïve CD4 negative selection kit, Stemcell Technologies) of the indicated strain. Purified CD4 T cells show  $\geq 99\%$  purity by FACS analysis. DCs were incubated with 10  $\mu\text{g}/\text{ml}$  (or as indicated) of OVA<sub>323–339</sub> or ESAT-6<sub>1–20</sub> peptide for 6 hours, washed with PBS, and infected with Mtb with or without CD40LT for 24 hours. DCs were then washed twice with PBS and co-cultured with antigen-specific CD4 T cells to achieve a 1:4 DC:T cell ratio for 72 hours. Cell free supernatants collected from co-cultured cells were analyzed for IFN- $\gamma$  (Mabtech, Cincinnati, OH), IL-17 (ELISA Ready-Set-Go, eBioscience), and IL-2 (BD Biosciences) by ELISA according to the manufacturers' instructions.

### Blockade of CD40-CD40L pathway

$2 \times 10^4$  CD11c-purified DCs were seeded in 96-well plates overnight, pulsed with relevant peptide and treated with the indicated conditions for 24 hours. Afterwards, purified antigen-specific CD4 T cells were incubated with 20  $\mu\text{g}/\text{ml}$  anti-CD40L (clone MR1) blocking antibody and co-cultured with DCs to achieve a 1:10 DC:T cell ratio. Co-cultured cells were incubated at 37°C with 5% CO<sub>2</sub> for 72 hours prior to harvest of supernatants for ELISAs.

### Intratracheal instillation of DCs and tissue harvest

CD11c-purified DCs were stimulated with indicated conditions for 24 hours. DCs were then washed twice and resuspended in sterile PBS at  $1 \times 10^6/50$   $\mu\text{l}$  and injected intratracheally into isoflurane-anesthetized mice. For some experiments, recipient mice (CD45.1<sup>+</sup>) received purified  $1 \times 10^6$  ESAT-6<sub>1–20</sub> TCR-Tg CD4 T cells (CD45.2<sup>+</sup>) one day prior to DC instillation by tail-vein injection. 6 and 12 days post-intratracheal instillation, lungs and mediastinal lymph nodes were harvested. Lungs were digested with 1 mg/ml collagenase D (Worthington) at 37°C for 30 min. For some experiments, the upper right lobe of the lung was used for determining CFU and the rest of the lung was used for cellular assays. Homogenized single-cell lung suspensions were obtained through mechanical disruption and filtered through a 70- $\mu\text{m}$  cell strainer (BD Biosciences), treated with RBC lysis buffer for 3–5 min, and washed twice with cell culture media. Cells were counted and used to set up stimulations for intracellular cytokine staining and flow cytometry. Single cell suspensions were stimulated with media, ESAT-6<sub>1–20</sub> (10  $\mu\text{g}/\text{ml}$ ), Mtb whole cell lysate (10  $\mu\text{g}/\text{ml}$ ), or PMA (80 ng/ml) and ionomycin (500 ng/ml) as indicated. BFA (5  $\mu\text{g}/\text{ml}$ ) and monensin (1:1500) were added to the stimulated cells after 1.5 hours and cells were cultured for an additional 4.5 hours, or 16 hours for whole cell lysate stimulations, and then stained for flow cytometry.

### Flow cytometry

Live cells were discriminated by a live/dead fixable aqua dead cell stain (Molecular Probes). For staining DCs, murine anti-CD11c PE-Cy7 (clone N418, eBioscience), anti-CD11b APC-Cy7 (clone M1/70, Biolegend), anti-CD40 PE-Cy5 (clone 1C10, eBioscience), anti-CD86

APC (clone GL1, eBioscience), and anti-MHC II PE (clone M5/114.15.2, BD) were utilized. For staining T cells, murine anti-CD3 V450 (clone 500A2, BD), anti-CD4 Alexa700 (clone RM4-5, BD), anti-CD8 PerCP (clone 53-6.7, BD), anti-TCR  $\gamma\delta$  BV605 (clone GL3, Biolegend), anti-CD44 APC-Cy7 (clone IM7, BD), anti-CD45.1 BV785 (clone A20, BioLegend), and anti-CD45.2 BV650 (clone 104, BioLegend) were utilized to stain for surface markers. Murine anti-ROR $\gamma$ t PE (clone B2D, eBioscience), anti-TNF $\alpha$  PE-Cy7 (clone MP6-XT22, BD), anti-IFN- $\gamma$  APC (clone XMG1.2, eBioscience), anti-IL-2 FITC (clone JES6-5H4, BD), and anti-IL-17 PE-CF594 (clone TC11-18H10, BD) were stained intracellularly with the BD Cytofix/Cytoperm or BD Transcription Factor kit as per manufacturer's instructions. Staining for cell-surface markers was done by resuspending  $\sim 1\text{-}2 \times 10^6$  cells in 100 ml PBS with 2% FBS containing the antibody mixture at 4°C for 30 min and then washing with PBS containing 2% FBS. Data were immediately acquired using an LSRII flow cytometer (BD Biosciences). Data were analyzed with FlowJo software (FlowJo LLC, Ashland, OR).

### Aerogenic infection of mice with Mtb

Mtb H37Rv was grown to OD<sub>600</sub> of  $\sim 0.6\text{-}0.8$ , washed two times in  $1 \times$  PBS. 1-ml aliquots were frozen at  $-80^\circ\text{C}$  and used for infection after thawing. Single-cell suspensions of these aliquots were used to deliver  $\sim 100$  CFU into 8–10 week old C57BL/6J mice using an aerosol apparatus manufactured by In-Tox Products (Moriarty, NM). Bacterial burden was estimated by plating serial dilutions of the lung homogenates on 7H10 agar plates on day 1 (for entry) or as indicated. CFU was enumerated after 21 days.

### Statistical analyses

The statistical significance of data was analyzed using the Student's unpaired t-test for comparisons between two groups or one-way analysis of variance (ANOVA) with a Tukey posttest correction for multiple comparisons for analysis of two or more groups (GraphPad Prism 6.0h). In order to calculate correlation, a linear regression was utilized to generate a best-fit line and Spearman's correlation coefficient calculated (GraphPad Prism 6.0h). Data are shown as mean  $\pm$  S.D. of one representative experiment from multiple independent experiments.

### Supporting information

**S1 Fig. CD40L is required for IFN- $\gamma$  and IL-2 responses from antigen-specific CD4 T cells *in vitro*.** DCs from C57BL/6 (B6) were pulsed with OVA<sub>323-339</sub> at 10  $\mu\text{g}/\text{ml}$  and infected with Mtb for 24 hours followed by co-culture with purified OT-II or CD40L<sup>-/-</sup> x OT-II TCR-Tg CD4 T cells. Cell-free supernatants were collected after 72 hours and assessed for the indicated cytokines by ELISA. Values are presented as mean  $\pm$  SD. Statistical significance was determined using a 2-tailed unpaired T test. \*  $p < 0.05$ . (TIFF)

**S2 Fig. CD40-CD40L interaction can be blocked using non-agonistic anti-CD40L antibody MR1.** To determine optimal concentrations of blocking antibody,  $1 \times 10^6$  splenocytes from OT-II TCR-Tg mice were plated with 5  $\mu\text{g}/\text{ml}$  anti-CD16/32 (Fc Block) and pulsed with 10  $\mu\text{g}/\text{ml}$  OVA<sub>323-339</sub> peptide for 6 hours in the presence or absence of non-agonistic anti-CD40L antibody (clone MR1) at the indicated concentrations. After 6 hours, PE-conjugated anti-CD40L antibody (clone MR1, 1:100) was spiked into the sample and left in the dark at 37°C for 18 hours. Cells were then washed, stained for viability, CD3 and CD4, and acquired immediately. Representative flow plots of recovered CD40L expression on live CD3<sup>+</sup> cells are shown

demonstrating titratable blockade of CD40L by MR1.  
(TIF)

**S3 Fig. CD40 engagement enhances cytokine production from DCs exposed to heat-killed Mtb.** B6 DCs were left uninfected or exposed to heat-killed Mtb in the presence or absence of 1 µg/ml multimeric CD40LT reagent (CD40LT) for 24 hours. Cell-free supernatants were collected after 24 hours and the indicated innate cytokines were measured by ELISA. Data are representative of 3 independent experiments. Values are presented as mean ± SD. Statistical significance was determined using a 2-tailed unpaired T-test. \* p<0.05.  
(TIFF)

## Acknowledgments

We gratefully thank Dana Tedesco and Dr. Arash Grakoui for anti-CD40L blocking antibody (MR1) and helpful input on CD40L blockade assays; Drs. David Pinelli and Mandy Ford for *CD40lg<sup>-/-</sup> × OT-II* TCR transgenic mice and input on breeding strategy; Dr. Joel Ernst for aid with intratracheal instillation technique. We also thank Melanie Quezada and members of the Rengarajan lab for helpful discussions.

## Author Contributions

**Conceptualization:** Jonathan Kevin Sia, Ranjna Madan-Lala, Jyothi Rengarajan.

**Data curation:** Jonathan Kevin Sia.

**Formal analysis:** Jonathan Kevin Sia, Jyothi Rengarajan.

**Funding acquisition:** Jyothi Rengarajan.

**Investigation:** Jonathan Kevin Sia, Erica Bizzell.

**Methodology:** Jonathan Kevin Sia, Ranjna Madan-Lala, Jyothi Rengarajan.

**Project administration:** Jonathan Kevin Sia, Jyothi Rengarajan.

**Resources:** Jyothi Rengarajan.

**Validation:** Jonathan Kevin Sia.

**Visualization:** Jonathan Kevin Sia, Jyothi Rengarajan.

**Writing – original draft:** Jonathan Kevin Sia, Jyothi Rengarajan.

**Writing – review & editing:** Jonathan Kevin Sia, Erica Bizzell, Ranjna Madan-Lala, Jyothi Rengarajan.

## References

1. Ernst JD. The immunological life cycle of tuberculosis. *Nat Rev Immunol.* 2012; 12(8):581–91. <https://doi.org/10.1038/nri3259> PMID: 22790178.
2. Robinson RT, Orme IM, Cooper AM. The onset of adaptive immunity in the mouse model of tuberculosis and the factors that compromise its expression. *Immunological Reviews.* 2015; 264(1):46–59. Epub 2015/02/24. <https://doi.org/10.1111/imr.12259> PMID: 25703551.
3. Reiley WW, Calayag MD, Wittmer ST, Huntington JL, Pearl JE, Fountain JJ, et al. ESAT-6-specific CD4 T cell responses to aerosol *Mycobacterium tuberculosis* infection are initiated in the mediastinal lymph nodes. *Proc Natl Acad Sci U S A.* 2008; 105(31):10961–6. <https://doi.org/10.1073/pnas.0801496105> PMID: 18667699; PubMed Central PMCID: PMC2504808.

4. Urdahl KB, Shafiani S, Ernst JD. Initiation and regulation of T-cell responses in tuberculosis. *Mucosal Immunol.* 2011; 4(3):288–93. <https://doi.org/10.1038/mi.2011.10> PMID: 21451503; PubMed Central PMCID: PMC3206635.
5. Wolf AJ, Desvignes L, Linas B, Banaiee N, Tamura T, Takatsu K, et al. Initiation of the adaptive immune response to *Mycobacterium tuberculosis* depends on antigen production in the local lymph node, not the lungs. *The Journal of Experimental Medicine.* 2008; 205(1):105–15. Epub 2007/12/26. <https://doi.org/10.1084/jem.20071367> PMID: 18158321; PubMed Central PMCID: PMC2234384.
6. Tameris MD, Hatherill M, Landry BS, Scriba TJ, Snowden MA, Lockhart S, et al. Safety and efficacy of MVA85A, a new tuberculosis vaccine, in infants previously vaccinated with BCG: a randomised, placebo-controlled phase 2b trial. *Lancet.* 2013; 381(9871):1021–8. [https://doi.org/10.1016/S0140-6736\(13\)60177-4](https://doi.org/10.1016/S0140-6736(13)60177-4) PMID: 23391465; PubMed Central PMCID: PMC3542467.
7. Andersen P, Urdahl KB. TB vaccines; promoting rapid and durable protection in the lung. *Current Opinion in Immunology.* 2015; 35:55–62. Epub 2015/06/27. <https://doi.org/10.1016/j.coi.2015.06.001> PMID: 26113434; PubMed Central PMCID: PMC4641675.
8. Bhatt K, Verma S, Ellner JJ, Salgame P. Quest for correlates of protection against tuberculosis. *Clinical and Vaccine Immunology.* 2015; 22(3):258–66. <https://doi.org/10.1128/CVI.00721-14> PMID: 25589549; PubMed Central PMCID: PMC4340894.
9. Wozniak TM, Saunders BM, Ryan AA, Britton WJ. *Mycobacterium bovis* BCG-specific Th17 cells confer partial protection against *Mycobacterium tuberculosis* infection in the absence of gamma interferon. *Infection and Immunity.* 2010; 78(10):4187–94. <https://doi.org/10.1128/IAI.01392-09> PMID: 20679438; PubMed Central PMCID: PMC2950338.
10. Scriba TJ, Kalsdorf B, Abrahams DA, Isaacs F, Hofmeister J, Black G, et al. Distinct, specific IL-17- and IL-22-producing CD4+ T cell subsets contribute to the human anti-mycobacterial immune response. *Journal of Immunology.* 2008; 180(3):1962–70. D—NLM: PMC2219462. PMID: 18209095; PubMed Central PMCID: PMC2219462.
11. Okamoto Yoshida Y, Umemura M, Yahagi A, O'Brien RL, Ikuta K, Kishihara K, et al. Essential role of IL-17A in the formation of a mycobacterial infection-induced granuloma in the lung. *Journal of Immunology.* 2010; 184(8):4414–22. <https://doi.org/10.4049/jimmunol.0903332> PMID: 20212094.
12. Khader SA, Guglani L, Rangel-Moreno J, Gopal R, Junecko BA, Fountain JJ, et al. IL-23 is required for long-term control of *Mycobacterium tuberculosis* and B cell follicle formation in the infected lung. *Journal of Immunology.* 2011; 187(10):5402–7. Epub 2011/10/18. <https://doi.org/10.4049/jimmunol.1101377> PMID: 22003199; PubMed Central PMCID: PMC3208087.
13. Freches D, Korf H, Denis O, Havaux X, Huygen K, Romano M. Mice genetically inactivated in interleukin-17A receptor are defective in long-term control of *Mycobacterium tuberculosis* infection. *Immunology.* 2013; 140(2):220–31. <https://doi.org/10.1111/imm.12130> PMID: 23721367; PubMed Central PMCID: PMC3784168.
14. Gopal R, Monin L, Slight S, Uche U, Blanchard E, Fallert Junecko BA, et al. Unexpected role for IL-17 in protective immunity against hypervirulent *Mycobacterium tuberculosis* HN878 infection. *PLoS Pathogens.* 2014; 10(5):e1004099. <https://doi.org/10.1371/journal.ppat.1004099> PMID: 24831696; PubMed Central PMCID: PMC34022785.
15. Cruz A, Torrado E, Carmona J, Fraga AG, Costa P, Rodrigues F, et al. BCG vaccination-induced long-lasting control of *Mycobacterium tuberculosis* correlates with the accumulation of a novel population of CD4(+)IL-17(+)TNF(+)IL-2(+) T cells. *Vaccine.* 2015; 33(1):85–91. Epub 2014/12/03. <https://doi.org/10.1016/j.vaccine.2014.11.013> PMID: 25448107.
16. Khader SA, Bell GK, Pearl JE, Fountain JJ, Rangel-Moreno J, Cillely GE, et al. IL-23 and IL-17 in the establishment of protective pulmonary CD4+ T cell responses after vaccination and during *Mycobacterium tuberculosis* challenge. *Nature Immunology.* 2007; 8(4):369–77. Epub 2007/03/14. <https://doi.org/10.1038/ni1449> PMID: 17351619.
17. Torrado E, Cooper AM. IL-17 and Th17 cells in tuberculosis. *Cytokine Growth Factor Rev.* 2010; 21(6):455–62. <https://doi.org/10.1016/j.cytogfr.2010.10.004> PMID: 21075039; PubMed Central PMCID: PMC3032416.
18. Gopal R, Lin Y, Obermajer N, Slight S, Nuthalapati N, Ahmed M, et al. IL-23-dependent IL-17 drives Th1-cell responses following *Mycobacterium bovis* BCG vaccination. *Eur J Immunol.* 2012; 42(2):364–73. <https://doi.org/10.1002/eji.201141569> PMID: 22101830; PubMed Central PMCID: PMC3490408.
19. Gopal R, Rangel-Moreno J, Slight S, Lin Y, Nawar HF, Fallert Junecko BA, et al. Interleukin-17-dependent CXCL13 mediates mucosal vaccine-induced immunity against tuberculosis. *Mucosal Immunol.* 2013; 6(5):972–84. <https://doi.org/10.1038/mi.2012.135> PMID: 23299616; PubMed Central PMCID: PMC3732523.

20. Rengarajan J, Murphy E, Park A, Krone CL, Hett EC, Bloom BR, et al. Mycobacterium tuberculosis Rv2224c modulates innate immune responses. *Proc Natl Acad Sci U S A*. 2008; 105(1):264–9. <https://doi.org/10.1073/pnas.0710601105> PMID: 18172199; PubMed Central PMCID: PMC2224198.
21. Madan-Lala R, Sia JK, King R, Adekambi T, Monin L, Khader SA, et al. Mycobacterium tuberculosis impairs dendritic cell functions through the serine hydrolase Hip1. *Journal of Immunology*. 2014; 192(9):4263–72. Epub 2014/03/25. <https://doi.org/10.4049/jimmunol.1303185> PMID: 24659689; PubMed Central PMCID: PMC3995873.
22. Wolf AJ, Linas B, Trevejo-Nunez GJ, Kincaid E, Tamura T, Takatsu K, et al. Mycobacterium tuberculosis infects dendritic cells with high frequency and impairs their function in vivo. *Journal of Immunology*. 2007; 179(4):2509–19. Epub 2007/08/07. PMID: 17675513.
23. Srivastava S, Ernst JD. Cell-to-cell transfer of M. tuberculosis antigens optimizes CD4 T cell priming. *Cell Host Microbe*. 2014; 15(6):741–52. <https://doi.org/10.1016/j.chom.2014.05.007> PMID: 24922576; PubMed Central PMCID: PMC4098643.
24. Grace PS, Ernst JD. Suboptimal Antigen Presentation Contributes to Virulence of Mycobacterium tuberculosis In Vivo. *Journal of Immunology*. 2016; 196(1):357–64. <https://doi.org/10.4049/jimmunol.1501494> PMID: 26573837; PubMed Central PMCID: PMC4684992.
25. Merad M, Sathe P, Helft J, Miller J, Mortha A. The dendritic cell lineage: ontogeny and function of dendritic cells and their subsets in the steady state and the inflamed setting. *Annual Review of Immunology*. 2013; 31:563–604. Epub 2013/03/23. <https://doi.org/10.1146/annurev-immunol-020711-074950> PMID: 23516985; PubMed Central PMCID: PMC3853342.
26. Sia JK, Georgieva M, Rengarajan J. Innate Immune Defenses in Human Tuberculosis: An Overview of the Interactions between Mycobacterium tuberculosis and Innate Immune Cells. *Journal of Immunology Research*. 2015; 2015:747543. Epub 2015/08/11. <https://doi.org/10.1155/2015/747543> PMID: 26258152; PubMed Central PMCID: PMC4516846.
27. Srivastava S, Ernst JD, Desvignes L. Beyond macrophages: the diversity of mononuclear cells in tuberculosis. *Immunological Reviews*. 2014; 262(1):179–92. <https://doi.org/10.1111/imr.12217> PMID: 25319335; PubMed Central PMCID: PMC4203409.
28. Lazarevic V, Myers AJ, Scanga CA, Flynn JL. CD40, but not CD40L, is required for the optimal priming of T cells and control of aerosol M. tuberculosis infection. *Immunity*. 2003; 19(6):823–35. Epub 2003/12/13. PMID: 14670300.
29. Jenkins MK, Taylor PS, Norton SD, Urdahl KB. CD28 delivers a costimulatory signal involved in antigen-specific IL-2 production by human T cells. *Journal of Immunology*. 1991; 147(8):2461–6. Epub 1991/10/15. PMID: 1717561.
30. Norton SD, Zuckerman L, Urdahl KB, Shefner R, Miller J, Jenkins MK. The CD28 ligand, B7, enhances IL-2 production by providing a costimulatory signal to T cells. *Journal of Immunology*. 1992; 149(5):1556–61. Epub 1992/09/01. PMID: 1380533.
31. Korn T, Bettelli E, Oukka M, Kuchroo VK. IL-17 and Th17 Cells. *Annual Review of Immunology*. 2009; 27:485–517. Epub 2009/01/10. <https://doi.org/10.1146/annurev-immunol.021908.132710> PMID: 19132915.
32. Ferrer IR, Liu D, Pinelli DF, Koehn BH, Stempora LL, Ford ML. CD40/CD154 blockade inhibits dendritic cell expression of inflammatory cytokines but not costimulatory molecules. *Journal of Immunology*. 2012; 189(9):4387–95. Epub 2012/09/25. <https://doi.org/10.4049/jimmunol.1201757> PMID: 23002440; PubMed Central PMCID: PMC3478479.
33. Demangel C, Palendira U, Feng CG, Heath AW, Bean AG, Britton WJ. Stimulation of dendritic cells via CD40 enhances immune responses to Mycobacterium tuberculosis infection. *Infection and Immunity*. 2001; 69(4):2456–61. <https://doi.org/10.1128/IAI.69.4.2456-2461.2001> PMID: 11254607; PubMed Central PMCID: PMC398179.
34. Harris NL, Ronchese F. The role of B7 costimulation in T-cell immunity. *Immunology and Cell Biology*. 1999; 77(4):304–11. Epub 1999/08/24. <https://doi.org/10.1046/j.1440-1711.1999.00835.x> PMID: 10457196.
35. Rengarajan J, Tang B, Glimcher LH. NFATc2 and NFATc3 regulate T(H)2 differentiation and modulate TCR-responsiveness of naive T(H) cells. *Nature Immunology*. 2002; 3(1):48–54. Epub 2001/12/12. <https://doi.org/10.1038/ni744> PMID: 11740499.
36. Ivanov II, McKenzie BS, Zhou L, Tadokoro CE, Lepelley A, Lafaille JJ, et al. The orphan nuclear receptor RORgamma directs the differentiation program of proinflammatory IL-17+ T helper cells. *Cell*. 2006; 126(6):1121–33. Epub 2006/09/23. <https://doi.org/10.1016/j.cell.2006.07.035> PMID: 16990136.
37. Tascon RE, Soares CS, Ragno S, Stavropoulos E, Hirst EM, Colston MJ. Mycobacterium tuberculosis-activated dendritic cells induce protective immunity in mice. *Immunology*. 2000; 99(3):473–80. D—NLM: PMC2327172. PubMed Central PMCID: PMC2327172. <https://doi.org/10.1046/j.1365-2567.2000.00963.x> PMID: 10712679

38. McShane H, Behboudi S, Goonetilleke N, Brookes R, Hill AV. Protective immunity against Mycobacterium tuberculosis induced by dendritic cells pulsed with both CD8(+) and CD4(+) T-cell epitopes from antigen 85A. *Infection and Immunity*. 2002; 70(3):1623–6. Epub 2002/02/21. PubMed Central PMCID: PMC127749. <https://doi.org/10.1128/IAI.70.3.1623-1626.2002> PMID: 11854254
39. Madan-Lala R, Peixoto KV, Re F, Rengarajan J. Mycobacterium tuberculosis Hip1 dampens macrophage proinflammatory responses by limiting toll-like receptor 2 activation. *Infection and Immunity*. 2011; 79(12):4828–38. Epub 2011/09/29. <https://doi.org/10.1128/IAI.05574-11> PMID: 21947769; PubMed Central PMCID: PMC3232659.
40. Naffin-Olivos JL, Georgieva M, Goldfarb N, Madan-Lala R, Dong L, Bizzell E, et al. Mycobacterium tuberculosis Hip1 modulates macrophage responses through proteolysis of GroEL2. *PLoS Pathogens*. 2014; 10(5):e1004132. Epub 2014/05/17. <https://doi.org/10.1371/journal.ppat.1004132> PMID: 24830429; PubMed Central PMCID: PMC34022732.
41. Hanekom WA, Mendillo M, Manca C, Haslett PA, Siddiqui MR, Barry C, 3rd, et al. Mycobacterium tuberculosis inhibits maturation of human monocyte-derived dendritic cells in vitro. *The Journal of Infectious Diseases*. 2003; 188(2):257–66. Epub 2003/07/11. <https://doi.org/10.1086/376451> PMID: 12854081.
42. Iezzi G, Sonderegger I, Ampenberger F, Schmitz N, Marsland BJ, Kopf M. CD40-CD40L cross-talk integrates strong antigenic signals and microbial stimuli to induce development of IL-17-producing CD4+ T cells. *Proc Natl Acad Sci U S A*. 2009; 106(3):876–81. <https://doi.org/10.1073/pnas.0810769106> PMID: 19136631; PubMed Central PMCID: PMC2630101.
43. Perona-Wright G, Jenkins SJ, O'Connor RA, Zienkiewicz D, McSorley HJ, Maizels RM, et al. A pivotal role for CD40-mediated IL-6 production by dendritic cells during IL-17 induction in vivo. *Journal of Immunology*. 2009; 182(5):2808–15. Epub 2009/02/24. <https://doi.org/10.4049/jimmunol.0803553> PMID: 19234175.
44. Hsia BJ, Whitehead GS, Thomas SY, Nakano K, Gowdy KM, Aloor JJ, et al. Trif-dependent induction of Th17 immunity by lung dendritic cells. *Mucosal Immunol*. 2015; 8(1):186–97. <https://doi.org/10.1038/mi.2014.56> PMID: 24985082; PubMed Central PMCID: PMC4267961.
45. Sakai S, Kauffman KD, Schenkel JM, McBerry CC, Mayer-Barber KD, Masopust D, et al. Cutting edge: control of Mycobacterium tuberculosis infection by a subset of lung parenchyma-homing CD4 T cells. *Journal of Immunology*. 2014; 192(7):2965–9. <https://doi.org/10.4049/jimmunol.1400019> PMID: 24591367; PubMed Central PMCID: PMC4010124.
46. Griffiths KL, Ahmed M, Das S, Gopal R, Horne W, Connell TD, et al. Targeting dendritic cells to accelerate T-cell activation overcomes a bottleneck in tuberculosis vaccine efficacy. *Nature Communications*. 2016; 7:13894. Epub 2016/12/23. <https://doi.org/10.1038/ncomms13894> PMID: 28004802; PubMed Central PMCID: PMC5192216.
47. Schulz O, Edwards AD, Schito M, Aliberti J, Manickasingham S, Sher A, et al. CD40 triggering of heterodimeric IL-12 p70 production by dendritic cells in vivo requires a microbial priming signal. *Immunity*. 2000; 13(4):453–62. PMID: 11070164.
48. Chandel HS, Pandey SP, Shukla D, Lalsare K, Selvaraj SK, Jha MK, et al. Toll-like receptors and CD40 modulate each other's expression affecting Leishmania major infection. *Clinical and Experimental Immunology*. 2014; 176(2):283–90. Epub 2014/01/07. <https://doi.org/10.1111/cei.12264> PMID: 24387292; PubMed Central PMCID: PMC3992041.
49. Campos-Neto A, Owendale P, Bement T, Koppi TA, Fanslow WC, Rossi MA, et al. CD40 ligand is not essential for the development of cell-mediated immunity and resistance to Mycobacterium tuberculosis. *Journal of Immunology*. 1998; 160(5):2037–41. Epub 1998/03/14. PMID: 9498737.
50. Ryan ES, Micci L, Fromentin R, Paganini S, McGary CS, Easley K, et al. Loss of Function of Intestinal IL-17 and IL-22 Producing Cells Contributes to Inflammation and Viral Persistence in SIV-Infected Rhesus Macaques. *PLoS Pathogens*. 2016; 12(2):e1005412. Epub 2016/02/02. <https://doi.org/10.1371/journal.ppat.1005412> PMID: 26829644; PubMed Central PMCID: PMC4735119.
51. Aguilo N, Alvarez-Arguedas S, Uranga S, Marinova D, Monzon M, Badiola J, et al. Pulmonary but Not Subcutaneous Delivery of BCG Vaccine Confers Protection to Tuberculosis-Susceptible Mice by an Interleukin 17-Dependent Mechanism. *The Journal of Infectious Diseases*. 2016; 213(5):831–9. Epub 2015/10/24. <https://doi.org/10.1093/infdis/jiv503> PMID: 26494773.
52. Cowley SC, Elkins KL. CD4+ T cells mediate IFN-gamma-independent control of Mycobacterium tuberculosis infection both in vitro and in vivo. *Journal of Immunology*. 2003; 171(9):4689–99. Epub 2003/10/22. PMID: 14568944.
53. Gallegos AM, van Heijst JW, Samstein M, Su X, Pamer EG, Glickman MS. A gamma interferon independent mechanism of CD4 T cell mediated control of M. tuberculosis infection in vivo. *PLoS Pathogens*. 2011; 7(5):e1002052. Epub 2011/06/01. <https://doi.org/10.1371/journal.ppat.1002052> PMID: 21625591; PubMed Central PMCID: PMC3098235.

54. Sakai S, Kauffman KD, Sallin MA, Sharpe AH, Young HA, Ganusov VV, et al. CD4 T Cell-Derived IFN-gamma Plays a Minimal Role in Control of Pulmonary Mycobacterium tuberculosis Infection and Must Be Actively Repressed by PD-1 to Prevent Lethal Disease. *PLoS Pathogens*. 2016; 12(5):e1005667. Epub 2016/06/01. <https://doi.org/10.1371/journal.ppat.1005667> PMID: [27244558](https://pubmed.ncbi.nlm.nih.gov/27244558/); PubMed Central PMCID: [PMC4887085](https://pubmed.ncbi.nlm.nih.gov/PMC4887085/).
55. Okada S, Markle JG, Deenick EK, Mele F, Averbuch D, Lagos M, et al. Impairment of immunity to *Candida* and *Mycobacterium* in humans with bi-allelic RORC mutations. *Science*. 2015; 349(6248):606–13. <https://doi.org/10.1126/science.aaa4282> PMID: [26160376](https://pubmed.ncbi.nlm.nih.gov/26160376/); PubMed Central PMCID: [PMC4668938](https://pubmed.ncbi.nlm.nih.gov/PMC4668938/).
56. Cruz A, Khader SA, Torrado E, Fraga A, Pearl JE, Pedrosa J, et al. Cutting edge: IFN-gamma regulates the induction and expansion of IL-17-producing CD4 T cells during mycobacterial infection. *Journal of Immunology*. 2006; 177(3):1416–20. Epub 2006/07/20. PMID: [16849446](https://pubmed.ncbi.nlm.nih.gov/16849446/).
57. Cruz A, Fraga AG, Fountain JJ, Rangel-Moreno J, Torrado E, Saraiva M, et al. Pathological role of interleukin 17 in mice subjected to repeated BCG vaccination after infection with *Mycobacterium tuberculosis*. *The Journal of Experimental Medicine*. 2010; 207(8):1609–16. <https://doi.org/10.1084/jem.20100265> PMID: [20624887](https://pubmed.ncbi.nlm.nih.gov/20624887/); PubMed Central PMCID: [PMC2916141](https://pubmed.ncbi.nlm.nih.gov/PMC2916141/).
58. Nandi B, Behar SM. Regulation of neutrophils by interferon-gamma limits lung inflammation during tuberculosis infection. *The Journal of Experimental Medicine*. 2011; 208(11):2251–62. <https://doi.org/10.1084/jem.20110919> PMID: [21967766](https://pubmed.ncbi.nlm.nih.gov/21967766/); PubMed Central PMCID: [PMC3201199](https://pubmed.ncbi.nlm.nih.gov/PMC3201199/).

Adapted from

Maria Georgieva, Jonathan Kevin Sia<sup>\*</sup>, Erica Bizzell<sup>\*</sup> *et al.* (2017)

*Mycobacterium tuberculosis* GroEL2 modulates dendritic cell responses

<sup>\*</sup> These authors contributed equally to this work

Accepted to Infection and Immunity November 2017

Contribution(s):

I conducted the experiment for figure 3B of this manuscript (pg. 193). Specifically, I stimulated DCs with the indicated amounts of GroEL2 protein and analyzed their cytokine responses via ELISA.

**ABSTRACT**

*Mycobacterium tuberculosis* (Mtb) successfully subverts the host immune response to promote disease progression. In addition to its known intracellular niche in macrophages, Mtb interferes with the functions of dendritic cells (DCs), which are the primary antigen presenting cells in the immune system. We previously showed that Mtb dampens proinflammatory responses and impairs DC functions through the cell envelope-associated serine protease, Hip1. Here we present data showing that Mtb GroEL2, a substrate of Hip1, modulates DC functions. Full length GroEL2 protein elicited robust proinflammatory responses from DCs and promoted DC maturation and antigen presentation to T cells. In contrast, the cleaved form of GroEL2, which predominates in Mtb, was poorly immunostimulatory and was unable to promote DC maturation and antigen presentation. Moreover, DCs exposed to full length, but not cleaved GroEL2, induced strong antigen-specific IFN- $\gamma$ , IL-2, and IL-17A cytokine responses from CD4<sup>+</sup> T cells. Moreover, expression of cleaved GroEL2 into the *hip1* mutant restored the robust T cell responses to wild type levels, suggesting that proteolytic cleavage of GroEL2 allows Mtb to prevent optimal DC-T cell crosstalk during Mtb infection.

## INTRODUCTION

*Mycobacterium tuberculosis* (Mtb) is a highly successful human pathogen that has evolved multiple mechanisms to evade and manipulate host innate and adaptive immunity [1-3]. While CD4<sup>+</sup> T cell responses are important for mycobacterial control, Mtb delays the onset of antigen-specific T cell responses, which are unable to effectively eliminate the pathogen from infected hosts. These sub-optimal CD4<sup>+</sup> T cell responses are in part due to the ability of Mtb to impair dendritic cell (DC) functions such as migration of infected DCs from the lung to draining lymph nodes, DC maturation and antigen presentation to naïve CD4<sup>+</sup> T cells [4-6]. As the primary antigen-presenting cells of the immune system, DCs serve as a bridge between innate and adaptive immunity. By impairing DC functions, Mtb prevents optimal crosstalk between DCs and CD4<sup>+</sup> T cells and shapes T cell responses to its benefit. However, the bacterial factors that contribute to Mtb-mediated impairment of DCs are poorly defined.

We previously demonstrated that the Mtb protein GroEL2, which encodes a chaperone-like immunomodulatory protein, modulates macrophage proinflammatory responses. While these studies have focused on the role of the full length (FL) GroEL2 protein, our data suggests that a cleaved form of GroEL2 predominates in wild type Mtb and that cleavage of GroEL2 serves to dampen innate immune responses to Mtb infection. We showed that FL GroEL2 protein has a multimeric conformation, is exported to the cell wall of Mtb, and secreted extracellularly [7]. In wild type Mtb, FL GroEL2 is proteolytically cleaved at its N-terminus between amino acid residues Arg<sub>12</sub> and Gly<sub>13</sub> by

the serine protease Hip1 into a smaller form GroEL2(cl) that has a monomeric conformation [7]. Cleavage of GroEL2 does not occur in the absence of Hip1 protease activity and an Mtb *hip1* mutant harbors FL GroEL2 but not GroEL2(cl) protein. Moreover, the *hip1* mutant induced significantly higher levels of proinflammatory cytokines compared to wild type Mtb during macrophage infection. This was in part attributed to the enhanced immunostimulatory effect of FL GroEL2 in the *hip1* mutant compared to GroEL2(cl), which predominates in wild type Mtb. The immunomodulatory effects of GroEL2 on macrophage functions suggests that GroEL2 may also play a role in modulating DCs and downstream T cell responses. Therefore, we sought to investigate whether cleavage of GroEL2 impacts DC functions. We hypothesized that FL GroEL2 and GroEL2(cl) proteins would differentially impact DC functions and thereby shape the type of antigen-specific T cell responses elicited during infection with Mtb. We show that FL GroEL2, but not cleaved GroEL2, induced robust proinflammatory cytokines from DCs and significantly greater expression of the costimulatory molecules CD40 and CD86 on DCs. We also show that FL GroEL2 promoted efficient antigen presentation and polarization of antigen-specific CD4<sup>+</sup> T cells into T-helper (Th) subsets that secreted IFN- $\gamma$ , IL-2, and IL-17. In contrast GroEL2(cl) was poorly stimulatory and unable to promote antigen presentation to T cells. Moreover, expressing GroEL2(cl) within the *hip1* mutant restored T cell responses to levels induced by wild type Mtb in DC-T cell co-culture assays. Our studies suggest that Hip1-mediated cleavage of GroEL2 compromises the ability of DCs to initiate optimal antigen-specific T cell responses, thus dampening the host response to infection.

## RESULTS

### **Enhanced maturation of DCs by FL GroEL2 compared to GroEL2(cl)**

At sites of infection, immature DCs undergo maturation upon contact with antigens; mature DCs are characterized by high surface expression of costimulatory molecules such as CD40 and CD86, which interact with ligands on T cells to optimally induce T cell activation. To investigate how proteolytic cleavage alters the immunostimulatory capacity of the GroEL2 protein, we first compared the ability of purified recombinant FL GroEL2 and GroEL2(cl) proteins to induce cell surface expression of key costimulatory molecules on DCs (Figure 1). Recombinant proteins were generated as described previously [7] and endotoxin levels in these protein preparations were determined to be below detection levels (data not shown). We exposed bone marrow-derived DCs (BMDCs) from C57BL/6 mice to either FL or GroEL2(cl), and measured the expression of CD40, CD86, and MHC class II on the cell surface by flow cytometry. FL GroEL2 induced robust expression of CD40 and CD86 (Figure 1); in contrast, GroEL2(cl) induced significantly lower levels of these two markers. Under these conditions, neither form of GroEL2 induced further expression of MHC class II above baseline (data not shown). Overall, these data indicate that cleavage of GroEL2 blunts its capacity to induce maturation of DCs.

### **Cleavage of Mtb GroEL2 attenuates its ability to induce cytokine responses in DCs.**

As DCs undergo maturation, they produce key proinflammatory cytokines such as IL-12 and IL-6 that are important for polarizing naïve T helper (Th) cells into Th subsets such

as IFN- $\gamma$ -producing Th<sub>1</sub> cells [8]. We therefore compared the levels of IL-12p40 and IL-6 induced by recombinant GroEL2 and GroEL2(cl) proteins (Figure 2). We exposed BMDCs to varying concentrations of FL GroEL2 and GroEL2(cl) and measured levels of IL-12p40 and IL-6 in the supernatants after 24 hours. FL GroEL2 induced high levels of both IL-12p40 and IL-6 in DCs at each concentration tested. Cytokine levels induced by FL were comparable to those induced by Pam<sub>3</sub>CysSerLys<sub>4</sub> (Pam<sub>3</sub>CSK<sub>4</sub>). In contrast, GroEL2(cl) was unable to induce these two cytokines above background levels at all concentrations of the protein tested. We did not detect IL-10, TNF- $\alpha$  or IL-1 $\beta$  production under the conditions tested (data not shown). These data indicate that FL GroEL2 has the capacity to induce proinflammatory cytokine production in DCs but that Hip1-mediated cleavage of GroEL2 abrogates its immunostimulatory capacity.

We next investigated whether Hip1-dependent cleavage of GroEL2 contributes to impaired DC functions during infection in the context of live wild type and *hip1* mutant Mtb strains. As shown in Figure 3A, the *hip1* mutant, which harbors only FL GroEL2, induced higher levels of IL-6 and IL-12 cytokines in infected BMDCs compared to wild type Mtb (Figure 3) [9]. Complementation of the *hip1* mutant with Hip1 (*hip1* comp) restored wild type levels of these cytokines (Figure 3A). To assess the contribution of GroEL2 cleavage to the *hip1* mutant phenotype, we used an engineered *hip1* mutant strain that ectopically expressed secreted GroEL2(cl). We previously confirmed that the levels of GroEL2(cl) in the supernatant fraction of the *hip1* mutant+GroEL2(cl) strain were comparable to wild type Mtb [7]. Importantly, expression of GroEL2(cl) in the *hip1* mutant background restored wild type levels of IL-12p40 and IL-6 in infected BMDCs,

comparable to levels seen in the *hip1* comp strain. These data suggest that cleavage of GroEL2 in wild type Mtb dampens DC cytokine responses. To more directly assess the immunomodulatory capacity of GroEL2(cl), we compared the effect of exposing BMDCs to both GroEL2(cl) and FL GroEL2 together. We found that the levels of cytokines induced by a 1:1 molar ratio of GroEL2 and GroEL2(cl) in combination was less than the additive effect of each individual protein (Figure 3B). Together, these studies suggest that GroEL2(cl) is capable of dampening the stimulatory effect of FL GroEL2.

### **FL GroEL2, but not GroEL2(cl), augments antigen-specific T cell responses.**

Based on our observation of differential production of proinflammatory cytokines and expression of co-stimulatory markers by DCs in response to GroEL2 and GroEL2(cl), we sought to test whether cleavage of GroEL2 impacted DC antigen presentation to naïve antigen-specific CD4<sup>+</sup> T cells. We used an *in vitro* antigen presentation assay involving co-culture of DCs with CD4<sup>+</sup> T cells isolated from OT-II mice, which are T Cell Receptor-transgenic (TCR-Tg) mice specific for the ovalbumin (OVA)<sub>323-339</sub> peptide. We first pulsed BMDCs with OVA<sub>323-339</sub> peptide and then exposed DCs to FL or GroEL2(cl) for 24 hours. We then co-cultured BMDCs with OT-II TCR-Tg CD4<sup>+</sup> T cells, collected supernatants 72 hours after co-culture, and assayed for IFN- $\gamma$ , IL-2 and IL-17 by ELISA (Figure 4A). FL GroEL2 but not GroEL2(cl) stimulated robust presentation of OVA<sub>323-339</sub> peptide as assessed by production of IL-2. Further, DCs stimulated with FL GroEL2 induced significantly higher levels of IFN- $\gamma$  and IL-17 compared to BMDCs stimulated with GroEL2(cl). Thus, FL GroEL2 enhanced both the capacity of BMDCs to present antigens to CD4<sup>+</sup> T cells and to induce Th<sub>1</sub> and Th<sub>17</sub> cytokines, consistent with the

enhanced levels of IL-12p40 and IL-6 produced by BMDCs exposed to FL GroEL2. In contrast, BMDCs stimulated with GroEL2(cl), which predominates during Mtb infection, activated CD4<sup>+</sup> T cells poorly. Overall, these results suggest that cleavage of GroEL2 contributes to modulation of DC-T cell crosstalk during Mtb infection.

To further investigate whether GroEL2(cl) modulates antigen-specific T cell responses during live Mtb infection, we used DC-T cell co-culture assays to assess the production of Th1 and Th17 cytokines. We infected BMDCs with wild type, *hip1* mutant, and *hip1* mutant + GroEL2(cl) Mtb strains. To assess the ability of DCs infected with each of these strains to polarize naive Mtb-specific CD4 T cell towards Th1 and Th17 subsets, we co-cultured infected BMDCs with purified ESAT-6 TCR-transgenic (Tg) CD4<sup>+</sup> T cells (Figure 4B). Supernatants were harvested 80 hours after co-culture and assayed for IL-17A, IL-2, and IFN- $\gamma$  cytokines by ELISA. *Hip1* mutant Mtb-infected BMDCs induced elevated levels of IL-17A, IL-2, and IFN- $\gamma$  cytokines relative to wild type Mtb-infected DCs. However, BMDCs infected with *hip1* mutant + GroEL2(cl) Mtb strain produced significantly lower IL-17A, IL-2, and IFN- $\gamma$  cytokine levels, comparable to BMDCs infected with wild type Mtb. Overall, these data suggest that GroEL2(cl) effectively blunts the magnitude of T cell responses during infection, and that cleavage of GroEL2 is a strategy employed by Mtb to modulate DC-T cell crosstalk.

## DISCUSSION

While it is known that Mtb impairs DC functions, the underlying bacterial mechanisms are poorly defined. In this study, we characterized the contribution of FL and cleaved forms of Mtb GroEL2 protein in modulating the DC-T cell interface. While most studies on GroEL2 have focused on the ability of FL protein to modulate innate immune responses, our studies are the first to show that cleavage of GroEL2 prevents robust DC activation and impacts crosstalk between DC and CD4<sup>+</sup> T cells [10-20]. Since GroEL2 is present predominantly as a cleaved monomeric protein in wild type Mtb, our studies provide new insights about the way cleavage of GroEL2 impacts DC-T cell crosstalk.

Our studies using purified recombinant FL and cleaved GroEL2 proteins suggest that cleavage of GroEL2 abrogates its immunostimulatory capacity towards DCs and significantly limits production of key cytokine mediators such as IL-12 and IL-6 (Figure 2). These studies extend previous findings in macrophages showing that recombinant full length GroEL2 induces pro-inflammatory cytokines in a TLR-dependent manner [7, 21]. To investigate the role of GroEL2 cleavage during Mtb infection of DCs, we took advantage of Mtb bacterial strains that predominantly harbored cleaved GroEL2 (wild type Mtb, *hip1* mutant complemented), FL GroEL2 (*hip1* mutant Mtb) or a strain that was engineered to express GroEL2(cl) within the *hip1* mutant. We found that ectopic expression of cleaved GroEL2 in the *hip1* mutant background significantly diminished the hyperinflammatory phenotype of the *hip1* mutant Mtb (Figure 3A). These data suggest that cleavage of GroEL2 in wild type Mtb directly contributes to impaired DC functions during infection and is likely to be a major contributor to the *hip1* mutant

phenotype. Furthermore, we found that addition of GroEL2(c1) dampens proinflammatory responses of DCs (Figure 3B). The differential functions of GroEL2 and GroEL2(c1) are reminiscent of studies on other immunostimulatory heat-shock family proteins. Fong *et al.* report that heat-shock protein 70 (Hsp70), similar to GroEL2(c1), is secreted from cells and is capable of activating the immunomodulatory Siglec receptors on monocytes and neutrophils [22]. Intriguingly, Hsp70 delivers both anti-inflammatory and pro-inflammatory signals through Siglec activation, pointing to important functional polymorphisms of extracellular Hsp proteins. In the context of these findings, our own data suggest that the two forms of Mtb GroEL2 are likely to be functionally distinct and that the balance between the amounts of the two form of GroEL2 during DC infection will influence the type of host immune response generated. We also show that FL GroEL2, but not GroEL2(c1) leads to upregulation of cell surface-associated costimulatory molecules on DCs such as CD40 and CD86 (Figure 1) and elicits significantly higher levels of IFN- $\gamma$ , IL-2, and IL-17 from antigen-specific CD4<sup>+</sup> T cells (Figure 4A). Furthermore, in the context of live infection during DC-T cell co-culture, GroEL2(c1) modulates antigen-specific T cell responses and thus promotes sub-optimal immune responses (Figure 4B). These results are consistent with previous reports on the ability of FL Mtb GroEL2 to enhance antigen cross presentation during DC-T cell co-culture [10]. Further, biochemical and structural studies indicate that GroEL2 may be involved in promoting antigen presentation. GroEL2 possesses specific protein domains that have the potential to bind peptide substrates, a process that likely facilitates their subsequent association with MHC molecules [23, 24]. Together, our results highlight

GroEL2 cleavage as a mechanism employed by Mtb to modulate DC-mediated immunity during infection.

Our studies add insight to a growing body of data implicating GroEL2 in modulating host immune responses to Mtb infection. *Mycobacteria* are unusual among bacteria in possessing two GroEL proteins, the cytoplasmic protein GroEL1, which is highly homologous to the *E. coli* GroEL chaperonin, and GroEL2 [25, 26]. While GroEL1 is cytoplasmic, GroEL2 is localized to the cell envelope and secreted extracellularly. Interestingly, GroEL2 is reported to be among the most abundant Mtb proteins *in vivo* and a dominant contributor to the potent immune response elicited by Mtb Purified Protein Derivative (PPD) [27, 28]. Indeed, several studies investigated GroEL2 as a vaccine adjuvant, showing that FL GroEL2 boosts the magnitude of the immune response against infection, thereby improving vaccine mediated protection against Mtb [17-20]. These studies show that FL GroEL2 appears to mediate its efficacy via a cellular response dominated by IFN- $\gamma$  producing Th<sub>1</sub> cells [18]. Our results on the functional differences between FL and cleaved GroEL2 add credence to these findings and highlight a potential use for GroEL2 as an immunomodulatory component in strategies aimed at improving vaccine-induced immunity to Mtb infection.

## MATERIAL AND METHODS

### Plasmid construction

a) for expression in *E. coli*

Mtb *groEL2* was cloned into pACYCDuet-1 (Merck Millipore, Darmstadt, Germany) via the restriction sites *EcoRI* and *KpnI* using the InFusion cloning system following the manufacturer's protocol. Mtb *groEL2* was amplified using the primers 5'-GCCAGGATCCGAATTCGATGGCCAAGACAATTGCGTACGAC-3' and 5'-TTACCAGACTCGAGGGTACCGAAATCCATGCCACCCATGTCGCC-3', yielding a construct bearing an in-frame N-terminal 6XHis-tag and a C-terminal S-tag, yielding pACYCDuet-1 GroEL2. Using LC/MS/MS analysis, we previously identified GroEL2 is cleaved between amino acid positions 12 and 13 at the N-terminus to produce the cleaved GroEL2 protein [7]. Using this information, we constructed Mtb *groEL2(cl)* using primers 5'-TCCACGGAATTCGGGCCTCGAGCGGGGCTTGAACGCC-3' and 5'-TCCAGTGGTACCTCAGAAATCCATGCCACCCATGTC -3', yielding a pACYCDuet-1 GroEL2(cl) construct bearing an in-frame N-terminal 6XHis-tag and a C-terminal S-tag.

b) for expression in Mtb

Secreted GroEL2(cl)-myc: To express the cleaved form of GroEL2, GroEL2 (cl), the *groEL2* gene (minus the first 13 amino acids) was amplified from the Mtb genome using forward primer 5'-ACGCAGCTGGGCCTCGAGCGGGGCTTGAACGCC-3' and reverse primer 5'-

AGTAAGCTTTCACAGATCTTCTTCAGAAATAAGTTTTTGTTCGAAATCCATGC

CACC-3' and cloned into the *PvuII* and *HindIII* sites of pMV762, downstream of the predicted N-terminal signal sequence from Mtb antigen 85 complex B NH<sub>2</sub>-MTDVSRKIRAWGRRLMIGTAAAVVLPGLVGLAGGAATAGA-OH and an in-frame C-terminal Myc tag.

**Expression and preparation of recombinant proteins GroEL2 and GroEL2(cl) from *E. coli***

The plasmids, pACYCDuet-1 GroEL2 and pACYCDuet-1 GroEL2(cl) were separately transformed into *E. coli* BL21 Star (DE3) (Invitrogen, Carlsbad, CA) for protein expression. LB broth (1L) containing 34 µg/mL chloramphenicol was inoculated with 5 mL of overnight culture and incubated at 37°C to an OD<sub>600</sub> of 0.6 to 0.8. The cells were cooled to room temperature for 15-30 minutes after which 1 mM IPTG was added and the cells were incubated overnight at 28°C. The cells were then centrifuged at 10,000 rpm for 1 hour. The cell pellet containing GroEL2 or GroEL2(cl) was resuspended in binding buffer (20 mM Tris-HCl, 500 mM NaCl, 5 mM Imidazole, pH 7.9, 200 µg/ml lysozyme, 1.8 µg/µl DNase) plus protease inhibitor cocktail (Santa Cruz Biotechnology, Dallas, TX), sonicated and centrifuged at 16,000 x g for 90 min to remove cellular debris and clarify. The soluble fraction was added to Ni<sup>2+</sup>-charged beads in a gravity column. The cell lysate in the gravity column was first washed with wash buffer 1 (20 mM Tris-HCl, 500 mM NaCl, 60 mM imidazole, pH 7.9) and then wash buffer 2 (10 mM Tris-HCl) to remove residual salts from the column. To remove endotoxin, the cell lysate was washed with 0.5% ASB-14 (Millipore, Billerica, MA) in 10 mM Tris-HCl. Finally, the lysate was washed with 10 mM Tris-HCl to remove any excess detergent. The protein

was eluted with 1M imidazole in 10 mM Tris-HCl and dialyzed overnight in 1× PBS buffer. The protein was further purified by size exclusion chromatography on GE Superdex 75 10/300 GL column. The purified protein was then concentrated. The endotoxin levels for each protein were  $<10 \text{ ng}^{-1} \text{ ml}^{-1} \text{ mg}^{-1}$  as determined using LAL Chromogenic endotoxin quantitation kit (Thermo Scientific, Rockford, IL). Proteins were subjected to SDS-PAGE and visualized as a single band by staining with 0.05% Coomassie blue R-250. The concentrations of purified proteins were determined by Bradford method using bovine serum albumin (BSA) as the standard.

### **Bacterial strains and media**

Mtb H37Rv, the *hip1* mutant strain (described previously) [29, 30] and Mtb strain expressing GroEL2(cl) were grown at 37°C in Middlebrook 7H9 broth or 7H10 supplemented with 10% oleic acid-albumin-dextrose-catalase (OADC) (Becton Dickinson, Franklin Lakes, NJ), 0.02 % glycerol, and 0.05% Tween 80 (for broth), with the addition of 25 µg/ml kanamycin (Sigma-Aldrich, St. Louis, MO) for the *hip1* mutant, and, for complemented strains, 10 µg/ml streptomycin (Sigma-Aldrich, St. Louis, MO) or 50 µg/ml hygromycin (Roche Diagnostics, Indianapolis, IN) was added.

### **Mice**

All mice were housed under specific pathogen-free conditions in filter- top cages within the vivarium at the Yerkes National Primate Center, Emory University, and provided with sterile water and food ad libitum. C57BL/6 mice were purchased from The Jackson Laboratory. OTH-transgenic (Tg) mice specific for OVA<sub>323–339</sub> peptide originally

generated in the laboratory of Dr. F. Carbone (University of Melbourne, Melbourne, VIC, Australia) were bred at the Yerkes animal facility.

### **Dendritic cells and cytokine assays**

For generating murine bone marrow–derived DCs (BMDCs), bone marrow cells from C57BL/6 mice were flushed from excised femurs and tibias and grown in RPMI 1640 medium (Lonza, Walkersville, MD) with 10% heat-inactivated FBS (HyClone, Logan, UT), 2 mM glutamine, 13 2-ME, 10 mM HEPES, 1 mM sodium pyruvate, 13 nonessential amino acids, and 20 ng/ml murine recombinant GM-CSF (R&D Systems, Minneapolis, MN). Incubations were carried out at 37°C with 5% CO<sub>2</sub>. Fresh medium with GM-CSF was added on days 3 and 6, and cells were used on day 7 for all experiments. We routinely obtained ~75% CD11c<sup>+</sup> CD11b<sup>+</sup> cell purity by flow cytometry. BMDCs were further purified by using magnetic beads coupled to CD11c<sup>+</sup> mAb and passed through an AutoMACS column as per the manufacturer's instructions, where indicated (Miltenyi Biotec, Auburn, CA). For all experiments, cells were maintained throughout in medium containing GM-CSF.

For infection, BMDCs were plated onto 24-well plates ( $3 \times 10^5$  per well). Bacteria were filtered through 5 micron filters, resuspended in complete medium containing 20 ng/ml GM-CSF, and sonicated twice for 5 s each before addition to the adherent monolayers. Each bacterial strain was used for infection (in duplicate or triplicate) at a multiplicity of infection (MOI) of 5 or as indicated. Infection of BMDCs was carried out for 4 h, after which monolayers were washed four times with PBS before replacing with RPMI 1640 medium containing 20 ng/ml GM-CSF. To determine intracellular CFU, one set of DCs

was lysed in PBS containing 0.5% Triton X-100 and plated on 7H10 agar plates containing the appropriate antibiotics.

For stimulation of BMDCs with recombinant GroEL2 protein, endotoxin-free GroEL2 and GroEL2(cl) in supplemented RPMI 1640 (as described above) were added to C57BL/6 BMDCs for 24 hours. Cell-free supernatants from DC monolayers were isolated at indicated points and assayed for cytokines by ELISA using Duo Set kits for IL-12p40, IL-6, and IL-10 (BD Biosciences, San Jose, CA). Assays were carried out according to the manufacturer's instructions. Uninfected BMDCs were used as controls for each experiment.

#### **DC-T cell coculture assays**

##### a) with live Mtb strains

BMDCs were differentiated and plated as described above. BMDCs were infected (in triplicate) with wild type, *hip1* mutant or *hip1* mutant + GroEL2(cl) Mtb strains at a multiplicity of infection (MOI) of 10. Infection of BMDCs was carried out for 4 hours, after which monolayers were incubated with amikacin (200 µg/ml; Sigma-Aldrich) for 45 minutes to kill extracellular bacteria and then washed four times with PBS before incubating for 24 hours in complete medium. Following washing, to determine intracellular CFU, one set of DCs was lysed in PBS containing 0.5% Triton X-100 and plated on 7H10 agar plates containing the appropriate antibiotics. On the following day, BMDCs were co-cultured with ESAT-6-specific TCR-Tg CD4<sup>+</sup> T cells at 1: 4 DC: T cell ratio for 80 hours. CD4<sup>+</sup> T cells were purified from single-cell suspensions of spleen and lymph nodes from 6–8-week-old transgenic mice using MACS Miltenyi CD4<sup>+</sup> positive

selection kit (L3T4). Purified CD4<sup>+</sup> T cells showed  $\geq 99\%$  purity by FACS analysis. Cell free supernatants collected from co-cultured cells were analyzed for IFN- $\gamma$  (Mabtech, Cincinnati, OH), IL-17A (ELISA Ready-Set-Go, eBioscience), and IL-2 (BD Biosciences) by ELISA according to the manufacturers' instructions.

b) with recombinant GroEL2 protein

CD4<sup>+</sup> T cells were purified from single-cell suspensions of spleen and lymph nodes from 6–8-week-old OTII-Tg mice using the EasySep naïve CD4<sup>+</sup> T cell isolation kit (Stemcell Technologies). BMDCs were incubated in 24-well plates ( $3 \times 10^5$ /well) with varying amounts of OVA<sub>323–339</sub> peptide (1  $\mu\text{g/ml}$ , 10  $\mu\text{g/ml}$ , 50  $\mu\text{g/ml}$ ) for 6 hours and then stimulated with either recombinant GroEL2 (10  $\mu\text{M}$ ) or GroEL2(cl) (10  $\mu\text{M}$ ) for 24 hours. Then, BMDCs were washed twice with PBS and co-cultured with OVA<sub>323–339</sub>-specific TCR-Tg CD4<sup>+</sup> T cells at a 1:4 ratio for 72 h. Supernatants collected from these cells were analyzed for IFN- $\gamma$  (Mabtech), IL-2 (BD Biosciences), and IL-17A (eBioscience) by ELISA according to the manufacturers' instructions.

### **Flow cytometry**

Murine anti-CD11c allophycocyanin (clone N418) and anti-CD11b FITC (clone M1/70) were obtained from BioLegend; anti-CD40 PE (clone 3//23), anti-CD86 PE (clone GL1) and anti-MHC II PE (clone M5/ 114.15.2) were purchased from BD Biosciences.

Staining for cell-surface markers was done by resuspending  $\sim 1 \times 10^6$  cells in 200 ml PBS with 2% FBS containing the antibody mixture. Cells were incubated at 4 °C for 30 min and then washed with PBS containing 2% FBS. Data were immediately acquired using an

LSR flow cytometer (BD Biosciences). Data were analyzed with FlowJo software (Tree Star, San Carlos, CA).

### **Statistical analysis**

The statistical significance of data was analyzed using the Student's unpaired t-test (GraphPad Prism 5.0a). Data are shown as mean  $\pm$ S.D. of one representative experiment from three independent experiments.

### **Author contributions**

Conceived and designed the experiments: JR, MG, EB, JKS, RML. Performed the experiments: MG, EB, JKS, RML. Analyzed the data: JR, MG, EB, JKS. Contributed reagents/materials/analysis tools: JR. Wrote the manuscript: JR, MG.

### **Acknowledgements**

This work was supported by grants from the National Institute of Allergy and Infectious Diseases, National Institutes of Health: 5R01AI083366-05 and 2R56AI083366-06A1 (to JR), a Yerkes National Primate Center Base grant: RR000165 and a Center for AIDS Research (CFAR) Immunology Core grant (to Emory University): P30AI050409.

## FIGURE LEGENDS AND FIGURES

**Figure 1. Expression of co-stimulatory molecules CD40 and CD86 on DCs in response to full length GroEL2 and GroEL2(cl).** We stimulated C57BL/6 BMDCs with recombinant GroEL2 or GroEL2(cl) for 24 hours and analyzed cell surface expression of CD40 and CD86. Representative histograms and MFI values for the CD11c<sup>+</sup> DC subpopulation are shown. Isotype and Pam<sub>3</sub>CSK<sub>4</sub> control are shown as gray and green outlines respectively. Data are shown as mean  $\pm$ S.D. of one representative experiment from three independent experiments.

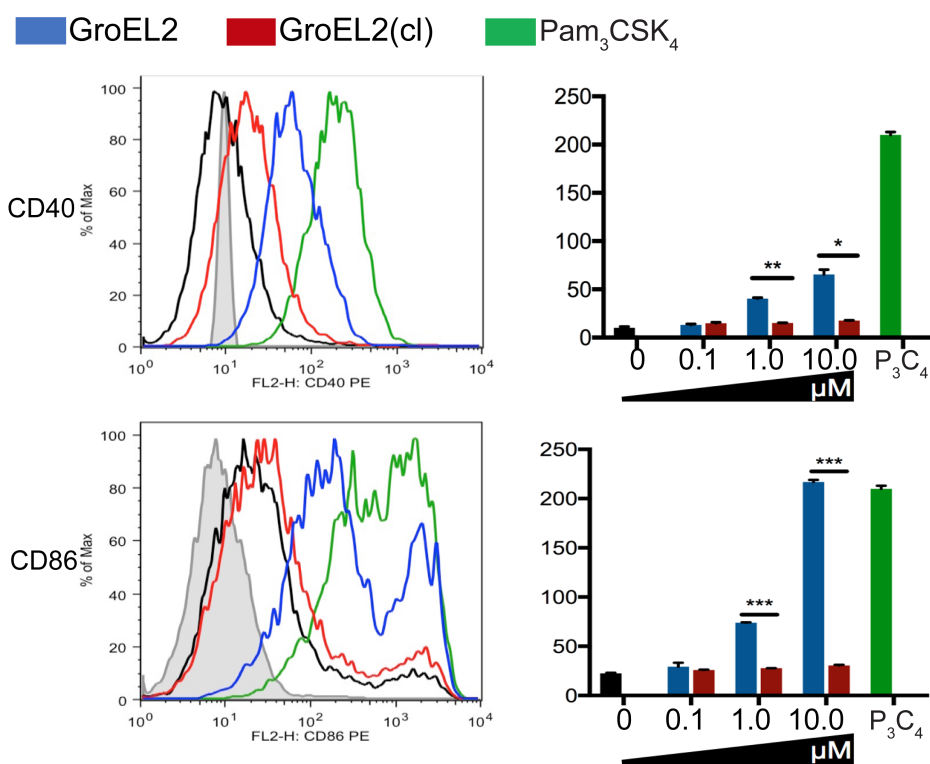


**Figure 2. Differential stimulation of proinflammatory cytokines from dendritic cells by GroEL2 and GroEL2(cl).** We measured levels of IL-6 and IL-12p40 cytokines produced by C57BL/6 BMDCs 24 hours after stimulation with varying levels of recombinant GroEL2 or GroEL2(cl). Data are shown as mean  $\pm$ S.D. of one representative experiment from three independent experiments.

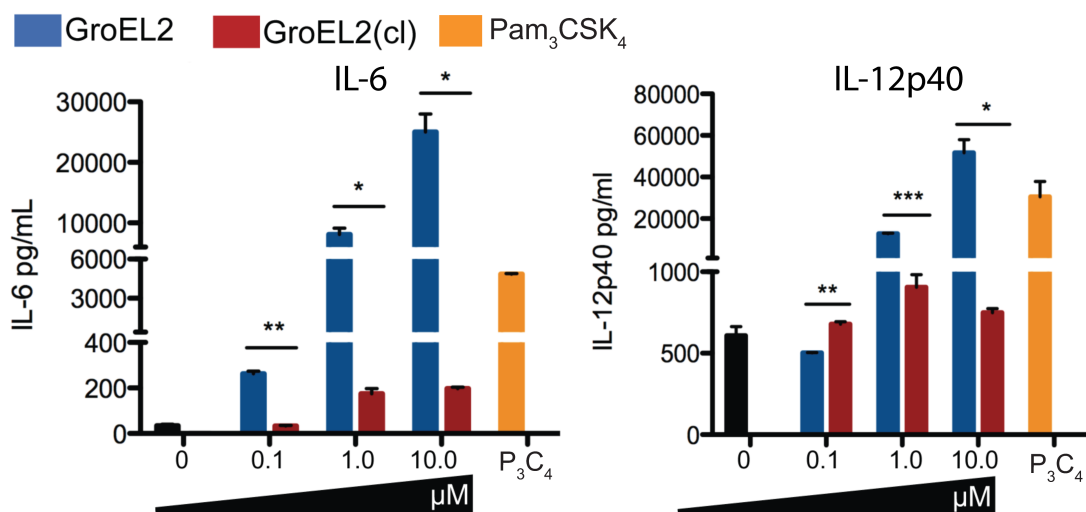


**Figure 3. GroEL2(cl) restores wild type levels of proinflammatory cytokine responses in dendritic cells and dampens the stimulatory capacity of full length GroEL2.**

**GroEL2.** (A) We measured IL-6 and IL-12p40 cytokines produced by C57BL/6 BMDCs 24 hours after infection with live Mtb strains. (B) We incubated C57BL/6 BMDCs with recombinant GroEL2 and GroEL2(cl) either alone (5  $\mu$ M) or together (5  $\mu$ M each) for 24 hours. The calculated additive effect of GroEL2 and GroEL2(cl) is represented as a sum of the cytokine levels for each protein alone. Data are shown as mean  $\pm$ S.D. of one representative experiment from three independent experiments.

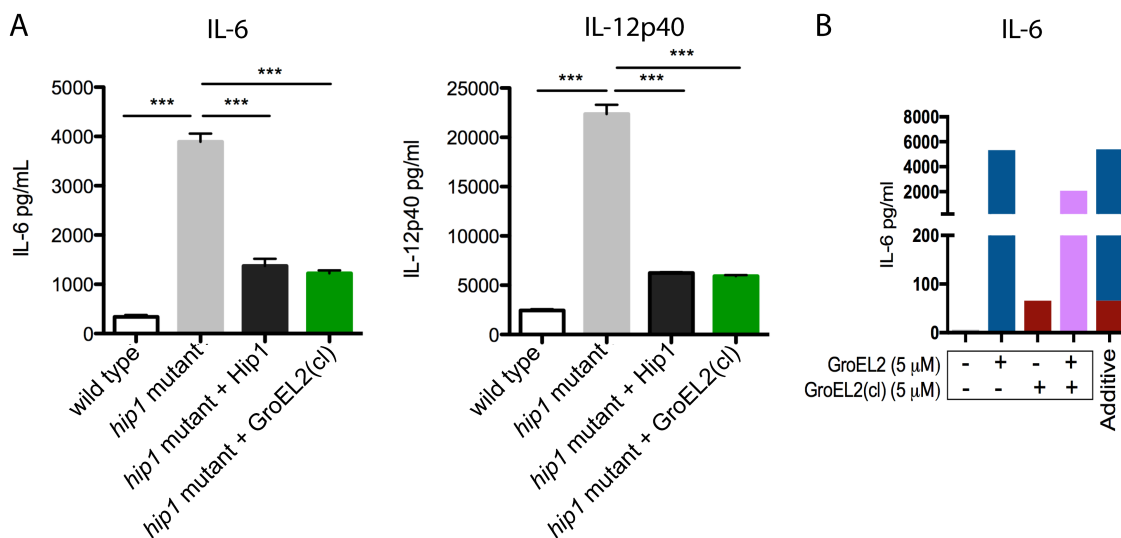
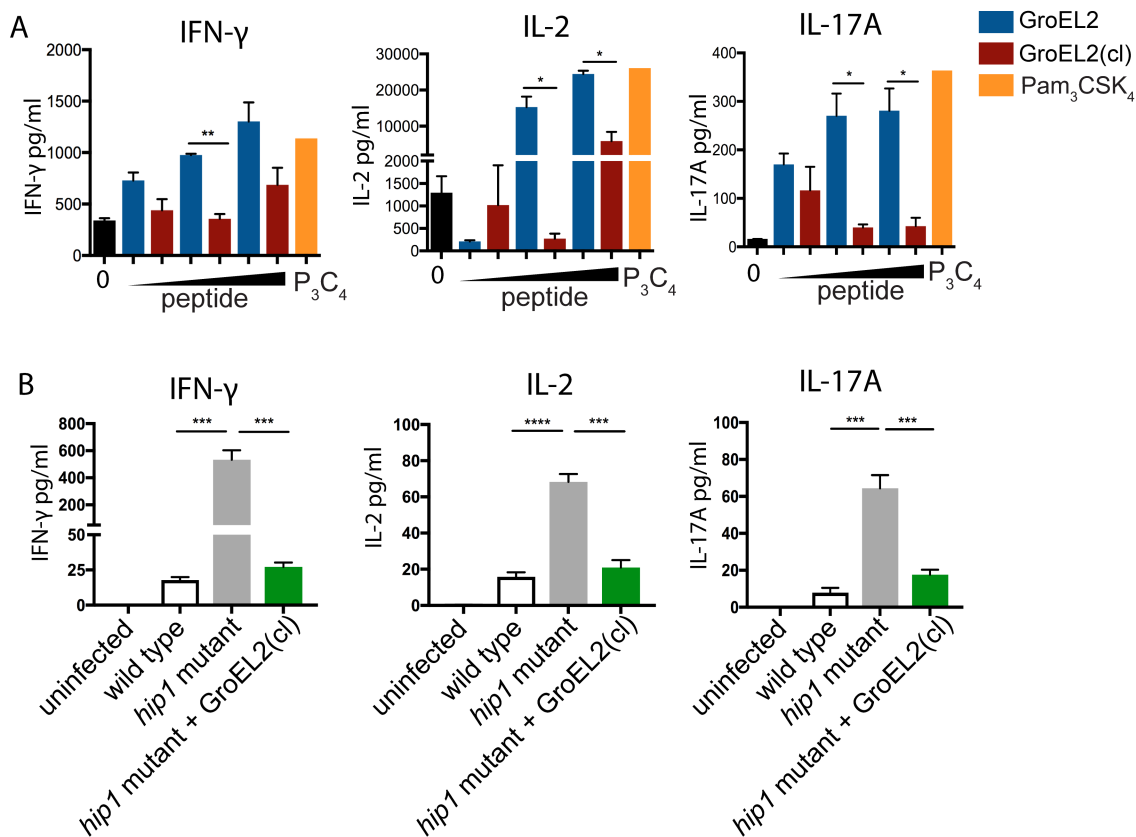


#### Figure 4. GroEL2 proteolysis modulates DC antigen presentation and T cell

**polarization.** (A) We pulsed DCs with varying amounts of OVA<sub>323-339</sub> peptide (1  $\mu\text{g/ml}$ , 10  $\mu\text{g/ml}$ , 50  $\mu\text{g/ml}$ ) for 6 hours and then stimulated with either recombinant GroEL2 or GroEL2(cl) for 24 hours. Following co-culture with antigen-specific TCR-Tg CD4<sup>+</sup> T cells for 72 hours, we assayed for cytokines IFN- $\gamma$ , IL-2 and IL-17A ELISA. (B) We infected DCs with live Mtb strains and then co-cultured them with purified ESAT-6-specific TCR-Tg CD4<sup>+</sup> T cells. After 80 hours, cell-free supernatants were collected and assessed for cytokines IFN- $\gamma$ , IL-2 and IL-17A ELISA. Data are shown as mean  $\pm$ S.D. of one representative experiment from three independent experiments.



**BIBLIOGRAPHY**

1. Ehrt S, Schnappinger D. Mycobacterial survival strategies in the phagosome: defence against host stresses. *Cellular microbiology*. 2009;11(8):1170-8. doi: 10.1111/j.1462-5822.2009.01335.x. PubMed PMID: 19438516; PubMed Central PMCID: PMC3170014.
2. Philips JA, Ernst JD. Tuberculosis pathogenesis and immunity. *Annual review of pathology*. 2012;7:353-84. doi: 10.1146/annurev-pathol-011811-132458. PubMed PMID: 22054143.
3. Russell DG. Mycobacterium tuberculosis: here today, here tomorrow. *Nature Reviews*. 2001;2:569-77.
4. Wolf AJ, Linas B, Trevejo-Nunez GJ, Kincaid E, Tamura T, Takatsu K, Ernst JD. Mycobacterium tuberculosis Infects Dendritic Cells with High Frequency and Impairs Their Function In Vivo. *The Journal of Immunology*. 2007;179(4):2509-19. doi: 10.4049/jimmunol.179.4.2509.
5. Hanekom WAM, M.; Manca, C.; Haslett, P.A.J.; Siddiqui, M.R.; Barry, C.; Kaplan, G. Mycobacterium tuberculosis inhibits maturation of human monocyte-derived dendritic cells in vitro. *Journal of Infectious Diseases*. 2003;188:257-66.
6. Marino S, Pawar S, Fuller CL, Reinhart TA, Flynn JL, Kirschner DE. Dendritic Cell Trafficking and Antigen Presentation in the Human Immune Response to Mycobacterium tuberculosis. *The Journal of Immunology*. 2004;173(1):494-506. doi: 10.4049/jimmunol.173.1.494.
7. Naffin-Olivos JLG, M.; , Goldfarb NM-L, R.; Dong, L.; Bizzell, E.; Valinetz, E.; Brandt, G.S.; Yu, S.; Shabashvili, D.E.; Ringer, D.; Dunn, B.M.; Petsko, G.A.;

- Rengarajan, J. Mycobacterium tuberculosis Hip1 modulates macrophage responses through proteolysis of GroEL2 .pdf. PLoS pathogens. 2014. doi: 10.1371/journal.ppat.1004132.
8. Mihret A. The role of dendritic cells in Mycobacterium tuberculosis infection. Virulence. 2012;3(7):654-9. doi: 10.4161/viru.22586. PubMed PMID: 23154283; PubMed Central PMCID: PMC3545947.
  9. Madan-Lala R, Sia JK, King R, Adekambi T, Monin L, Khader SA, Pulendran B, Rengarajan J. Mycobacterium tuberculosis impairs dendritic cell functions through the serine hydrolase Hip1. Journal of immunology. 2014;192(9):4263-72. doi: 10.4049/jimmunol.1303185. PubMed PMID: 24659689; PubMed Central PMCID: PMC3995873.
  10. Chen K, Lu J, Wang L, Gan YH. Mycobacterial heat shock protein 65 enhances antigen cross-presentation in dendritic cells independent of Toll-like receptor 4 signaling. Journal of leukocyte biology. 2004;75(2):260-6. doi: 10.1189/jlb.0703341. PubMed PMID: 14597728.
  11. Cehovin A, Coates AR, Hu Y, Riffo-Vasquez Y, Tormay P, Botanch C, Altare F, Henderson B. Comparison of the moonlighting actions of the two highly homologous chaperonin 60 proteins of Mycobacterium tuberculosis. Infection and immunity. 2010;78(7):3196-206. doi: 10.1128/IAI.01379-09. PubMed PMID: 20421377; PubMed Central PMCID: PMC2897374.
  12. Hickey TB, Thorson LM, Speert DP, Daffe M, Stokes RW. Mycobacterium tuberculosis Cpn60.2 and DnaK are located on the bacterial surface, where Cpn60.2 facilitates efficient bacterial association with macrophages. Infection and immunity.

2009;77(8):3389-401. doi: 10.1128/IAI.00143-09. PubMed PMID: 19470749; PubMed Central PMCID: PMC2715658.

13. Hickey TB, Ziltener HJ, Speert DP, Stokes RW. Mycobacterium tuberculosis employs Cpn60.2 as an adhesin that binds CD43 on the macrophage surface. *Cellular microbiology*. 2010;12(11):1634-47. doi: 10.1111/j.1462-5822.2010.01496.x. PubMed PMID: 20633027.

14. Khan N, Alam K, Mande SC, Valluri VL, Hasnain SE, Mukhopadhyay S. Mycobacterium tuberculosis heat shock protein 60 modulates immune response to PPD by manipulating the surface expression of TLR2 on macrophages. *Cellular microbiology*. 2008;10(8):1711-22. doi: 10.1111/j.1462-5822.2008.01161.x. PubMed PMID: 18419772.

15. Lewthwaite JC, Clarkin CE, Coates AR, Poole S, Lawrence RA, Wheeler-Jones CP, Pitsillides AA, Singh M, Henderson B. Highly homologous Mycobacterium tuberculosis chaperonin 60 proteins with differential CD14 dependencies stimulate cytokine production by human monocytes through cooperative activation of p38 and ERK1/2 mitogen-activated protein kinases. *International immunopharmacology*. 2007;7(2):230-40. doi: 10.1016/j.intimp.2006.10.005. PubMed PMID: 17178391.

16. Lewthwaite JC, Coates AR, Tormay P, Singh M, Mascagni P, Poole S, Roberts M, Sharp L, Henderson B. Mycobacterium tuberculosis chaperonin 60.1 is a more potent cytokine stimulator than chaperonin 60.2 (Hsp 65) and contains a CD14-binding domain. *Infection and immunity*. 2001;69(12):7349-55. doi: 10.1128/IAI.69.12.7349-7355.2001. PubMed PMID: 11705907; PubMed Central PMCID: PMC98821.

17. Lima KM, Santos SA, Lima VM, Coelho-Castelo AA, Rodrigues JM, Jr., Silva CL. Single dose of a vaccine based on DNA encoding mycobacterial hsp65 protein plus

- TDM-loaded PLGA microspheres protects mice against a virulent strain of *Mycobacterium tuberculosis*. *Gene therapy*. 2003;10(8):678-85. doi: 10.1038/sj.gt.3301908. PubMed PMID: 12692596.
18. Silva CL, Bonato VL, Coelho-Castelo AA, De Souza AO, Santos SA, Lima KM, Faccioli LH, Rodrigues JM. Immunotherapy with plasmid DNA encoding mycobacterial hsp65 in association with chemotherapy is a more rapid and efficient form of treatment for tuberculosis in mice. *Gene therapy*. 2005;12(3):281-7. doi: 10.1038/sj.gt.3302418. PubMed PMID: 15526006.
19. Silva CL, Lowrie DB. A single mycobacterial protein (hsp65) expressed by a transgenic antigen-presenting cell vaccinates mice against tuberculosis. *Immunology*. 1994;82:244-8.
20. Silva CLP, R.L.R.; Januario, A.; Bonato, V.L.D.; Lima, V.M.F.; da Silva, M.F.; Lowrie, D.B. Protection against tuberculosis by bone marrow expressing mycobacterial hsp65. *Immunology*. 1995;86:519-24.
21. Bulut Y, Michelsen KS, Hayrapetian L, Naiki Y, Spallek R, Singh M, Arditi M. *Mycobacterium tuberculosis* heat shock proteins use diverse Toll-like receptor pathways to activate pro-inflammatory signals. *The Journal of biological chemistry*. 2005;280(22):20961-7. doi: 10.1074/jbc.M411379200. PubMed PMID: 15809303.
22. Fong JJ, Sreedhara K, Deng L, Varki NM, Angata T, Liu Q, Nizet V, Varki A. Immunomodulatory activity of extracellular Hsp70 mediated via paired receptors Siglec-5 and Siglec-14. *EMBO J*. 2015;34(22):2775-88. doi: 10.15252/embj.201591407. PubMed PMID: 26459514; PubMed Central PMCID: PMC4682649.

23. Chilukoti N, Kumar CM, Mande SC. GroEL2 of *Mycobacterium tuberculosis* Reveals the Importance of Structural Pliability in Chaperonin Function. *Journal of bacteriology*. 2015;198(3):486-97. doi: 10.1128/JB.00844-15. PubMed PMID: 26553853; PubMed Central PMCID: PMC4719451.
24. Shahar A, Melamed-Frank M, Kashi Y, Shimon L, Adir N. The dimeric structure of the Cpn60.2 chaperonin of *Mycobacterium tuberculosis* at 2.8 Å reveals possible modes of function. *Journal of molecular biology*. 2011;412(2):192-203. doi: 10.1016/j.jmb.2011.07.026. PubMed PMID: 21802426.
25. Goyal K, Qamra R, Mande SC. Multiple gene duplication and rapid evolution in the groEL gene: functional implications. *Journal of molecular evolution*. 2006;63(6):781-7. doi: 10.1007/s00239-006-0037-7. PubMed PMID: 17103057.
26. Dekker C, Willison KR, Taylor WR. On the evolutionary origin of the chaperonins. *Proteins*. 2011;79(4):1172-92. doi: 10.1002/prot.22952. PubMed PMID: 21322032.
27. Cho YS, Dobos KM, Prenni J, Yang H, Hess A, Rosenkrands I, Andersen P, Ryoo SW, Bai GH, Brennan MJ, Izzo A, Bielefeldt-Ohmann H, Belisle JT. Deciphering the proteome of the in vivo diagnostic reagent "purified protein derivative" from *Mycobacterium tuberculosis*. *Proteomics*. 2012;12(7):979-91. doi: 10.1002/pmic.201100544. PubMed PMID: 22522804.
28. Yang H, Troudt J, Grover A, Arnett K, Lucas M, Cho YS, Bielefeldt-Ohmann H, Taylor J, Izzo A, Dobos KM. Three protein cocktails mediate delayed-type hypersensitivity responses indistinguishable from that elicited by purified protein derivative in the guinea pig model of *Mycobacterium tuberculosis* infection. *Infection*

and immunity. 2011;79(2):716-23. doi: 10.1128/IAI.00486-10. PubMed PMID: 21134965; PubMed Central PMCID: PMC3028861.

29. Rengarajan J, Murphy E, Park A, Krone CL, Hett EC, Bloom BR, Glimcher LH, Rubin EJ. Mycobacterium tuberculosis Rv2224c modulates innate immune responses. Proceedings of the National Academy of Sciences of the United States of America. 2008;105(1):264-9. doi: 10.1073/pnas.0710601105. PubMed PMID: 18172199; PubMed Central PMCID: PMC2224198.

30. Madan-Lala R, Peixoto KV, Re F, Rengarajan J. Mycobacterium tuberculosis Hip1 dampens macrophage proinflammatory responses by limiting toll-like receptor 2 activation. Infection and immunity. 2011;79(12):4828-38. doi: 10.1128/IAI.05574-11. PubMed PMID: 21947769; PubMed Central PMCID: PMC3232659.